MIINA OJANSIVU

Characterization of Osteogenic Differentiation Mechanisms of Human Adipose Stem Cells in Response to BMP-2 and Bioactive Glasses

MIINA OJANSIVU

Characterization of Osteogenic Differentiation Mechanisms of Human Adipose Stem Cells in Response to BMP-2 and Bioactive Glasses

■

ACADEMIC DISSERTATION
To be presented, with the permission of
the Board of the BioMediTech of the University of Tampere,
for public discussion in the auditorium F115 of the Arvo building,
Lääkärinkatu 1, Tampere,
on 16 September 2016, at 12 o'clock.

UNIVERSITY OF TAMPERE

MIINA OJANSIVU

Characterization of Osteogenic Differentiation Mechanisms of Human Adipose Stem Cells in Response to BMP-2 and Bioactive Glasses

UNIVERSITY
OF TAMPERE

Supervised by
Docent Susanna Miettinen
University of Tampere
Finland
PhD Sari Vanhatupa
University of Tampere
Finland

Reviewed by
Professor Maria Helena Fernandes
University of Porto
Portugal
Professor Jeffrey Gimble
Tulane University
United States

The originality of this thesis has been checked using the Turnitin OriginalityCheck service
in accordance with the quality management system of the University of Tampere.

Cover design by
Mikko Reinikka

441 729
Painotuote

Abstract

Due to the aging population, the incidence of bone defects, caused either by trauma or disease, is constantly increasing. Bone tissue engineering (TE), combining a biomaterial scaffold, cells and cell growth and differentiation stimulating factors, has recently emerged as a promising approach to treat these defects without the drawbacks associated with the traditionally used bone grafts. With respect to bone TE, adipose stem cells (ASCs) are considered a highly favorable cell choice due to their multipotent differentiation capability and high abundance in the easily obtainable adipose tissue. In fact, bone TE treatments utilizing adipose stem cells have already shown promising results in a number of clinical case studies. However, despite the fast progress of the bone TE approaches, the molecular level cellular responses to the various chemical and biomaterial-elicited stimuli are still poorly understood.

In this thesis, the osteogenic and adipogenic differentiation responses stimulated by bone morphogenetic protein-2 (BMP-2) and bioactive glass (BaG), as well as the underlying intracellular signaling events in human ASCs (hASCs), were evaluated. Accepted also for clinical use, BMP-2 is thought to be a strong bone formation inducer, but based on recent findings, it seems to elicit highly variable cellular responses. To shed light on this, the effect of BMP-2 on osteogenic and adipogenic differentiation, as well as on the canonical Smad signaling pathway was analyzed in hASCs derived from several donors. Moreover, the role of the culture medium (either human serum (HS) or fetal bovine serum (FBS) supplemented) and the production origin of BMP-2 (Escherichia coli or mammalian cells) in the BMP-2 function was evaluated. With respect to the biomaterial component of the bone TE approach, BaGs have been considered highly advantageous due to their inherent ability to stimulate osteogenic differentiation. However, the exact mechanism of this favorable phenomenon is not well known. Thus, the osteogenesis-stimulating effect of ionic extracts from the BaGs S53P4, 2-06, 1-06 and 3-06, in the absence of the cell-biomaterial contact, was determined. Secondly, the mechanisms of BaG-induced early osteogenic differentiation, with respect to cell attachment and attachment-mediated signaling, were evaluated when hASCs were cultured on S53P4 and 1-06 BaG discs.

The stimulation with BMP-2 was observed to elicit functional canonical Smad signaling response in all the hASC donor lines studied. However, with respect to differentiation, hASCs from some donors adopted an osteogenic fate while hASCs from other donors committed towards adipocytes in response to BMP-2. Moreover, the cellular response to BMP-2 was observed to be the strongest in HS condition and with mammalian cells originated BMP-2. With respect to the BaG ionic extracts, the combination of the ions released from the BaGs and the traditionally used osteogenic medium (OM) induced exceptionally fast and extensive osteogenic differentiation of hASCs when compared to the control OM. Of the different BaGs, 2-06 and 3-06 OM extracts seemed to be the strongest stimulators of osteogenic differentiation. As such, however, the BaG extracts could not induce the osteogenic commitment of hASCs. When the hASCs were cultured in contact with the S53P4 and 1-06 discs, the glasses stimulated the early osteogenic differentiation even in the absence of OM. The cell attachment mode on the BaGs was shown to be atypical, with small and dispersed focal adhesion sites and disorganized actin cytoskeleton, but increased production of integrinβ1 and vinculin. The cells also modified the BaG surface underneath them. The BaG-induced early osteogenic differentiation was shown to be highly dependent on focal adhesion kinase (FAK) and mitogen-activated protein kinases (MAPKs) extracellular signal-regulated kinase 1/2 (ERK1/2) and c-Jun N-terminal kinase (JNK), whereas the role of MAPK p38 was less significant.

In conclusion, the BMP-2-induced cellular responses were observed to be highly dependent on the hASC donor but also on culture medium composition and BMP-2 production origin, which poses challenges to the clinical utility of this growth factor. Moreover, despite the varying differentiation responses, the BMP-2-induced Smad signaling was similar in all the hASC donor lines, implying that additional signaling mechanisms must be involved in the BMP-2-induced differentiation. In case of the BaG extracts, the exceptionally strong osteogenesis-inducing ability of the OM-based BaG extracts might be highly applicable in various approaches requiring effective osteogenic differentiation. When cultured in direct contact with the BaGs, a unique cell attachment mode of hASCs was observed and, furthermore, the attachment-related FAK-MAPK signaling pathway was shown to play a central role in the BaG-induced early osteogenic response. These observations set the basis for a more detailed evaluation of the cell signaling events on BaGs, an area with currently only very little knowledge.

Tiivistelmä

Väestön ikääntymisen myötä onnettomuuksien ja sairauksien aiheuttamien luuvaurioiden määrä kasvaa jatkuvasti. Luun kudosteknologia on nuori tieteenala, joka yhdistää biomateriaalitukirakenteen, solut sekä solujen proliferaatiota ja erilaistumista tukevia tekijöitä, ja tarjoaa näin lupaavan menetelmän luuvaurioiden hoitoon ilman perinteisenä hoitomuotona käytettyjen luusiirteiden haittoja. Luun kudosteknologiaa ajatellen rasvan kantasolut ovat suotuisa soluvalinta, sillä ne ovat erilaistumiskyvyltään multipotentteja ja eristettävissä suurella saannolla helposti saatavilla olevasta rasvakudoksesta. Luun kudosteknologiaan perustuvat, rasvan kantasoluja käyttävät hoidot ovatkin jo tuottaneet lupaavia tuloksia useissa yksittäisissä potilastapauksissa. Huolimatta kudosteknologisten menetelmien nopeasta kehityksestä, molekyylitason soluvasteet erilaisiin kemiallisiin sekä biomateriaalin aikaansaamiin ärsykkeisiin tunnetaan kuitenkin vielä huonosti.

Tässä väitöskirjatyössä tutkittiin luun morfogeneettinen proteiini-2 (BMP-2) – kasvutekijän sekä bioaktiivisen lasin aiheuttamia luu- ja rasvaerilaistumisvasteita sekä niihin liittyviä solunsisäisiä signalointivaikutuksia ihmisen rasvan kantasoluissa. Kliinisestikin käytettyä BMP-2:a pidetään voimakkaana luuerilaistajana, mutta viimeisimmän tutkimustiedon valossa sen aiheuttamat soluvasteet eivät ole yhteneviä. Tämän vuoksi BMP-2:n vaikutusta luu- ja rasvaerilaistumiseen sekä kanoniseen Smad-signalointireittiin analysoitiin usealta eri luovuttajalta peräisin olevissa rasvan kantasoluissa. Lisäksi tutkittiin kasvatusliuoksen (ihmisseerumi-/naudan seerumipohjainen) sekä BMP-2:n tuottoalkuperän (Escherichia coli/nisäkässolut) vaikutusta kasvutekijän toimintaan. Mitä tulee luun kudosteknologiassa käytettyihin biomateriaaleihin, bioaktiivisia laseja pidetään erityisen hyödyllisinä niiden luuerilaistumista stimuloivain vaikutuksen vuoksi. Ilmiön tarkkaa mekanismia ei kuitenkaan juuri tunneta. Tämän vuoksi S53P4-, 2-06-, 1-06- ja 3-06-laseista valmistettujen ekstraktien luuerilaistavaa vaikutusta tutkittiin ilman suoraa solu-biomateriaali-kontaktia. Lisäksi lasien aiheuttaman varhaisen luuerilaistumisen mekanismeja liittyen solujen kiinnittymiseen ja kiinnittymisen käynnistämään signalointiin tutkittiin kasvattamalla rasvan kantasoluja S53P4- ja 1-06-bioaktiivisista laseista valmistetuilla levyillä.

BMP-2-stimuloinnin havaittiin aiheuttavan toiminnallisen kanonisen Smad-signalointivasteen kaikilta luovuttajilta peräisin olevissa rasvan kantasoluissa. Tästä huolimatta eri luovuttajien solujen erilaistumisvasteet erosivat merkittävästi toisistaan: toisten luovuttajien solut erilaistuivat BMP-2:n vaikutuksesta luun ja toisten rasvan suuntaan. BMP-2:n aiheuttama soluvaste oli voimakkain ihmisen seerumia sisältävässä mediumissa sekä nisäkässoluissa tuotetulla kasvutekijällä. Mitä tulee lasiekstrakteihin, lasista vapautuneet ionit sekä perinteisesti käytetyt kemialliset luuerilaistustekijät yhdistävä kasvatusliuos aiheutti poikkeuksellisen nopean ja voimakkaan luuerilaistusvasteen rasvan kantasoluissa verrattuna lasi-ionittomaan luuerilaistusmediumiin. Lasiekstrakteista 2-06 ja 3-06 indusoivat luuerilaistumista voimakkaimmin. Ilman luuerilaistusmediumia lasiekstraktit eivät kuitenkaan aiheuttaneet luuerilaistumista. Viljeltäessä S53P4- ja 1-06-biolasilevyillä ilman kemiallisia luuerilaistustekijöitä rasvan kantasolut ilmensivät luuerilaistumisen varhaisia markkereita. Solut kiinnittyivät lasilevyille epätyypillisellä mekanismilla: fokaaliadheesiokohdat olivat pieniä ja tasaisesti ympäri soluja levittäytyneitä, ja aktiinitukiranka oli epäjärjestynyt, mutta tästäkin huolimatta integriiniβ1:n sekä vinkuliinin tuoton havaittiin lisääntyvän lasien vaikutuksesta. Solut myös muokkasivat allaan olevaa biolasipintaa. Bioaktiivisen lasin aiheuttaman varhaisen luuerilaistumisen havaittiin riippuvan fokaaliadheesiokinaasista (FAK) sekä mitogeeniaktivoituvista proteiinikinaaseista (MAPK) ERK1/2 ja JNK. MAPK p38 oli sen sijaan toiminnaltaan merkityksettömämpi.

Yhteenvetona BMP-2:n aiheuttamien soluvasteiden havaittiin olevan voimakkaasti riippuvaisia rasvan kantasolujen luovuttajasta, mutta myös kasvatusmediumin koostumuksesta sekä kasvutekijän tuottoalkuperästä, mikä aiheuttaa haasteita BMP-2:n onnistuneelle kliiniselle käytölle. Kaksijakoisesta erilaistumisvasteesta huolimatta BMP-2:n aiheuttama Smad-signalointi oli yhtenevää kaikissa soluissa, minkä vuoksi myös muiden signalointimekanismien täytyy säädellä BMP-2:n indusoimaa erilaistumisvastetta. Mitä tulee biolasiekstrakteihin, luuerilasitustekijöiden läsnä ollessa lasi-ionien luuerilaistava vaikutus oli poikkeuksellisen voimakas, mikä saattaa tarjota näille mediumeille lukuisia käyttökohteita tehokasta luuerilaistumista edellyttävissä sovelluksissa. Viljeltäessä rasvan kantasoluja biolasilevyillä, solujen huomattiin kiinnittyvän laseille poikkeuksellisella tavalla, ja kiinnittymiseen kytkeytyvän FAK-MAPK–signalointireitin havaittiin olevan merkittävässä asemassa lasien aiheuttaman varhaisen luuerilaistumisen säätelyssä. Nämä havainnot luovat pohjaa bioaktiivisten lasien aiheuttaman solusignalointivasteen tarkemmille analyyseille.

Contents

Abbreviations

ACP	amorphous calcium phosphate
ActR	activin receptor
ALP	alkaline phosphatase
AM	adipogenic medium
α-MEM	alpha modified Eagle's medium
aP2	adipocyte protein 2
ASC	adipose stem cell
ATF4	activating transcription factor 4
BaG	bioactive glass
BCP	biphasic calcium phosphate
BM	basic cell culture medium
BMI	body mass index
BMP	bone morphogenetic protein
BMPR	BMP receptor
BMSC	bone marrow-derived mesenchymal stem cell
BSP	bone sialoprotein
CADM1	cell adhesion molecule 1
CaP	calcium phosphate
CD	cluster of differentiation
C/EBP	CCAAT enhancer-binding protein
CHO	Chinese hamster ovary
co-Smad	common partner Smad
CPC	calcium phosphate ceramic
CREB	cyclic AMP response element-binding protein
DAPI	4',6-diamidino-2-phenylindole
DCC	dextran coated charcoal
DLX5	distal-less homeobox transcription factor 5
DMEM/F-12	Dulbecco's modified Eagle's medium/Ham's nutrient mixture F-12
ECM	extracellular matrix
E. coli	Escherichia coli
EDXA	energy dispersive X-ray analysis

EGF	epidermal growth factor
EGFR	epidermal growth factor receptor
ELISA	enzyme-linked immunosorbent assay
ERK	extracellular signal-regulated kinase
ESC	embryonic stem cell
FA	focal adhesion
FABP4	fatty acid binding protein 4
FAK	focal adhesion kinase
FBS	fetal bovine serum
FCS	fetal calf serum
FDA	Food and Drug Administration
FGF	fibroblast growth factor
GLUT4	glucose transporter 4
Grb2	growth factor receptor binding protein 2
GSK3	glycogen synthase kinase 3
HA	hydroxyapatite
hASC	human adipose stem cell
hBMSC	human bone marrow-derived mesenchymal stem cell
HCA	hydroxycarbonate apatite
HLA-DR	human leukocyte antigen - antigen D related
hMSC	human mesenchymal stem cell
HS	human serum
Hsp27	heat shock protein 27
IBMX	isobutylmethylxanthin
ICC	immunocytochemical staining
ICP-OES	inductively-coupled plasma optical emission spectrometry
IFATS	International Federation of Adipose Therapeutics and Science
IGF	insulin-like growth factor
iPSC	induced pluripotent stem cell
ISCT	International Society for Cellular Therapy
I-Smad	inhibitory Smad
JNK	c-Jun N-terminal kinase
KLF	Krüppel-like factor
LPL	lipoprotein lipase
LRP6	low-density lipoprotein receptor-related protein 6
MAPK	mitogen-activated protein kinase
MAPKK	MAPK kinase

MAPKKK	MAPK kinase kinase
miRNA	micro RNA
MSC	mesenchymal stem cell/multipotent mesenchymal stromal cell
MSX2	Msh homeobox transcription factor 2
nRTK	non-receptor tyrosine kinase
OM	osteogenic medium
PCL	polycaprolactone
PDGF	platelet-derived growth factor
PI3K	phosphatidylinositol 3-kinase
PKA	protein kinase A
PKC	protein kinase C
PLA	polylactide
PLGA	poly(lactide-co-glycolide)
PPARγ	peroxisome proliferator-activated transcription factor γ
qALP	quantitative alkaline phosphatase activity
qRT-PCR	quantitative real-time polymerase chain reaction
RPLP0	large ribosomal protein P0
rhBMP	recombinant human BMP
ROCK	Rho-associated protein kinase
RSK2	ribosomal S6 kinase 2
R-Smad	receptor-activated Smad
RUNX2	runt-related transcription factor 2
SAPK	stress-activated protein kinase
SDS-PAGE	sodium dodecyl sulfate polyacrylamide gel electrophoresis
SEM	scanning electron microscopy
Smad	mothers against decapentaplegic homolog protein
Smurf	Smad specific E3 ubiquitin protein ligase
Sox9	SRY-related high-mobility group box 9 transcription factor
SREBP-1	sterol response element-binding protein-1
STAT3	signal transducer and activator of transcription 3
SVF	stromal vascular fraction
TAZ	transcriptional co-activator with PDZ-binding motif
TCP	tricalcium phosphate
TE	tissue engineering
TGF-β	transforming growth factor β
VEGF	vascular endothelial growth factor

Original publications

This thesis is based on the following original publications, referred to in the text by their Roman numerals (**I-III**):

I   Vanhatupa S, **Ojansivu M**, Autio R, Juntunen M, Miettinen S. BMP-2 induces donor dependent osteogenic and adipogenic differentiation in human adipose stem cells. *Stem Cells Transl Med*. 2015 Dec;4(12):1391-402.

II   **Ojansivu M**, Vanhatupa S, Björkvik L, Häkkänen H, Kellomäki M, Autio R, Ihalainen JA, Hupa L, Miettinen S. Bioactive glass ions as strong enhancers of osteogenic differentiation in human adipose stem cells. *Acta Biomater*. 2015 Jul 15;21:190-203.

III **Ojansivu M**, Vanhatupa S, Wang X, Kellomäki M, Hupa L, Miettinen S. The role of mitogen-activated protein kinases and cell attachment mechanism on bioactive glasses S53P4 and 1-06 in glass-induced osteogenic differentiation of human adipose stem cells. *Submitted*.

The original publications are reproduced with the permission of the copyright holders.

1   Introduction

Tissue engineering (TE), originally introduced in the beginning of 1990s, is a branch of science aiming to develop biological substitutes that restore, maintain, or improve tissue function (Langer & Vacanti, 1993). Among other tissues in the human body, the TE approach has been extensively studied for the creation of bone. Traditionally, large bone defects have been treated with either autografts, often tempered by inadequate amount, poor quality and donor-site morbidity, or allografts, which pose the risk of disease transmission and immunorejection (Burg et al., 2000; Jakob et al., 2012). Considering these severe drawbacks of the current treatment methods, as well as the constantly increasing incidence of bone defects as a consequence of the aging population, there is clearly a huge demand for novel orthopedic interventions, for which the bone TE approach has the potential to provide an answer.

A typical TE-based solution combines a biomaterial scaffold, cells and cell growth and differentiation stimulating factors (Vacanti & Langer, 1999). With respect to the choice of cells, adipose stem cells (ASCs) have turned out to be a highly promising cell type due to their multipotency, high yield and the general abundance of their source material, i.e. adipose tissue (Lindroos et al., 2011). Moreover, ASCs have low immunogenicity which might enable the use of allogenic cells, a potential "off-the-shelf" product of the future (McIntosh et al., 2006; Niemeyer et al., 2007). Out of the large variety of biomaterials exploited for bone TE, bioactive glass (BaG), invented by Larry Hench over 40 years ago (Hench et al., 1971), has gained considerable attention because of its advantageous properties, including strong bonding to bone and ability to support cell attachment, growth and osteogenic differentiation (Jones, 2015). In fact, the combination of autologous ASCs and BaG granules has been already successfully used in bone TE-based treatments of three patients with frontal sinus defects (Sandor et al., 2014). The performance of TE constructs is often boosted with supplemental chemical agents, such as growth factors. Out of the different growth factors tested for the applications of bone TE, bone morphogenetic proteins (BMPs) are probably the most widely studied due to the strong bone formation-inducing capacity of a subset of these proteins (Argintar et al., 2011; X. Zhang et al., 2014). Because it has been approved for clinical use, BMP-2 has received particular attention with respect to bone TE.

Traditionally, the design of a bone TE construct has been tackled with a "top-down" approach, which focuses on the large-scale tissue-level performance of the cell-biomaterial structure and thus provides fast-track solutions to create usable implants (Bodle et al., 2011). However, this approach is highly oversimplified and disregards the cellular level mechanisms, the understanding of which is nowadays thought to be crucial for the proper functionality as well as the optimized development of the TE constructs. Therefore, a more basic-level "bottom-up" approach has started to emerge and shift the focus towards the cellular responses to the various environmental stimuli within the bone TE construct (Bodle et al., 2011). This closer evaluation of the cell-level responses has been accompanied with new standpoints to many issues previously taken for granted. For example, with respect to the osteogenesis-stimulating effect of BMP-2, many studies have recently observed a negligible or even negative role for BMP-2 as an inducer of stem cell osteogenic differentiation (Chou et al., 2011; Cruz et al., 2012; Tirkkonen et al., 2013; Waselau et al., 2012; Yi et al., 2016; Zuk et al., 2011). This clearly shakes the established position of this widely used growth factor and calls for a more detailed analysis of its functionality. The "bottom-up" approach has also started to draw attention to the biomaterial-elicited cellular responses, extending all the way to the level of intracellular signaling. In case of the BaGs, there is evidence that the ionic products released from these reactive biomaterials have a profound effect on the cellular actions (Hoppe et al., 2011), but more evidence is required to elucidate this matter. With respect to the signaling level changes induced by the BaGs, the knowledge is currently even scarcer.

This thesis work aimed to shed light on the mechanisms of the cellular responses elicited by the BMP-2 growth factor and BaG biomaterials, either in the form of ionic extracts or disc-shaped cell culture substrates. In this work, the functionality of the BMP-2 signaling route was evaluated in human ASCs (hASCs) in different culture conditions and with growth factor protein from different production origins. Several donor lines were tested with respect to both the signaling response and the differentiation outcome under BMP-2 stimulus. To analyze the mechanism of BaG-induced osteogenic differentiation of hASCs, the osteogenesis-inducing effect of BaG ionic extracts, in the absence of any cell-biomaterial contact, was determined. With respect to the cell-BaG contact, the cell attachment mechanisms on BaGs as well as the attachment-initiated signaling responses responsible for the BaG-induced early osteogenic differentiation, were investigated.

2 Literature review

2.1 Stem cells

By definition, stem cells are able to both self-renew and to produce differentiated progeny (Brignier & Gewirtz, 2010; Choumerianou et al., 2008). Due to these properties, stem cell research provides excellent tools for the basic understanding of the differentiation mechanisms, testing of drugs and, most importantly, for the treatment of diseases and traumas by the means of cell therapy and TE-based solutions (Jung, 2009). Stem cells can be classified based on their differentiation capacity (Brignier & Gewirtz, 2010; Choumerianou et al., 2008). Totipotent stem cells, the cells of the embryo until the 4- to 8-cell stage, are able to produce an entire organism, i.e. all the embryonic as well as the extraembryonic (e.g. placenta) tissues. Pluripotent stem cells, like the embryonic stem cells (ESCs) derived from the inner cell mass of a 5 to 14 days old blastocyst, are defined by their ability to differentiate to all the cell types present in the three embryonic germ layers, namely ectoderm, mesoderm and endoderm. The first ESC lines were generated from mouse blastocysts in 1981 by two independent research groups (Evans & Kaufman, 1981; Martin, 1981), and 17 years later the first human ESC lines were established (Thomson et al., 1998). In addition to ESC isolation, another significant milestone in the pluripotent stem cell research occurred in 2006 when mouse fibroblasts were successfully reprogrammed back to stem cells by retrovirally introducing the genes of four transcription factors, *Oct3/4, Sox2, Klf2* and *c-Myc,* into the fibroblasts (Takahashi & Yamanaka, 2006). The reprogramming was soon accomplished also with human fibroblasts (Takahashi et al., 2007) resulting in a Nobel prize for Shinya Yamanaka in 2012. These induced pluripotent stem cells (iPSCs) have similar properties to the ESCs, including the almost unlimited self-renewal capacity, but unlike ESCs, they do not have ethical problems related to the destruction of embryos or concerns about the immunorejection. Since 2010 the pluripotent stem cells have finally reached the clinical trials, which currently focus on the treatment of spinal cord injury, ocular diseases, type I diabetes and heart failure (Kimbrel & Lanza, 2015).

When the stem cell differentiation capacity is further restricted, the stem cells are called multipotent (Brignier & Gewirtz, 2010; Choumerianou et al., 2008). Adult stem cells, found in differentiated tissues, are typically multipotent and their differentiation capacity is thus mainly restricted to the cell types of the tissue from which they originated. Adult stem cells can be divided into three categories based on their germ layer origin: cells of ectodermal origin (e.g. pulmonary epithelial stem cells and gastrointestinal tract stem cells), cells of mesodermal origin (e.g. bone marrow-derived mesenchymal stem cells (BMSCs) and ASCs) and cells of endodermal origin (e.g. neural and skin stem cells) (Choumerianou et al., 2008). A bit misleadingly, also stem cells of the fetal tissues, umbilical cord and placenta are considered adult stem cells of multipotent nature. Finally, stem cells being able to differentiate to only one cell type, e.g. basal cells of the epidermis and satellite cells of the muscles, are considered unipotent (Visvader & Clevers, 2016).

2.2   Mesenchymal stem cells

Mesenchymal stem cells (MSCs), a type of adult stem cells able to undergo mesodermal lineage-specific differentiation, were first isolated from bone-marrow by Friedenstein and co-workers in 1968 (Friedenstein et al., 1968). This adherent fibroblast-like cell population, first called colony-forming unit fibroblasts, consisted of non-hematopoietic progenitors able to differentiate to stromal precursors. Since their recovery, the colony-forming unit fibroblasts were extensively studied under non-consistent nomenclature until Arnold Caplan suggested the term "mesenchymal stem cell", which became commonly used (Caplan, 1991). Later on, MSCs have been isolated from many other tissues, such as adipose tissue (Zuk et al., 2001), dental pulp (Gronthos et al., 2000), tendon (Salingcarnboriboon et al., 2003), Wharton's jelly of the umbilical cord (Troyer & Weiss, 2008) and placenta (Igura et al., 2004). Indeed, it is currently thought that MSCs can be found from virtually all the organs (da Silva Meirelles et al., 2006). Recently, MSCs have been also successfully generated from iPSCs (K. Hynes et al., 2014).

Due to the inherent heterogeneity of the MSC population (Russell et al., 2010), there has been a lot of debate about the "true" stemness of these cells, i.e. the long-term survival with retention of the self-renewal and differentiation capacities. Therefore, the Mesenchymal and Tissue Stem Cell Committee of International Society for Cellular Therapy (ISCT) proposed that, instead of "mesenchymal stem cell" (which is reserved for the subpopulation that meets the stem cell criteria), these

cells should be collectively called "multipotent mesenchymal stromal cells", independent of the tissue of origin (Horwitz et al., 2005). However, the acronym "MSC" may be used for both cell populations as long as it is clearly defined.

Since MSCs cannot be identified based on a single universal surface marker, ISCT has defined minimal criteria the MSCs have to fulfill (Dominici et al., 2006). First, MSCs must be plastic-adherent under standard culture conditions. Second, ≥95% of the MSC population has to express the cluster of differentiation (CD) surface markers CD73, CD90 and CD105, and lack the expression of CD45, CD34, CD14 or CD11b, CD79α or CD19, and human leukocyte antigen - antigen D related (HLA-DR) (≤2%). Third, MSCs must be able to differentiate to osteoblasts, adipocytes and chondroblasts *in vitro*.

Despite the trilineage differentiation requirement defined by ISCT, there is evidence that in reality the differentiation potential of MSCs is considerably wider (Strioga et al., 2012). For example, MSCs can be induced to differentiate to other mesodermal tissues such as tendon (Vuornos et al., 2016), skeletal muscle (De Bari et al., 2003), myocardium (Shim et al., 2004) and endothelium (Oswald et al., 2004). Furthermore, MSCs have shown also plasticity, i.e. differentiation to cells of endodermal and ectodermal origin (e.g. neurons, hepatocytes) (Krampera et al., 2007; Teng et al., 2015), although the efficacy of the nonmesodermal differentiation of MSCs is typically very low.

In addition to their multilineage differentiation potential, MCSs possess also other beneficial properties when considering the MSC-based clinical applications. Due to the low expression of major histocompatibility complexes I and II, MSCs are low-immunogenic, which allows their allogenic transplantation (Myers et al., 2010; S. Wang et al., 2011). Moreover, MSCs are shown to be immunosuppressive, non-tumorigenic and to have a strong homing tendency, i.e. they tend to migrate to the site of injury where they regulate the healing process via active paracrine, e.g. proangiogenic and anti-apoptotic, actions (Myers et al., 2010; Ren et al., 2012). Indeed, it has been suggested that, instead of providing an injured tissue with mature cells via differentiation, MSCs exert their therapeutic potential mainly via paracrine functions (Myers et al., 2010; Strioga et al., 2012). Either way, there are currently 549 registered MSC-utilizing clinical trials going on (clinicaltrials.gov), illustrating the huge interest in MSCs as a potential treatment means for conditions ranging from the treatment of complex fistulas, often related to Crohn's disease, to the treatment of joint disorders (e.g. osteoarthritis), neurological disorders (e.g. Parkinson's disease, spinal cord injury and multiple sclerosis), cardiovascular diseases (e.g. myocardial infarction) and immunological disorders (e.g. type I diabetes, graft-

versus-host disease). In particular, the number of clinical trials evaluating the safety and efficacy of hASCs for various medical disorders has increased exponentially in the last couple of years. Whereas in 2010 there were only 18 clinical trials utilizing either hASCs or stromal vascular fraction of adipose tissue (Lindroos et al., 2011), in April 2016 the amount of clinical trials using hASCs as a medical intervention had increased to a total of 162 (www.clinicaltrials.gov; search term: "adipose* stem cell").

When considering the MSC-based therapeutic approaches, a challenge remains in choosing the best source of MSCs for a particular treatment. Even though fulfilling the ISCT criteria, MSCs from different sources have a certain amount of variation with respect to surface marker expression, differentiation potential as well as immunomodulatory properties (Murray et al., 2014). Moreover, the yield of MSCs varies a lot between different tissues but also due to the differences in isolation procedures and patient demographic characteristics, as recently reviewed (Vangsness et al., 2015).

2.2.1 Osteogenic differentiation

The commitment of MSCs to a differentiated phenotype is a complex and highly regulated process orchestrated by a myriad of environmental cues. This and the following section will give an overview of the sequence of events associated with osteogenic and adipogenic differentiation, respectively. The various induction methods used to accomplish the differentiation *in vitro* are described in detail for ASCs in section 2.3.1. The regulatory aspects of osteogenesis, on the other hand, will be covered in section 2.4.

The generation of osteoblasts from MSCs can proceed via two distinct processes: intramembranous ossification, i.e. by a direct differentiation to osteoblasts, or endochondral ossification through a cartilage intermediate step (Almubarak et al., 2016; Berendsen & Olsen, 2015). During vertebrate development, most of the bones are formed by endochondral ossification and only certain bones of the skull form via intramembranous route. In case of the TE approaches, there are indications that, especially with respect to vascularization, the endochondral approach might give a better healing outcome (Bahney et al., 2014; Harada et al., 2014; Thompson et al., 2016). However, currently the majority of the bone TE approaches rely on the direct intramembranous model-based *in vitro* osteogenic differentiation of MSCs, which is why the focus here will be on this route.

Based on the analysis of protein and gene markers, histological stainings and cell morphological changes, the osteogenic differentiation from a progenitor cell to a

mature osteocyte can be divided into three distinct periods: proliferation, matrix maturation and mineralization (Lian & Stein, 1995; Lian et al., 2012). Each period has its characteristic set of markers, as depicted in Figure 1, even though there might be slight variation in the gene expression routes leading to the same outcome (Madras et al., 2002). Furthermore, it should be kept in mind that the data concerning the sequence of events leading to mature osteocytes are derived mainly from osteoblasts (Lian & Stein, 1995) and many details of the exact order of events in MSCs still require clarification.

The proliferation stage is characterized by strong mitotic activity with increased expression of cell cycle and growth related genes, as well as the genes of several extracellular matrix (ECM) proteins (e.g. *collagen-I*, *fibronectin*) (Lian & Stein, 1995). An important transcription factor regulating the early stages of osteogenic differentiation is Runt-related transcription factor 2 (Runx2) (Long, 2011). Runx2 is indispensable for osteogenic differentiation as evidenced by the total lack of mature osteoblasts in mice with homozygous deletion of Runx2 (Komori et al., 1997; F. Otto et al., 1997). The expression of the genes of many osteogenic markers, e.g. *osteocalcin*, *ALP*, *collagen-I* and *osteopontin* is regulated by Runx2, whereas Runx2 itself is shown to synergize with many nuclear factors, including Distal-less homeobox transcription factor 5 (Dlx5), transcriptional co-activator with PDZ-binding motif (TAZ), Msh homeobox transcription factor 2 (Msx2) and activating transcription factor 4 (Atf4) (Long, 2011; Vimalraj et al., 2015). Of these factors, especially Dlx5 has been observed to have an important role in osteogenesis as an activator of *Runx2* expression (M. H. Lee et al., 2005). A key transcription factor in osteogenic differentiation is also Osterix, acting directly downstream of Runx2 (Long, 2011). In Osterix null mice no bone is formed (Nakashima et al., 2002).

The proliferative phase of osteogenic differentiation switches to matrix maturation as the collagenous ECM gradually forms and the level of alkaline phosphatase (ALP) activity transiently peaks (Lian & Stein, 1995). ALP is a membrane-bound enzyme, the activity of which has been considered to be indispensable for the onset of mineralization (Murshed & McKee, 2010). A dual role has been proposed for ALP as an initiator of mineral formation: it generates inorganic phosphate, a raw material for calcium phosphates (CaPs), by hydrolyzing various substrates, but even more importantly, it decreases the level of pyrophosphate, an inhibitor of mineralization, by degrading it (Millan, 2013). Therefore, due to the presence of inhibitory pyrophosphate, a sole increase in the phosphate concentration was not observed to be enough to support mineralization (Murshed et al., 2005). In addition to ALP activity, the formation of mature collagen-I containing ECM is also

a necessary prerequisite for the mineralization step since it serves as a platform for mineral crystal growth (Landis & Silver, 2009; Y. Wang et al., 2012). Characteristic to the last phase of osteogenesis, in addition to the CaP mineral deposition, is the increased production of proteins associated with the mineralized matrix, including osteopontin and osteocalcin (Lian & Stein, 1995). Osteopontin is expressed in low level also in the early proliferative phase, whereas osteocalcin is not found in the absence of mineralization. Both of these proteins bind to the CaP mineral and negatively regulate mineral growth (Zoch et al., 2016). Moreover, by bridging the collagen-I ECM to the mineral matrix, they have been proposed to have a role in preventing crack propagation in bone fractures (Zoch et al., 2016).
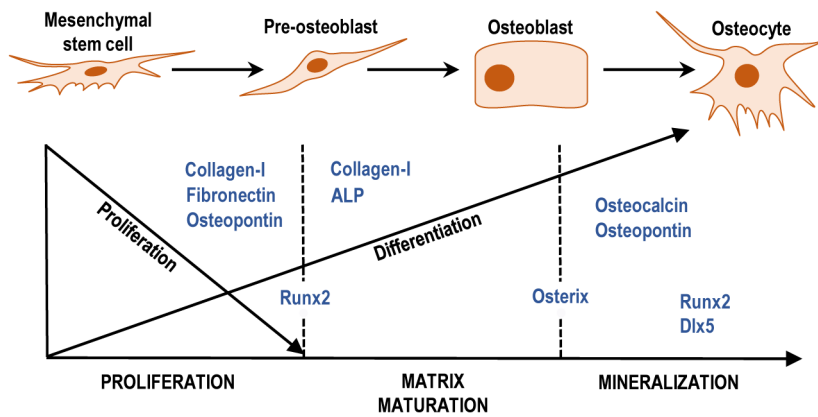
Figure 1. The process of osteogenic differentiation. The molecular events illustrated are based on osteoblast-derived data due to the lack of knowledge of the exact sequence of events in MSCs. Image modified from (Lian & Stein, 1995; Lian et al., 2012).

2.2.2 Adipogenic differentiation

Adipogenesis, schematically presented in Figure 2, is generally divided into two consecutive phases: determination of MSCs to a preadipocyte fate and terminal differentiation leading to mature adipocytes (Cristancho & Lazar, 2011; Muruganandan et al., 2009; Rosen & MacDougald, 2006). During determination, the stem cell is converted to a preadipocyte, morphologically indistinguishable from the precursor cell, but now able to differentiate only to adipocytes. Preadipocytes proliferate until they reach confluency and become then growth-arrested at the G_1/S

phase of the cell cycle (Avram et al., 2007; Tang & Lane, 2012). Growth arrest is required for the cells to proceed to the differentiation phase.

The differentiation phase can be initiated with a cocktail of inducers, typically including insulin, dexamethasone and isobutylmethylxanthin (IBMX) (Avram et al., 2007; Moseti et al., 2016; Tang & Lane, 2012). After induction, clonal preadipocytes enter the cell cycle and undergo 1-2 rounds of mitosis (mitotic clonal expansion), followed by exit from the cell cycle. However, the necessity of the mitotic clonal expansion for the terminal differentiation remains controversial since not all cell lines, including human MSCs (hMSCs), require this clonal expansion step to become mature adipocytes (Janderova et al., 2003). Regardless of the realization of the mitotic clonal expansion, hormonal induction triggers the activation of a transcription factor cascade which ultimately leads to the formation of mature adipocytes. An important factor in the early phase is cyclic AMP response element-binding protein (CREB), which is responsible for the activation of CCAAT enhancer-binding protein (C/EBP) β expression (T. C. Otto & Lane, 2005; Tang & Lane, 2012). C/EBPβ and C/EBPδ then transcriptionally activate the expression of the two master regulators of adipogenesis, peroxisome proliferator-activated transcription factor γ (PPARγ) and C/EBPα. PPARγ and C/EBPα stimulate each other's expression which is sustained in high level throughout the lifetime of an adipocyte (Moseti et al., 2016). Of these two, PPARγ has been shown to be indispensable for adipogenesis since no factor can stimulate normal adipogenesis in its absence (Rosen & MacDougald, 2006). In addition to the aforementioned, there are also multiple other factors regulating the progression of adipogenesis, including Krüppel-like factors (KLFs) and sterol response element-binding protein-1 (SREBP1), just to mention a few (Moseti et al., 2016; Rosen & MacDougald, 2006).

When reaching terminal differentiation, cells are permanently withdrawn from the cell cycle and the expression of genes associated with glucose and lipid metabolism is greatly increased, enabling the processes of lipid synthesis and transport as well as the secretion of adipocyte specific proteins (Avram et al., 2007; Moseti et al., 2016). These genes include *glucose transporter 4* (*GLUT4*), *fatty acid binding protein 4/adipocyte protein 2* (*FABP4/aP2*), *adiponectin*, *leptin* and *lipoprotein lipase* (*LPL*), several of which are directly regulated by PPARγ and/or C/EBPα. Terminal differentiation phase is also accompanied with prominent changes in cell shape (Avram et al., 2007). Stellate-shaped preadipocytes become spherical and start to accumulate lipids, which are initially in the form of small droplets, but later on fuse into one large lipid droplet filling the whole cell. Even fully differentiated

adipocytes continue to grow in size as a consequence of additional lipid accumulation.
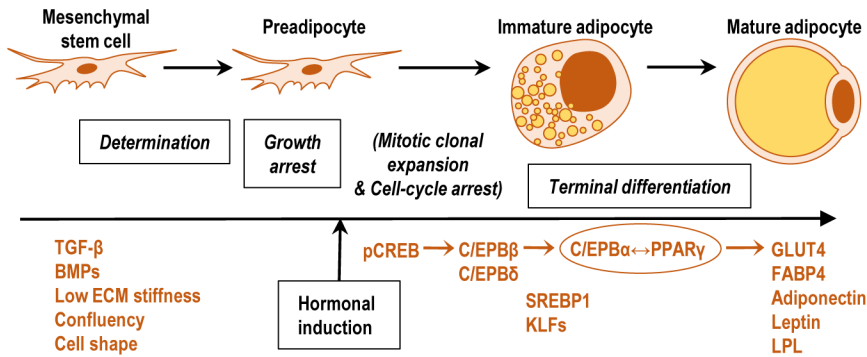
Figure 2. The process of adipogenic differentiation. Commitment of MSCs to an adipogenic lineage is driven by various external factors, including growth factors (transforming growth factor β (TGF-β), BMPs), low ECM stiffness, high cell confluency and rounded cell shape. Mitotic clonal expansion and the following cell cycle arrest are depicted in parentheses since they do not occur with all cell types (e.g. hMSCs). Image modified from (Avram et al., 2007; Cristancho & Lazar, 2011; Lefterova & Lazar, 2009; Margoni et al., 2012).

2.3   Adipose stem cells

Adipose tissue, like bone-marrow, originates from embryonic mesenchyme and contains a well-defined stroma, which led scientists to speculate whether there is a BMSC-like MSC population residing also in the adipose tissue. Indeed, on the verge of the 21st century, several studies proved the existence of such a multipotent MSC population within the adipose tissue (Halvorsen et al., 2000; Halvorsen et al., 2001; Zuk et al., 2001; Zuk et al., 2002). Like the MSCs, this newly-discovered cell population was initially identified by multiple names, such as adipose-derived stem/stromal cells (ASCs), adipose tissue-derived MSCs (AT-MSCs) and adipose tissue-derived stromal cells (ATSCs), until the International Federation of Adipose Therapeutics and Science (IFATS) recommended the use of the acronym ASC for this new adipose-derived MSC population (Daher et al., 2008). Due to the fact that adipose tissue is easily accessible in large quantities and with a minimally invasive harvesting procedure, ASCs have raised a lot of interest in the field of regenerative medicine (Baer & Geiger, 2012; Lindroos et al., 2011). Moreover, there is evidence that the yield of ASCs from a specified volume of tissue is considerably higher than

that of BMSCs (4.7×10^3-1.5×10^6 ASCs/ml for adipose tissue and 30-3.2×10^5 BMSCs/ml for bone-marrow) (Vangsness et al., 2015), further supporting the use of adipose tissue as an alternative MSC source for research and therapeutic purposes.

Adipose tissue is composed of lipid-laden adipocytes and a heterogeneous cell population surrounding and supporting them (Lindroos et al., 2011). Upon isolation, this supporting cell population is called stromal vascular fraction (SVF) and it includes several distinct cell types, such as ASCs, endothelial cells, vascular smooth muscle cells and hematopoietic cells. Already in 1964, Martin Rodbell, while developing a method for isolation of mature adipocytes and adipogenic progenitor cells, described a procedure for SVF separation from adipose tissue (Rodbell, 1964). Briefly, the tissue was minced into small fragments, enzymatically digested and centrifuged, which resulted in a floating supernatant of adipocytes and a pellet containing the SVF components. Later on, Zuk and coworkers demonstrated that ASCs can be selected from the SVF based on their plastic adherence (Zuk et al., 2001; Zuk et al., 2002). The SVF and ASC isolation methods developed by Rodbell and Zuk and co-workers are still the basis of most of the current methods used to isolate ASCs from adipose tissue.

In order for the ASCs to retain the multilineage differentiation capacity but still be able to proliferate without spontaneous differentiation, optimal culturing conditions are needed. Typically, the culture medium is based on either alpha modified Eagle's medium (α-MEM), Dulbecco's Modified Eagle Medium (DMEM) or DMEM/Ham's Nutrient Mixture F-12 (DMEM/F-12) and contains 1% antibiotics (e.g. penicillin and streptomycin), 1% L-glutamine and 10% fetal bovine serum (FBS)/fetal calf serum (FCS) (Haimi et al., 2009a; Halvorsen et al., 2001; Mitchell et al., 2006; Zuk et al., 2001; Zuk et al., 2002). FBS or FCS are typically used because they contain high levels of factors stimulating cell growth and adhesion (Mannello & Tonti, 2007). However, when considering the clinical applications of ASCs, the animal origin of FBS and FCS poses severe risks of immune rejection and infections, which has led to the increased use of human serum (HS) as a xeno-free alternative to FBS/FCS (Bieback et al., 2009; Lindroos et al., 2010; Tirkkonen et al., 2011; Waselau et al., 2012). In addition to HS, other human-derived alternatives to FBS/FCS include platelet lysate and platelet-rich plasma, each of which have induced increased proliferation and osteogenic differentiation but decreased adipogenesis when compared to the traditional FBS (Amable et al., 2014; Castegnaro et al., 2011; Escobar & Chaparro, 2016).

When considering the clinical use of ASCs, there are several factors (e.g. donor age, gender, body mass index (BMI) and adipose tissue harvest site) which affect the

ASC characteristics and therefore need to be taken into account when evaluating the therapeutic potential of ASCs. For example, several reports have shown that the proliferation and osteogenic differentiation of human hASCs decrease with age (Alt et al., 2012; Choudhery et al., 2014; de Girolamo et al., 2009; Kornicka et al., 2015). However, with respect to the correlation of donor age and adipogenesis, contradictory data exist (Alt et al., 2012; Choudhery et al., 2014; de Girolamo et al., 2009; Kornicka et al., 2015; H. J. Yang et al., 2014). When considering the gender, Aksu and co-workers demonstrated that male hASCs differentiate towards bone more efficiently than female hASCs (Aksu et al., 2008), whereas Yang et al. did not find any gender-related differences in adipogenic or osteogenic differentiation of hASCs (H. J. Yang et al., 2014). No consensus exists about the role of donor BMI. Whereas Yang and co-workers demonstrated that adipogenesis and osteogenesis are enhanced for hASCs from obese donors (BMI>30) (H. J. Yang et al., 2014), two other studies reported a decreasing effect of obesity on hASC osteogenesis (Frazier et al., 2013; Strong et al., 2016). With respect to the effect of adipose tissue harvest site on hASC characteristics, there seems to be agreement that the hASCs from subcutaneous depots have better differentiation potential when compared to the hASCs from deeper depots such as omentum (Aksu et al., 2008; Shah et al., 2014; Toyoda et al., 2009).

2.3.1 Characterization of adipose stem cells

Initially, ASCs were considered MSCs when they fulfilled the minimal criteria defined by ISCT (Dominici et al., 2006) (described in detail in section 2.2). However, in 2013 ISCT and IFATS created a joint statement, which provided literature-based phenotypic and functional criteria for the characterization of both SVF and ASCs (Bourin et al., 2013). The goal of the statement was to create "living" guidelines, which will be modified in response to new data, and which will promote the best clinical practices and safety aspects in the ASC-based cell therapies.

Immunophenotype
According to the joint statement of ISCT and IFATS, ASCs should be selected from the SVF by plastic adhesion and they should exhibit a certain pattern of surface marker expression as determined by multi-color flow cytometric analysis (Bourin et al., 2013). Similar to the MSC criteria, ASCs should have a positive expression (>90%) for CD73 and CD90. CD105, on the other hand, is recommended to be replaced by CD13, which has a higher and more stable expression and commercial

antibodies targeted to it exhibit higher specificity and signal intensity when compared to the antibodies targeted to CD105. The expression of hematopoietic markers CD11b and CD45 should be negative (<2%) in ASCs. In order to distinguish ASCs from BMSCs, the analysis of CD36 and CD106 expression is suggested, since ASCs, unlike BMSCs, are positive for CD36 but do not express CD106 (De Ugarte et al., 2003; Pachon-Pena et al., 2011; Varma et al., 2007). To further strengthen the characterization of ASCs, additional positive markers (e.g. CD10, CD26, CD49d, CD49e and CD146) and negative markers (e.g. CD3, CD11b and CD49f) may be used. All in all, it is recommended that at least two positive and two negative surface markers should be used in the same analysis in order to adequately identify the ASCs. However, due to the inherent heterogeneity of the ASC populations, it is likely that, even though the expressions of the defined surface markers would meet the suggested criteria, additional surface markers show variable expression patterns. For example, it has been observed that the expression of CD34, typically not detected in BMSCs, is high in the early phase of ASC culture but then declines with continued cell divisions and passaging (Maumus et al., 2011; Mitchell et al., 2006; Patrikoski et al., 2013; Varma et al., 2007). Finally, the studies setting the basis for the characterization criteria are for the most part conducted in the traditional FBS medium. However, there is evidence that the serum condition has an effect on certain surface markers, including CD34, CD45, CD105 and CD54 (Patrikoski et al., 2013; Rajala et al., 2010), pointing out a need for a further clarification of this issue.

Due to the high variation in the surface marker expression, a novel epigenetics-based MSC classification method was recently developed by de Almeida and co-workers (de Almeida et al., 2016). With this method, MSCs could be efficiently distinguished from fibroblasts based on only two differentially methylated CpG sites. Moreover, with another two CpG sites a distinction could be also made between BMSCs and ASCs, suggesting that epigenetic evaluation might be a promising tool to characterize MSCs.

Differentiation potential

Similar to MSCs from other sources, ASCs can differentiate to mesodermal lineages, such as osteoblasts, adipocytes, chondrocytes, myoblasts, endothelial cells and tenocytes (Bekhite et al., 2014; Halvorsen et al., 2001; Vuornos et al., 2016; Zuk et al., 2002), but there are also reports indicating their ability to give rise to cells of endodermal and ectodermal origin, such as hepatocytes (Han et al., 2015; X. Li et al., 2014) and neuronal cells (Gao et al., 2014; Jang et al., 2010). However, despite

this wide differentiation capacity, the trilineage differentiation potential, i.e. osteogenic, adipogenic and chondrogenic differentiation, is enough to verify the multipotency of ASCs, as stated by ISCT and IFATS (Bourin et al., 2013). Therefore, this section will concentrate on the induction and analysis of these three differentiation routes, the main focus being in the osteogenic differentiation.

The osteogenic differentiation of ASCs is typically induced by culture medium supplemented with ascorbic acid, β-glycerophosphate, dexamethasone and/or 1.25 vitamin D_3 (Gimble & Guilak, 2003; Gupta et al., 2007; Halvorsen et al., 2001; Zuk et al., 2002). However, in the literature there has been no consensus regarding the specific concentrations of these substances. Tirkkonen and co-workers conducted a comparison of compositionally different osteogenic media and observed that the osteogenic differentiation of ASCs is optimal with 250 μM L-ascorbic acid 2-phosphate (a more stable analogue of ascorbic acid), 10 mM β-glycerophosphate and 5 nM dexamethasone (Kyllönen et al., 2013). Each of these components has a specific role in supporting the osteogenic commitment (Langenbach & Handschel, 2013; Vater et al., 2011). Ascorbic acid is an important co-factor of an enzyme hydroxylating proline and lysine in pro-collagen, and in the absence of ascorbic acid no properly formed collagen-I is produced or secreted (Langenbach & Handschel, 2013). In addition to promoting osteogenesis, ascorbic acid has been also shown to increase MSC proliferation (Fernandes et al., 2010). β-glycerophosphate, enzymatically degraded by ALP, serves as a crucial source of inorganic phosphate to initiate the CaP mineral formation (Fratzl-Zelman et al., 1998; Vater et al., 2011). The osteogenic function of dexamethasone, a synthetic glucocorticoid, is not fully elucidated but it has been shown to regulate Runx2 in both transcriptional and functional level, via multistep intracellular signaling cascades (Hamidouche et al., 2008; Hong et al., 2009; Phillips et al., 2006).

In addition to the aforementioned chemical substances, osteogenic differentiation of ASCs can be also stimulated via growth factors, such as BMP-2 (Panetta et al., 2010; Song et al., 2011) and vascular endothelial growth factor (VEGF) (Behr et al., 2011; C. J. Li et al., 2015). The signaling mechanism and cellular responses to BMP-2 are discussed in detail in section 2.4.1. Also certain biomaterials, such as BaGs (see section 2.5.2) and β-tricalcium phosphate (β-TCP), can induce osteogenic differentiation of ASCs even without any added chemical supplements (Haimi et al., 2009b; Marino et al., 2010; Waselau et al., 2012). Furthermore, an additional regulatory level to the osteogenic induction is brought by micro RNAs (miRNAs) (Lian et al., 2012). While certain miRNAs act as osteogenesis enhancers (S. Huang et al., 2012; Liao et al., 2014; Xie et al., 2016; W. B. Zhang et al., 2014), others

clearly inhibit it (H. Li et al., 2013). Finally, osteogenic differentiation of ASCs can be also enhanced by various mechanical stimuli, such as vibration loading (Pre et al., 2011; Tirkkonen et al., 2011), stretching (X. Yang et al., 2010) and fluid shear stress (Knippenberg et al., 2005).

Adipogenic induction of ASCs is typically accomplished with dexamethasone, IBMX, insulin, indomethacin, pantothenate and biotin (Halvorsen et al., 2001; Lindroos et al., 2009; Mitchell et al., 2006; Zuk et al., 2002). Dexamethasone stimulates adipogenesis in high concentrations (100nM-1000nM) whereas in lower concentrations (≤100 nM) it is required for the osteogenesis-inducing cocktail (Scott et al., 2011). IBMX, a cAMP-elevating agent, is used to amplify the effect of glucocorticoids, such as dexamethasone (Vater et al., 2011). Via elevation of cAMP levels and protein kinase A (PKA) activation, IBMX stimulates the expression of PPARγ, C/EBPβ and C/EBPδ (S. P. Kim et al., 2010; Scott et al., 2011). Also insulin, a peptide hormone produced in the pancreas, has an increasing effect on the PPARγ expression and protein production, but this is achieved via Akt-TSC2-mTORC1 pathway (H. H. Zhang et al., 2009). Moreover, the insulin effect can be further enhanced by insulin sensitizing chemical agents, like rosiglitazone and troglitazone (Scott et al., 2011; Vater et al., 2011). Indomethacin is a non-steroidal anti-inflammatory drug which directly binds to PPARγ and thus activates it (Lehmann et al., 1997). Furthermore, as with the osteogenic induction, the adipogenesis of ASCs can be also enhanced with several growth factors, such as fibroblast growth factor-2 (FGF-2) (Kakudo et al., 2007). Finally, in addition to the chemical induction, it has been observed that high plating density is required for the adipogenic differentiation of MSCs (McBeath et al., 2004).

Effective chondrogenesis of ASCs requires a 3D culture system, such as micro-mass, pellet or scaffold-based culture, which increases the cell-cell interactions and thus mimics the precartilage condensation occurring in the embryonic development (Estes et al., 2010; Stromps et al., 2014; Vater et al., 2011; Wei et al., 2007). In addition, chemical induction of ASC chondrogenesis, typically conducted with serum-free or low-serum (1%) medium supplemented with slightly varying combinations of insulin, L-ascorbic-acid 2-phosphate, TGF-β, sodium pyruvate, L-proline, BMP-6, insulin-like growth factor-1 (IGF-1), transferrin, sodium selenite, albumin and linoleic acid, is needed (Diekman et al., 2010; Estes et al., 2010; Lindroos et al., 2009; Patrikoski et al., 2013; Q. Zhou et al., 2016; Zuk et al., 2002). Also additional growth factors, such as fibroblast growth factor-2 (FGF-2), BMP-4 and BMP-2, have been shown to stimulate ASC chondrogenesis (Chiou et al., 2006; Shi et al., 2013; Wei et al., 2007). Moreover, there is evidence that hypoxic

conditions (1-5% oxygen), mimicking the *in vivo* niche of chondrocytes, favor ASC chondrogenesis (Merceron et al., 2010; Weijers et al., 2011). Chondrogenic differentiation is characterized by the formation of highly organized cell-surrounding ECM consisting of collagens (mainly collagen II), proteoglycans (e.g. aggrecan) and glycosaminoglycans (e.g. chondroitin sulfate and keratin sulfate) (Estes et al., 2010; Vater et al., 2011). At the transcriptional level, SRY-related high-mobility group box 9 (Sox9) transcription factor is one of the major regulators of the initiation of chondrogenesis (Vater et al., 2011).

In order to analyze the differentiation outcome, ISCT and IFATS recommend that, in addition to qualitative staining methods, quantitative analyzing tools, e.g. quantitative real-time reverse transcription polymerase chain reaction (qRT-PCR), Western blot and enzyme-linked immunosorbent assay (ELISA), should be used (Bourin et al., 2013). Table 1 lists the specific histological stainings as well as biomarkers suggested by ISCT and IFATS to verify the osteogenic, adipogenic and chondrogenic differentiation of ASCs.

Table 1. Characterization of ASC multipotency. Histological stainings and biomarkers suggested by ISCT and IFATS to determine adipogenic, osteogenic and chondrogenic differentiation of ASCs. Modified from (Bourin et al., 2013). BSP=bone sialoprotein

Osteogenic differentiation	Adipogenic differentiation	Chondrogenic differentiation
Histological staining: Alizarin red S, von Kossa	Histological staining: Oil red O, Nile red	Histological staining: Alcian blue, Safranin O
Biomarkers: ALP, BSP, osteocalcin, osterix, Runx2	Biomarkers: adiponectin, leptin, PPARγ, FABP4/aP2, C/EBPα	Biomarkers: aggrecan, collagen II, Sox9

2.4   Molecular mechanisms regulating osteogenic differentiation

Osteogenic differentiation consists of a strictly orchestrated sequence of events leading to the mature osteoblastic phenotype, as discussed in section 2.2.1. Execution of such an elaborate process requires the proper function of a vast amount of complex and interconnected intracellular signaling pathways activated in response to various extracellular stimuli. This section will give an overview of the osteogenesis-regulating signaling cascades. Due to the relatively small amount of studies evaluating these signaling mechanisms, the discussion here is not strictly limited to MSCs. Instead, also studies conducted with various osteoblastic cell lines will be referred to.

However, the use of different cell types, along with the non-standardized culture conditions and cells originated from different animals, might explain some contradictions in the literature with respect to many of the signaling pathways reviewed in this section.

2.4.1 Bone morphogenetic protein signaling

Even though the existence of bone formation inducing agents in the bone matrix was reported already in 1965 in the pioneering work of Dr. Urist (Urist, 1965), the identification of these factors took place only in the late 1980s when the purification and sequencing of BMP-3, as well as the cloning of human BMP-1, BMP-2 and BMP-3, were successfully accomplished (Luyten et al., 1989; Wozney et al., 1988). Since then, around 20 BMP family members have been identified with varying roles in the development of bone, but also other tissues, such as kidney, muscle, brain and intestine (Modica & Wolfrum, 2013; Nohe et al., 2004). BMPs belong to the TGF-β superfamily and rely on their signals via type I and type II transmembrane serine/threonine kinase receptors (Sanchez-Duffhues et al., 2015). In humans seven type I and five type II receptors have been found, of which type I receptors BMP receptor IA (BMPR-IA, also known as ALK-3), BMPR-IB (ALK-6), ALK-1 and ALK-2, and type II receptors activin receptor type IIa (ActR-IIa), ActR-IIb and BMPR-II work in conjunction with BMPs. The signaling cascade is initiated when the homodimeric BMP ligand binds to the receptor complex, leading to an increase in the hetero-oligomerization of the two receptor types and, intracellularly, to the induction of phosphorylation and activation of type I receptor by type II. Once activated, the type I receptor phosphorylates a receptor-activated mothers against decapentaplegic homolog protein (R-Smad), which is now able to form a complex with a common partner Smad (co-Smad) and translocate to the nucleus to regulate the gene expression of various target genes (e.g. *Runx2*, *Osterix*), in association with several transcription co-activators and repressors, such as Runx2. In fact, there is evidence that formation of a Smad-Runx2 complex is indispensable for BMP-2-induced osteogenesis (Javed et al., 2009).

In addition to the canonical BMP-Smad signaling scheme, also Smad-independent non-canonical signaling routes, generally involving the mitogen-activated protein kinases (MAPKs) p38, extracellular signal-regulated kinase (ERK) and c-Jun N-terminal kinase (JNK), but also other factors such as phosphatidylinositol 3-kinase (PI3K), have been observed to be activated in response to BMP stimulus (Ghosh-Choudhury et al., 2013; Ryoo et al., 2006). However, the

activation mechanisms of these routes are far less understood than those of the canonical signaling. The most studied of the non-canonical pathways is TAK1-p38 route which has been shown to be activated when BMP-2 binds first to type I receptor leading to the recruitment of type II receptor, whereas BMP-2 binding to preformed receptor complex was shown to activate the canonical Smad pathway (Nohe et al., 2002). Moreover, especially with respect to BMP-ERK non-canonical pathway, a lot of contradicting results exist. While others state that ERK is indispensable for BMP-2-induced bone formation in mouse myoblast cell line C2C12, mouse multipotent mesenchymal cell line C3H10T1/2 and human osteoblast cells (Gallea et al., 2001; Lai & Cheng, 2002; Lou et al., 2000), other studies suggest that ERK is a negative regulator of BMP-2 and BMP-4-induced osteogenesis in C2C12 cells, MC3T3-E1 mouse osteoblastic cells and skeletal-muscle-derived stem cells (Higuchi et al., 2002; Kozawa et al., 2002; Payne et al., 2010). The negative effect of ERK on the BMP-signaling is likely related to its ability to phosphorylate Smad to a linker region, thus causing the Smad specific E3 ubiquitin protein ligase 1 (Smurf1)-dependent degradation of Smad1 (Sapkota et al., 2007).

The Smad proteins are typically divided to three subclasses: R-Smads (Smad1/2/3/5/8), co-Smad (Smad4) and inhibitory Smads (I-Smads; Smad6/7) (Miyazono et al., 2010; Nohe et al., 2004). Of the R-Smads Smad1/5/8 operate in the BMP signaling pathway and Smad2/3 in TGF-β route, whereas the co-Smad Smad4 is shared between the different pathways. I-Smads, on the other hand, represent an important level of BMP signaling regulation by down-regulating the BMP signaling responses. In addition to I-Smads, the BMP signaling is highly regulated by various other means, e.g. with extracellular BMP antagonists (e.g. noggin), intracellular Smurf-dependent degradation mechanisms and miRNAs (Derynck & Zhang, 2003; Fan et al., 2013; H. Li et al., 2013; Luzi et al., 2008; Sanchez-Duffhues et al., 2015). The antagonizing role of noggin, however, is still slightly controversial since in hBMSC noggin suppression was observed to decrease BMP-2-induced osteogenic differentiation, suggesting that noggin is a osteogenesis-stimulatory agent (C. Chen et al., 2012), whereas in mouse and human ASCs the knock-down of noggin had a stimulatory effect on osteogenesis (Fan et al., 2013; Fan et al., 2016; Ramasubramanian et al., 2011). Interestingly, also cell shape seems to be an important factor in BMP-signaling since the restriction of cell spreading, cytoskeletal tension or RhoA/Rho-associated protein kinase (ROCK) signaling prevented BMP-2-induced canonical signaling and osteogenesis of hMSCs (Y. K. Wang et al., 2012). Lastly, there is extensive and complex cross-talk between BMP-

signaling and several other signaling cascades, which naturally has a profound effect on the cell behavioral outcome in response to BMP stimulus. Some examples of the cross-talk are presented in the following sections. The BMP signaling scheme is schematically presented in Figure 3.

Of the different BMPs, the strongest osteogenic capacity has been associated with BMP-2, BMP-4, BMP-6, BMP-7 and BMP-9, out of which BMP-2 is probably the most studied inducer of bone formation both *in vitro* and *in vivo* (Bragdon et al., 2011; G. Chen et al., 2012; Kang et al., 2009; Ryoo et al., 2006). The strong osteogenic potential of BMPs has been also evidenced by the Food and Drug Administration (FDA) approval of recombinant human BMP-2 (rhBMP-2) and rhBMP-7 for the clinical treatment of acute tibial fracture, long bone non-unions, lumbar spinal fusions, and in case of rhBMP-2, certain oral and maxillofacial indications (Argintar et al., 2011). In addition, rhBMP-2 has been also used to augment the bone formation in clinical bone TE applications (Mesimäki et al., 2009; Sandor et al., 2014; Taylor, 2010). However, the increased clinical use of BMPs, typically applied in considerably high doses to achieve the desired healing outcome, has been accompanied with an increased amount of adverse side-effects, including ectopic bone formation, osteoclast-mediated bone resorption, inappropriate adipogenesis, inflammation, swelling and urogenital complications (James et al., 2016). This has prompted the scientific community to evaluate BMPs in a more critical fashion and to develop novel techniques to utilize the bone formation capacity of BMPs more safely and efficiently.

In *in vitro* cell culture rhBMP-2 is typically used in concentrations ranging from 10 ng/ml to 1000 ng/ml, but the optimal effect on osteogenesis is generally achieved with approximately 100 ng/ml of rhBMP-2 in osteogenic medium (OM) (Mehrkens et al., 2012; Panetta et al., 2010; Park et al., 2012; Shiraishi et al., 2012; Song et al., 2011; X. Zhang et al., 2014). Apart from the studies of Mehrkens et al. and Shiraishi et al., who showed that high concentrations (300 and 500 ng/ml) of rhBMP-2 can induce osteogenesis of SVF cells and hASCs without OM (Mehrkens et al., 2012; Shiraishi et al., 2012), the osteogenesis-inducing effect of rhBMP-2 is typically achieved in OM conditions (Panetta et al., 2010; Park et al., 2012; Song et al., 2011; X. Zhang et al., 2014). The requirement of OM might be explained by the crucial role of the BMP pathway also in the adipogenic differentiation (Modica & Wolfrum, 2013). For example, BMP-2, in addition to its osteogenesis-inducing effect, has been shown to stimulate the adipogenesis of C3H10T1/2 cells and human alveolar bone-derived stromal cells both *in vitro* and *in vivo* (Hata et al., 2003; H. Huang et al., 2009; Park et al., 2012). Similar to osteogenesis, the BMP-signaling mechanism in

adipogenesis is thought to involve both the canonical Smad pathway and non-canonical routes, such as the p38 pathway, but instead of Runx2, they lead to the activation and up-regulation of PPARγ (Hata et al., 2003; Modica & Wolfrum, 2013).

Since the major cause of BMP-related adverse effects in the clinics has been thought to be caused by high and transient dosages (James et al., 2016), there has been an attempt to develop sustained and local delivery systems, and alternative BMP delivery methods to circumvent this problem. For example, incorporation of BMP-2 to different biomaterial scaffolds has resulted in a release profile with beneficial effects on bone formation *in vitro* and *in vivo* (Chou et al., 2011; C. Li et al., 2006; Talley et al., 2016; Yi et al., 2016). Moreover, the need for exogenous BMP-2 protein has been able to circumvent by means of gene technology, e.g. by delivering *BMP-2* gene to the stem cells (Y. Liu et al., 2012; Ramasubramanian et al., 2011). Recently, Balmayor and co-workers introduced stable chemically modified BMP-2 mRNA to rat BMSCs and ASCs, leading to increased osteogenesis both *in vitro* and *in vivo* (Balmayor et al., 2016). BMP-2-signaling utilizing osteogenesis of mouse ASCs has been also accomplished completely without BMP-2 protein/gene/mRNA supplementation, by combined action of noggin suppression and administration of phenamil, a positive regulator of BMP signaling (Fan et al., 2016).

Finally, despite the vast amount of literature demonstrating the efficacy of BMPs in bone formation, there are also contradictory studies reporting no effect or even a negative effect for BMP-2 treatment on stem cell osteogenesis (Chou et al., 2011; Cruz et al., 2012; Tirkkonen et al., 2013; Waselau et al., 2012; Yi et al., 2016; Zuk et al., 2011). In *in vitro* cell culture, two studies reported no enhancement in the osteogenic differentiation of hASCs in OM supplemented with rhBMP-2 (Cruz et al., 2012; Zuk et al., 2011). Moreover, in the study of Zuk and co-workers, rhBMP-2 failed to induce the Smad1/5/8 signaling in hASCs even though the signaling was functional in C3H10T1/2 cells stimulated with the same growth factor (Zuk et al., 2011). Furthermore, the osteogenic differentiation of hASCs cultured on different bioceramics in OM was observed to decrease in response to rhBMP-2 or rhBMP-7 stimulation (Tirkkonen et al., 2013; Waselau et al., 2012). With respect to the *in vivo* bone TE, it has been demonstrated that the presence of cells, either transduced with *BMP-2* gene or not, does not improve the performance of rhBMP-2-incorporated scaffolds in the treatment of rat calvarial or femoral defects (Chou et al., 2011; Yi et al., 2016). However, without the cells the incorporation of rhBMP-2 into the scaffolds was observed to be beneficial for the healing.
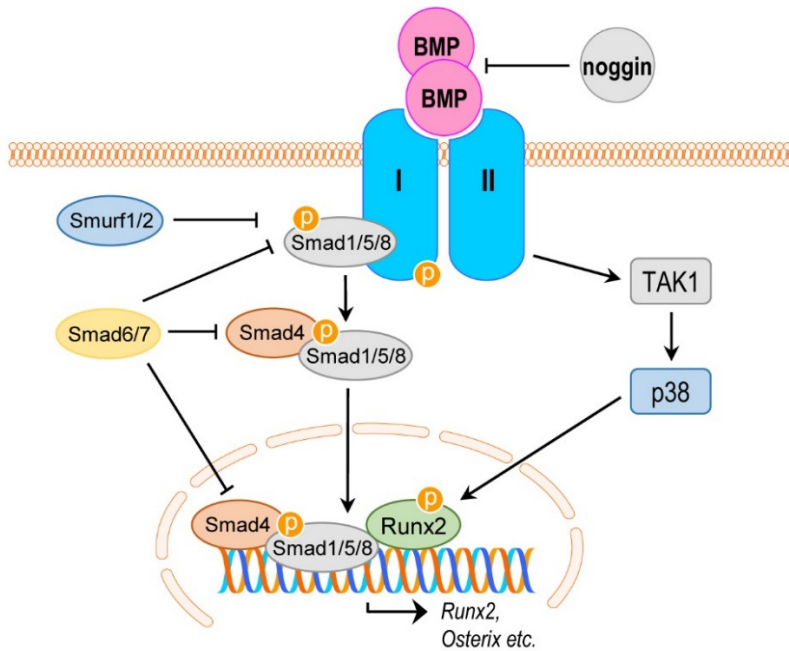
Figure 3. BMP signaling pathways. Canonical Smad-dependent pathway and non-canonical TAK1-p38 pathway are presented. In the regulation of osteogenic differentiation, both of these pathways converge to Runx2. In addition to the TAK1-p38 route also other, less-well understood, non-canonical BMP signaling pathways have been suggested (including ERK, JNK and PI3K-mediated signaling). I-Smads (Smad6/7) form non-functional complexes with Smad4, thus inhibiting BMP signaling. They also prevent the activation of R-Smads (Smad1/5/8) by type I receptors and the formation of a functional Smad/DNA complex. Smurf1/2 interact with R-Smads and BMP receptors and target them for degradation. Smurf1/2 also induce nuclear export of I-Smads and facilitate their interaction with type I receptors. For simplicity, BMPs, BMP receptors and Smad4-Smad1/5/8 are represented as dimers even though in reality they form oligomeric complexes. Image modified from (G. Chen et al., 2012; Modica & Wolfrum, 2013).

2.4.2   Integrin-focal adhesion kinase signaling

Anchorage-dependent cells, such as MSCs, attach to the growth surface via transmembrane proteins called integrins, which are composed of two noncovalently bound glycoprotein units, the α chain and the β chain (Danen & Sonnenberg, 2003; Giancotti & Ruoslahti, 1999; R. O. Hynes, 2002). In humans, 24 different functional integrins, consisting of various combinations of 18 α and eight β subunits, have been identified, each with its own binding specificity (Danen & Sonnenberg, 2003; R. O. Hynes, 2002). Integrins, clustered in the plane of the cell membrane into large aggregates, form the core of focal adhesions (FAs), specialized cell membrane regions responsible for the cell adhesion and connection of the ECM to

the cytoskeleton (Burridge & Chrzanowska-Wodnicka, 1996; Petit & Thiery, 2000). As part of the dynamic FA structures, integrins have to withstand high attachment-related forces, but in addition to this, they have a major role in conveying signals in both directions (Danen & Sonnenberg, 2003; Giancotti & Ruoslahti, 1999). Achieved via large conformational changes in the integrin subunits, the ECM binding ability can be regulated from inside of the cell (inside-out signaling) whereas the binding-related forces can be transmitted to the interior of the cells (outside-in signaling) and then translated into biochemical signals, a process called mechanotransduction. However, since integrins lack enzymatic activity, the biochemical translation relies primarily on non-receptor tyrosine kinases (nRTKs) which associate with the integrin cytoplasmic tails. The most notable of these nRTKs is focal adhesion kinase (FAK), which binds several FA proteins, such as integrin β chains, talin and paxillin, and gets activated presumably via integrin-induced conformational change (Schaller, 2001; Schlaepfer et al., 1999; Tomakidi et al., 2014). Subsequent autophosphorylation of tyrosine residue 397 creates a docking site for Src, which phosphorylates other tyrosines and thus fully activates FAK. Once activated, FAK can directly activate other key signaling proteins, such as PI3K, growth factor receptor binding protein 2 (Grb2), Shc and p130[Cas], and downstream of these a broad spectrum of other factors including Ras, Rac, ERK, JNK and Akt, just to mention a few. Of note, there is evidence that in certain cases FAK activation can be increased also integrin-independently, e.g. via signals through G-protein linked receptors and transmembrane growth factor receptors (Schlaepfer et al., 1999). Figure 4 presents a simplified illustration of the signaling cascades mediated by integrin-FAK complex upon cell attachment.

Apart from its role in various cellular processes, such as migration, proliferation, cell survival and differentiation, integrin-mediated signaling has been shown to regulate also osteogenesis on various biomaterials (Biggs & Dalby, 2010). For example, it has been observed that natural ECM simulating collagen-I, collagen-II and laminin surfaces support osteogenic differentiation of MSCs and osteoblastic cells via integrinα2β1-FAK-ERK/JNK signaling route (Chiu et al., 2014; Shih et al., 2011; Takeuchi et al., 1997; Viale-Bouroncle et al., 2014b). However, in contrast to this, Tsai and co-workers reported that collagen-I-induced osteogenesis of hMSCs was not dependent on adhesion via integrinα2β1, and no FAK activation was detected even though ERK and Akt got activated (Tsai et al., 2010). Klees and co-workers, on the other hand, demonstrated that, instead of integrinα2β1, the osteogenesis of hBMSCs on laminin-5 occurs via integrinα3β1-stimulated ERK-Runx2 signaling (Klees et al., 2005). In general, Runx2 seems to be a key mediator

in attachment-stimulated osteogenesis since many studies identify it as a target of the integrin-FAK-ERK pathway (Klees et al., 2005; Lu & Zreiqat, 2010; Lu et al., 2012; Salasznyk et al., 2007a; Salasznyk et al., 2007b).

In addition to the ECM proteins, cell attachment-mediated signaling events have been also studied on ceramic biomaterials and polymer-ceramic composites (Au et al., 2010; G. H. Kim et al., 2015; Lu & Zreiqat, 2010; Lu et al., 2012; Marino et al., 2010; Shie & Ding, 2013; Woo et al., 2007; J. Zhang et al., 2015). The majority of these studies, however, evaluated only the gene expression or the activation status of the various signaling factors, but did not determine the role of these proteins in the osteogenic differentiation (Au et al., 2010; G. H. Kim et al., 2015; Marino et al., 2010; Woo et al., 2007; J. Zhang et al., 2015). Still, Lu and coworkers were able to demonstrate that, similar to the ECM-based biomaterials, integrinα2β1-ERK-Runx2 pathway mediates the osteogenesis stimulated by β-TCP and 3D biphasic calcium phosphate (BCP)-polycaprolactone (PCL)-hydroxyapatite (HA) composite (Lu & Zreiqat, 2010; Lu et al., 2012).

Interestingly, in addition to the cell attachment-related osteogenesis, it has been suggested that FAK is also required for the BMP-2-initiated bone formation in MC3T3-E1 cells (Tamura et al., 2001). Specifically, Tamura and co-workers observed that the inhibition of FAK hinders the transcriptional activity of Smad1. In addition to this, two other studies reported the inhibition of BMP-2 signaling when the binding of integrinα2β1 to collagen-I was disrupted (Jikko et al., 1999; Suzawa et al., 2002). In the study of Suzawa and co-workers, the transcriptional activity of Smad1 was augmented by direct phosphorylation by ERK, which could work as a direct link between BMP-2 and integrin signaling pathways (Suzawa et al., 2002). Moreover, Bilem and co-workers recently demonstrated that immobilization of integrin-binding RGD peptide and BMP-2 peptide on the hBMSC growth substrate synergistically enhanced the osteogenesis of these cells even in the absence of OM (Bilem et al., 2016). Therefore, it seems that there is a strong cross-talk between the BMP-2 signaling pathway and the integrin-mediated signaling in the regulation of osteogenic differentiation.
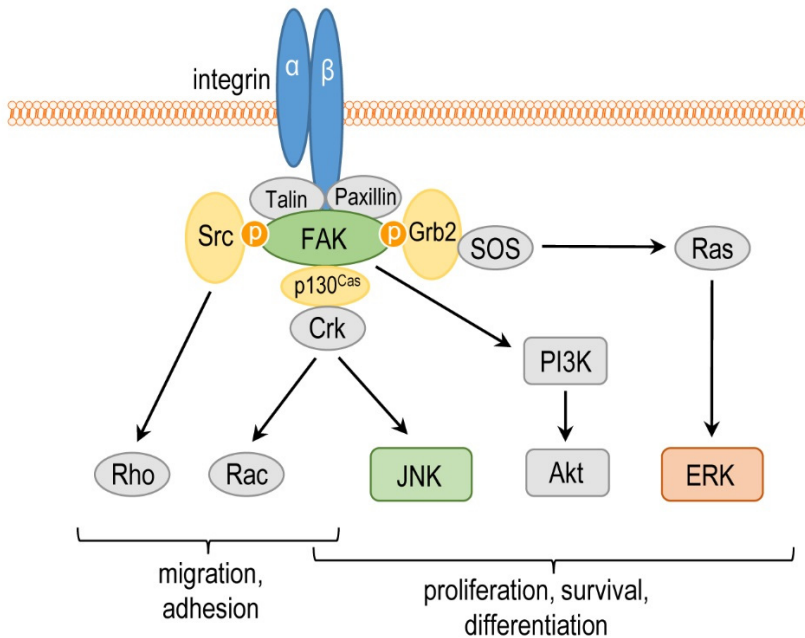
Figure 4. Integrin-FAK signaling. The image is a simplified representation of the numerous signaling cascades initiated by integrin-FAK complex upon cell attachment. Once activated, the kinases JNK, Akt and ERK phosphorylate both nuclear and cytosolic substrates which ultimately leads to changes in cellular behavior, including osteogenic differentiation. p indicates phosphorylation. Image modified from (Giancotti & Ruoslahti, 1999; Millard et al., 2011).

2.4.3   Mitogen-activated protein kinases

MAPK cascades, highly abundant and conserved in all eukaryotic cells, consist of three protein kinases acting in series: MAPK kinase kinase (MAPKKK), MAPK kinase (MAPKK) and, as the final member, MAPK (Pearson et al., 2001; Roux & Blenis, 2004; Rubinfeld & Seger, 2005). The MAPK cascades propagate the signal by phosphorylations and work in a highly sophisticated manner by receiving and coordinating inputs from a large amount of signaling pathways. Of the MAPKs, ERK, JNK and p38 form the three most essential and the best studied groups, each of which is discussed below.

ERK
The family of ERK consists of two MAPKs, ERK1 and ERK2, both of which are ubiquitously expressed and thought to be functionally redundant (Cobb, 1999; Roux & Blenis, 2004; Rubinfeld & Seger, 2005). Although generally considered to be

activated mainly via mitogen stimuli (e.g. growth factors) and to regulate proliferative cell responses, there is also an increasing amount of data indicating a major role for ERK in the regulation of osteoblast functions and osteogenesis of progenitor cells (Greenblatt et al., 2013). ERK is essential for osteoblast mineralization, since mice with a germline deletion of *Erk1* and a conditioned deletion of *Erk2* in limb mesenchyme, show greatly reduced bone mineralization and correspondingly increased ectopic chondrogenesis (Matsushita et al., 2009). In the molecular level, ERK can directly phosphorylate and activate Runx2 (Ge et al., 2009; Xiao et al., 2000) which is probably the best-known osteogenesis-regulating mechanism of ERK, although ERK can also activate other factors contributing to osteogenesis, such as Smad1 and ATF4 (Greenblatt et al., 2013; Suzawa et al., 2002). Moreover, it was recently shown that the proper function of both ERK and p38 is required for the interaction of Runx2 and Osterix, leading to co-operative induction of several osteogenesis-related genes (Artigas et al., 2014).

In addition to the important role for ERK in the cell-attachment mediated osteogenesis discussed in the previous section, several studies have also demonstrated that ERK is an important regulator of OM-induced osteogenic differentiation of hMSCs (Jaiswal et al., 2000; Kilian et al., 2010; Lai et al., 2001; Q. Liu et al., 2009). Moreover, Byun and co-workers showed that ERK is required for the FGF-2-induced bone formation in C3H10T1/2 cells (Byun et al., 2014). Interestingly, there is also evidence that the mechanically-induced bone formation is dependent on ERK-Runx2 signaling (Kanno et al., 2007; P. Zhang et al., 2012). However, some studies report a negative role for ERK in osteogenesis induced by OM, BMP-2, BMP-4 or BMP-9 (Higuchi et al., 2002; Kono et al., 2007; Kozawa et al., 2002; Payne et al., 2010; Zhao et al., 2012).

p38

The p38 family consists of four isoforms, namely p38α, p38β, p38γ and p38δ (Cuenda & Rousseau, 2007; Ono & Han, 2000; Roux & Blenis, 2004). p38γ is found mainly in skeletal muscle and p38δ in lung, kidney, testis, pancreas and small intestine, whereas p38α and p38β are abundant in all tissues. The discussion here is limited to these two abundant isoforms, which will be simply referred to as p38 unless otherwise mentioned. While p38 is traditionally thought to be activated by various types of environmental stresses and inflammatory cytokines, the function of p38 is now known to be extended beyond immune responses. The role of p38 in regulating osteogenesis is a good example of this. The deletion of *p38* in mice results in various location-dependent skeletal disorders, highlighting the importance of p38

in bone formation (Greenblatt et al., 2010). Recently, also BMSC-specific *p38* ablation has been connected to impaired bone development and remodeling *in vivo* (Cong et al., 2016). Similar to ERK, the effect of p38 on osteogenic differentiation is at least partially exerted via direct phosphorylation of Runx2 (Greenblatt et al., 2010). However, Ge and co-workers suggested that BMP-2/7-induced Runx2 phosphorylation and transcriptional activity in osteoblasts are predominantly mediated via ERK rather than p38 (Ge et al., 2012). Under BMP-2 stimulation, also Osterix and Dlx5 have been shown to be direct targets of p38 phosphorylation (Ortuno et al., 2010; Ulsamer et al., 2008), further explaining the importance of p38 for osteogenesis.

With respect to the cell attachment-mediated osteogenesis, there are currently only few reports suggesting a role for p38 in this process (Ivaska et al., 1999; Shie & Ding, 2013; W. Wang et al., 2014). Interestingly, Zhou and co-workers demonstrated that p38 is essential for the osteogenic differentiation of rat BMSCs in 3D human bone-derived scaffolds under hypoxic conditions (Y. Zhou et al., 2013). Concerning chemically-induced differentiation, p38 seems to be required for the osteogenesis of MSCs and osteoblastic cells induced by OM, BMP-2, BMP-4, BMP-9 and Wnt4 (Chang et al., 2007; Guicheux et al., 2003; Kozawa et al., 2002; Lai & Cheng, 2002; Nöth et al., 2003; Payne et al., 2010; Tominaga et al., 2005; Zhao et al., 2012). However, Kilian et al. failed to show any impact of p38 inhibition on osteogenesis or adipogenesis of hMSCs cultured on different micropatterns in mixed OM/adipogenic medium (AM) (Kilian et al., 2010). In line with this, BMP-2 induced osteogenesis of C2C12 cells was not affected by p38 inhibition either (Vinals et al., 2002).

JNK
JNK1, JNK2 and JNK3 (also known as stress-activated protein kinases, SAPKs) form the third major family of MAPKs (Davis, 2000; Greenblatt et al., 2013; Pearson et al., 2001; Rubinfeld & Seger, 2005). JNK1 and JNK2 are found in all tissues whereas JNK3 is mainly produced in the nervous system. Due to the large amount of common MAPKKKs, JNKs and p38 are often activated by the same stimuli, e.g. cytokines and environmental stresses, although also specific activation occurs via distinct MAPKKs. Since no bone phenotype of JNK-deficient mice has been reported yet, the role of JNK pathway in osteogenesis is by far the less understood of the MAPKs (Greenblatt et al., 2013). However, there is evidence that the inhibition of JNK attenuates the OM and BMP-2 induced osteogenesis of hMSCs, suggesting an important role for JNK as a regulator of osteogenic differentiation (Gu et al.,

2015; Guicheux et al., 2003; Kilian et al., 2010; Tominaga et al., 2005). Interestingly, Qiu and co-workers observed that stimulation of hBMSCs with Wnt3a activates a non-canonical signaling pathway leading to c-Jun activation via JNK (Qiu et al., 2011). Moreover, the inhibition of JNK also decreased the Wnt3a-induced osteogenesis. Related to this, Wu et al. reported that the nuclear accumulation of β-catenin in the canonical Wnt signaling pathway requires β-catenin phosphorylation by JNK2 (X. Wu et al., 2008). These data suggest that JNK is a key player in both canonical and non-canonical Wnt signaling. Of note, both ERK and p38 have been also linked to the Wnt signaling via their ability to phosphorylate glycogen synthase kinase 3β (GSK3β) and thus inhibit it, causing the nuclear accumulation of β-catenin (Ding et al., 2005; Thornton et al., 2008). In addition, all the MAPKs are able to promote Wnt/β-catenin signaling by phosphorylating the Wnt co-receptor low-density lipoprotein receptor-related protein 6 (LRP6) (Cervenka et al., 2011).

In addition to the Wnt signaling, JNK was also observed to be required for the NELL-1-induced mineralization of Saos-2 human osteosarcoma cells (F. Chen et al., 2012). Moreover, in the gene expression level, the late stages of osteogenesis of MC3T3-E1 cells were shown to be dependent on JNK-induced *Atf4* expression (Matsuguchi et al., 2009). With respect to the cell attachment-mediated osteogenesis, Chiu and co-workers demonstrated that JNK activation is required for hBMSC osteogenesis on collagen-I and collagen-II, and blocking of integrinα2β1 on collagen-II impeded JNK phosphorylation (Chiu et al., 2012; Chiu et al., 2014). However, on Ca silicate cements no activation of JNK or role in hBMSC or human dental pulp cell osteogenesis could be detected (Shie & Ding, 2013). Interestingly, Hwang et al. showed that the activation of both JNK and ERK in hMSCs increase with increasing stiffness of the growth substrate, and upon inhibition of these kinases the osteogenesis is decreased via a TAZ-dependent mechanism (Hwang et al., 2015).

Figure 5 summarizes the various signaling molecules activated directly by the MAPKs and having an established role in the osteogenesis regulation as discussed in this section.
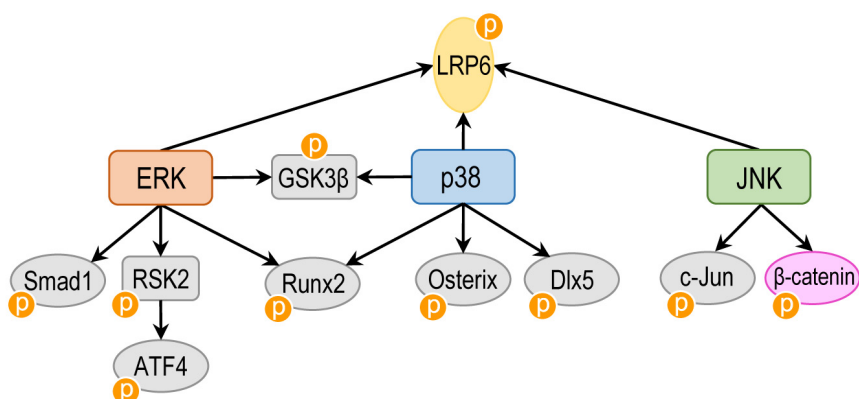
Figure 5. MAPKs and their target molecules in the regulation of osteogenesis. Only targets of direct MAPK phosphorylation with an established role in the regulation of osteogenesis are depicted. RSK2=ribosomal S6 kinase 2. p indicates phosphorylation. Image modified from (Greenblatt et al., 2013).

2.4.4 Other major signaling pathways regulating osteogenic differentiation

In addition to the signaling pathways and molecules discussed above, there are a considerable number of other signaling mechanisms regulating the sequence of events leading to the osteogenic commitment (Hayrapetyan et al., 2015; James, 2013). For instance, Wnt, Hedgehog and Notch pathways, as well as signaling induced by NELL-1, Ca and several growth factors (e.g. FGF, IGF, platelet-derived growth factor (PDGF)) have been shown to play central roles in bone formation (Agas et al., 2013; F. Chen et al., 2012; Hilton et al., 2008; James et al., 2012; Jin et al., 2014; Leucht et al., 2013; Viti et al., 2016; Xian et al., 2012). The majority of these pathways ultimately affect the expression and/or activation of Runx2 and PPARγ, the two master regulators of osteogenesis and adipogenesis, respectively (James, 2013). Therefore, apart from IGF and BMPs being able to induce both osteogenesis and adipogenesis, the majority of these signaling mechanisms simultaneously induce osteogenesis and inhibit adipogenesis, or vice versa.

An additional level of complexity to the signaling scene is brought by the extensive cross-talk between the various signaling pathways. For example, FGF-2 has been shown to be necessary for the BMP-2-induced nuclear accumulation and co-localization of Runx2 and pospho-Smad1/5/8 in mouse primary calvarial osteoblasts, leading to the expression of osteogenic differentiation markers (Agas et al., 2013). In contrast to this, Biver et al. observed that FGF-2 inhibits hMSC osteogenesis by

decreasing the expression of BMPs and their receptors, and this inhibitory effect of FGF-2 was abrogated by ERK or JNK inhibition (Biver et al., 2012). An interconnection has been also found between the BMP and Wnt signaling routes, with evidence of a synergistic effect of BMP-2 and Wnt3a in promoting bone formation in *in vivo* mouse models (Aquino-Martinez et al., 2016; Fuentealba et al., 2007). Interestingly, also two other pairs of signaling factors, namely Sonic Hedgehog & NELL-1, and BMP-6 & VEGF, have shown synergism in inducing osteogenic differentiation of hASCs (James et al., 2012; C. J. Li et al., 2015). In the case of the latter pair, the cross-talk was observed to be dependent on p38 (C. J. Li et al., 2015). All in all, despite the gradually accumulating data about the various osteogenesis-regulating signaling mechanisms, the overall picture of the signaling scheme still remains unclear, and a lot of research is required to fill the gaps in the complex signaling map.

2.4.5   Predicting cell fate

Despite the enormous potential of MSCs for bone TE applications, the therapeutic efficacy of these cells still faces the problem of a huge donor-to-donor variability and, consequently, a lack of specific markers to predict the *in vivo* bone forming capacity based on the *in vitro* cell behavior. Interestingly, analysis of the cell signaling events has emerged as a potential means to solve the problem related to the osteogenic differentiation capacity prediction (Bolander et al., 2016; Mentink et al., 2013; Platt et al., 2009). Platt and co-workers created an osteogenesis-predictive computational model by analyzing the activation of eight intracellular signaling proteins (epidermal growth factor receptor (EGFR), Akt, ERK, heat shock protein 27 (Hsp27), c-Jun, GSK3α/β and signal transducer and activator of transcription 3 (STAT3)) in hBMSCs on epidermal growth factor (EGF) presenting polymeric substrates (Platt et al., 2009). It was observed that the 7-day signaling status was the strongest predictor of the 21-day mineralization outcome, and the model was also able to successfully predict the osteogenesis of hBMSCs cultured on collagen-I. Mentink and co-workers, on the other hand, were able to identify a single gene, *cell adhesion molecule 1 (CADM1)*, the expression of which strongly correlated with the *in vivo* bone forming capacity of hBMSCs in a data set of 62 cell donors (Mentink et al., 2013). No such correlation could be found between the osteogenic markers or donor features and the *in vivo* bone formation. Lastly, Bolander et al. recently presented a mathematical model able to successfully predict the *in vivo* bone formation capacity of different CaP/collagen-based scaffolds seeded with human periosteum-derived

cells (Bolander et al., 2016). The combination of five measurements, β-catenin, phospho-β-catenin, phospho-protein kinase C (PKC) and phospho-Smad1/5/8 at day 3, and Ca-release after 24h, could predict the quantity of bone formed *in vivo* with the accuracy of 96%. All in all, these data suggest that the use of cell signaling data combined with an appropriate computational model could be a useful tool to predict cell differentiation outcome, a process that could potentially save a lot of time, money and animals, and improve the clinical efficacy of MSC-based treatments.

2.5   Biomaterials in bone tissue engineering

The treatment of bone defects too large to be healed by the bone's natural renewal capacity has traditionally relied on autologous bone grafts, typically harvested from the iliac crest of the patient (Burg et al., 2000; Jakob et al., 2012; Stevens et al., 2008; Välimäki & Aro, 2006). However, this strategy has severe limitations such as donor-site morbidity and pain, limited supply and poor quality of the bone. As an alternative option, allografts, typically obtained from the femoral heads or human cadavers, have been widely utilized in the past for the treatment of large bone traumas, but they also have drawbacks, mainly associated with the risk of immunological reactions and disease transmission. Consequently, the unsolved problems of these traditional treatment methods have paved the way for the development of absorbable biomaterials and TE-based interventions to treat large bone defects.

The basic concept of TE was originally introduced by Robert Langer and Joseph Vacanti (Langer & Vacanti, 1993). Based on their definition TE is "an interdisciplinary field that applies the principles of engineering and life sciences toward the development of biological substitutes that restore, maintain, or improve tissue function" (Vacanti & Langer, 1999). In practice, the TE-based tissue regeneration is typically achieved with a construct combining cells, a biomaterial scaffold and possibly also differentiation stimulating factors (e.g. growth factors), implanted to the defect site. With respect to the biomaterial, a functional scaffold for bone TE should fulfill a long list of essential requirements (Drosse et al., 2008; Jones, 2015; Rahaman et al., 2011; Rezwan et al., 2006). For example, the scaffold needs to be biocompatible (i.e. not to elicit adverse inflammatory responses *in vivo*), porous with interconnected pores to facilitate cell ingrowth and vascularization, biodegradable with the degradation rate matching the formation of the new tissue,

and strong enough to withstand the mechanical loading *in vivo*. Moreover, the design should mimic the natural structure of bone and the construct should be easily manageable in the operation theatre. So far, a material which would fulfill all the aforementioned criteria has not been developed, but a lot of research has been conducted to find optimal biomaterial solutions for the needs of bone TE.

The biomaterials used in bone TE are often roughly divided to natural polymers, synthetic polymers and bioceramics (Rezwan et al., 2006; Zanetti et al., 2013). Especially bioceramics, including HA, β-TCP and BaGs, have proved to be highly beneficial for bone TE due to their close resemblance to the inorganic matrix of natural bone (Barrere et al., 2006; Zanetti et al., 2013). This section will give a brief overview on the calcium phosphate ceramics (CPCs) followed by a closer description of BaGs and their utilization in bone TE. Moreover, since combining materials from the different classes to composite structures (e.g. polymer-ceramic composites) has often led to a dramatically improved performance, examples of *in vitro* and *in vivo* studies evaluating BaG-containing composites will be also presented.

2.5.1 Calcium phosphate ceramics

Synthetic CPCs, chemical salts of orthophosphoric acid (H_3PO_4), have been successfully used in medical applications of cranio-maxillofacial, dental and orthopedic surgery from the beginning of the 1970s (Barrere et al., 2006; Hench, 1991). The favorable performance of these materials is to a large part explained by their close resemblance to bone, of which around 60 wt-% consists of inorganic HA ($Ca_{10}(PO_4)_6(OH)_2$) (Rezwan et al., 2006). Furthermore, due to the specific surface reactions, a common characteristic of all the bioceramics (including BaGs) is the formation of a biologically active hydroxycarbonate apatite (HCA) layer on the material surface in physiological fluids (Hench, 1991; Rezwan et al., 2006). Consequently, the HCA layer mediates strong bonding to bone, defined as bioactivity (Hench, 1988). Therefore, in addition to the use of CPCs as bone fillers in the form of granules or cements, the bioactivity makes them also excellent coating materials for various metallic and polymeric implants (Barrere et al., 2006). However, for load-bearing sites pure CPCs are generally too brittle.

Initially, HA was the most abundantly used CPC since its composition is closest to the inorganic matrix of bone. However, it has poor solubility and, despite being osteoconductive (i.e. supportive of bone growth on the surface), it is not osteoinductive (i.e. able to stimulate the osteogenic differentiation of undifferentiated cells) (Albrektsson & Johansson, 2001; Samavedi et al., 2013).

Therefore, more soluble and osteoinductive CPCs, such as TCPs, amorphous calcium phosphates (ACPs) and BCPs (mixtures of HA and TCPs in varying ratios) have been gradually replacing HA in the regeneration of bone (Barrere et al., 2006; Samavedi et al., 2013). When considering the situation *in vivo*, the properties of CPCs (e.g. surface roughness, solubility, porosity and surface charge) have a major effect on protein adsorption and, consequently, on cell adhesion, proliferation and differentiation, which ultimately defines their clinical performance (Samavedi et al., 2013). Thus far, different CPCs, either as such or as a part of a composite scaffold, have shown promising results with respect to cell attachment, proliferation and differentiation in various bone TE-based approaches both *in vitro* (Haimi et al., 2009a; Hattori et al., 2006; Khanna-Jain et al., 2012; C. Li et al., 2006; Marino et al., 2010) and *in vivo* (Cowan et al., 2004; Jeon et al., 2008; Khojasteh et al., 2013). Moreover, β-TCP granules have been successfully used in clinical case studies describing bone-TE-based treatment of cranio-maxillofacial defects, which illustrates the potential of CPCs beyond the traditional applications as bone fillers and implant coatings (Mesimäki et al., 2009; Sandor et al., 2014).

2.5.2   Bioactive glasses

The invention of the first BaG by Larry Hench in 1969 at the University of Florida (Hench et al., 1971) was inspired by a conversation with a US Army colonel, just returned from Vietnam, who was asking about the possibility to develop a material which could survive the hostile environment of the human body (Hench, 2006). At that time the implant materials available were mainly bioinert metals and polymers which often failed due to the fibrous encapsulation and weak binding to tissues. BaG, on the other hand, was different. Due to its inherent bioactivity, BaG formes a strong bond to bone and moreover, it is biocompatible as well as biodegradable. Thus, not surprisingly, the invention of BaG denoted a significant milestone for regenerative medicine and the original BaG, later termed 45S5 and trademarked with the name Bioglass® (45 wt-% SiO_2, 24.5 wt-% Na_2O, 24.5 wt-% CaO, and 6 wt-% P_2O_2) entered the clinics already in 1984 as a monolithic ear prosthesis (Rust et al., 1996). Currently, the commercial clinical BaG products are mainly particulates intended for bone fillers in various dental and orthopedic applications (Jones, 2015). Examples of these are 45S5-based PerioGlas® and NovaBone as well as the even more widely used BonAlive®, a Finnish product based on S53P4 glass with a similar composition to 45S5 but with slightly slower reactivity. Moreover, the 45S5 particulate

NovaMin®, as a component of a tooth paste, has turned out to be efficient in treating hypersensitivity (Jones, 2015).

Due to their advantageous properties BaGs have gained a lot of attention also in the field of bone TE. After an introduction to the different BaG compositions and properties, the utilization of BaGs in bone TE applications *in vitro* and *in vivo* will be reviewed.

Compositions and properties

Formation of the HCA layer and, consequently, strong bonding to bone, is dependent on certain compositional features of BaGs. Unlike in the traditional soda-lime silicate glasses, in BaGs the SiO_2 content is considerably low (<60 mol-%), whereas the Na_2O and CaO contents and the ratio of $CaO:P_2O_5$ are high (Hench, 1998). Moreover, it has been observed that BaGs containing 45-52 wt-% SiO_2 bond to both soft and hard tissues, glasses with 55-60 wt-% SiO_2 only bond to hard tissues (e.g. bone) and with SiO_2 content raising above 60 wt-% the bioactivity of the melt-derived glasses is totally lost (Välimäki & Aro, 2006). Lowering the silica-content (e.g. by replacing silica with sodium) leads to a less connected silica network, which is more prone to dissolution and therefore explains the increased reactivity. The processing characteristics and the degradation profiles of BaGs can be also adjusted by supplementation with network modifiers such as MgO, K_2O, Al_2O_3 and B_2O_3, whereas doping glasses with elements such as cobalt, silver and strontium may have a positive effect on the biological performance (e.g. vascularization, antibacterial properties and osteogenic differentiation) (Jones, 2015). Of note, in addition to the traditional silicate BaGs based on a 3D glass-forming SiO_2 network, also borate and phosphate-based BaGs, generally more reactive than the silicate glasses, have been developed for the purposes of regenerative medicine (Hoppe et al., 2011; Rahaman et al., 2011). However, the focus here will be on silicate BaGs.

As already mentioned, the bioactivity of BaGs is associated with the formation of a HCA layer and the consequent bone bonding, but also with the biological interactions at the host bone-HCA interface, such as protein adsorption as well as cell attachment and differentiation (Jones, 2015). The understanding of the HCA layer formation is a key to understand the glass reaction kinetics and the biological responses. The formation of the HCA layer, either *in vivo* or in simulated body fluid *in vitro*, can be divided into five consecutive stages (Hench, 1991). Briefly, in the first stage (I) Na^+ and Ca^{2+} are released from the glass surface and H^+ and H_3O^+ are acquired from the solution, leading to the creation of silanols (Si-OH) on the glass surface. Next, as a consequence of the increased pH of the solution, silica dissolutes

from the glass surface in the form of silicic acid ($Si(OH)_4$) (II). In the third step (III) a silica-rich layer condensates and polymerizes on the glass surface. Ca^{2+} and $(PO_4)^-$ ions are then migrated from the glass and from the solution on top of the silica-rich layer to form an amorphous CaP film (IV). Finally, the CaP layer crystallizes to the bioactive HCA layer (V).

BaGs can be made by two different methods: the traditional, high temperature requiring melt-quenching route leading to dense non-porous structures, and the chemistry-based sol-gel synthesis taking place at lower temperatures and producing inherently nanoporous structures which may retain their bioactivity with up to 90 mol-% of SiO_2 (Jones, 2015; Rahaman et al., 2011). With respect to bone TE, a challenge remains in producing 3D scaffolds from the glasses, since BaGs, regardless of the manufacturing method, are generally too brittle for load-bearing applications. Moreover, 3D scaffold production from melt-derived glasses is typically achieved with sintering, which often results in crystallization and, consequently, to the loss of bioactivity (Jones, 2015). With direct ink writing, an additive manufacturing technique, it has been possible to produce BaG scaffolds with compressive strength comparable to that of cortical bone (100-150 MPa) (Q. Fu, Saiz, & Tomsia, 2011a; Q. Fu, Saiz, & Tomsia, 2011b). However, the brittleness of the glass still compromises these structures in sites under cyclic load. Consequently, considerable expectations have been put on the BaG-containing composites, although they also have challenges to overcome, such as problems associated with the differing degradation rates of the two phases and the masking of the BaG by the another component (Jones, 2015).

Apart from their inherent bioactivity and osteoconductivity, BaGs are highly osteoinductive materials capable of stimulating the osteogenesis of stem and progenitor cells without any added chemical supplements (Bosetti & Cannas, 2005; Gough et al., 2004; Haimi et al., 2009b; Waselau et al., 2012). Moreover, BaGs can induce new bone formation away from the implant-bone interface, likely via their dissolution products, which is commonly called osteoproduction (Jones, 2015). With respect to TE, a highly advantageous property of BaGs is also their ability to stimulate the secretion of angiogenic growth factors and tubule formation *in vitro* as well as vascularization *in vivo* (Day et al., 2004; Day, 2005; Day et al., 2005; Gerhardt et al., 2011; Leu & Leach, 2008; Waselau et al., 2012). Finally, BaGs, especially S53P4, seem to have a strong antimicrobial effect on a large variety of clinically relevant aerobic and anaerobic bacteria, mediated through the glass dissolution-induced pH rise in the vicinity of the glasses (Leppäranta et al., 2008; Munukka et al., 2008; Stoor et al., 1998; D. Zhang et al., 2010). The angiogenic

and antimicrobial properties, as well as the ability of some of the BaGs to bond to soft tissues, has increased the interest in using the BaGs also for wound healing and soft tissue repair, as reviewed by Miguez-Pacheco and co-workers (Miguez-Pacheco et al., 2015).

In vitro studies with stem and progenitor cells

Several *in vitro* studies with stem and progenitor cells have shown favorable cell responses, e.g. good cell attachment and viability as well as increased proliferation and osteogenic differentiation, upon culturing the cells on granules, 3D scaffolds and other monolithic BaG substrates (Bosetti & Cannas, 2005; Detsch et al., 2015; Gough et al., 2004; Haimi et al., 2009b; Jones et al., 2007; Loty et al., 2001; Waselau et al., 2012; C. Wu et al., 2013). Moreover, the osteogenic response has been observed to be further enhanced on rough and nanopatterned BaG surfaces (Gough et al., 2004; Lei et al., 2010), highlighting the crucial role of the surface topography on cell behavior. However, there are also contradicting reports regarding the osteogenesis-supporting role of BaGs. Reilly and co-workers observed no stimulation of osteogenesis of hBMSCs cultured on 45S5 discs in either BM or OM, even though rat BMSCs responded to the glass by increased ALP activity (Reilly et al., 2007). Furthermore, Rath et al. demonstrated that 45S5 scaffolds induced the osteogenic differentiation of ASCs even without OM, but with BMSCs this was not detected (Rath et al., 2013). There is also evidence that osteogenesis of hBMSCs on 45S5 granules, unlike on HA/TCP, is hindered due to the alkaline pH caused by the glass dissolution (Monfoulet et al., 2014). Human ASCs, on the other hand, showed better osteogenesis on S53P4 granules, very close in composition to 45S5, than on β-TCP granules (Waselau et al., 2012). All in all, it seems that the cellular response to the BaGs is highly dependent on the cell source and animal origin.

In addition to the structures of pure BaG, also BaG containing composites have been widely studied in *in vitro* cell culture for bone TE. Bioactive glass, typically either as a coating or a filler, has been shown to improve the cellular response to both polymeric (e.g. polylactide (PLA), PCL, poly(lactide-co-glycolide) (PLGA)) and CPC scaffolds (S. Chen et al., 2015; Larranaga et al., 2015; Lu et al., 2015; Oh et al., 2010; Pamula et al., 2011; S. Yang et al., 2014). Furthermore, the mixing of BaG particles of submicron or nanoscale with different hydrogels (e.g. collagen, alginate) has been observed to be a promising approach for bone TE with enhanced proliferation and osteogenic differentiation of gel encapsulated stem and progenitor cells when compared to the corresponding gels without the BaGs (Marelli et al., 2011; Olmos Buitrago et al., 2015; Zeng et al., 2014).

Even though the unique biological properties of bioactive glasses have been recognized and extensively studied for the applications of regenerative medicine since the discovery of the Bioglass® in the early 1970s, only from the beginning of the 21st century more attention has been paid to the specific properties of the BaGs inducing the favorable cellular responses (Hoppe et al., 2011; Xynos et al., 2000; Xynos et al., 2001). In particular, increasing evidence has started to accumulate that, in addition to the BaG surface properties (e.g. roughness, topography), porosity and crystallinity, also the ionic dissolution products play a significant role in regulating cell behavior (Hoppe et al., 2011; Lakhkar et al., 2013). Many of the ions released from the BaGs, such as Ca, Si, P, Mg, K and B, have well-established roles as regulators of bone metabolism, and therefore it is logical to think that they will also have an effect on the osteogenic differentiation of stem cells and osteoprogenitor cells *in vitro*.

Despite the emerging concept of the ionic dissolution product-mediated mechanism stimulating the osteogenic differentiation, only a handful of studies have analyzed the proliferative and osteogenic cellular responses in culture media conditioned with ions released from BaGs. These studies and their main findings are listed in Table 2. In general, the treatment with BaG extracts seems to have a positive effect on osteogenic differentiation even without any additional OM supplements (Alves et al., 2015; Gong et al., 2014; Tsigkou et al., 2009), although in most of the studies the osteogenic outcome has been achieved in ion-supplemented OM (Bielby et al., 2005; Saffarian Tousi et al., 2013; Varanasi et al., 2009; Varanasi et al., 2011). Moreover, in addition to the positive results, there are also studies reporting no effect for the BaG extract treatment on the osteogenic differentiation (Christodoulou et al., 2005; Jell et al., 2008; Valerio et al., 2004). Of note, thus far no knowledge exists about the response of MSCs to the BaG ionic extracts and the choice of BaG compositions used in the dissolution studies is still quite restricted.

A major shortcoming of the studies evaluating the cellular response to BaG dissolution products is the lack of standardization, e.g. with respect to cell type, glass particle size as well as dissolution protocol (glass:medium ratio, incubation time, temperature, medium composition etc.). This makes the comparison of the current studies extremely challenging. To simplify the experimental setup, many studies have analyzed the effect of single ionic species added to the culture medium (e.g. Ca, Si) instead of the combination of various ions dissolved from BaGs (An et al., 2012; Dvorak et al., 2004; Maeno et al., 2005; Reffitt et al., 2003; Shie et al., 2011; Takagishi et al., 2006). However, the beneficial effect of the BaG dissolution products might be caused by the combinatorial effect of the different ions and thus

cannot necessarily be achieved with the addition of a single ionic species. Finally, in addition to determining the optimal ion concentrations for the stimulation of stem cell osteogenesis, a huge challenge remains in the field of bone TE to develop a scaffold with an optimal and predetermined ion release profile to support bone formation both *in vitro* and *in vivo*.

In vivo studies

In addition to the extensive studies *in vitro*, BaGs, either as such or combined with cells, have been also widely evaluated in animal models in both ectopic (typically subcutaneous) and orthotopic (e.g. calvarium, femur) locations. Whereas the ectopic implantation may provide useful information about the osteoinductivity of the construct itself, orthotopic implantation to the bone defect simulates more closely the clinical situation, even though the specific contribution of the construct-related factors on the healing might be impossible to distinguish. One widely used model in the biomaterial testing *in vivo* is the Oonishi model, which was initially described by Oonishi and co-workers (Oonishi et al., 2000). They drilled 6 mm diameter critical-sized holes in the femoral condyles of rabbits and filled them with 100-300 μm granules of either 45S5, HA or apatite-wollastonite ceramic. Out of these, 45S5 induced the most rapid bone formation and it was also resorbed faster than the others. In addition to 45S5, also S53P4 granules have been shown to be superior to HA with respect to bone formation and resorption, when used in the obliteration of rabbit frontal sinuses and calvarial defects (Peltola et al., 2001). In order to further improve the handling of the granules, they may be mixed with either blood or some synthetic carrier. Wang and co-workers demonstrated that applying a putty of NovaBone (45S5) granules and polyethylene glycol-glycerine into the vertebral body defects of sheep improves the initial bone formation when compared to the NovaBone granules applied as such (Z. Wang et al., 2011).

The addition of BaG to a composite structure, as a coating or a filler, has been also observed to be a beneficial approach to improve the bone formation *in vivo*. For example, BaG coating of both PLLA and polyethersulphone nanofibers led to an increased bone formation in rat critical-sized calvarial defects (Ardeshirylajimi et al., 2015; Dinarvand et al., 2011). In silk scaffolds, the presence of BaG greatly increased the bone formation in calvarial defects of mice (C. Wu et al., 2011). Moreover, 45S5 particles in dense collagen hydrogel stimulated mineralization, vascularization and cell infiltration when injected subcutaneously in rats (Miri et al., 2016).

Table 2. Studies evaluating the effect of different BaG extracts on proliferation and osteogenic response of various cell types.

Reference	Cell type	BaG	Extract preparation	Results
Alcaide et al., 2010	Saos-2, L929 fibroblasts	MBG85 powder	100mg/100ml, 3h, 3d, 7d only BM	proliferation ↓ good viability no T-cell response
Alves et al., 2015	canine osteoblasts	BG60S <137 µm	6g/1L, 12h +6°C BM and OM	ALP activity ↑ in BM but ↓ in OM, mineralization ↑in both media, osteogenic marker genes ↑ in OM
Bielby et al., 2005	murine ESCs	58S 300-710 µm	0.1-0.5g/100ml, 24h, +37°C only OM	ALP activity and mineralization ↑
Christodoulou et al., 2005	human fetal osteoblasts	58S 710-790 µm	0.05-0.2g/100ml, 1-24h, 37°C only OM	no effect on osteogenic differentiation
Christodoulou et al., 2006	human fetal osteoblasts	58S 710-790 µm	0.2g/100ml, 3h, +37°C only OM	differences in gene expression (e.g. *ERK1, IGF-1, gp130*) (microarray)
Gong et al., 2014	dental pulp cells	58S (10-100 nm), 58S (2-20 µm), 45S5 (1-10 µm)	1 mg/ml, 24h, +37°C only BM	nano-58S induced odontogenic gene expression and mineralization
Jell et al., 2008	human fetal osteoblasts	45S5	1g/100ml, o/n, +37°C only BM	*ALP* and *BSP* ↑ in protein level no effect
Saffarian Tousi et al., 2013	MC3T3-E1	45S5 and 6P53-b 100-300 µm	0.8, 1.6 ja 2.4 g/50 ml 72h at +37°C only OM	mineralization and OC production ↑, 45S5 more effective
Tsigkou et al., 2009	human fetal osteoblasts	45S5 300-710 µm	1% w/v, 24h, +37°C only BM	mineralization, OC & col-I production and osteogenic marker gene expression ↑
Valerio et al., 2004	rat osteoblasts	BG60S 38 µm	0.5 g/50 ml, 5 h +37°C only BM	col-I production and cell viability ↑, no effect on ALP activity
Varanasi et al., 2009	MC3T3-E1	45S5, 6P53-b discs 1x1x0.2 cm	2d in +37°C (after 10d in SBF) BM±AA	proliferation ↑ (-AA); *OC, ALP, Runx2, col-1* ↑ and OC & col-I production ↑ (+AA)
Varanasi et al., 2011	periodontal ligament fibroblasts	45S5, 6P53-b powder	3d BM+AA	*col-I, OC, ALP* ↑ mineralization ↑ OC production ↑
Xynos et al., 2000	human osteoblasts	45S5 300-710 µm	1% w/v, 24h, +37°C only BM	proliferation ↑
Xynos et al., 2001	human osteoblasts	45S5 300-710 µm	1% w/v, 24h, +37°C only BM	strong effect on gene expression (microarray)

BM=basic cell culture medium, OM=osteogenic medium, ALP=alkaline phosphatase, BSP=bone sialoprotein, OC=osteocalcin, col-I=collagen-I, AA=ascorbic acid, ↑=increase, ↓=decrease. MBG85: $85SiO_2$-$10CaO$-$5P_2O_5$ (mol-%); BG60S: $60SiO_2$-$36CaO$-$4P_2O_5$ (mol-%); 58S: $60SiO_2$-$36CaO$-$4P_2O_5$ (mol-%; sol-gel-derived BaG); 6P53-b: $53SiO_2$-$18CaO$-$10Na_2O$-$3K_2O$-$10MgO$-$6P_2O_5$ (wt-%); 45S5: $46SiO_2$-$27CaO$-$24Na_2O$-$3P_2O_5$ (mol-%).

In addition to the promising *in vivo* results obtained with BaG-containing scaffolds without cells, there is also evidence that the seeding of the scaffolds with MSCs prior to implantation further improves the bone formation in rats, in both subcutaneous sites (Q. Fu et al., 2010; Gomide et al., 2012) and femoral defects (Xu et al., 2011). Moreover, Gomide and co-workers reported that the subcutaneous osteoid tissue formation with rat BMSC seeded polyvinylalcohol-BaG scaffolds required osteogenic differentiation of the cells before seeding to the scaffolds (Gomide et al., 2012). In contrast to these studies, Sacak and co-workers did not detect any difference in the bone formation in rat critical-sized calvarial defects filled with either S35P4 granules combined with rat ASCs or S53P4 granules alone (Sacak et al., 2016). However, both of these treatments still increased the bone formation and density, indicating that the presence of the cells did not compromise the healing.

2.5.3   Clinical case reports of adipose stem cell-based bone tissue engineering

Apart from one terminated phase II trial (NCT01532076; www.clinicaltrials.gov), the clinical evidence of hASC-utilizing bone TE treatments is currently based on a handful of case reports describing the treatment of few cases (Lendeckel et al., 2004; Mesimäki et al., 2009; Pak, 2011; Pak, 2012; Sandor et al., 2013; Sandor et al., 2014; Taylor, 2010; Thesleff et al., 2011; Wolff et al., 2013). Whereas the majority of these reports describe the treatment of various defects in the cranio-maxillofacial area (Mesimäki et al., 2009; Sandor et al., 2014; Taylor, 2010), two studies demonstrate that hASCs, when combined with platelet-rich plasma, hyaluronic acid and calcium chloride, might potentially be a promising intervention for femoral head osteonecrosis as well as osteoarthritis (Pak, 2011; Pak, 2012).

In the first reported case of hASC-based bone TE, an initial titanium plate-based treatment of a 7-year-old girl with a fall-induced closed multifragment calvarial fracture had failed and, consequently, the defect was treated with autologous SVF cells mixed with milled autologous bone from the iliac crest (Lendeckel et al., 2004). After three months marked ossification had occurred with no reported complications. Even though the outcome of the study of Lendeckel and co-workers was clearly encouraging, their strategy to use autologous bone as a biomaterial component is not a sustainable solution due to the unsolvable problems related to the adequate availability and donor-site morbidity. Mesimäki and co-workers presented a solution to this problem by using autologous hASCs combined with β-TCP granules and rhBMP-2 in the treatment of a 65-year-old male, who had undergone a hemimaxillectomy due to a large keratocyst (Mesimäki et al., 2009). A

preformed titanium cage filled with the construct was inserted in the patient's abdominis muscle for eight months. After the eight months the structure was ossified, vascularized and was now transplanted into the maxillary defect area. The healing was uneventful leading to a successful outcome.

The pioneering work by Mesimäki and co-workers was subsequently improved on by another study conducted also in collaboration with University of Tampere (Thesleff et al., 2011). In this study, four patients with large calvarial defects were successfully treated with hASC-seeded β-TCP granules. Unlike in the case study of Mesimäki and colleagues (Mesimäki et al., 2009), this time the constructs were directly administered to the defect areas and no external growth factor stimulus was used. Moreover, instead of a titanium mesh, the team used resorbable meshes to support the structures. In 2014 Sandor and co-workers published the first multipatient case series describing the treatment of 13 patients with cranio-maxillofacial bone defects at four different anatomical sites: frontal sinus, cranial bone, mandible and nasal septum (Sandor et al., 2014). All the patients were treated with autologous hASCs combined with either β-TCP or BaG (S53P4, BonAlive®) granules, with or without rhBMP-2 supplementation. Ten out of the 13 cases resulted in a successful outcome. Of note, no complications occurred in either of the three cases treated with BaG granules (all frontal sinus defects).

In summary, the clinical cases treated with ASC-utilizing bone TE strategies have thus far shown more or less encouraging outcomes with no severe complications reported. However, a challenge still remains in translating these novel and comparatively complicated treatment methods to routine techniques for the treatment of large bone defects. To reach that goal, more evidence about the safety and efficacy of these methods is definitely required. Therefore, in addition to more thorough basic level research *in vitro* and *in vivo*, large-scale clinical trials will be needed.

3 Aims of the study

The aim of this thesis was to conduct a closer evaluation of the osteogenic differentiation mechanisms of hASCs in response to the BMP-2 growth factor stimulus and BaG biomaterials. The main focus was in the intracellular signaling events responsible for the cell fate decisions under these stimuli. The specific aims for each study are listed below:

I   To evaluate the osteogenic and adipogenic differentiation outcome of hASCs from different donors in response to BMP-2 stimulus, to study the molecular mechanism of BMP-2 signaling, and to assess the effect of production origin (Escherichia coli (E. coli) versus mammalian cells) and the culture conditions (HS versus FBS) on BMP-2 function.

II   To determine whether ionic extracts from BaGs can stimulate hASC osteogenic differentiation in the absence of cell-BaG contact, and to compare the osteogenesis-inducing ability of BaG extracts prepared from different BaG compositions (S53P4, 2-06, 1-06 and 3-06).

III   To compare the efficacy of S53P4 and 1-06 BaG discs in inducing osteogenic differentiation of hASCs, to study the mode of cell attachment on BaGs, and to determine the role of cell attachment-related FAK-MAPK signaling cascade in the BaG-induced early osteogenic differentiation of hASCs.

4 Materials and methods

4.1 Adipose tissue samples and ethical considerations

This study was conducted in accordance with the Ethics Committee of the Pirkanmaa Hospital District, Tampere, Finland (ethical approvals R03058 and R15161). The hASCs were isolated from breast and abdomen originated adipose tissue samples which were acquired from surgical procedures conducted in the Department of Plastic surgery, Tampere University Hospital, Tampere, Finland. All the adipose tissue donors gave a written informed consent for the utilization of the tissue samples in research settings. The adipose tissue samples in study **I** were obtained from ten female donors (mean age 46±25), in study **II** from five female donors (mean age 52±12) and in study **III** from five female donors (mean age 56±8 years).

4.2 Biomaterial manufacturing, pretreatment and characterization

The BaGs used in studies **II** and **III** were manufactured using the traditional melt-quenching route as described in detail in the original publications. In study **II**, the glass blocks were crushed and sieved to give a 500–1000 μm size range fraction. In study **III**, the glass rods were cut into circular discs (thickness 1.5 mm and diameter either 14 mm or 10 mm), both sides of which were polished. The oxide compositions of the studied glasses are shown in Table 3.

Table 3. The compositions of the BaGs used in studies **II** and **III**.

	wt-%						
	Na_2O	K_2O	MgO	CaO	P_2O_5	B_2O_3	SiO_2
S53P4	23.0	0.0	0.0	20.0	4.0	0.0	53.0
1-06	5.9	12.0	5.3	22.6	4.0	0.2	50.0
2-06	12.1	14.0	0.0	19.8	2.5	1.6	50.0
3-06	24.6	0.0	0.0	21.6	2.5	1.3	50.0

4.2.1 Bioactive glass pretreatment

Prior to the use in cell culture, BaG granules and discs were disinfected with ethanol treatment (10 min in absolute ethanol and 10 min in 70% ethanol), followed by drying at room temperature for 1-2 hours. Before plating the cells on the discs in study **III**, the discs were pre-incubated in basic cell culture medium (BM, the composition described in section 4.3) in the cell culture incubator overnight. In study **III**, BaG discs of the compositions S53P4 and 1-06 were used.

4.2.2 Bioactive glass extract preparation

Bioactive glass extract media, used in study **II**, were prepared from all the BaG compositions presented in Table 3, following the workflow of Figure 6. The extraction medium consisted of DMEM/F-12 (Invitrogen, Thermo Fisher Scientific, Waltham, MA, USA) supplemented with 1 % L-glutamine (GlutaMAX I, Life Technologies, Thermo Fisher Scientific) and 1 % antibiotics (100 U/ml penicillin and 0.1 mg/ml streptomycin; BioWittaker, Lonza, Basel, Switzerland). After incubation the extracts were sterile filtered (0.2 µm) and HS (PAA Laboratories, GE Healthcare, Little Chalfont, Buckinghamshire, United Kingdom) was added to 5 %. This medium composition is referred to as basic medium extract (BM extract). The osteomedium extracts (OM extracts) were obtained by supplementing the BM extracts with osteogenic supplements (250 µM L-ascorbic acid 2-phosphate, 10 mM β-glycerophosphate and 5 nM dexamethasone; Sigma-Aldrich, St. Louis, MO, USA). Fresh BaG extracts were made for each 2 week experiment so that the maximum storage time for the extracts was 14 days at +4°C. No visible precipitate was formed during this period.

4.2.3 Determination of the ion concentrations

In study **II**, the ion concentrations of the different extracts were analyzed from sterile filtrated extract samples prior to the addition of HS or the osteogenic supplements. In study **III**, the ionic release profile of the BaG discs during the culture period was determined. Specifically, a medium sample was collected at the time of each medium change from both blank and cell containing samples. The ion concentrations of the different samples were determined by inductively-coupled plasma optical emission spectrometry (ICP-OES; Optima 5300 DV, Perkin Elmer, Waltham, MA, USA).

The elements analyzed by ICP-OES were Na (k = 589.592 nm), K (k = 766.490 nm), Mg (k = 285.213 nm), Ca (k = 317.933 nm), P (k = 213.617 nm), B (k = 249.667 nm) and Si (k = 251.611 nm).
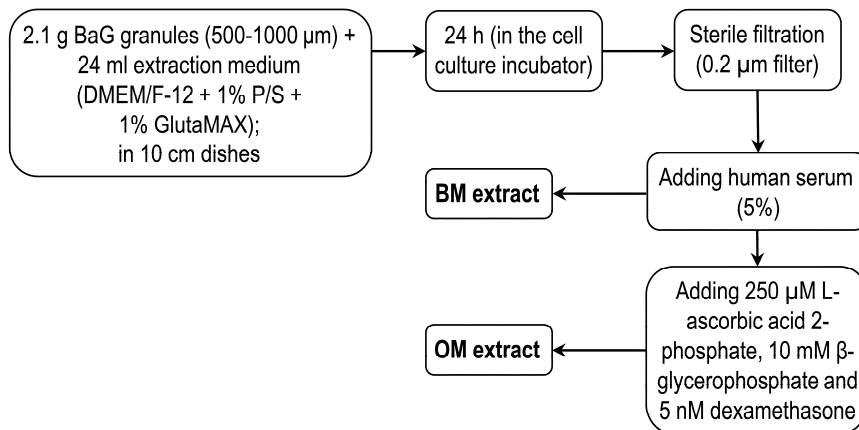
Figure 6. Workflow of the BaG extract preparation in study **II**.

4.2.4   Scanning electron microscopy

In study **III**, the changes in the BaG disc surfaces, in the cell morphology on the BaGs and in the reaction layer formation during the experimental period were assessed with scanning electron microscopy (SEM; Leo 1530, combined with energy dispersive X-ray analysis (EDXA, UltraDry, Thermo Fisher Scientific) after 7d and 21d of culture. Both blank and cell containing samples were analyzed. The reaction layer formation was analyzed from the disc cross-sections, for which the discs were cast in epoxy plastic, cut in half with a diamond blade and polished, which generated a smooth finish for the SEM imaging.

4.3   Adipose stem cell isolation, characterization and culture

4.3.1   Cell isolation from adipose tissue

The isolation of hASCs from the adipose tissue samples was conducted using a mechanical and enzymatic procedure described originally by Zuk and co-workers

(Zuk et al., 2001) and depicted in detail in the original publications **I-III**. The isolated cells were cultured in BM consisting of DMEM/F-12 (Invitrogen, Thermo Fisher Scientific) supplemented with 5% HS (PAA Laboratories, GE Healthcare), 1 % L-glutamine (GlutaMAX I, Life Technologies, Thermo Fisher Scientific) and 1 % antibiotics (100 U/ml penicillin and 0.1 mg/ml streptomycin; BioWittaker, Lonza). The cells used for the experiments were in passages 1-5.

4.3.2   Surface marker expression

To verify the mesenchymal origin of the hASCs used in all the studies (**I-III**), the immunophenotype was determined at passage 1 with flow cytometric analysis (FACSAria, Becton, Dickinson and Company, Erembodegem, Belgium). The studied surface markers and their expressions are listed in Table 4.

4.3.3   Cell culture in different biomaterials and culture media

The plating densities of the cells in the studies **I-III** are depicted in Table 5. In studies **I** and **II** the cells were cultured in Thermo Scientific™ Nunc™ 48-well, 24-well and 6-well cell culture plates, with the exception of the longer lasting mineralization analyses in study **I**, which were conducted in CellBIND plates (Corning, New York, USA) in order to avoid cell detachment. In study **III** the cells were cultured in S53P4 and 1-06 discs, and the polystyrene of the Thermo Scientific™ Nunc™ plates served as a control material.

   The different culture media and the added supplements used in studies **I-III** are listed in Table 6. The cells were always plated in BM and the supplemented media were given to the cells the following day (0d). During the experiments, the medium was changed twice a week. In study **I**, the cells cultured for the Western blot and immunocytochemical signaling analyses were cultured in starvation medium (1% HS or 1% FBS (Gibco, Thermo Fisher, Scientific)) in order to minimize the serum-induced signaling stimuli. The starvation medium was given to the cells 24h before the initiation of the growth factor stimulus. In study **III**, the serum of the BM was treated with dextran coated charcoal (DCC; Sigma-Aldrich) which strips hormones and thus diminishes the background signaling. All the experiments of study **III** were conducted in BM to see the osteogenic differentiation induced solely by the BaGs.

Table 4. Cell surface markers analyzed from the hASCs used in all the studies (**I-III**). The surface marker expression is depicted as average ± standard deviation of the 13 hASC donor lines used.

Antigen	Surface protein	Expression	Fluorophore	Manufacturer
CD3	T-cell surface glycoprotein	0.3±0.2	phycoerythrin (PE)	BD Biosciences, Franklin Lakes, NJ, USA
CD11a	Lymphocyte function-associated antigen 1	0.4±0.2	allophycocyanin (APC)	R&D Systems, Minneapolis, MN, USA
CD14	Serum lipopolysaccharide binding protein	1.0±0.8	phycoerythrincyanine (PECy7)	BD Biosciences
CD19	B lymphocyte-lineage differentiation antigen	0.7±0.7	PECy7	BD Biosciences
CD34	Sialomucin-like adhesion molecule	20.3±18.9	APC	Immunotools, Friesoythe, Germany
CD45	Leukocyte common antigen	1.7±1.0	APC	BD Biosciences
CD54	Intercellular adhesion molecule 1	14.0±11.0	fluorescein icothiocyanate (FITC)	BD Biosciences
CD73	Ecto-5'-nucleotidase	78.3±18.6	PE	BD Biosciences
CD80	B-lymphocyte activation antigen B7	0.5±0.4	PE	R&D Systems
CD86	B-lymphocyte activation antigen B7-2	0.8±0.5	PE	R&D Systems
CD90	Thy-1 (T cell surface glycoprotein)	98.2±2.4	APC	BD Biosciences
CD105	SH-2, endoglin	91.9±10.8	PE	R&D Systems
HLA-DR	Major histocompatibility class II antigens	0.6±0.3	PE	Immunotools

Table 5. Cell plating densities used in studies **I-III**.

	Study I	Study II	Study III
Cell density	300 cells/cm^2 (Western blot: 4200 cells/cm^2)	400 cells/cm^2	1100 cells/cm^2 (Western blot: 11 100 cells/cm^2)

Table 6. Media compositions used in the studies **I-III**.

Study	Basic culture medium	Osteogenic medium	Growth factors	BaG Ions	Inhibitors
I	BM (DMEM/F-12 + 5% HS + 1% P/S + 1% GlutaMAX) starvation BM (1% HS or 1% FBS)	BM supplemented with 200 µM L-ascorbic acid 2-phosphate, 10 mM β-glycerophosphate and 5 nM dexamethasone	rhBMP-2 (produced in E. Coli (Sigma-Aldrich) or in Chinese Hamster Ovary (CHO) cells (R&D Systems)), 0-100 ng/ml	-	-
II	BM (DMEM/F-12 + 5% HS + 1% P/S + 1% GlutaMAX)	BM supplemented with 250 µM L-ascorbic acid 2-phosphate, 10 mM β-glycerophosphate and 5 nM dexamethasone	-	S53P4, 2-06, 1-06 and 3-06 extracts (BM and OM)	-
III	DCC BM (hormones stripped from HS with dextran coated charcoal (DCC))	-	-		FAK, ERK, p38 and JNK inhibitors (see Table 13)

4.4 Isolation, characterization and culture of osteoblasts and bone marrow-derived mesenchymal stem cells

In addition to hASCs, the BMP-2 signaling mechanisms in study **I** were assessed in human osteoblasts and hBMSCs. Human osteoblasts were isolated from bone samples, obtained with surgical procedures performed in Department of Surgery, Oulu University Hospital (ethical approval R08009). Human BMSCs were purchased from Lonza and their immunophenotype was verified by the supplier with the analysis of the following surface markers: CD105, CD166, CD29, CD44, CD14, CD34 and CD45. Both osteoblasts and hBMSCs were cultured in the same conditions and in the same densities as hASCs.

4.5 Adipose stem cell viability and proliferation

In order to evaluate the cell viability and proliferation in the studied culture conditions, Live/Dead staining (Invitrogen, Thermo Fisher Scientific) (studies **II-III**) and CyQUANT Cell Proliferation Assay (Invitrogen, Thermo Fisher Scientific) (studies **I-III**), respectively, were conducted, according to the protocols provided by the manufacturers and described in detail in the original publications. The Live/Dead staining was visualized with a fluorescence microscope (Olympus, Tokyo, Japan). In study **II**, in addition to the DNA-based CyQUANT assay, the total protein amounts were measured from the same samples. The total protein amounts can also give information about the cell amounts in the samples and are thus used as an alternative way to normalize ALP activity. The total protein levels were determined by Pierce® BCA Protein Assay Kit (Thermo Fisher Scientific). Figure 7 indicates the time points of the viability and proliferation analyses in studies **I-III**.
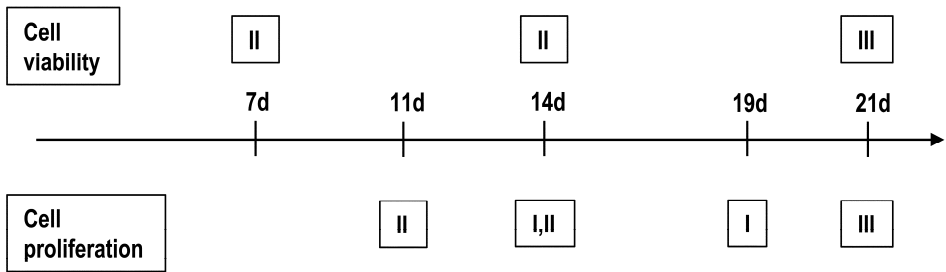
Figure 7. Timeline of the cell viability and proliferation assays conducted in studies **I-III**.

4.6 Differentiation analyses of adipose stem cells

In study **I** the effect BMP-2 stimulus on hASC osteogenic and adipogenic differentiation was evaluated. Studies **II** and **III** concentrated on the osteogenic response of hASC to BaG extracts and BaG discs combined with FAK and MAPK inhibitors, respectively. In study **I** the studied hASC donor lines were divided in two groups based on their differentiation response to BMP-2: group I representing the hASCs differentiating towards bone and group II the hASCs differentiating towards fat in response to BMP-2.

4.6.1 Osteogenic differentiation

Table 7 lists the various methods used to assess the osteogenic differentiation of hASCs in response to BMP-2 (study **I**), BaG extracts (study **II**) as well as BaG discs and inhibitor treatment (study **III**). These methods are briefly described below.

ALP activity
ALP activity was determined quantitatively (qALP) in studies **I-III** using the Sigma ALP (Sigma-Aldrich) procedure and the resulting absorbances were measured with Victor 1420 Multilabel Counter (Wallac, PerkinElmer) at 405 nm. The same cell lysates were used for the ALP analysis as for the CyQUANT and Pierce® BCA assays. The qALP activity values were presented either as such or normalized by dividing with the CyQUANT cell proliferation values or the total protein values.

qRT-PCR
qRT-PCR was used to analyze the expression of osteogenic marker genes *OSTERIX* and *RUNX2a* in study **III**. Briefly, the total mRNA was isolated from the samples using NucleoSpin RNA II kit (Macherey-Nagel, Düren, Germany) and the isolated mRNA was reverse transcribed to cDNA with the High-Capacity cDNA Reverse Transcriptase Kit (Applied Biosystems, Thermo Fisher Scientific). The expression data were normalized to the expression of housekeeping gene *RPLP0* (large ribosomal protein P0). *RPLP0* was chosen because it has been shown to have stable expression in adipose tissue (Fink et al., 2008; Gabrielsson et al., 2005). The relative expressions were calculated using a previously described mathematical model (Pfaffl, 2001). The sequences of the primers (Oligomer Oy, Helsinki, Finland) used in qRT-PCR and the accession numbers of the corresponding genes are depicted in Table 8.

Alizarin red S staining
In order to assess mineralization, an indicator of late osteogenesis, Alizarin red S staining, which stains the calcium minerals red, was conducted in studies **I** and **II**. In study **III**, Alizarin red S staining could not be used due to the high background staining of the BaG discs.

Raman spectroscopy
In study **II**, the mineral produced by the cells was further characterized with Raman spectroscopy, for which the cells were cultured in phenol red free medium (DMEM/F-12, +glutamine, -phenol red; Invitrogen, Thermo Fisher Scientific) because phenol red strongly interferes with Raman. For these analyses the cells were

cultured only in OM (control and extracts) due to the lack of mineral formation in extract BMs. The samples were collected with sterile H_2O and the Raman spectra were obtained as previously described (Ruokola et al., 2014).

Immunocytochemical stainings

In order to further study the osteogenic differentiation and extracellular matrix formation in study **II**, immunocytochemical staining (ICC) of osteocalcin, a marker of late osteogenic differentiation, and collagen-I, a major component of bone ECM, was conducted. The primary antibodies are presented in Table 9. The secondary antibody donkey anti-mouse Alexa Fluor® 488 IgG (Invitrogen, Thermo Fisher Scientific; dilution 1:1000) was used. In collagen-I ICC the actin cytoskeleton was stained with phalloidin-TRITC (Sigma-Aldrich; dilution 1:500). The nuclei were stained with 4',6-diamidino-2-phenylindole (DAPI; Molecular Probes, Thermo Fisher Scientific; dilution 1:2000) and the samples were imaged with a fluorescent microscope (Olympus).

Table 7. Analyses of osteogenic differentiation in studies **I-III**.

Study	Differentiation marker(s)	Technique	Time point(s)
I	qALP activity	ALP assay	14d
	mineralization	Alizarin red S staining	14d, 19d
II	qALP activity	ALP assay	11d, 14d
	mineralization	Alizarin red S staining	11d, 14d
	mineralization	Raman spectroscopy	17d
	collagen-I and osteocalcin production	ICC	13d
III	qALP activity	ALP assay	21d
	expression of *OSTERIX* and *RUNX2a*	qRT-PCR	14d, 21d

Table 8. The sequences of the primers used in qRT-PCR in studies **I** and **III**.

Name	5'-Sequence-3'	Product size (bp)	Accession number	Study
aP2	forward GGTGGTGGAATGCGTCATG reverse CAACGTCCCTTGGCTTATGC	71	NM_001442	**I**
OSTERIX	forward TGAGCTGGAGCGTCATGTG reverse TCGGGTAAAGCGCTTGGA	79	AF477981	**III**
RPLP0	forward AATCTCCAGGGGCACCATT reverse CGCTGGCTCCCACTTTGT	70	NM_001002	**I,III**
RUNX2a	forward CTTCATTCGCCTCACAAACAAC reverse TCCTCCTGGAGAAAGTTTGCA	62	NM_001024630.3	**III**

Table 9. Primary antibodies used in the osteogenic differentiation assessing ICCs in study **II**.

Antibody	Host	Dilution	Manufacturer	Study
collagen-I	mouse	1:2000	Abcam (Cambridge, United Kingdom)	**II**
osteocalcin	mouse	1:100	Abcam	**II**

4.6.2   Adipogenic differentiation

In study **I**, the effect of BMP-2 stimulus on adipogenic differentiation of hASCs was analyzed with qRT-PCR of adipogenic marker gene *aP2* (primer sequences in Table 8), and with Oil red O staining of lipid vacuoles combined with DAPI (Molecular Probes, Thermo Fisher Scientific; dilution 1:2000) staining of the nuclei. The staining was visualized with a fluorescence microscope (Olympus). The different analyses and corresponding time points to assess adipogenesis are listed in Table 10.

Table 10. Analyses of adipogenic differentiation in study **I**.

Study	Differentiation marker(s)	Technique	Time point(s)
I	*aP2* expression	qRT-PCR	14d
	lipid vacuole formation	Oil red O staining	19d

4.7 Analyses of cell attachment and signaling

4.7.1 Activation and production of signaling and attachment proteins

The activation (phosphorylation) of Smad1/5 in response to BMP-2-stimulus in study **I** as well as the activation of FAK and MAPKs in response to BaG contact in study **III** were analyzed with sodium dodecyl sulfate polyacrylamide gel electrophoresis (SDS-PAGE) and Western blotting. The same techniques were also used to analyze the production of cell attachment related proteins integrinβ1 and vinculin in hASCs grown on BaG discs in study **III**. The target proteins were probed with the primary antibodies listed in Table 11. The following horseradish peroxidase-conjugated secondary antibodies were used: goat anti-mouse IgG (Santa Cruz Biotechnology, Dallas, Texas, USA; dilution 1:2000) and anti-rabbit IgG (Cell Signaling Technology, Danvers, Massachusetts, USA; dilution 1:2000). For the analysis of the basal levels of non-phosphorylated proteins, the blots were stripped and blotted again by the primary antibodies listed in Table 11.

4.7.2 Intracellular localization of signaling and attachment proteins

In study **I**, the translocation of activated Smad1/5 into the nucleus was studied with ICC after 30min and 2h of BMP-2 stimulus. In these analyses also the intermediate filament protein vimentin was stained in order to better visualize the cells. In study **III**, the formation of FAs on BaG discs was analyzed with ICC of FA protein vinculin after 24h and 7d of culture. Vinculin staining was combined with the phalloidin-TRITC staining of actin cytoskeleton and DAPI staining of the nuclei. The primary antibodies used in the signaling and cell attachment ICCs are listed in Table 12. The secondary antibodies used were donkey anti-rabbit Alexa Fluor® 488 IgG (Invitrogen, Thermo Fisher Scientific; dilution 1:800) and anti-goat Alexa Fluor® 568 (Invitrogen, Thermo Fisher Scientific; dilution 1:800). The pSmad1/5 and vimentin double staining was visualized with the Olympus fluorescence microscope whereas the vinculin staining, requiring higher magnifications, was visualized with Zeiss Axio Scope.A1 fluorescence microscope (Zeiss, Oberkochen, Germany).

Table 11. Primary antibodies used in the Western blot analyses of studies **I** and **III**. The prefix "p" indicates phosphorylated form of the protein.

Antibody	Host	Dilution	Manufacturer	Study
β-actin	mouse	1:2000	Santa Cruz Biotechnology	**I, III**
p-c-Jun	rabbit	1:1000	Cell Signaling Technology	**III**
c-Jun	rabbit	1:1000	Cell Signaling Technology	**III**
pERK1/2	rabbit	1:2000	Cell Signaling Technology	**III**
ERK2	rabbit	1:500	Santa Cruz Biotechnology	**III**
pFAK	rabbit	1:1000	Cell Signaling Technology	**III**
FAK	rabbit	1:1000	Cell Signaling Technology	**III**
integrinβ1	mouse	1:500	Santa Cruz Biotechnology	**III**
pJNK	rabbit	1:1000	Cell Signaling Technology	**III**
JNK	mouse	1:500	Santa Cruz Biotechnology	**III**
p-p38	rabbit	1:1000	Cell Signaling Technology	**III**
p38α	rabbit	1:100	Santa Cruz Biotechnology	**III**
pSmad1/5	rabbit	1:1000	Cell Signaling Technology	**I**
Smad1	rabbit	1:1000	Cell Signaling Technology	**I**
vinculin	rabbit	1:500	Life Technologies, Thermo Fisher Scientific	**III**

Table 12. Primary antibodies used in the signaling and cell attachment ICCs of studies **I** and **III**. The prefix "p" indicates phosphorylated form of the protein.

Antibody	Host	Dilution	Manufacturer	Study
pSmad1/5	rabbit	1:200	Cell Signaling Technology	**I**
vimentin	goat	1:200	Invitrogen, Thermo Fisher Scientific	**I**
vinculin	rabbit	1:100	Life Technologies, Thermo Fisher Scientific	**III**

4.7.3 The role of signaling proteins in osteogenic differentiation

In order to determine the role of FAK and MAPKs in BaG-induced osteogenic differentiation in study **III**, these proteins were inhibited during the culture with the specific inhibitors depicted in Table 13. The effect of these inhibitions on qALP activity and the expression of osteogenic marker genes *RUNX2a* and *OSTERIX* was evaluated. Furthermore, the effect of FAK inhibition on downstream signaling and cell attachment was evaluated with Western blotting and vinculin ICC. Fresh inhibitors were provided for the cells at the time of each medium change (twice a week).

Table 13. The inhibitors used in study **III**.

| Target	Inhibitor	Final concentration	Manufacturer
FAK	PF562271	2 µM	Selleckchem, Munich, Germany
MEK-ERK	PD98059	60 µM	Calbiochem, Merck Millipore, Billerica, MA, USA
p38	SB202190	2 µM	Calbiochem, Merck Millipore
JNK	SP600125	10 µM	Selleckchem

4.8   Statistical analyses

Statistical analyses were performed with SPSS Statistics version 22 (IBM, Armonk, NY, USA). All the quantitative data are presented as mean and standard deviation. The quantitative cell analyses of ALP, cell proliferation and mineralization were repeated with hASCs from 3-5 donors, with 3-4 parallel samples in each culturing condition (n=9-20). Gene expression analyses were conducted with hASCs from 3-4 donors with no parallel samples (n=3-4). The statistical significances between the different conditions were evaluated with non-parametric statistics using Kruskal-Wallis one-way analysis of variance by ranks to determine whether there are significant differences within a data set, and with Mann-Whitney post hoc test to analyze the specific sample pairs for significant differences. Non-parametric testing was chosen because, due to the relatively small n, an assumption of a normally distributed data would have been unjustified. In order to control the familywise error-rate, all the resulted p-values were corrected using Bonferroni adjustment based on the number of planned comparisons. The result was considered statistically significant when the adjusted p-value < 0.05.

5   Results

5.1   Bioactive glass surface structures and dissolution

The BaG disc surfaces and the glass reaction layer formation were analyzed with SEM in study **III** in order to characterize the material surface affecting the behavior of the cells cultured in direct contact with the BaGs. As seen in Figure 8, a heavy cell-covering CaP precipitate was formed on the S53P5 surface, whereas on 1-06 no such precipitate was detected. The presence of the precipitate on S53P5 but not on 1-06 implies to a higher rate of reactivity of S53P4. In order to further study the glass reactivity, the BaG discs were cut and the cross-sections were imaged with SEM (Figure 8). When comparing the two glass types, the uppermost CaP layer was totally missing from the 1-06 samples whereas in S53P4 21d blank sample it was well visible. The cross-section data of the reaction layers thus give further evidence about the higher reactivity of S53P4 when compared to 1-06 in cell culture medium. Interestingly, when comparing the blank and the cell containing samples after 21d of culture, the reaction layers seem to be thinner in cell-containing samples, suggesting that the presence of the cells has a distinct effect on BaG surface reactions.

In order to analyze the BaG dissolution behavior, the concentrations of the ions released from the glasses were measured from the medium with ICP-OES technique in studies **II** and **III**. The ion concentrations of the BaG extracts used as cell culture media in study **II** are listed in Table 14. As a reference, the ion concentrations were also measured from the DMEM/F-12 medium. All the extracts contained Ca, but the concentrations were highest in 2-06 and 3-06 extracts. Potassium levels were elevated only in 1-06 and 2-06 extracts since these were the only glass compositions containing K. Similarly, only Mg containing 1-06 released Mg to the medium. Phosphorous levels dropped below the limit of quantification in S53P4, 2-06 and 3-06 extracts, and were very low also in 1-06 extract, due to the specific glass surface reactions during the dissolution. Silicon, which was not present in DMEM/F-12, was found in all the extracts in similar levels. Also Na release from the glasses was somewhat equal with only slightly lower concentration in 1-06 extract. Finally, 2-06 and 3-06 contained trace amounts of B in the extract composition.
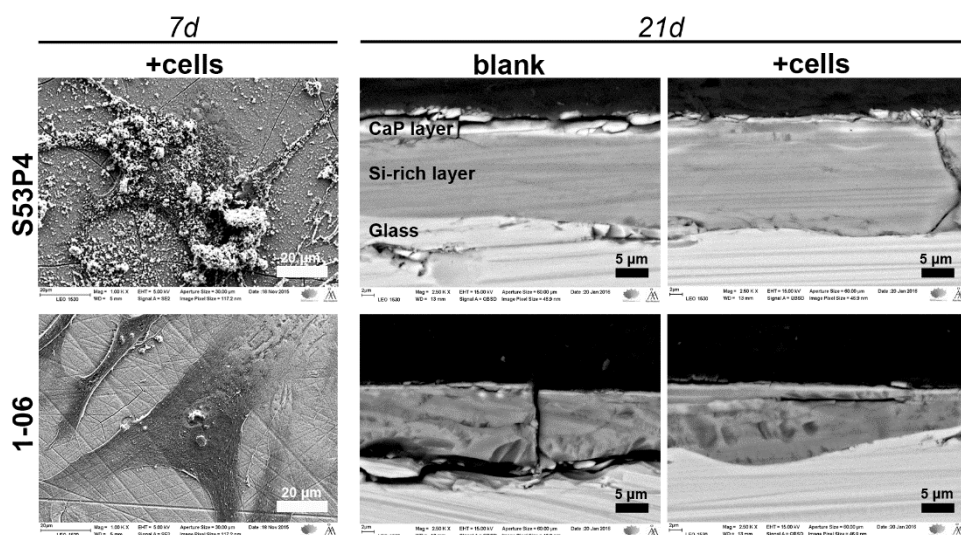
Figure 8. SEM analysis of BaG discs in study **III**. SEM images of hASCs on the glass surface after 7d of culture as well as cross-section SEM images of the blank and cell-containing samples after 21d of culture. The typical glass reaction layers (CaP layer, Si-rich layer and the bulk glass) are indicated in the 21d S53P4 blank sample.

In study **III** the cells were cultured in direct contact with the glass discs, but they were still exposed to the influence of the glass dissolution products. This prompted us to analyze the ion concentrations from the medium samples collected at each medium change (Figure 9). Since only 1-06 glass contains K, Mg and B in its formulation, elevated concentrations of these ions were only detected in 1-06 samples. With respect to Si, the release kept constant throughout the cell culture period for both S53P4 and 1-06. In the case of Ca and P, a more profound depletion of these ions was observed in the S53P4 samples than in the 1-06 samples, implying that more CaP was precipitated onto S53P4 than onto 1-06. This is in line with the heavy CaP precipitate on S53P4 glass and the formation of a visible CaP layer at 21d time point as seen in the cross-section image of a S53P4 disc (Figure 8).

When comparing the cell-containing and blank samples, in the 1-06 cell-containing samples, unlike in the blank samples, K and Mg concentrations kept increasing during the culture period (Figure 9). Similarly, the release of B, even though quite low in general, was somewhat higher from the cell-containing 1-06 samples than from the blanks samples. Moreover, higher Ca concentrations were also seen in both S53P4 and 1-06 cell-containing samples than in the blanks. It therefore seems evident that the presence of cells on the glass surface affects the BaG reactivity with respect to both reaction layer formation and ion release from the glasses.

Table 14. Ion concentrations of the BaG extracts in study **II**. All the concentrations are mg/kg and they were analyzed after 24h of extraction by ICP-OES. The samples contained antibiotics and GlutaMAX but no serum or osteogenic supplements. (<LOQ = below limit of quantification)
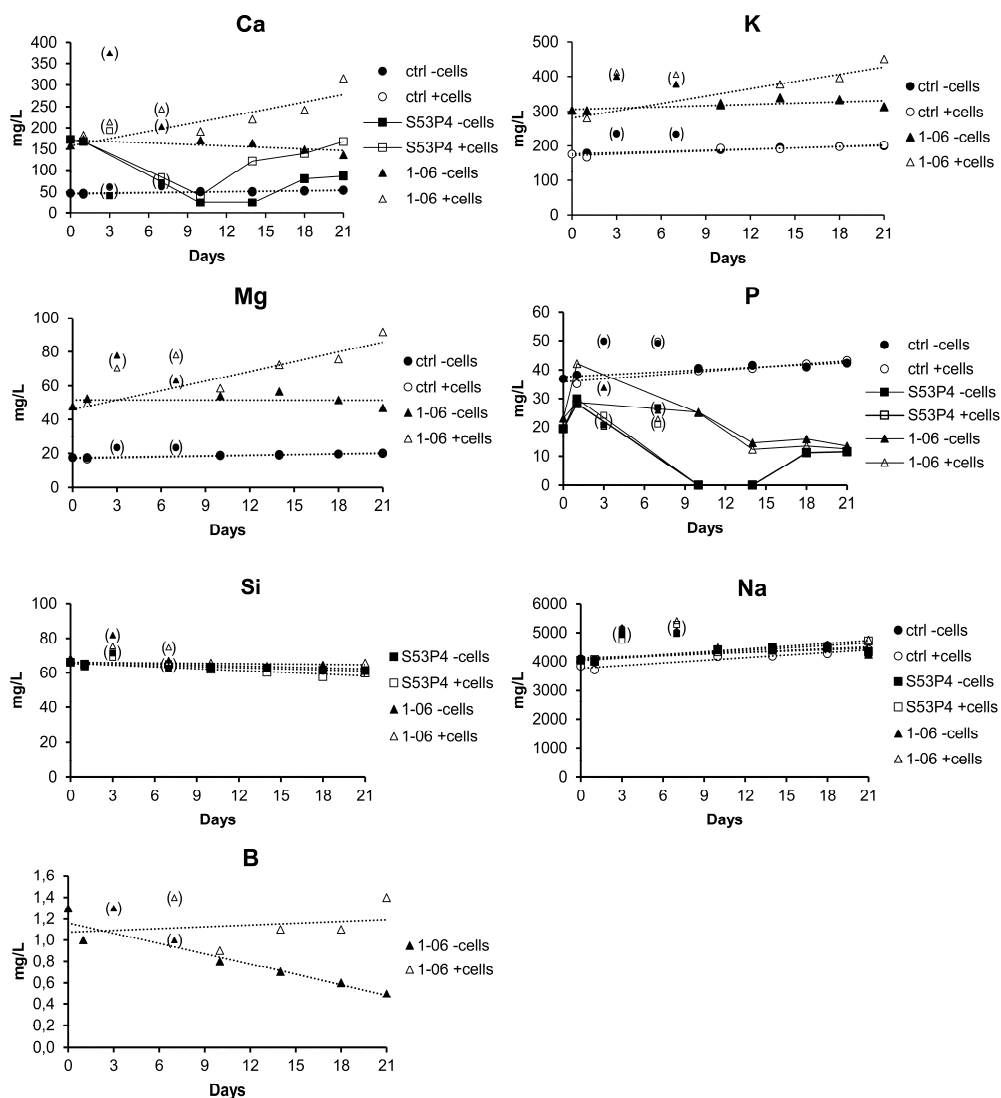
	Ca	K	Mg	P	Si	Na	B
DMEM/F-12	41	173	18	30	<LOQ	3480	<LOQ
S53P4	115	180	16	<LOQ	61	3760	<LOQ
2-06	153	360	16	<LOQ	53	3730	3.4
1-06	116	243	40	21	52	3620	<LOQ
3-06	131	172	16	<LOQ	56	3750	2.6

5.2   Cell proliferation and viability

The influence of the different culturing conditions on hASC proliferation was evaluated with CyQUANT cell proliferation assay (Invitrogen, Thermo Fisher Scientific) in studies **I-III**. The viability of the hASCs was studied with Live/dead staining (Invitrogen, Thermo Fisher Scientific) in studies **II** and **III**.

In study **I** the BMP-2 treatment significantly decreased the proliferation of hASCs in both group I and group II after 14 and 19 days of culture, regardless of the culturing medium (BM/OM). In study **II** the effect of the BaG extracts on the hASC proliferation seemed to be dependent on the base medium. Specifically, all the BM extracts increased the proliferation at 11d and 14d when compared to the control BM, and at 14d the difference was even statistically significant with 1-06, 2-06 and 3-06. On the contrary, all the OM extracts significantly decreased the proliferation at 14d when compared to the OM control. At 11d, however, the decrease was statistically significant only with S53P4 OM and the magnitude still considerably small. Therefore, the proliferation was not initially compromised in either of the extracts, and the cell amount dropped in the extract OMs only between 11 and 14 days of culture. The viability staining showed that, despite the changes in the cell amounts, none of the extracts negatively affected the cell viability.

In study **III** the hASC proliferation was significantly increased on both of the BaG discs (S53P4 and 1-06) after 21 days of culture. Moreover, of the different inhibitors only FAK inhibitor significantly reduced the cell amount on the glasses, whereas in control cells grown on polystyrene also ERK and JNK inhibitors significantly decreased the proliferation. However, there were still a lot of cells in all the culture conditions enabling further analysis with these inhibitor concentrations. Furthermore, none of the culture conditions compromised cell viability.

Figure 9. Ion release from of the BaG discs in study **III**. Ion concentrations of Ca, K, Mg, P, Si, Na and B were analyzed with ICP-OES from medium samples collected at each medium change. Both blank samples (-cells) and cell-containing samples (+cells), from both control wells and BaG disc wells, were analyzed. A linear trendline (dash line) was fitted when the release was approximately linear. In Ca and P graphs a continuous line was added to the BaG samples to make the temporal fluctuation in the ionic levels clearer. Measurement values of the 3d and 7d samples are shown in parentheses due to their systematically too high values, possibly caused by concentration of these particular samples due to transient humidity change in the cell culture incubator. Ctrl=control (polystyrene). No Si or B was present in the control medium, and no K, Mg or B was detected in the S53P4 samples.

5.3   Cell attachment on BaGs

When the cells are cultured in direct contact with the BaG, as we did in study **III**, the attachment mode and attachment-related mechanisms are likely to have a considerable effect on the cellular behavior. Therefore, the hASC attachment on S53P4 and 1-06 BaG discs was analyzed with Western blotting of integrinβ1 and vinculin, as well as vinculin ICC combined with phalloidin staining of actin cytoskeleton. As seen in Figure 10, the production of integrinβ1 was clearly increased on both glasses after 3d and 7d of culture. With vinculin the enhanced production was detected at all the time points studied. Interestingly, the inhibition of FAK did not seem to have a clear effect on the production of either of these proteins.

The Western blot analysis demonstrated that the BaGs had an influence on the hASC attachment, possibly making it stronger when compared to the polystyrene. However, when the mature focal adhesion sites were visualized with vinculin ICC, some atypical characteristics were observed in the focal adhesions on the glasses (Figure 11). After 24h of culture (Figure 11A) the focal adhesions were still small on all the substrates. At 7d (Figure 11B), however, typical-looking large adhesion sites were observed on the control polystyrene at the end of the actin fibers, whereas on both of the glasses the focal adhesions were still small but present in large amounts and dispersed throughout the cell. Moreover, the actin fibers of the cells grown on the BaGs were not as stretched or orientated as the fibers of the control cells on polystyrene. At some points the actin fibers on the BaGs seemed to be even partially disorganized. As with the integrinβ1 and vinculin production, the inhibition of FAK did not affect the vinculin amount or arrangement nor the appearance of the actin fibers on the glasses. On control polystyrene, on the other hand, it impeded the formation of large focal adhesion sites at 7d and made the actin fibers even thicker.
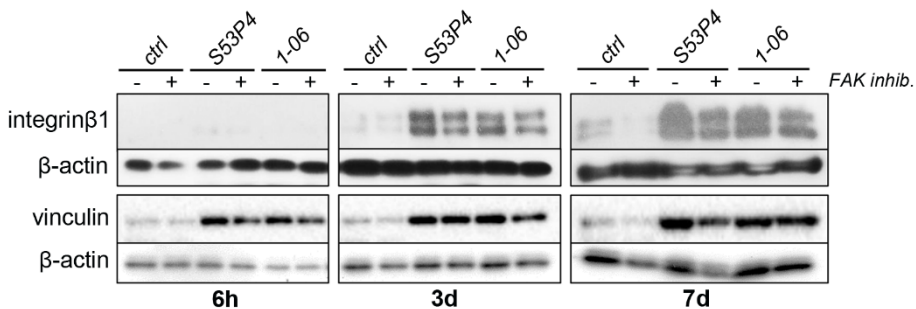
Figure 10. The production of integrinβ1 and vinculin on BaG discs in study **III**. Integrinβ1 and vinculin production was studied with Western blotting after 6h, 3d and 7d of culture. β-actin served as a loading control. FAK inhibitor PF562271 (2 µM) was used. ctrl=control (polystyrene).
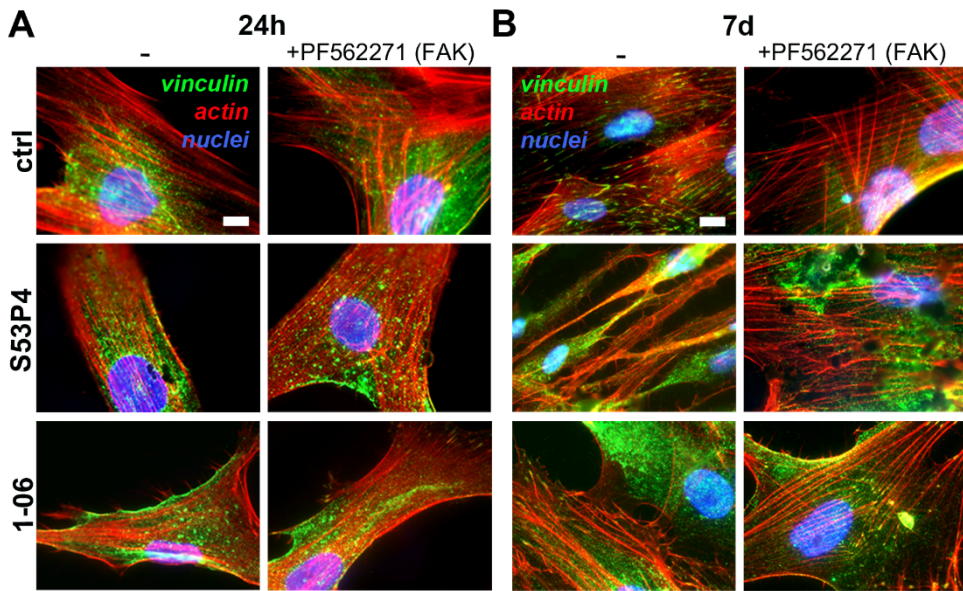
Figure 11. Focal adhesions and cytoskeleton on BaG dics in study **III.** Mature focal adhesions were visualized with vinculin ICC after 24h (**A.**) and 7d (**B.**) of culture. Vinculin is stained green, actin cytoskeleton red with phalloidin and nuclei blue with DAPI. Scale bars 10 μM. FAK inhibitor PF562271 (2 μM) was used. ctrl=control (polystyrene).

5.4 Activation of intracellular signaling

### 5.4.1 BMP-2-induced Smad signaling in hASCs, hBMSCs and osteoblasts

In study **I** the activation and functionality of the BMP-2 induced Smad1/5 signaling route was evaluated in hASCs, hBMSCs and osteoblasts. Furthermore, the effect of the rhBMP-2 production origin (E. coli versus CHO cells) as well as the culture condition (HS versus FBS) on the signaling response was determined. BMP-2-induced Smad1/5 activation was detected after 24h and 7d of stimulus in the hASCs from both group I and group II, as seen in Figure 12A. The Smad1/5 activation levels were clearly higher with rhBMP-2 produced in CHO cells when compared to the protein produced in E. coli. Once activated, Smad1/5 was successfully translocated into the nucleus in hASCs from both groups, regardless of the BMP-2 source (Figure 12B). The BMP-2-induced nuclear translocation of pSmad1/5 occurred also in hBMSCs and osteoblasts (data not shown). When comparing the Smad1/5 activation in HS and FBS media, it was observed that in HS conditions the

BMP-2-induced activation was considerably stronger in all the three cell types studied (hASCs, hBMSCs and osteoblasts) (Figure 13). The strength of the Smad1/5 activation correlated positively with the BMP-2 concentration. All in all, the BMP-2-Smad1/5 signaling pathway seems to be functional in hASCs from both group I and group II, as well as in hBMSCs and osteoblasts, although the BMP-2 source and culture conditions cause differences in the signal strength.
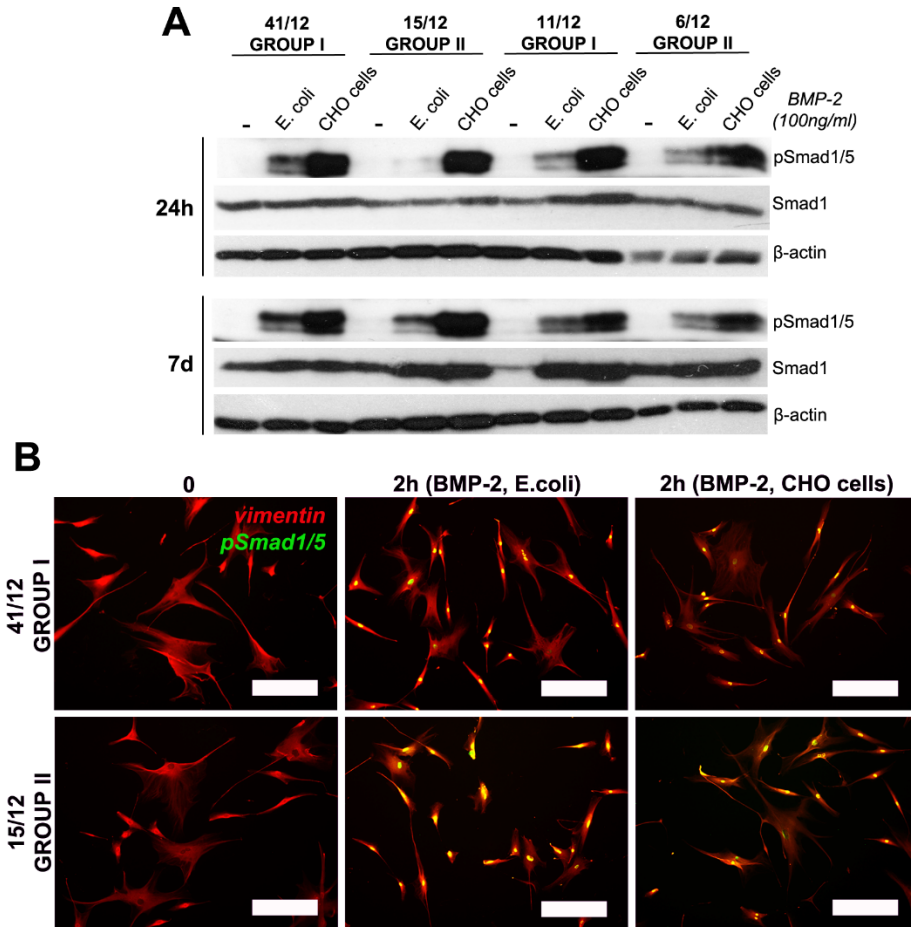
Figure 12. Smad1/5 activation and translocation to the nucleus in hASCs stimulated by BMP-2 produced in E. coli or in CHO cells (study **I**). **A.** Western blot analysis of Smad1/5 activation (phosphorylation; pSmad1/5) after 24h and 7d of BMP-2 stimulation. Also the basal levels of Smad1 were analyzed. β-actin served as a loading control. **B.** Translocation of pSmad1/5 to the nucleus after 2h of BMP-2 stimulation, analyzed by ICC. Scale bars 200 μm. ctrl=unstimulated cells. rhBMP-2 produced either in CHO cells (R&D Systems) or in E. coli (Sigma-Aldrich), 100 ng/ml. 41/12, 15/12, 11/12 and 6/12 denote hASCs donor lines, 15/12 and 6/12 belonging to group II and 41/12 and 11/12 to group I.
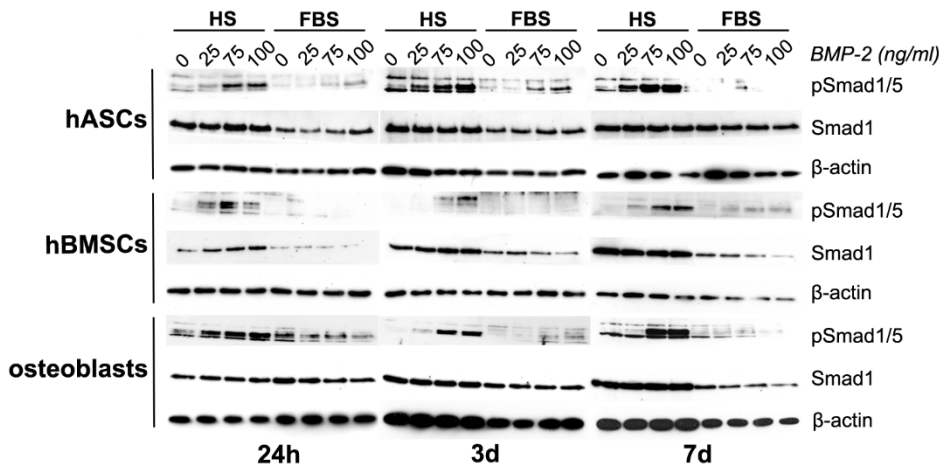
Figure 13. BMP-2-induced Smad1/5 activation in hASCs, hBMSCs and osteoblasts in HS and FBS culture conditions (study **I**). Western blot analysis of Smad1/5 activation (phosphorylation; pSmad1/5) after 24h, 3d and 7d of stimulation with increasing BMP-2 concentrations in HS and FBS media. Also the basal levels of Smad1 were analyzed. β-actin served as a loading control. rhBMP-2 produced in E. coli (Sigma-Aldrich).

5.4.2   BaG-induced FAK and MAPK signaling in hASCs

To evaluate the signaling response of hASCs on BaG discs S53P4 and 1-06 in study **III**, the activation of FAK and MAPKs was analyzed with Western blot method after 6h, 3d and 7d of culture. As seen in Figure 14A, no FAK activation could be detected at 6h and 3d time points, but at 7d the activation of FAK was clearly increased on both of the glasses when compared to the polystyrene control. The inhibition of FAK abolished the FAK activation, as expected. Interestingly, the glasses had an elevating effect also on the basal levels of FAK at 3d and 7d time points. When it comes to ERK1/2, the activation was initially observed only on the control polystyrene (Figure 14B). However, at later time points (3d and 7d), the ERK1/2 activation was increased by both glasses, but unlike with FAK, no elevation in basal levels could be seen. The inhibition of FAK seemed to have a decreasing effect on ERK1/2 activation. With respect to p38, there was an initial lack of activation on BaGs similar to ERK1/2, but unlike with FAK and ERK1/2, the activation levels of p38 on the glasses did not clearly exceed the activation on control polystyrene at the later time points (Figure 14C). On the contrary, on 1-06 the p38 activation was decreased at 3d and, in the presence of FAK inhibition, totally abolished. In the case of JNK no activation could be detected in either of the samples or conditions (data not shown), which led us to analyze the activation of JNK downstream target c-Jun in order to

obtain information about the JNK signaling on the BaGs. Interestingly, c-Jun was activated on both of the glasses after 3d and 7d of culture (Figure 14D). The inhibition of FAK, however, did not seem to greatly affect the c-Jun activation status. Similar to FAK, the BaGs also upregulated the production of c-Jun.
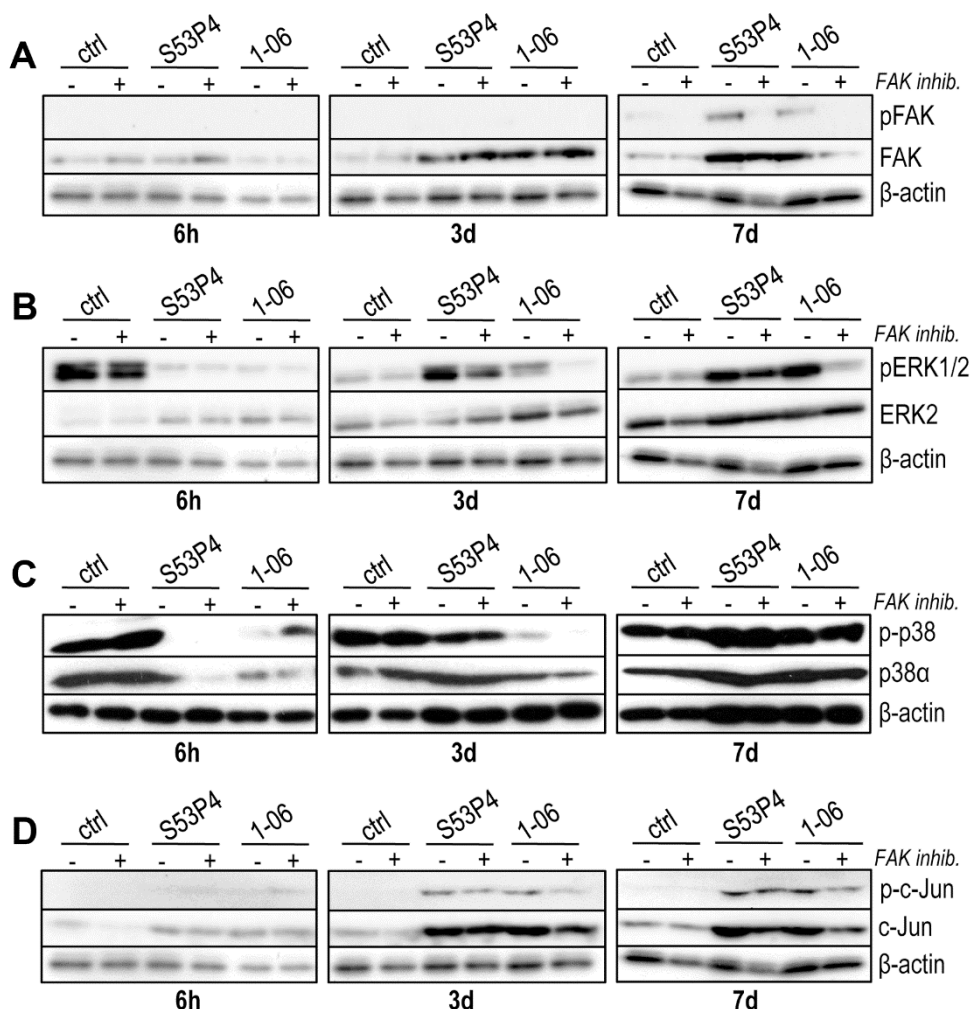

Figure 14. The activation of FAK, ERK1/2, p38 and c-Jun on BaG discs in study **III**. **A.** Western blot analysis of FAK activation (phosphorylation; pFAK) on the different materials at 6h, 3d and 7d. **B.** Western blot analysis of pERK1/2 activation (phosphorylation; pERK1/2) on the different materials at 6h, 3d and 7d. **C.** Western blot analysis of p38 activation (phosphorylation; p-p38) on the different materials at 6h, 3d and 7d. **D.** Western blot analysis of JNK downstream target c-Jun activation (phosphorylation; p-c-Jun) on the different materials at 6h, 3d and 7d. FAK inhibitor PF562271 (2 μM). Also the basal levels of each of these proteins were analyzed. β-actin served as a loading control. ctrl=control (polystyrene).

5.5 Osteogenic differentiation

5.5.1 The dual effect of BMP-2 on hASC osteogenic differentiation

In study **I**, the effect of BMP-2 stimulus on hASC osteogenic differentiation was evaluated. As seen in Figure 15A, the BMP-2 treatment in OM increased the qALP activity of the hASC donor lines of group I but, on the contrary, decreased it in group II. In BM the BMP-2 had a slightly decreasing effect on qALP in both groups but the qALP activities were very low in general. A similar trend was seen in the mineralization of the hASCs (Figure 15B): BMP-2 significantly increased the mineral formation in the OM condition in group I but decreased it in group II. In BM basically no mineralization was detected. Interestingly, when comparing the rhBMP-2 produced in E. coli and in mammalian CHO cells, the rhBMP-2 produced in mammalian cells induced a bigger increase in the qALP activity in a hASC donor line from group I, whereas in a hASC line from group II it decreased the qALP activity to a greater extent than the rhBMP-2 produced in E. coli. A similar BMP-2 origin-dependent effect was observed also in the mineralization levels. To summarize, the treatment with BMP-2 seems to either increase or decrease the osteogenic differentiation, depending on the hASC donor line and the effect is more pronounced with the rhBMP-2 produced in mammalian cells.
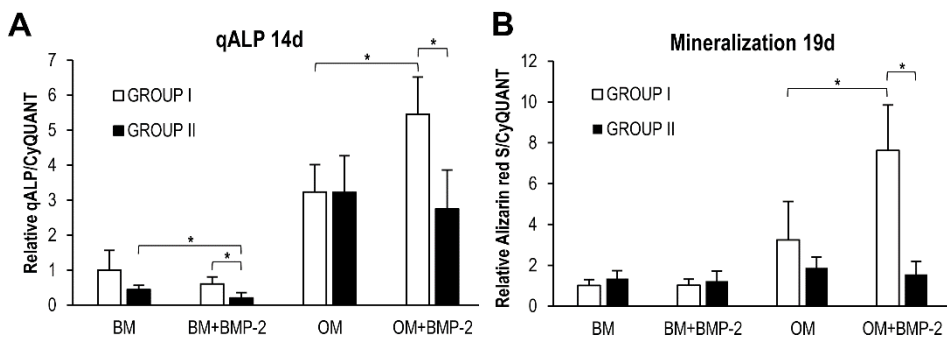
Figure 15. Osteogenic differentiation induced by BMP-2 in study **I**. **A.** Quantitative ALP activity normalized with the cell amount (determined by CyQUANT) at 14d. The results are relative to the group I BM. n=9. *$p<0.05$ between indicated groups. rhBMP-2 (R&D Systems, produced in CHO cells), 100 ng/ml. **B.** Quantified mineralization analyzed by Alizarin red S staining at 19d and normalized with the cell amount (determined by CyQUANT). The results are relative to the group I BM. n=12. *$p<0.05$ between indicated groups. rhBMP-2 (R&D Systems, produced in CHO cells), 100 ng/ml.

5.5.2 Discrepancy in the BaG extract induced ALP activity results

In order to analyze the early osteogenic differentiation induced by the BaG extracts in study **II**, the quantification of the ALP activity was conducted. Against the expectations, the total qALP activity at 11d was not affected by the extracts in either BM or OM, and at 14d all the four OM extracts significantly decreased the qALP (Figure 16A). By studying the qALP at 2d intervals from 4d to 14d with control OM and 2-06 OM samples, we also ruled out the possibility that qALP activity reached its peak outside the time points analyzed in the first place (Figure 16B). However, when the qALP activity was normalized with the cell amount determined by the DNA-based CyQUANT method, the result was almost the opposite (Figure 16C). BM extracts decreased the normalized qALP but in OM condition the extracts actually increased it. Also with closer inspection of the control OM and 2-06 OM samples the normalized qALP activity with 2-06 OM exceeded that of control OM after the 12d time point (Figure 16D). This discrepancy prompted us to test still an alternative method to present the qALP data, i.e. by normalizing the qALP with the total protein amount (Figure 16E and F). Unlike the qALP data normalized with CyQUANT, the normalization with the total protein amount gave a similar result as the total qALP activity with no normalization (Figure 16A and B). In summary, the qALP results may vary a lot between the different presentation modes.

5.5.3 BaG extracts with traditional OM supplements are superior inducers of late osteogenesis

Despite the discrepancy in the BaG extract induced qALP activities, the osteogenic differentiation in the extracts in study **II** was studied further by determining the mineralization, an indicator of the late stages of osteogenic commitment. As seen in Figure 17A, all the four OM extracts induced excessive mineral formation already after 14d of culture, whereas in control OM basically no mineral was detected at such an early time point. When quantified (Figure 17B), the difference was also statistically significant. Of the four OM extracts 2-06 and 3-06 turned out to be the strongest mineralization inducers. At the 11d time point or in either of the BM conditions, however, no signs of mineralization were observed. In order to further characterize the mineral produced by the cells, a Raman spectroscopic measurement of the OM samples was conducted (Figure 17C). All the OM extract samples had a peak in the Raman spectra corresponding to the peak detected in pure HA, whereas

in control OM no such peak was detected. Therefore, the CaP mineral produced by the cells in the extract OM samples was most likely HA.
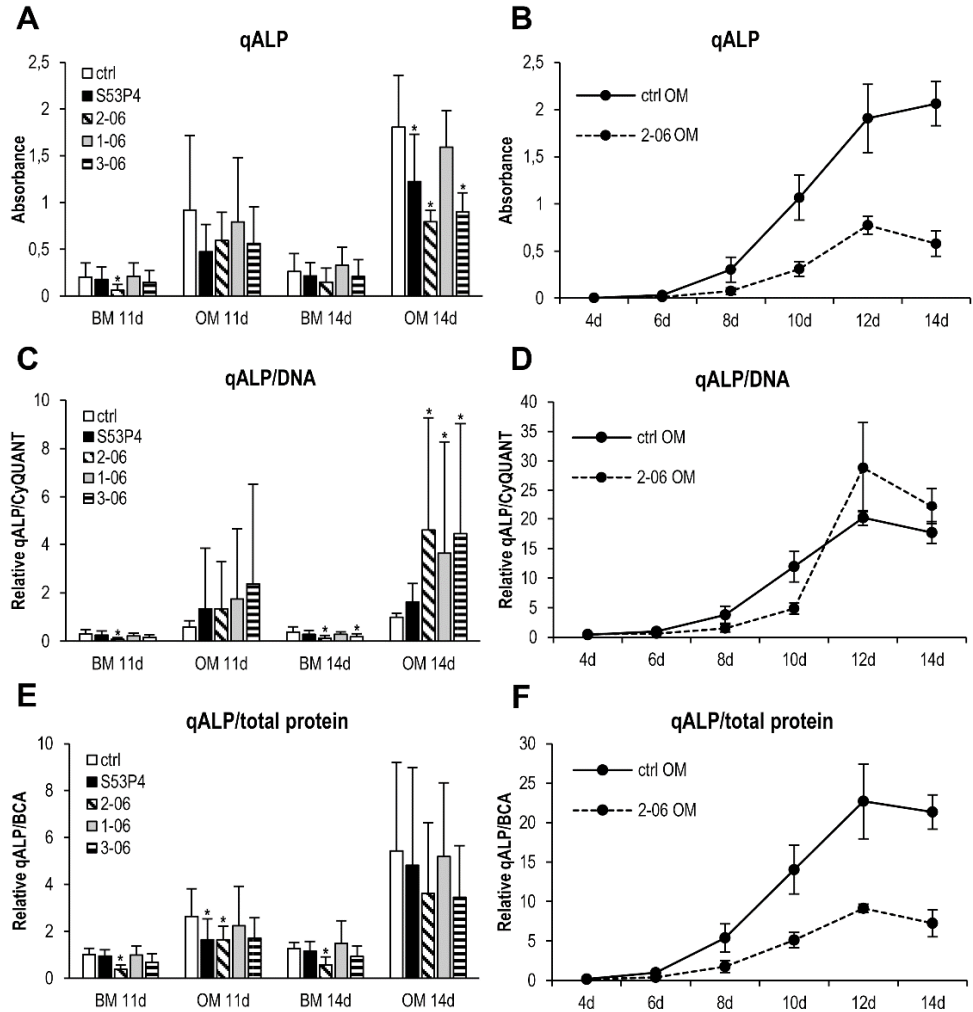

Figure 16. ALP activities induced by the BaG extracts in study **II**. **A.** Total quantitative ALP activity for all the samples at 11d and 14d. n=20. *$p<0.05$ between indicated group and the control (ctrl) BM/OM at the same time point. **B.** Total qALP activity for control (ctrl) OM and 2-06 OM extract samples assessed at 2d intervals from 4d to 14d. n=3. **C.** Quantitative ALP activity normalized with the cell amount (determined by CyQUANT). n=20. *$p<0.05$ between indicated group and the control (ctrl) BM/OM at the same time point. **D.** Quantitative ALP activity normalized with CyQUANT activity for control (ctrl) OM and 2-06 OM extract samples assessed at 2d intervals from 4d to 14d. n=3. **E.** Quantitative ALP activity normalized with the total protein amount (determined by BCA assay). n=20. *$p<0.05$ between indicated group and the control (ctrl) BM/OM at the same time point. **F.** Quantitative ALP activity normalized with total protein for control (ctrl) OM and 2-06 OM extract samples assessed at 2d intervals from 4d to 14d. n=3.

To further confirm the osteogenic phenotype induced by the OM extracts, collagen-I and osteocalcin ICCs were conducted after 13d of culture (Figures 18 and 19, respectively). With respect to collagen-I, all the OM conditions stimulated the production of this protein, but unlike in control OM, in which the collagen-I was still clearly inside the cells, in all the extract OMs collagen-I was secreted to the ECM. Moreover, in some spots the collagen-I had started to organize into fibrils. In case of osteocalcin, all the four OM extracts stimulated osteocalcin production, whereas in control OM no sign of this protein was detected. The BM conditions of both of these ICCs are omitted from the figures since only minimal amounts of collagen-I and osteocalcin were produced in the BMs. The ICC results are well in line with the mineralization data and thus confirm the osteogenesis-stimulating effect of the OM extracts.
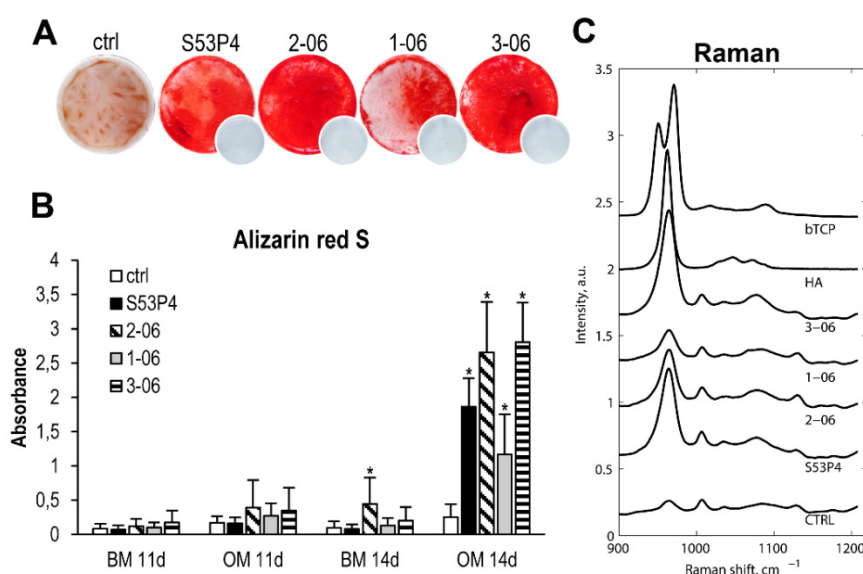

Figure 17. Mineralization induced by the BaG extracts in study **II**. **A.** Alizarin red S staining of control (ctrl) OM and OM extract samples at 14d. A representative sample well (area 1.8 cm^2) is depicted for each sample. Smaller images represent the blank samples (extracts incubated in the wells with no cells for the whole culturing period). The mineral is stained red. **B.** Quantification of the Alizarin red S staining. n=16. *p<0.05 between indicated group and the control (ctrl) BM/OM at the same time point. **C.** A Raman spectra of the studied samples, and standard samples of HA and β-TCP in the range of PO$_4^{3-}$ and CO$_3^{2-}$ vibration modes. The 960 cm^{-1}, 1008 cm^{-1}, 1030 cm^{-1}, and the broad band between 1060 and 1100 cm^{-1} originate from, PO$_4^{3-}$, phenylalanine, PO$_4^{3-}$, and PO$_4^{3-}$ and CO$_3^{2-}$ bands, respectively.
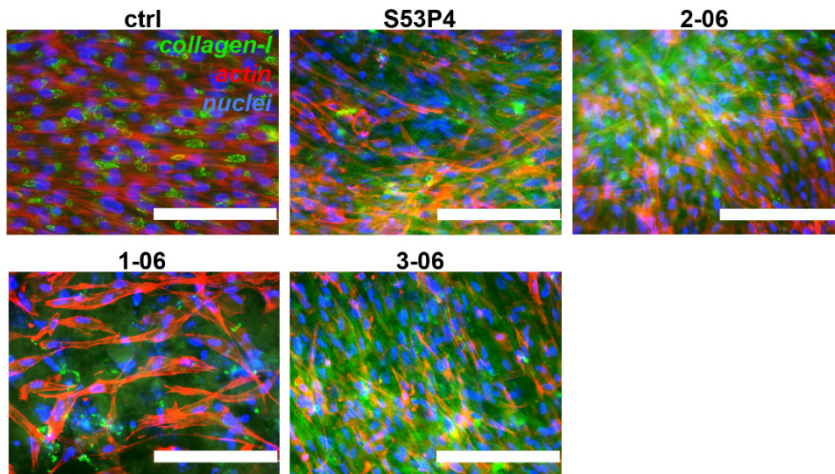
Figure 18. Collagen-I production in hASCs cultured in BaG OM extracts for 13d in study **II**. Collagen-I production was analyzed with ICC. Collagen-I is stained green, actin cytoskeleton red with phalloidin and nuclei blue with DAPI. ctrl=OM (with no glass ions). Scale bars 200 μm.
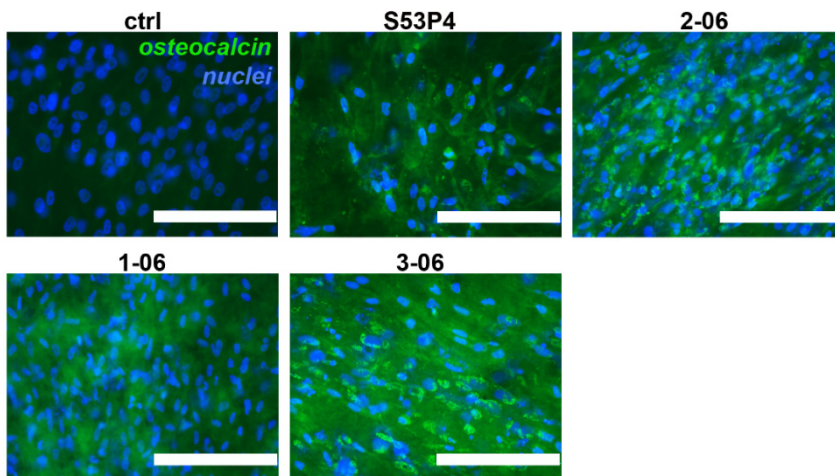
Figure 19. Osteocalcin production in hASCs cultured in BaG OM extracts for 13d in study **II**. Osteocalcin production was analyzed with ICC. Osteocalcin is stained green and nuclei blue with DAPI. ctrl=OM (with no glass ions). Scale bars 200 μm.

5.5.4 BaG disc-induced osteogenic differentiation and the effect of FAK and MAPK inhibition on it

In study **III**, hASCs were cultured on S53P4 and 1-06 discs in BM in order to study the osteogenic differentiation induced solely by the glasses and not affected by the

82

chemical substituents present in OM. Figure 20A shows that both of the glass types significantly increased the qALP activity when compared to the cells grown on control polystyrene. Moreover, 1-06 induced a significantly higher qALP activity than S53P4, suggesting that 1-06 might be a stronger inducer of early osteogenic differentiation. Both glasses also increased the expression of the osteogenic marker genes *RUNX2a* and *OSTERIX* (Figure 20B and 20C, respectively), although in the gene expression level no clear differences between the glass types were observed.

After determining the osteoinductive capacity of the BaGs we were interested to study the intracellular signaling mechanisms regulating the BaG-induced early osteogenic differentiation. For that, hASCs were cultured on the discs in the presence of specific inhibitors for FAK, ERK1/2, p38 and JNK. The inhibition of FAK, ERK1/2 and JNK significantly decreased the ALP activity on both of the glasses (Figure 20D) and also decreased the expression of *RUNX2a* and *OSTERIX* (Figure 20E and 20F, respectively), suggesting an important role for these molecules in BaG-induced early osteogenic differentiation. With respect to p38, the inhibition slightly decreased the ALP activity on both S53P4 and 1-06 (Figure 20D), but in the gene expression level the effect was negligible (Figure 20E and 20F). Therefore, the role of p38 in BaG-induced early osteogenic differentiation seemed to be less significant.
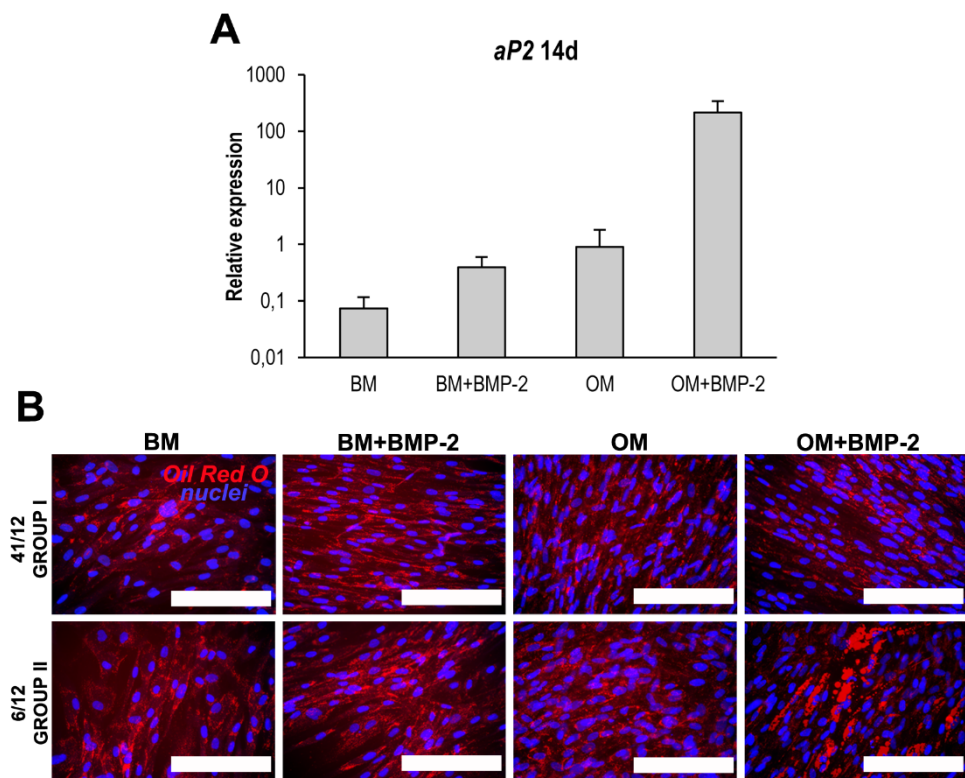
5.6   Adipogenic differentiation

5.6.1   The effect of BMP-2 on adipogenic differentiation of hASCs

In study **I**, the hASC donor lines from group I differentiated towards bone in response to BMP-2 stimulus but in group II the hASCs showed no indications of osteogenic commitment. Moreover, lipid vacuoles were detected in the group II hASCs with light microscopy (data not shown), necessitating a closer evaluation of the adipogenic fate of hASCs under BMP-2-stimulus. In Figure 21A the expression of adipogenic marker gene *aP2* is depicted. Since the donor lines in group I and group II behaved similarly with respect to the gene expression, the graph in Figure 21A represents combined data from hASCs donor lines from both groups. In OM condition the BMP-2-stimulus induced a several hundred-fold increase in the *aP2* expression levels, indicating a strong adipogenic response. However, when adipogenesis was evaluated with Oil red O staining of lipid vacuoles, BMP-2 in OM induced lipid formation only in the hASC donor lines from group II (Figure 21B).
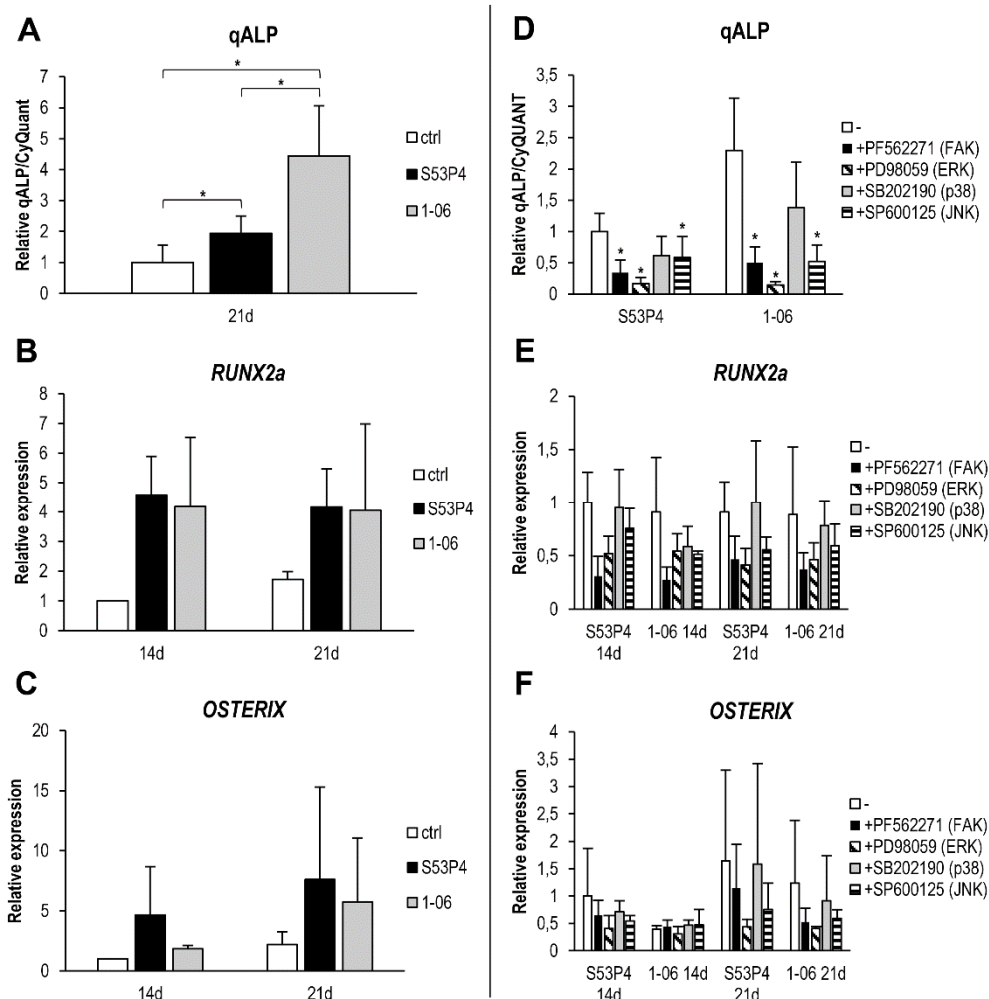
Figure 20. Osteogenic differentiation of hASCs on S53P4 and 1-06 BaG discs and the effect of FAK and MAPK inhibition on it in study **III**. **A.** Quantitative ALP activity normalized with the cell amount (determined by CyQUANT). hASCs were cultured on control (ctrl) polystyrene and BaG discs in DCC BM. The results are relative to the ctrl. n=12. *p<0.05 between indicated groups. **B.** *RUNX2a* expression of hASCs cultured on control (ctrl) polystyrene and BaG discs in DCC BM. The results are relative to the 14d ctrl. n=4. **C.** *OSTERIX* expression of hASCs cultured on control (ctrl) polystyrene and BaG discs in DCC BM. The results are relative to the 14d ctrl. n=4. **D.** The effect of the FAK and MAPK inhibitors on CyQUANT-normalized qALP on BaG discs in DCC BM. The results are relative to the S53P4 (-). n=12. *p<0.05 between the indicated group and the (-) sample of the same glass. **E.** The effect of the FAK and MAPK inhibitors on *RUNX2a* expression on BaG discs in DCC BM. The results are relative to the 14d S53P4 (-). n=4. **F.** The effect of the FAK and MAPK inhibitors on *OSTERIX* expression on BaG discs in DCC BM. The results are relative to the 14d S53P4 (-). n=4.

Figure 21. The effect of BMP-2 on adipogenic differentiation of hASCs in study **I**. **A.** The expression of *aP2* at 14d. n=3. **B.** Oil red O staining of lipid vacuoles at 19d. Oil red O stains lipid vacuoles red. Nuclei are stained blue with DAPI. Scale bars 200 μm. BMP-2 (R&D Systems, produced in CHO cells) 100 ng/ml.

6 Discussion

6.1 The effect of BMP-2 on human adipose stem cell differentiation is donor-dependent

Being approved for clinical use as a recombinant human protein for the treatment of bone traumas and disorders, BMP-2 has established its position as a strong bone formation inducing agent. However, due to the recent findings, the research community has started to adopt a more critical approach to this widely exploited growth factor. First of all, the increased clinical use has been accompanied with a variety of undesired and harmful side-effects, such as inflammation, swelling and inappropriate adipogenesis (James et al., 2016). Moreover, recent *in vitro* and *in vivo* findings strongly suggest that the use of BMP-2 does not always enhance the osteogenic differentiation of stem cells and might actually even decrease it (Chou et al., 2011; Cruz et al., 2012; Tirkkonen et al., 2013; Waselau et al., 2012; Yi et al., 2016; Zuk et al., 2011). These emerging data prompted us to conduct a closer evaluation of the BMP-2 responses in hASCs in order to obtain more evidence about the utility of BMP-2 use in the bone TE applications.

Based on our data, the stimulation of all the donor hASC lines, as well as hBMSCs and osteoblasts, with BMP-2 resulted in increased Smad1/5 activation and efficient translocation of the activated Smad1/5 to the nucleus, indicating a fully functional signaling route. In contrast to our observations, Zuk and co-workers could not detect the activation of the Smad1/5 signaling in hASCs stimulated with the same concentration of BMP-2 as used in study I, even though the cells were shown to express the necessary BMP receptors on their surface (Zuk et al., 2011). However, the experiments of Zuk and co-workers were conducted in FBS-containing culture medium, which might have a negative effect on the rhBMP-2 bioactivity and therefore explain the non-functional BMP-2 signaling. Indeed, when we analyzed the Smad1/5 activation in HS versus FBS containing culture medium, there were constantly higher activation levels in the HS condition in all hASCs, hBMSCs and osteoblasts, which supports this hypothesis.

Despite the fully functional canonical BMP-2 signaling route in all the hASCs donor lines evaluated, the differentiation outcome was clearly donor-dependent:

whereas other hASC donor lines responded to the BMP-2 stimulus by differentiating towards bone, other donor lines were committed to the adipogenic fate. The adipogenic commitment was not totally unexpected since there is evidence that BMP-2 can also stimulate adipogenic differentiation (Hata et al., 2003; H. Huang et al., 2009; Kang et al., 2009; Park et al., 2012). However, unlike in the study of Park and co-workers, who observed the BMP-2 induced adipogenesis of human alveolar bone-derived stromal cells in AM (Park et al., 2012), in study **I** the BMP-2-induced adipogenesis of hASCs occurred in OM. It is conceivable that some hASC donor lines have such a strong and inherent adipogenic tendency that, despite of the osteogenic stimulus provided by the OM, they adopt an adipogenic fate when stimulated by BMP-2. Interestingly, in the gene expression level, also the donor lines differentiating towards bone in response to BMP-2 showed increased expression of the adipogenic marker gene *aP2*, suggesting that all the hASCs, possibly related to their tissue of origin, possess a certain level of adipogenic tendency. However, Kang and co-workers demonstrated that the osteogenesis and adipogenesis of C3H10T1/2 cells upon BMP-2, BMP-4, BMP-6, BMP-7 and BMP-9 stimulation was mutually exclusive even though the cells undergoing osteogenic and adipogenic differentiation were closely located (Kang et al., 2009). This might suggest that also in study **I** the *aP2* expressing subpopulation of the hASCs was distinct from the subpopulation committing towards osteogenesis in the same sample. On the other hand, Kang et al. also observed that the overexpression of *PPARγ* enhanced not only adipogenesis but also osteogenesis induced by the BMPs and, conversely, the knockdown of this adipogenesis master regulator inhibited both of these differentiation fates (Kang et al., 2009). Therefore, in the level of transcriptional regulation, the osteogenic and adipogenic commitment might be even more closely intertwined than generally expected.

Regardless of the ultimate differentiation outcome, the canonical BMP-2 signaling seemed to be similarly activated in all the hASC donor lines. This means that there must be other mechanisms regulating the BMP-2 response and explaining the variable differentiation behavior. It has been suggested that, in the receptor level, BMPR-1B might be primarily responsible for osteogenic responses whereas BMPR-1A is mainly involved in adipogenesis (McArdle et al., 2014; Wan et al., 2006; Zielins et al., 2016), thus providing one possible mechanism explaining the divergence of the BMP-2-induced osteogenesis and adipogenesis. Of course, there is also extensive and complex cross-talk between BMP-2 signaling and various other signaling pathways, such as integrin, MAPK, Wnt and FGF-2 signaling (Agas et al., 2013; Aquino-Martinez et al., 2016; Fuentealba et al., 2007; Guicheux et al., 2003;

Suzawa et al., 2002), which enables the fine-tuning of the ultimate behavioral responses. However, the exact signaling mechanisms responsible for the divergence of the BMP-2-induced osteogenesis and adipogenesis are still mainly unknown. Figure 22 sums up the observations made about the BMP-2-induced signaling responses and differentiation outcomes in study I.

In study I, we also evaluated the effect of the production origin, i.e. mammalian cells versus bacteria, on the cellular responses of rhBMP-2. Even though the rhBMP-2 from both of the production origins induced essentially similar responses with respect to signaling activation, proliferation and differentiation, the responses to the rhBMP-2 produced in mammalian cells, either positive or negative, were constantly stronger. Since post-translational glycosylation can be only conducted in mammalian cells but not in bacteria, the rhBMP-2 produced in CHO cells is likely to have a more physiological conformation and thus higher bioactivity than the rhBMP-2 produced in E. coli. Indeed, when comparing the effect of glycosylated and non-glycosylated BMP-2 on C2C12 cells, van de Watering and co-workers observed that the glycosylated form induced significantly higher ALP activities than the non-glycosylated form (van de Watering et al., 2012). Therefore, in addition to the culture conditions (e.g. differentiation medium and serum supplementation), the production origin of rhBMP-2 might be also one factor explaining the varying cellular BMP-2 responses reported in the literature.

So far, rhBMP-2 supplementation has been utilized in some of the hASC-based clinical bone TE treatments (Mesimäki et al., 2009; Sandor et al., 2013; Taylor, 2010; Wolff et al., 2013), but since these case reports cannot provide comparative data about the outcome without rhBMP-2, the ultimate benefits of using this growth factor as part of the treatment remain unclear. In light of our current data and the studies of others, the advantages of using BMP-2 as a bone formation inducing agent seem to be highly questionable. Even though some of the negative effects of BMP-2 on osteogenesis *in vitro* can be possibly explained by the varying culture conditions as well as the BMP-2 production origin, it seems clear that the donor-dependent factors, likely related to varying signaling mechanisms, arrangement of the BMP receptors and pre-commitment of the cell populations, play a major role in defining the ultimate differentiation outcome. Still, there are studies reporting no beneficial effect of BMP-2 stimulus on *in vivo* bone formation with cell-biomaterial constructs, but increased bone formation with BMP-2-incorporated materials without the seeded cells (Chou et al., 2011; Yi et al., 2016). Therefore, the endogenous cells might still respond favorably to BMP-2 even though the implanted cells would not, adding a further level of complexity to the BMP signaling scheme.
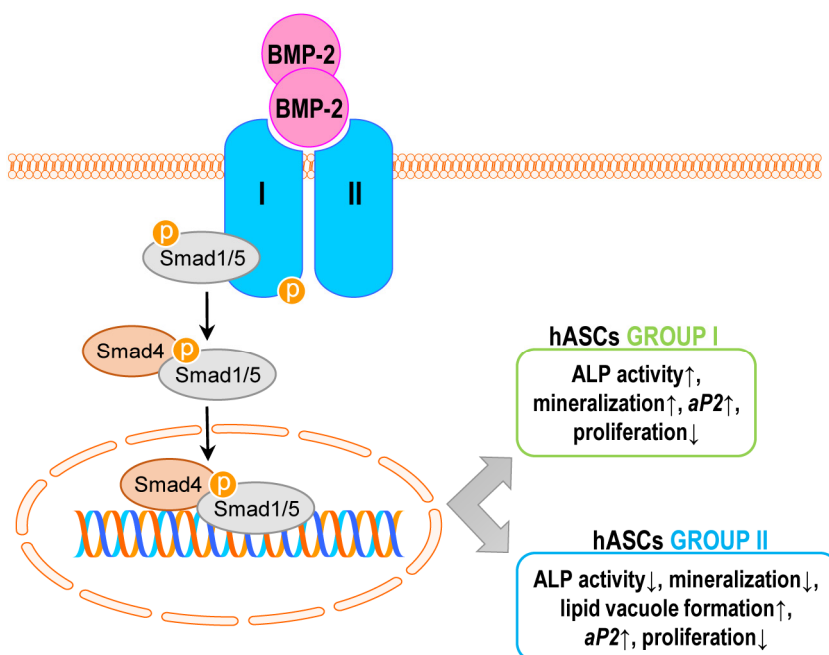
Figure 22. BMP-2 signaling events and differentiation responses observed in study **I**. Despite the equivalent signaling mechanisms for BMP-2 in all the hASC donor lines studied, the differentiation outcome varied. Whereas some cell lines (group I) responded to BMP-2 stimuli with increased osteogenesis, others (group II) preferentially differentiated towards adipocytes. However, the expression of *aP2* was increased in all the hASC donor lines in response to BMP-2. Moreover, BMP-2 decreased cell proliferation regardless of the differentiation fate. The observations about the BMP-2-induced differentiation responses were made in OM culture condition; in BM the BMP-2 treatment had only minor effects on hASC differentiation. ↑=increase, ↓=decrease.

6.2 Osteogenic medium supplemented with BaG ions is a superior osteoinducer when compared to the non-supplemented OM

The invention of BaG by Larry Hench (Hench et al., 1971) has undoubtedly been a remarkable milestone for the field of biomaterial research. However, despite the wide-spread exploitation of various BaG formulations in the clinics, only relatively recently there has started to be an increasing interest in the specific mechanisms by which the glasses affect the cell behavior. Specifically, in addition to the glass surface properties, the ionic dissolution products from the glasses have gained some attention as potential regulators of cellular responses (Hoppe et al., 2011; Lakhkar et al., 2013). Thus far, however, the cellular responses to the BaG extracts have not been studied with MSCs and, moreover, the choice of the BaG compositions used in the

dissolution studies has been somewhat restricted (Table 2). Therefore, we were determined to broaden the knowledge about this important matter in study **II** by analyzing the hASC viability, proliferation and osteogenesis in BaG ions containing extracts prepared from S53P4, commercially known as the BonAlive® glass, and three experimental silicate glasses, namely 2-06, 1-06 and 3-06.

Based on the observations that ions from the BaGs BG60S, 58S and 45S5, in concentrations comparable to our extracts, could stimulate the osteogenic differentiation even without any OM supplements added (Alves et al., 2015; Gong et al., 2014; Tsigkou et al., 2009), we hypothesized that this would be the case also with our BM extracts. However, none of the BM extracts could induce the osteogenic differentiation of hASCs within the time frame studied (up to 14 days). The OM extracts, on the other hand, induced an extensive and fast osteogenic response, as determined by mineralization and osteocalcin and collagen-I production. The reason for the lack of the late osteogenic differentiation in the BM extracts might be at least partially explained by the extremely low phosphorous, and thus phosphate, concentration in all the four extract. As a result of the glass surface reactions, not much phosphate was leaked into the medium and consequently, there was no source for this essential raw material for the mineralization to occur. In OM extracts, on the other hand, the supplemented β-glycerophosphate and L-ascorbic acid-2-phosphate served as the necessary phosphate sources. Another factor potentially explaining the progressed osteogenesis in the OM extracts but not in the BM extracts is the OM extract-induced production, secretion and, to some extent, the organization of collagen-I, which was not observed in the BM conditions. It has been shown that the formation of mature collagen-I containing ECM is a prerequisite for mineralization since it functions as a platform for mineral crystal growth (Landis & Silver, 2009; Y. Wang et al., 2012). Ascorbic acid, present only in OM conditions, is considered an essential substance for the proper formation and secretion of collagen-I (Langenbach & Handschel, 2013), and therefore it is not surprising that the BM extracts as such could not support the collagen-I production. Interestingly, despite the presence of ascorbic acid, the hASCs in control OM did not secrete the collagen-I even though in the OM extracts they clearly did. Therefore, the ionic dissolution products must play a role in the collagen-I containing ECM formation. In fact, it has been observed that of the different ions in the BaG extracts at least Si has the ability to stimulate collagen-I synthesis (Reffitt et al., 2003).

The unexpected extent and rate of the mineralization in the OM extracts prompted us to verify the result with an alternative method, in addition to the traditional Alizarin red S mineralization staining. Therefore, Raman spectroscopic

analysis was conducted for the OM samples and the results of this measurement confirmed the presence of large amounts of (calcium-)phosphate in all the OM extracts. The Raman spectra of these samples were quite similar to the spectra of pure HA, suggesting that the mineral formed in the extracts probably consisted mainly of HA, which is also the main CaP species in the structure of bone.

An additional goal in study **II** was to compare the osteogenesis-inducing capability of the different BaG extracts. Based on Alizarin red S staining and visual evaluation of the amounts of osteocalcin and collagen-I, 2-06 and 3-06 OM extracts seemed to be the strongest stimulators of hASCs' osteogenic differentiation. Probably not coincidentally, these two extracts contained the highest concentrations of Ca, an essential component of the CaP mineral. Apart from its role as a raw material for mineralization, Ca-induced cell signaling events have been also tightly coupled to the regulation of osteogenic differentiation (Barradas et al., 2012; Bolander et al., 2016; Samavedi et al., 2013; Shin et al., 2008). These studies suggest that the stimulation of osteogenesis by Ca might involve Ca channels, Ca sensing receptors, as well as ERK1/2, PKC and BMP signaling pathways. In addition to the high Ca concentrations, 2-06 and 3-06 extracts, unlike the other extracts, contained also traces of B, which in small concentrations has been considered an osteogenesis-stimulator (H. Fu et al., 2009; Hakki et al., 2010; Ying et al., 2011). The slightly poorer performance of 1-06, on the other hand, might be caused by the elevated Mg concentration in this extract. Based on previous studies, high Mg concentration can work as a negative regulator of osteogenesis (Leidi et al., 2011; Saffarian Tousi et al., 2013). Lastly, also Si has been shown to support osteogenic differentiation, (Reffitt et al., 2003; Shie et al., 2011), but due to the similar levels in all the four extracts, this ion cannot explain the differences between the BaGs.

All in all, even though it is tempting to speculate the separate role of each individual ion in the extract media, it is likely that the ultimate cellular response in caused by the specific combination of the different ions. Therefore, no matter how appealing, the favorable outcome achieved with the OM extracts might not be possible to reach by supplementing the medium with single ionic species. With respect to this matter, Saffarian Tousi and co-workers, after observing the osteogenesis-enhancing effect of 45S5 and 6P53-b extracts on MC3T3-E1 cells, made an attempt to evaluate the role of single or double ion supplementation on osteogenic differentiation (Saffarian Tousi et al., 2013). Even though Ca, Si and Ca+Si all enhanced osteogenic differentiation in OM conditions when compared to the control OM, the Ca+Si double supplementation did not perform any better than the Si supplementation alone. Unfortunately, these supplementations were not

compared to the original extracts and, in addition to the *osteocalcin* expression, no other differentiation markers were evaluated. Thus, further comparative analyses are needed to confirm whether the multi-ion composition of the extracts is truly the superior one or if the enhanced osteogenesis is possible to achieve with more simplified medium compositions, which would naturally be preferable for large scale production of well-defined clinical-grade products. Moreover, the field of research evaluating the effect of ionic dissolution products on cellular behavior would certainly benefit from standardized methods and procedures, since currently the comparison of the studies is seriously hampered by the highly varying experimental setups. Due to different cell types, glass compositions, medium supplements, differentiation markers as well as versatile extraction protocols, it is not surprising that the results obtained thus far are somewhat inconsistent (Table 2). In general, the cellular responses to BaG ionic dissolution products is a topic which is little by little establishing its position as an important sector of the BaG research but currently the amount of studies concentrating on this aspect is still surprisingly small, and there is certainly a huge need for a more thorough evaluation.

6.3 Alkaline phosphatase activity - a reliable indicator of bone formation?

In literature, ALP activity is probably the single most utilized indicator of osteogenic differentiation. Indeed, the activity of this membrane-bound enzyme is thought to be indispensable for the onset of mineralization, since it generates inorganic phosphate for the formation of CaP minerals but also decreases the levels of inhibitory pyrophosphates (Millan, 2013; Murshed & McKee, 2010), thus reasoning its established position as a marker of osteogenic differentiation. In line with this, the analysis of ALP activity was also conducted in all the studies (**I-III**) of this work. In study **I**, the ALP activity data, normalized with the DNA amount determined by CyQUANT assay, supported well the mineralization staining, thus raising no doubts on the reliability of this marker. In study **III**, the Alizarin red S mineralization staining was not possible due to technical limitations (i.e. the strong staining of the HCA surface of the glass), but when compared to the gene expression of *RUNX2* and *OSTERIX*, there were no remarkable contradictions in the CyQUANT normalized ALP activity, further supporting the use of ALP activity as an osteogenic marker. However, in study **II** the situation was more complicated. Despite the tremendous increase in the mineral production induced by the OM extracts, the ALP

activity values, not yet normalized at the initial stage, seemed to either stay unaffected or even decrease in response to the extract treatment. Although there is evidence that such a decrease in ALP activity levels could be explained by the high Ca concentration in the culture medium (An et al., 2012; Maeno et al., 2005; Takagishi et al., 2006; Xynos et al., 2000), we were determined to evaluate the ALP activity in a bit more detail.

In literature, ALP activity is typically presented either as such (i.e. the total ALP activity) or then normalized to the cell amount (using either total DNA or total protein as the measure of cell number), the latter being often more favorable since it eliminates the distorting effect of varying cell amounts on the ALP activity. Due to the unexpected total ALP activity results in study **II**, we tested both of these two normalization methods to our data, which resulted in highly contradicting outcomes. Whereas normalization with total protein amounts gave a similar outcome as the total ALP activity, normalization with DNA turned the situation upside down, giving the highest ALP activity values to the OM extracts. Also the closer inspection with 2d intervals, aiming to rule out the possibility of ALP activity peaks outside the time points studied, provided a similar contradictory result with constantly lower total ALP activity and ALP activity/total protein values for the 2-06 OM extract than for the control OM, but ALP activity/DNA values exceeding those of the control at later time points. Which one of these ALP activity presentation modes should be then used? One might say that the DNA amount is a better measure of cell number than the total protein, which does not necessarily increase linearly with increasing cell amount, but still, normalizing enzymatic activity with the total protein amount in the sample is an established mode favored by many researchers. On the other hand, in some cases the comparison of the total ALP activities might serve the purpose better than the comparison of the normalized ALP activity values. Either way, the fact that the final result seems to be highly dependent on the ALP activity presentation mode is clearly alarming, and seriously attenuates the comparability as well as the reliability of the ALP activity results in a myriad of studies. This certainly demands for a closer analysis of the role of ALP activity in osteogenesis and, ultimately, for a standardized method to conduct and present the ALP activity data.

In addition to the discrepancies in the ALP activity data presentation, there is also accumulating evidence that ALP activity might not serve as a reliable predictor of later stages of osteogenesis. For example, it has been observed that neither the expression of *ALP* nor ALP activity correlates well with hBMSC mineralization capacity *in vitro* (Marklein et al., 2016; Matsuoka et al., 2013). Moreover, *ALP* gene expression, ALP protein production and ALP activity also poorly predict the *in vivo*

bone formation outcome of hBMSCs-seeded CaP constructs (Larsen et al., 2010; Mendes et al., 2004; Mentink et al., 2013). Prins and co-workers, on the other hand, detected a correlation between ALP activity and *in vivo* bone formation, but this was only seen with ALP activity induction (fold-increase of 7d and 11d ALP values when compared to 1d values) and not with the absolute values, which could be actually lower in the *in vivo* bone forming cells (Prins et al., 2014).

All in all, in light of the recent data, ALP activity might not be suitable as a universal indicator of the ultimate bone formation outcome. It might serve well as a marker of early osteogenic differentiation but no conclusions should be made about the progression of the osteogenesis to the late stages based on ALP activity alone. It is plausible that, even though the mineralization cannot be initiated without the activity of ALP, the ALP activity might not need to be elevated above a certain threshold level to initiate the mineral nodule formation. This would explain why high ALP activity may not always be a necessity for increased mineralization or *in vivo* bone formation. Indeed, a reliable verification of osteogenic commitment likely requires a wide palette of markers, the optimal set of which still needs to be determined.

6.4   Cell attachment on bioactive glasses: a reciprocal interaction between the cells and the bioactive glass surface

With respect to TE, a proper interaction between the biomaterial and the cells, either seeded prior to implantation or migrating from the surrounding tissues *in situ*, is the key to successful healing. Most importantly, the biomaterial should support stem and progenitor cell attachment, which is mediated via cell surface integrins binding to the ECM proteins adsorbed on the biomaterial surface. Although it might appear relatively simple, the protein adsorption and, consequently, the cell attachment is a relatively complex process, which is strongly affected by the submicron and nanoscale features of the biomaterial surface (e.g. roughness, porosity) as well as surface charge, crystallinity and solubility (Samavedi et al., 2013). In the molecular level, the surface nanoscale features have been shown to induce modulations in the FA formation and cytoskeletal arrangement, ultimately leading to changes in cell signaling events responsible for various cellular outcomes, such as differentiation (Biggs et al., 2010). With respect to BaG biomaterials, we observed in study **II** that the released ions without the OM supplements could not stimulate the osteogenesis of hASCs, but the direct culture on the glasses, as shown in study **III** and studies by others (Haimi

et al., 2009b; Waselau et al., 2012), can stimulate the early osteogenic differentiation of hASCs even without any additional chemical supplements. This highlights the role of cell attachment in the BaG-induced osteogenesis and prompted us to conduct a more detailed evaluation of the cell-BaG interaction as one potential factor explaining the favorable effect of the BaGs on cell behavior. Despite the extensive characterization of BaGs *in vitro*, *in vivo* and also in clinical settings, the various aspects related to the cell attachments mechanisms and to the underlying signaling events are currently poorly understood.

Previous studies with hMSCs cultured on varying surface topographies and micropatterns created on synthetic polymer substrates have demonstrated that the formation of strong and mature FA sites, characterized by the presence of vinculin, is highly connected to the osteogenesis-inducing ability of these surfaces (Biggs et al., 2009; Kilian et al., 2010). In sharp contrast to these observations, we were not able to detect any large and prominent FA sites on either of the BaG discs during the evaluation period (up to 7 days), even though these materials were clearly inducing early osteogenic differentiation of hASCs. Initially (after 24h), the FAs were small, relatively scarce and evenly distributed throughout the cells on all the materials evaluated, but after 7 days of culture they had adopted a typical-looking appearance at the end of the actin fibers on control polystyrene. On BaGs, on the other hand, the FAs remained small and evenly dispersed, although their amount was considerably large as verified by the increased vinculin production on the BaGs detected by Western blot analysis. These observations challenge the previous data about the tight connection of large FAs and the occurrence of osteogenesis, and suggest that the size and distribution of the FAs as such might not dictate the cell fate exclusively. Interestingly, despite the lack of large FA sites, the glasses upregulated the production of not only vinculin but also integrinβ1, which might imply enhanced attachment mechanisms on the BaGs. Pennisi and co-workers observed a somewhat similar appearance of fibroblasts on roughened platinum surfaces, with an elongated shape accompanied by small and dispersed FAs (Pennisi et al., 2011), suggesting that the surface roughness of the BaGs, clearly evidenced in the SEM figures, might be an underlying factor explaining the atypical attachment of hASCs on the BaG surfaces. Furthermore, the BaG reactivity and, consequently, the continuous remodeling of the glass surface, is also likely affecting the cell attachment and might explain the lack of stable and prominent FAs on the BaGs. Such a dynamic growth surface may stimulate the attachment mechanisms with an alternative manner by inducing the formation of a vast amount of smaller, possibly less stable, attachment sites as observed on the glasses.

The surface properties of the biomaterial substrate, by affecting the cell attachment mode, modulate also the arrangement of the underlying actin cytoskeleton and, consequently, cell shape. During osteogenesis, the spindle-shaped MSCs typically turn into cuboidal shaped cells with the initially organized and parallel thin actin fibers rearranging into a robust network of reorganized thick stress fibers (Rodriguez et al., 2004; Yourek et al., 2007). Closely related to the actin arrangement, it has been observed that stiff matrices enabling cell spreading and high cellular tension favor osteogenesis of stem and progenitor cells (Biggs et al., 2009; Engler et al., 2006; Hsieh et al., 2016; Hwang et al., 2015; Khetan et al., 2013; Kilian et al., 2010; J. Lee et al., 2014; McBeath et al., 2004). Even though on the BaGs the actin cytoskeleton adopted a slightly disorganized appearance when compared to the more organized actin arrangement on the control polystyrene, thus supporting the observation of osteogenic differentiation, the thick stress fibers were still evidently missing and the shape of the cells was still more spindle-shaped than highly spread. Therefore, in addition to the atypical FAs, also the cell shape and actin arrangement on the BaGs deviated from the typical appearances associated with osteogenic differentiation. It is likely that the BaG surface roughness and reactivity are reflected to the actin cytoskeleton via the unorthodox attachment mode and are thus responsible for the distinctive cell morphology not typically associated with osteogenesis. Interestingly, Huebsch and co-workers demonstrated that, in 3D, the osteogenic cell fate did not correlate with cell morphology (Huebsch et al., 2010), suggesting that a specific morphology might not be the ultimate factor determining the cell fate. Moreover, with respect to the actin cytoskeleton, Rodriguez and colleagues observed, that even though the integrity of the actin cytoskeleton at the initial stage of differentiation seems to be highly important, later on rapid changes occur in the actin monomer/polymer equilibrium enabling the cytoskeletal reorganization associated with osteogenic differentiation (Rodriguez et al., 2004). Thus, depending on the time point analyzed, the actin cytoskeleton might transiently look disorganized and atypical, even though the cells are still committing towards an osteoblastic phenotype.

Based on the data obtained in study **III**, the surface properties of the BaGs have a distinct effect on the cell attachment and shape. However, when thinking a little bit further, one might speculate whether the cells also affect the BaG surface on which they are cultured. Indeed, this seems to be the case since we observed a slower accumulation of CaP and, consequently, a thinner CaP reaction layer on the cell-containing discs when compared to the blank discs. Moreover, slightly higher ion concentrations were measured from the medium of the cell-containing samples than

from the blank samples, indicating that in the presence of cells a larger number of the ions released from the glass network are free in the medium rather than entrapped in the formed CaP layer. Even though these results merely scratch the surface of the modifying action of the cells on the BaG surface, they clearly alleviate the need to take the reciprocal nature of the cell-BaG interaction into account when designing and evaluating BaG structures and their cellular responses for TE applications.

6.5 Bioactive glass induced early osteogenic differentiation is mediated by focal adhesion kinase and mitogen-activated protein kinases

Biomaterial surface features have a profound effect on the cell attachment mode as discussed above, but this does not only cause changes in the actin cytoskeleton, cell shape and tension, but also in intracellular signaling mechanisms leading ultimately to changes in cell behavior, such as commitment to certain lineages. It has become clear that these attachment-initiated integrin-mediated signaling mechanisms regulate also the osteogenic commitment, and involve the activation of FAK, MAPKs and, as a last link of the signaling chain, Runx2 (Biggs & Dalby, 2010). However, even though the central role of the integrinβ1-FAK-MAPK signaling scheme in the osteogenic differentiation has been established on ECM-based biomaterials (e.g. collagen-I, collagen-II, laminin) (Chiu et al., 2014; Shih et al., 2011; Takeuchi et al., 1997; Viale-Bouroncle et al., 2014b) and there is also evidence of the importance of this route on CPCs (Lu & Zreiqat, 2010; Lu et al., 2012), currently there is very little knowledge about the cell signaling response on BaGs. Therefore, in study **III** the analysis of the cell attachment mechanisms on the BaGs was extended to the analysis of the underlying signaling responses, the focus being on the integrinβ-FAK-MAPK signaling, which is known to be an important regulator of osteogenesis on other biomaterials.

Before digging into the signaling mechanisms, we wanted to confirm the osteogenesis-inducing ability of our glasses in the absence of any added osteogenic supplements. Based on the analysis of early osteogenic markers, namely ALP activity and *RUNX2a* and *OSTERIX* expression, both of the glasses stimulated the early osteogenic differentiation of hASCs. Interestingly, 1-06 induced a significantly higher ALP activity than S53P5, suggesting that it is a stronger stimulator of early osteogenic differentiation. This might be related to the glass compositions since 1-06, unlike S53P4, contains a small amount of B, which has been shown to be advantageous for the osteogenic differentiation of hBMSCs in a similar

concentration as released into the culture medium in study **III** (around 1 mg/L) (Ying et al., 2011). Moreover, the SEM analysis revealed that S53P4 was more reactive than 1-06, which resulted in heavy, cell-covering CaP precipitate on S53P4 already after 7 days of culture. Even though no clear differences were found between the glasses in the cell attachment analysis, the higher reactivity of the S53P4 surface might slightly hamper the cell-BaG interaction, and thus result in a weaker osteogenic response. Interestingly, in study **II** the S53P4 OM extract was a stronger osteoinducer than the 1-06 OM extract, but since this result was obtained in the absence of the cell-BaG contact and the surface phenomena, a direct comparison is somewhat questionable and therefore no contradiction necessarily exists. Moreover, study **III** focused on the early osteogenic events in the absence of any OM supplements whereas in study **II** the main findings were connected to the late stages of osteogenesis in OM-based BaG extracts, which further complicates the direct comparison of these studies.

After indicating the ability of both of the studied glasses to induce early osteogenic differentiation of hASCs, we were determined to elucidate the roles of FAK and MAPKs in the BaG-induced osteogenic commitment. With respect to FAK, both of the glasses were observed to stimulate FAK activation after 7d of culture and, upon FAK inhibition, the early BaG-induced osteogenic response was greatly diminished. Thus, similar to the observations made on ECM-based biomaterials (Chiu et al., 2014; Salasznyk et al., 2007a; Salasznyk et al., 2007b; Shih et al., 2011; Takeuchi et al., 1996; Viale-Bouroncle et al., 2014b), FAK seems to have a central role also in the BaG-induced early osteogenic differentiation. In addition, FAK activation has been previously observed on ceramic biomaterials as well as on BaG-containing composites (G. H. Kim et al., 2015; Marino et al., 2010; Shie & Ding, 2013; J. Zhang et al., 2015) but in these studies the role of FAK in the osteogenic differentiation was not directly measured. Interestingly, Hamilton and Brunette reported increased activation of FAK on various microfabribated topographies when compared to smooth surfaces (Hamilton & Brunette, 2007), suggesting that also with the BaGs the surface topography might be one underlying factor affecting the activation of FAK. Indeed, the surface roughness of the glasses might not only affect the cell attachment mechanisms but also the underlying signaling, as evidenced by the FAK activation which is known to be directly coupled to the integrin-mediated cell attachment. Moreover, the activation of FAK on the glasses further proves that, even though the attachment mode observed was not typical for the cells committing towards the bone phenotype, it still evokes cellular responses favoring the osteogenic differentiation. Furthermore, no dramatic changes were observed in the cell

morphology or in the FAs on the glasses upon FAK inhibition although the inhibition of FAK clearly hindered the early osteogenic differentiation of hASCs. Thus, the visual evaluation of the cell morphology and attachment mode might not always be indicative of the intracellular signaling events or the cell fate decisions and should be therefore interpreted cautiously.

With respect to ERK1/2, both glasses increased the activation of this signaling molecule after 3 and 7 days of culture when compared to the control polystyrene and, similar to FAK, the inhibition of ERK1/2 significantly attenuated the early osteogenic differentiation as determined by ALP activity and *RUNX2a* and *OSTERIX* expression. Moreover, the inhibition of FAK resulted in downregulation of the ERK1/2 activation, which is well in line with the previous observations about the connection of these signaling factors in the regulation of osteogenesis on ECM biomaterials (Salasznyk et al., 2007a; Salasznyk et al., 2007b; Shih et al., 2011; Takeuchi et al., 1997; Viale-Bouroncle et al., 2014a; Viale-Bouroncle et al., 2014b). However, the inhibition of FAK did not totally abolish the activation of ERK1/2, implying that in addition to the attachment-mediated signaling mechanisms ERK1/2 is also activated by other stimuli. Previous reports have identified ERK1/2 as an important player in the osteogenesis induced by OM (Jaiswal et al., 2000; Lai et al., 2001; Q. Liu et al., 2009) but since no OM was used in study **III**, this cannot explain the residual ERK1/2 activation. Gu and co-workers detected increased ERK1/2 activation in hASCs treated with akermanite extracts containing Ca, Mg and Si ions (Gu et al., 2011), suggesting that ERK1/2 might be also stimulated by the ionic dissolution products from the BaGs, thus possibly explaining the ERK1/2 activation in the presence of FAK inhibitor. Moreover, ERK1/2 is also a very prominent mediator of mitogenic stimuli and cell proliferation, which might be reflected in the ERK1/2 activation levels, especially when both of the BaGs were observed to increase the hASC proliferation.

In contrast to ERK1/2, the roles of p38 and JNK in the osteogenic differentiation, especially in relation to the attachment-related mechanisms, are generally far less established. However, there is some evidence that both of these kinases operate downstream of integrins in the regulation of osteogenic commitment on collagen-based biomaterials (Chiu et al., 2012; Chiu et al., 2014; Ivaska et al., 1999). Even though we could not detect any traces of JNK activation at either of the time points or materials, c-Jun, an immediate downstream target of JNK, was clearly activated on both of the BaGs after 3 and 7 days of culture, suggesting that the BaGs stimulate the JNK signaling. Moreover, the inhibition of JNK seriously hampered the early BaG-induced osteogenic response, which further supports the role of JNK in the

glass-induced osteogenic commitment. However, since the inhibition of FAK did not clearly affect the c-Jun activation levels, the activation of JNK signaling likely occurred via FAK-independent mechanisms. JNK has been previously shown to play an important role in the osteogenic differentiation stimulated by BMP-2, Wnt3a, and NELL-1 (F. Chen et al., 2012; Guicheux et al., 2003; Qiu et al., 2011), which might be differentially produced in hASCs cultured on the glasses, thus possibly explaining the elevated c-Jun activation. Interestingly, the glasses also upregulated the basal levels of c-Jun, as well as FAK, which indicates that, in addition to the effect on activation, also the production of these signaling proteins is affected by the BaGs.

Unlike the other signaling proteins studied, p38 was not activated by the glasses at any of the studied time points and the inhibition of p38 had only a mild effect on the ALP activity and basically no effect at all on *RUNX2a* and *OSTERIX* expression. Even though there are reports suggesting a crucial role for p38 in the osteogenic differentiation stimulated by both cell attachment and chemical factors (Ivaska et al., 1999; Suzuki et al., 2002; Tominaga et al., 2005), others reports were not able to demonstrate the significance of p38 for the osteogenic commitment (L. Fu et al., 2008; Kilian et al., 2010). Thus, it is possible that the early osteogenic differentiation stimulated by the BaGs occurs independently of p38. Interestingly, even though the attachment and signaling responses on both of the studied glass types were generally very similar, with respect to p38 activation there was a systematic difference between the glasses. After 3 days of culture, 1-06 clearly reduced the p38 activation, which was totally abolished in the presence of FAK inhibitor. However, with S53P4 such a dramatic reduction was not observed. It is tempting to speculate whether this difference could explain the upregulation of ALP activity on 1-06 when compared to S53P4, but since the inhibition of p38 in general did not seem to support the early osteogenic response in hASCs, this signaling difference between the glasses might not be the ultimate factor explaining the difference in the ALP activity. Thus, even though study **III** provided new information about the signaling mechanisms behind the BaG-induced early osteogenic differentiation of hASCs, more analyses are required to determine the signaling level events responsible for the slightly differing differentiation responses observed on S53P4 and 1-06 glasses.

Figure 23 summarizes the main observations made about the cell attachment and signaling in study **III**.
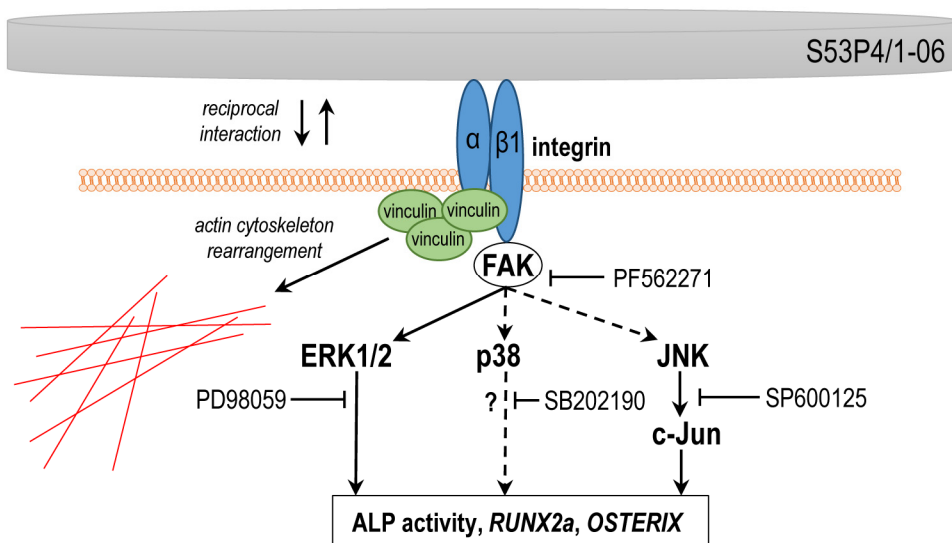
Figure 23. Bioactive glass-induced cell attachment and signaling response in study **III**. When cultured on the BaG discs S53P4 and 1-06, the production of integrinβ1 and vinculin was upregulated. Moreover, the actin cytoskeleton adopted a disorganized appearance. Both BaGs activated FAK, ERK1/2 and JNK downstream target c-Jun. FAK, ERK1/2 and JNK inhibition significantly reduced the early osteogenic differentiation induced by the glasses. FAK inhibition also attenuated ERK1/2 activation but not the activation of p38 or c-Jun, suggesting that ERK1/2 operates downstream of FAK but p38 and JNK possibly not. p38 inhibition had only a minor effect on ALP activity and no effect at all on *RUNX2a* and *OSTERIX* expression. Therefore, the role of p38 in the BaG-induced osteogenic differentiation remained unclear (hence the question mark). The cells cultured on the BaG discs also modified the glass surface as indicated by decreased CaP layer formation and increased ionic release in the presence of the cells (indicated in the figure by "reciprocal interaction").

6.6 Future perspectives

When considering the evolution of the ASC-based bone TE, the progress made within a relatively short period has been almost breathtaking. A kind of a culmination point occurred already in 2004 when Lendeckel and co-workers reported the first clinical treatment based on an SVF cells-utilizing bone TE strategy (Lendeckel et al., 2004). Since then, also other teams have published promising results regarding the clinical treatment of large bone defects by the means of hASC-based bone TE (Mesimäki et al., 2009; Pak, 2012; Sandor et al., 2014; Taylor, 2010). Such fast progress has drawn a lot of attention in the public and keeps raising high hopes for the wide-spread use of the TE-based treatment strategies. However, even though

mainly successful, the clinical treatments utilizing the bone TE approach have thus far been individual cases, and the routine use of such procedures is still considerably far on the horizon. To reach the ultimate goal of bone TE-based everyday treatments, a lot of basic level research is still required, since with respect to the biomaterial, cells and cell-stimulating factors no optimal combination with a superior functionality has yet been developed. It is becoming clear that, instead of focusing only on the tissue-level function of the TE construct, a lot more attention should be paid to the cellular level since, ultimately, the beneficial responses elicited at the level of single cells are the key to clinical success.

In the light of the results of this thesis, there are many fundamental aspects which require a more thorough evaluation. First of all, the unambiguous function of BMP-2 as an osteogenesis-stimulating factor was further questioned in study **I**, since some of the hASC donor lines committed adipogenic differentiation in response to BMP-2 stimulus, even in the presence of OM. Most notably, both the osteogenesis and adipogenesis involved the same canonical Smad1/5 signaling route, implying that additional signaling mechanisms must be participating in making the distinction between the ultimate differentiation fates. However, these mechanisms are currently not understood, which demands for a broader analysis of the BMP-2-induced signaling scheme regulating the cell fate decisions. In general, the dual effect of BMP-2 on hASCs differentiation poses severe challenges to the clinical use of this growth factor. Even if the BMP-2-induced signaling would be well defined, it would not probably be such a straightforward task to guide the cells to the desired direction under the BMP-2 stimulus. Therefore, the increasing trend among the scientific community to evaluate and develop novel bone formation stimulating factors is no doubt a reasonable approach to proceed towards enhanced bone TE applications.

Based on the results of study **II**, the OM-based BaG extracts might well have a potential to fill the need for a strong inducer of *in vitro* osteogenic differentiation. However, more development is still required in order to harness the *in vitro* power of these induction media for the clinical bone TE treatments. It might be possible to design biomaterial scaffolds releasing these ions with optimal kinetics but as observed in study **III**, the cell-biomaterial interaction has also a significant effect on the cell behavior, bringing an additional level of complexity and thus likely modifying the cellular responses to the BaG ions. Alternatively, the OM extracts could be used solely as *in vitro* inducers of hASC osteogenic differentiation before the implantation of the TE construct to the defect site. This might also improve the functionality of biomaterials with no inherent ability to stimulate stem cell osteogenesis. However, the utility of the stem cell osteogenic differentiation *in vitro* prior to the *in vivo*

implantation is currently somewhat questionable with highly contradicting results reported (Gomide et al., 2012; Jeon et al., 2008; H. P. Kim et al., 2012; Niemeyer et al., 2006; Ye et al., 2012; Yoon et al., 2007). This is also one key aspect which in future should be studied more carefully in order to be able to develop functional strategies for the clinical bone TE interventions.

When getting back to the cellular level responses to the various environmental stimuli, the topic of cell-biomaterial interactions, especially in the level of molecular signaling mechanisms, has not gained too much attention among the field of bone TE. This is especially true with the BaGs, which have been extensively studied in terms of many other aspects, but related to the cell attachment and the attachment-related signaling underlying the BaG-induced osteogenesis, very little knowledge exists. Study **III** provided novel information about this intriguing topic, thus laying the foundation for a more thorough evaluation of the signaling responses elicited by the BaGs. In order to form a more complete picture of this signaling scheme, future studies should approach this matter with high-throughput techniques exploiting advanced proteomics, which should be combined with bioinformatics tools to mine the relevant information from the vast amount of data. Interestingly, as recently demonstrated by three studies, the signaling changes might also have a potential to predict the ultimate cell differentiation fate both *in vitro* and *in vivo* already at the very beginning of the *in vitro* culture (Bolander et al., 2016; Mentink et al., 2013; Platt et al., 2009). This kind of approach might offer plenty of opportunities and a possibility to revolutionize the laboratory work by significantly shortening the time and money consuming experimental setups. All in all, it is presumable that the future of bone TE will be increasingly focusing on the elucidation of the various cellular responses, all the way to the cell signaling level, induced by the different osteogenesis-inducing stimuli. Such knowledge will be ideally serving as the base for the design and functionality prediction of the next generation TE constructs.

7 Conclusions

In this thesis, the osteogenic differentiation response of hASCs was evaluated in response to BMP-2 growth factor stimulus and BaG biomaterials, either in the form of ionic extracts or discs serving as a cell culture substrate. With respect to BMP-2 and the BaG discs the focus was on the underlying cell signaling and cell attachment-related mechanisms. The main findings and conclusions of each of the studies are briefly described below:

I   Regardless of the hASC donor line, the treatment with rhBMP-2 successfully activated the canonical Smad signaling pathway and resulted in the nuclear translocation of the activated Smad1/5 protein. However, the activation was clearly weaker in FBS-based culture medium when compared to the HS medium, suggesting that the bioactivity of rhBMP-2 might be affected by the serum conditions. Similar signaling-related observations were made also with human osteoblasts and hBMSCs. With respect to the differentiation outcome, hASCs could be roughly divided into donor lines responding to BMP-2 by osteogenic commitment and donor lines committing towards adipocytes. Thus, despite the identical Smad1/5 signaling response in all the hASCs, in the behavioral level the treatment with BMP-2 resulted in two distinct differentiation outcomes. This is probably explained by additional, thus far unidentified, signaling mechanisms fine-tuning the effect of BMP-2. Finally, it was observed that, with respect to both the signaling events and the differentiation response, the rhBMP-2 produced in mammalian cells induced constantly stronger responses than the rhBMP-2 produced in E. coli, likely due to the post-translational modifications present only in the mammalian cell originated protein.

II   When combined with the traditionally used OM supplements, BaG extracts prepared from the BaGs S53P4, 2-06, 1-06 and 3-06 induced exceptionally fast and extensive osteogenic differentiation of hASCs. This was achieved in the absence of any cell-biomaterial contact. Still, without the OM supplements none of the BaG extracts was able to stimulate the osteogenic differentiation. Of the different extracts, 2-06 and 3-06 OM extracts turned out to be the strongest inducers of osteogenic differentiation. These extracts contained the highest concentrations of Ca, which

serves as a raw material for mineralization but is also known to regulate osteogenesis-related cell signaling events. Moreover, 2-06 and 3-06 were the only extracts containing traces of boron, which in small amounts is able to stimulate osteogenic differentiation.

III S53P4 and 1-06 BaGs induced early osteogenic differentiation of hASCs cultured on the glass discs in the absence of any OM supplements. This response was stronger with 1-06, which released small amounts of B and was less reactive than S53P4. The cell attachment on the BaG discs was observed to be unorthodox, with small and evenly dispersed FAs, slightly disorganized actin cytoskeleton and increased production of integrinβ1 and vinculin, possibly explained by the surface roughness and reactivity of the BaGs. Moreover, the presence of cells also affected the glass surfaces by increasing the ionic release and decreasing the CaP surface layer formation. FAK and MAPKs ERK1/2 and JNK seemed to be crucial mediators of the BaG-induced early osteogenic response, whereas the role of p38 was less significant. ERK1/2 was shown to operate downstream of FAK, but no connection could be made between FAK and the other MAPKs. The cell attachment and signaling mechanisms were overall highly similar between the two glass types.

In summary, the BMP-2-induced differentiation outcome seems to be highly donor-dependent and is affected also by other factors, such as the culture medium and the production origin of the growth factor. These data certainly question the clinical utility of BMP-2 and highlights the need for more basic level studies to make the distinction in the signaling events between the BMP-2-induced osteogenesis and adipogenesis. OM-based ionic extracts prepared from the different BaGs turned out to be exceptionally strong osteo-inducers, which urges to utilize them as effective means to differentiate cells *in vitro*, for example when cultured in non-osteoinductive scaffold materials. BaG-induced early osteogenesis was shown to involve FAK and MAPKs and is likely affected by the reciprocal interaction between the cells and the glass surface. These novel data pave the way for more thorough analyses of the BaG-induced signaling responses, which provide means to further improve the future bone TE applications.

Acknowledgements

a lot longer time for this work to be completed. I would also like to express my gratitude to my fellow PhD students Laura Hyväri, Heidi Halonen and Sanni Virjula. Apart from sharing all the struggles related to the PhD project, your friendship outside the work has been invaluable for me.

I would like to thank all my friends for providing me all those joyful moments. They have been excellent counterbalance for the work. Special thanks to Toni and Anni, you are the best company I can imagine.

My deepest gratitude goes to all my close relatives and especially to my family: Mom, Dad and Emmi. Thank you for balancing my life and always believing in me. I truly appreciate all the weekends and holidays we have spent with you, away from all the work stress. Special thanks to our little black panther Miisu, the best therapy animal in the world.

Finally, my beloved Kimmo. Without your help and support, and constant encouragement, my life would be a mess (as would be my computer skills). I am deeply grateful for all the moments we have shared. Thank you for being always there for me, we are the best.

Tampere, July 2016

©Pertti Jarla/PIB

8 References

Agas, D., Sabbieti, M. G., Marchetti, L., Xiao, L., & Hurley, M. M. (2013). FGF-2 enhances runx-2/smads nuclear localization in BMP-2 canonical signaling in osteoblasts. *J.Cell.Physiol., 228*(11), 2149-2158.

Aksu, A. E., Rubin, J. P., Dudas, J. R., & Marra, K. G. (2008). Role of gender and anatomical region on induction of osteogenic differentiation of human adipose-derived stem cells. *Ann.Plast.Surg., 60*(3), 306-322.

Albrektsson, T., & Johansson, C. (2001). Osteoinduction, osteoconduction and osseointegration. *Eur.Spine J., 10 Suppl 2*, S96-101.

Alcaide, M., Portoles, P., Lopez-Noriega, A., Arcos, D., Vallet-Regi, M., & Portoles, M. T. (2010). Interaction of an ordered mesoporous bioactive glass with osteoblasts, fibroblasts and lymphocytes, demonstrating its biocompatibility as a potential bone graft material. *Acta Biomater., 6*(3), 892-899.

Almubarak, S., Nethercott, H., Freeberg, M., Beaudon, C., Jha, A., Jackson, W., Marcucio, R., Miclau, T., Healy, K., & Bahney, C. (2016). Tissue engineering strategies for promoting vascularized bone regeneration. *Bone, 83*, 197-209.

Alt, E. U., Senst, C., Murthy, S. N., Slakey, D. P., Dupin, C. L., Chaffin, A. E., Kadowitz, P. J., & Izadpanah, R. (2012). Aging alters tissue resident mesenchymal stem cell properties. *Stem Cell.Res., 8*(2), 215-225.

Alves, E. G., Serakides, R., Rosado, I. R., Pereira, M. M., Ocarino, N. M., Oliveira, H. P., Goes, A. M., & Rezende, C. M. (2015). Effect of the ionic product of bioglass 60s on osteoblastic activity in canines. *BMC Vet.Res., 11*, 247-015-0558-7.

Amable, P. R., Teixeira, M. V., Carias, R. B., Granjeiro, J. M., & Borojevic, R. (2014). Mesenchymal stromal cell proliferation, gene expression and protein production in human platelet-rich plasma-supplemented media. *PLoS One, 9*(8), e104662.

An, S., Gao, Y., Ling, J., Wei, X., & Xiao, Y. (2012). Calcium ions promote osteogenic differentiation and mineralization of human dental pulp cells: Implications for pulp capping materials. *J.Mater.Sci.Mater.Med., 23*(3), 789-795.

Aquino-Martinez, R., Rodriguez-Carballo, E., Gamez, B., Artigas, N., Carvalho-Lobato, P., Manzanares-Cespedes, M. C., Rosa, J. L., & Ventura, F. (2016). Mesenchymal stem cells within gelatin/CaSO4 scaffolds treated ex vivo with low doses of BMP-2 and Wnt3a increase bone regeneration. *Tissue Eng.Part A., 22*(1-2), 41-52.

Ardeshirylajimi, A., Farhadian, S., Adegani, F. J., Mirzaei, S., Zomorrod, M. S., Langroudi, L., Doostmohammadi, A., Seyedjafari, E., & Soleimani, M. (2015). Enhanced osteoconductivity of polyethersulphone nanofibres loaded with bioactive glass nanoparticles in in vitro and in vivo models. *Cell Prolif., 48*(4), 455-464.

Argintar, E., Edwards, S., & Delahay, J. (2011). Bone morphogenetic proteins in orthopaedic trauma surgery. *Injury, 42*(8), 730-734.

Artigas, N., Urena, C., Rodriguez-Carballo, E., Rosa, J. L., & Ventura, F. (2014). Mitogen-activated protein kinase (MAPK)-regulated interactions between osterix and Runx2 are critical for the transcriptional osteogenic program. *J.Biol.Chem., 289*(39), 27105-27117.

Au, A. Y., Au, R. Y., Demko, J. L., McLaughlin, R. M., Eves, B. E., & Frondoza, C. G. (2010). Consil bioactive glass particles enhance osteoblast proliferation and selectively modulate cell signaling pathways in vitro. *J.Biomed.Mater.Res.A., 94*(2), 380-388.

Avram, M. M., Avram, A. S., & James, W. D. (2007). Subcutaneous fat in normal and diseased states 3. adipogenesis: From stem cell to fat cell. *J.Am.Acad.Dermatol., 56*(3), 472-492.

Baer, P. C., & Geiger, H. (2012). Adipose-derived mesenchymal stromal/stem cells: Tissue localization, characterization, and heterogeneity. *Stem Cells Int., 2012*, 812693.

Bahney, C. S., Hu, D. P., Taylor, A. J., Ferro, F., Britz, H. M., Hallgrimsson, B., Johnstone, B., Miclau, T., & Marcucio, R. S. (2014). Stem cell-derived endochondral cartilage stimulates bone healing by tissue transformation. *J.Bone Miner.Res., 29*(5), 1269-1282.

Balmayor, E. R., Geiger, J. P., Aneja, M. K., Berezhanskyy, T., Utzinger, M., Mykhaylyk, O., Rudolph, C., & Plank, C. (2016). Chemically modified RNA induces osteogenesis of stem cells and human tissue explants as well as accelerates bone healing in rats. *Biomaterials, 87*, 131-146.

Barradas, A. M., Fernandes, H. A., Groen, N., Chai, Y. C., Schrooten, J., van de Peppel, J., van Leeuwen, J. P., van Blitterswijk, C. A., & de Boer, J. (2012). A calcium-induced signaling cascade leading to osteogenic differentiation of human bone marrow-derived mesenchymal stromal cells. *Biomaterials, 33*(11), 3205-3215.

Barrere, F., van Blitterswijk, C. A., & de Groot, K. (2006). Bone regeneration: Molecular and cellular interactions with calcium phosphate ceramics. *Int.J.Nanomedicine, 1*(3), 317-332.

Behr, B., Tang, C., Germann, G., Longaker, M. T., & Quarto, N. (2011). Locally applied vascular endothelial growth factor A increases the osteogenic healing capacity of human adipose-derived stem cells by promoting osteogenic and endothelial differentiation. *Stem Cells, 29*(2), 286-296.

Bekhite, M. M., Finkensieper, A., Rebhan, J., Huse, S., Schultze-Mosgau, S., Figulla, H. R., Sauer, H., & Wartenberg, M. (2014). Hypoxia, leptin, and vascular endothelial growth factor stimulate vascular endothelial cell differentiation of human adipose tissue-derived stem cells. *Stem Cells Dev., 23*(4), 333-351.

Berendsen, A. D., & Olsen, B. R. (2015). Bone development. *Bone, 80*, 14-18.

Bieback, K., Hecker, A., Kocaomer, A., Lannert, H., Schallmoser, K., Strunk, D., & Kluter, H. (2009). Human alternatives to fetal bovine serum for the expansion of mesenchymal stromal cells from bone marrow. *Stem Cells, 27*(9), 2331-2341.

Bielby, R. C., Pryce, R. S., Hench, L. L., & Polak, J. M. (2005). Enhanced derivation of osteogenic cells from murine embryonic stem cells after treatment with ionic dissolution products of 58S bioactive sol-gel glass. *Tissue Eng., 11*(3-4), 479-488.

Biggs, M. J., & Dalby, M. J. (2010). Focal adhesions in osteoneogenesis. *Proc.Inst.Mech.Eng.H., 224*(12), 1441-1453.

Biggs, M. J., Richards, R. G., & Dalby, M. J. (2010). Nanotopographical modification: A regulator of cellular function through focal adhesions. *Nanomedicine, 6*(5), 619-633.

Biggs, M. J., Richards, R. G., Gadegaard, N., McMurray, R. J., Affrossman, S., Wilkinson, C. D., Oreffo, R. O., & Dalby, M. J. (2009). Interactions with nanoscale topography: Adhesion quantification and signal transduction in cells of osteogenic and multipotent lineage. *J.Biomed.Mater.Res.A., 91*(1), 195-208.

Bilem, I., Chevallier, P., Plawinski, L., Sone, E. D., Durrieu, M. C., & Laroche, G. (2016). RGD and BMP-2 mimetic peptide crosstalk enhances osteogenic commitment of human bone marrow stem cells. *Acta Biomater., 36*, 132-142.

Biver, E., Soubrier, A. S., Thouverey, C., Cortet, B., Broux, O., Caverzasio, J., & Hardouin, P. (2012). Fibroblast growth factor 2 inhibits up-regulation of bone morphogenic proteins and their receptors during osteoblastic differentiation of human mesenchymal stem cells. *Biochem.Biophys.Res.Commun., 427*(4), 737-742.

Bodle, J. C., Hanson, A. D., & Loboa, E. G. (2011). Adipose-derived stem cells in functional bone tissue engineering: Lessons from bone mechanobiology. *Tissue Eng.Part B.Rev., 17*(3), 195-211.

Bolander, J., Chai, Y. C., Geris, L., Schrooten, J., Lambrechts, D., Roberts, S. J., & Luyten, F. P. (2016). Early BMP, wnt and ca(2+)/PKC pathway activation predicts the bone forming capacity of periosteal cells in combination with calcium phosphates. *Biomaterials, 86*, 106-118.

Bosetti, M., & Cannas, M. (2005). The effect of bioactive glasses on bone marrow stromal cells differentiation. *Biomaterials, 26*(18), 3873-3879.

Bourin, P., Bunnell, B. A., Casteilla, L., Dominici, M., Katz, A. J., March, K. L., Redl, H., Rubin, J. P., Yoshimura, K., & Gimble, J. M. (2013). Stromal cells from the adipose tissue-derived stromal vascular fraction and culture expanded adipose tissue-derived stromal/stem cells: A joint statement of the international federation for adipose therapeutics and science (IFATS) and the international society for cellular therapy (ISCT). *Cytotherapy, 15*(6), 641-648.

Bragdon, B., Moseychuk, O., Saldanha, S., King, D., Julian, J., & Nohe, A. (2011). Bone morphogenetic proteins: A critical review. *Cell.Signal., 23*(4), 609-620.

Brignier, A. C., & Gewirtz, A. M. (2010). Embryonic and adult stem cell therapy. *J.Allergy Clin.Immunol., 125*(2 Suppl 2), S336-44.

Burg, K. J., Porter, S., & Kellam, J. F. (2000). Biomaterial developments for bone tissue engineering. *Biomaterials, 21*(23), 2347-2359.

Burridge, K., & Chrzanowska-Wodnicka, M. (1996). Focal adhesions, contractility, and signaling. *Annu.Rev.Cell Dev.Biol., 12*, 463-518.

Byun, M. R., Kim, A. R., Hwang, J. H., Kim, K. M., Hwang, E. S., & Hong, J. H. (2014). FGF2 stimulates osteogenic differentiation through ERK induced TAZ expression. *Bone, 58*, 72-80.

Caplan, A. I. (1991). Mesenchymal stem cells. *J.Orthop.Res., 9*(5), 641-650.

Castegnaro, S., Chieregato, K., Maddalena, M., Albiero, E., Visco, C., Madeo, D., Pegoraro, M., & Rodeghiero, F. (2011). Effect of platelet lysate on the functional and molecular characteristics of mesenchymal stem cells isolated from adipose tissue. *Curr.Stem Cell.Res.Ther., 6*(2), 105-114.

Cervenka, I., Wolf, J., Masek, J., Krejci, P., Wilcox, W. R., Kozubik, A., Schulte, G., Gutkind, J. S., & Bryja, V. (2011). Mitogen-activated protein kinases promote WNT/beta-catenin signaling via phosphorylation of LRP6. *Mol.Cell.Biol., 31*(1), 179-189.

Chang, J., Sonoyama, W., Wang, Z., Jin, Q., Zhang, C., Krebsbach, P. H., Giannobile, W., Shi, S., & Wang, C. Y. (2007). Noncanonical wnt-4 signaling enhances bone regeneration of mesenchymal stem cells in craniofacial defects through activation of p38 MAPK. *J.Biol.Chem., 282*(42), 30938-30948.

Chen, C., Uludag, H., Wang, Z., & Jiang, H. (2012). Noggin suppression decreases BMP-2-induced osteogenesis of human bone marrow-derived mesenchymal stem cells in vitro. *J.Cell.Biochem., 113*(12), 3672-3680.

Chen, F., Walder, B., James, A. W., Soofer, D. E., Soo, C., Ting, K., & Zhang, X. (2012). NELL-1-dependent mineralisation of saos-2 human osteosarcoma cells is mediated via c-jun N-terminal kinase pathway activation. *Int.Orthop., 36*(10), 2181-2187.

Chen, G., Deng, C., & Li, Y. P. (2012). TGF-beta and BMP signaling in osteoblast differentiation and bone formation. *Int.J.Biol.Sci., 8*(2), 272-288.

Chen, S., Jian, Z., Huang, L., Xu, W., Liu, S., Song, D., Wan, Z., Vaughn, A., Zhan, R., Zhang, C., Wu, S., Hu, M., & Li, J. (2015). Mesoporous bioactive glass surface modified poly(lactic-co-glycolic acid) electrospun fibrous scaffold for bone regeneration. *Int.J.Nanomedicine, 10*, 3815-3827.

Chiou, M., Xu, Y., & Longaker, M. T. (2006). Mitogenic and chondrogenic effects of fibroblast growth factor-2 in adipose-derived mesenchymal cells. *Biochem.Biophys.Res.Commun., 343*(2), 644-652.

Chiu, L. H., Lai, W. F., Chang, S. F., Wong, C. C., Fan, C. Y., Fang, C. L., & Tsai, Y. H. (2014). The effect of type II collagen on MSC osteogenic differentiation and bone defect repair. *Biomaterials, 35*(9), 2680-2691.

Chiu, L. H., Yeh, T. S., Huang, H. M., Leu, S. J., Yang, C. B., & Tsai, Y. H. (2012). Diverse effects of type II collagen on osteogenic and adipogenic differentiation of mesenchymal stem cells. *J.Cell.Physiol., 227*(6), 2412-2420.

Chou, Y. F., Zuk, P. A., Chang, T. L., Benhaim, P., & Wu, B. M. (2011). Adipose-derived stem cells and BMP2: Part 1. BMP2-treated adipose-derived stem cells do not improve repair of segmental femoral defects. *Connect.Tissue Res., 52*(2), 109-118.

Choudhery, M. S., Badowski, M., Muise, A., Pierce, J., & Harris, D. T. (2014). Donor age negatively impacts adipose tissue-derived mesenchymal stem cell expansion and differentiation. *J.Transl.Med., 12*, 8-5876-12-8.

Choumerianou, D. M., Dimitriou, H., & Kalmanti, M. (2008). Stem cells: Promises versus limitations. *Tissue Eng.Part B.Rev., 14*(1), 53-60.

Christodoulou, I., Buttery, L. D., Saravanapavan, P., Tai, G., Hench, L. L., & Polak, J. M. (2005). Dose- and time-dependent effect of bioactive gel-glass ionic-dissolution products on human fetal osteoblast-specific gene expression. *J.Biomed.Mater.Res.B.Appl.Biomater., 74*(1), 529-537.

Christodoulou, I., Buttery, L. D., Tai, G., Hench, L. L., & Polak, J. M. (2006). Characterization of human fetal osteoblasts by microarray analysis following stimulation with 58S bioactive gel-glass ionic dissolution products. *J.Biomed.Mater.Res.B.Appl.Biomater., 77*(2), 431-446.

Cobb, M. H. (1999). MAP kinase pathways. *Prog.Biophys.Mol.Biol., 71*(3-4), 479-500.

Cong, Q., Jia, H., Biswas, S., Li, P., Qiu, S., Deng, Q., Guo, X., Ma, G., Ling Chau, J. F., Wang, Y., Zhang, Z. L., Jiang, X., Liu, H., & Li, B. (2016). p38alpha MAPK regulates lineage commitment and OPG synthesis of bone marrow stromal cells to prevent bone loss under physiological and pathological conditions. *Stem Cell.Reports, 6*(4), 566-578.

Cowan, C. M., Shi, Y. Y., Aalami, O. O., Chou, Y. F., Mari, C., Thomas, R., Quarto, N., Contag, C. H., Wu, B., & Longaker, M. T. (2004). Adipose-derived adult stromal cells heal critical-size mouse calvarial defects. *Nat.Biotechnol., 22*(5), 560-567.

Cristancho, A. G., & Lazar, M. A. (2011). Forming functional fat: A growing understanding of adipocyte differentiation. *Nat.Rev.Mol.Cell Biol., 12*(11), 722-734.

Cruz, A. C., Silva, M. L., Caon, T., & Simoes, C. M. (2012). Addition of bone morphogenetic protein type 2 to ascorbate and beta-glycerophosphate supplementation did not enhance osteogenic differentiation of human adipose-derived stem cells. *J.Appl.Oral Sci., 20*(6), 628-635.

Cuenda, A., & Rousseau, S. (2007). p38 MAP-kinases pathway regulation, function and role in human diseases. *Biochim.Biophys.Acta, 1773*(8), 1358-1375.

da Silva Meirelles, L., Chagastelles, P. C., & Nardi, N. B. (2006). Mesenchymal stem cells reside in virtually all post-natal organs and tissues. *J.Cell.Sci., 119*(Pt 11), 2204-2213.

Daher, S. R., Johnstone, B. H., Phinney, D. G., & March, K. L. (2008). Adipose stromal/stem cells: Basic and translational advances: The IFATS collection. *Stem Cells, 26*(10), 2664-2665.

Danen, E. H., & Sonnenberg, A. (2003). Integrins in regulation of tissue development and function. *J.Pathol., 201*(4), 632-641.

Davis, R. J. (2000). Signal transduction by the JNK group of MAP kinases. *Cell, 103*(2), 239-252.

Day, R. M. (2005). Bioactive glass stimulates the secretion of angiogenic growth factors and angiogenesis in vitro. *Tissue Eng., 11*(5-6), 768-777.

Day, R. M., Boccaccini, A. R., Shurey, S., Roether, J. A., Forbes, A., Hench, L. L., & Gabe, S. M. (2004). Assessment of polyglycolic acid mesh and bioactive glass for soft-tissue engineering scaffolds. *Biomaterials, 25*(27), 5857-5866.

Day, R. M., Maquet, V., Boccaccini, A. R., Jerome, R., & Forbes, A. (2005). In vitro and in vivo analysis of macroporous biodegradable poly(D,L-lactide-co-glycolide) scaffolds containing bioactive glass. *J.Biomed.Mater.Res.A., 75*(4), 778-787.

de Almeida, D. C., Ferreira, M. R., Franzen, J., Weidner, C. I., Frobel, J., Zenke, M., Costa, I. G., & Wagner, W. (2016). Epigenetic classification of human mesenchymal stromal cells. *Stem Cell.Reports, 6*(2), 168-175.

De Bari, C., Dell'Accio, F., Vandenabeele, F., Vermeesch, J. R., Raymackers, J. M., & Luyten, F. P. (2003). Skeletal muscle repair by adult human mesenchymal stem cells from synovial membrane. *J.Cell Biol., 160*(6), 909-918.

de Girolamo, L., Lopa, S., Arrigoni, E., Sartori, M. F., Baruffaldi Preis, F. W., & Brini, A. T. (2009). Human adipose-derived stem cells isolated from young and elderly women: Their differentiation potential and scaffold interaction during in vitro osteoblastic differentiation. *Cytotherapy, 11*(6), 793-803.

De Ugarte, D. A., Alfonso, Z., Zuk, P. A., Elbarbary, A., Zhu, M., Ashjian, P., Benhaim, P., Hedrick, M. H., & Fraser, J. K. (2003). Differential expression of stem cell mobilization-associated molecules on multi-lineage cells from adipose tissue and bone marrow. *Immunol.Lett., 89*(2-3), 267-270.

Derynck, R., & Zhang, Y. E. (2003). Smad-dependent and smad-independent pathways in TGF-beta family signalling. *Nature, 425*(6958), 577-584.

Detsch, R., Alles, S., Hum, J., Westenberger, P., Sieker, F., Heusinger, D., Kasper, C., & Boccaccini, A. R. (2015). Osteogenic differentiation of umbilical cord and adipose derived stem cells onto highly porous 45S5 bioglass(R)-based scaffolds. *J.Biomed.Mater.Res.A., 103*(3), 1029-1037.

Diekman, B. O., Rowland, C. R., Lennon, D. P., Caplan, A. I., & Guilak, F. (2010). Chondrogenesis of adult stem cells from adipose tissue and bone marrow: Induction by growth factors and cartilage-derived matrix. *Tissue Eng.Part A., 16*(2), 523-533.

Dinarvand, P., Seyedjafari, E., Shafiee, A., Jandaghi, A. B., Doostmohammadi, A., Fathi, M. H., Farhadian, S., & Soleimani, M. (2011). New approach to bone tissue engineering: Simultaneous application of hydroxyapatite and bioactive glass coated on a poly(L-lactic acid) scaffold. *ACS Appl.Mater.Interfaces, 3*(11), 4518-4524.

Ding, Q., Xia, W., Liu, J. C., Yang, J. Y., Lee, D. F., Xia, J., Bartholomeusz, G., Li, Y., Pan, Y., Li, Z., Bargou, R. C., Qin, J., Lai, C. C., Tsai, F. J., Tsai, C. H., & Hung, M. C. (2005). Erk associates with and primes GSK-3beta for its inactivation resulting in upregulation of beta-catenin. *Mol.Cell, 19*(2), 159-170.

Dominici, M., Le Blanc, K., Mueller, I., Slaper-Cortenbach, I., Marini, F., Krause, D., Deans, R., Keating, A., Prockop, D., & Horwitz, E. (2006). Minimal criteria for defining multipotent mesenchymal stromal cells. the international society for cellular therapy position statement. *Cytotherapy, 8*(4), 315-317.

Drosse, I., Volkmer, E., Capanna, R., De Biase, P., Mutschler, W., & Schieker, M. (2008). Tissue engineering for bone defect healing: An update on a multi-component approach. *Injury, 39 Suppl 2*, S9-20.

Dvorak, M. M., Siddiqua, A., Ward, D. T., Carter, D. H., Dallas, S. L., Nemeth, E. F., & Riccardi, D. (2004). Physiological changes in extracellular calcium concentration directly control osteoblast function in the absence of calciotropic hormones. *Proc.Natl.Acad.Sci.U.S.A., 101*(14), 5140-5145.

Engler, A. J., Sen, S., Sweeney, H. L., & Discher, D. E. (2006). Matrix elasticity directs stem cell lineage specification. *Cell, 126*(4), 677-689.

Escobar, C. H., & Chaparro, O. (2016). Xeno-free extraction, culture, and cryopreservation of human adipose-derived mesenchymal stem cells. *Stem Cells Transl.Med., 5*(3), 358-365.

Estes, B. T., Diekman, B. O., Gimble, J. M., & Guilak, F. (2010). Isolation of adipose-derived stem cells and their induction to a chondrogenic phenotype. *Nat.Protoc., 5*(7), 1294-1311.

Evans, M. J., & Kaufman, M. H. (1981). Establsihment in culture of pluripotential cells from mouse embryos. *Nature, 292*, 154-156.

Fan, J., Im, C. S., Guo, M., Cui, Z. K., Fartash, A., Kim, S., Patel, N., Bezouglaia, O., Wu, B. M., Wang, C. Y., Aghaloo, T. L., & Lee, M. (2016). Enhanced osteogenesis of adipose-derived stem cells by regulating bone morphogenetic protein signaling antagonists and agonists. *Stem Cells Transl.Med., 5*(4), 539-551.

Fan, J., Park, H., Tan, S., & Lee, M. (2013). Enhanced osteogenesis of adipose derived stem cells with noggin suppression and delivery of BMP-2. *PLoS One, 8*(8), e72474.

Fernandes, H., Mentink, A., Bank, R., Stoop, R., van Blitterswijk, C., & de Boer, J. (2010). Endogenous collagen influences differentiation of human multipotent mesenchymal stromal cells. *Tissue Eng.Part A., 16*(5), 1693-1702.

Fink, T., Lund, P., Pilgaard, L., Rasmussen, J. G., Duroux, M., & Zachar, V. (2008). Instability of standard PCR reference genes in adipose-derived stem cells during propagation, differentiation and hypoxic exposure. *BMC Mol.Biol., 9*, 98-2199-9-98.

Fratzl-Zelman, N., Fratzl, P., Horandner, H., Grabner, B., Varga, F., Ellinger, A., & Klaushofer, K. (1998). Matrix mineralization in MC3T3-E1 cell cultures initiated by beta-glycerophosphate pulse. *Bone, 23*(6), 511-520.

Frazier, T. P., Gimble, J. M., Devay, J. W., Tucker, H. A., Chiu, E. S., & Rowan, B. G. (2013). Body mass index affects proliferation and osteogenic differentiation of human subcutaneous adipose tissue-derived stem cells. *BMC Cell Biol., 14*, 34-2121-14-34.

Friedenstein, A. J., Petrakova, K. V., Kurolesova, A. I., & Frolova, G. P. (1968). Heterotopic of bone marrow. analysis of precursor cells for osteogenic and hematopoietic tissues. *Transplantation, 6*(2), 230-247.

Fu, H., Fu, Q., Zhou, N., Huang, W., Rahaman, M. N., Wang, D., & Liu, X. (2009). In vitro evaluation of borate-based bioactive glass scaffolds prepared by a polymer foam replication method. *Materials Science and Engineering: C, 29*(7), 2275-2281.

Fu, L., Tang, T., Miao, Y., Zhang, S., Qu, Z., & Dai, K. (2008). Stimulation of osteogenic differentiation and inhibition of adipogenic differentiation in bone marrow stromal cells by alendronate via ERK and JNK activation. *Bone, 43*(1), 40-47.

Fu, Q., Rahaman, M. N., Bal, B. S., Kuroki, K., & Brown, R. F. (2010). In vivo evaluation of 13-93 bioactive glass scaffolds with trabecular and oriented microstructures in a subcutaneous rat implantation model. *J.Biomed.Mater.Res.A., 95*(1), 235-244.

Fu, Q., Saiz, E., & Tomsia, A. P. (2011a). Bioinspired strong and highly porous glass scaffolds. *Adv.Funct.Mater., 21*(6), 1058-1063.

Fu, Q., Saiz, E., & Tomsia, A. P. (2011b). Direct ink writing of highly porous and strong glass scaffolds for load-bearing bone defects repair and regeneration. *Acta Biomater., 7*(10), 3547-3554.

Fuentealba, L. C., Eivers, E., Ikeda, A., Hurtado, C., Kuroda, H., Pera, E. M., & De Robertis, E. M. (2007). Integrating patterning signals: Wnt/GSK3 regulates the duration of the BMP/Smad1 signal. *Cell, 131*(5), 980-993.

Gabrielsson, B. G., Olofsson, L. E., Sjögren, A., Jernås, M., Elander, A., Lönn, M., Rudemo, M., & Carlsson, L. M. (2005). Evaluation of reference genes for studies of gene expression in human adipose tissue. *Obes.Res., 13*(4), 649-652.

Gallea, S., Lallemand, F., Atfi, A., Rawadi, G., Ramez, V., Spinella-Jaegle, S., Kawai, S., Faucheu, C., Huet, L., Baron, R., & Roman-Roman, S. (2001). Activation of mitogen-activated protein kinase cascades is involved in regulation of bone morphogenetic protein-2-induced osteoblast differentiation in pluripotent C2C12 cells. *Bone, 28*(5), 491-498.

Gao, S., Zhao, P., Lin, C., Sun, Y., Wang, Y., Zhou, Z., Yang, D., Wang, X., Xu, H., Zhou, F., Cao, L., Zhou, W., Ning, K., Chen, X., & Xu, J. (2014). Differentiation of human adipose-derived stem cells into neuron-like cells which are compatible with photocurable three-dimensional scaffolds. *Tissue Eng.Part A., 20*(7-8), 1271-1284.

Ge, C., Xiao, G., Jiang, D., Yang, Q., Hatch, N. E., Roca, H., & Franceschi, R. T. (2009). Identification and functional characterization of ERK/MAPK phosphorylation sites in the Runx2 transcription factor. *J.Biol.Chem., 284*(47), 32533-32543.

Ge, C., Yang, Q., Zhao, G., Yu, H., Kirkwood, K. L., & Franceschi, R. T. (2012). Interactions between extracellular signal-regulated kinase 1/2 and p38 MAP kinase pathways in the control of RUNX2 phosphorylation and transcriptional activity. *J.Bone Miner.Res., 27*(3), 538-551.

Gerhardt, L. C., Widdows, K. L., Erol, M. M., Burch, C. W., Sanz-Herrera, J. A., Ochoa, I., Stampfli, R., Roqan, I. S., Gabe, S., Ansari, T., & Boccaccini, A. R. (2011). The pro-angiogenic properties of multi-functional bioactive glass composite scaffolds. *Biomaterials, 32*(17), 4096-4108.

Ghosh-Choudhury, N., Mandal, C. C., Das, F., Ganapathy, S., Ahuja, S., & Ghosh Choudhury, G. (2013). C-abl-dependent molecular circuitry involving Smad5 and phosphatidylinositol 3-kinase regulates bone morphogenetic protein-2-induced osteogenesis. *J.Biol.Chem., 288*(34), 24503-24517.

Giancotti, F. G., & Ruoslahti, E. (1999). Integrin signaling. *Science, 285*(5430), 1028-1032.

Gimble, J., & Guilak, F. (2003). Adipose-derived adult stem cells: Isolation, characterization, and differentiation potential. *Cytotherapy, 5*(5), 362-369.

Gomide, V., Zonari, A., Ocarino, N., Goes, A., Serakides, R., & Pereira, M. (2012). In vitro and in vivo osteogenic potential of bioactiveglass-PVA hybrid scaffolds colonized by mesenchymal stem cells. *Biomed Mater., 7*(1)

Gong, W., Huang, Z., Dong, Y., Gan, Y., Li, S., Gao, X., & Chen, X. (2014). Ionic extraction of a novel nano-sized bioactive glass enhances differentiation and mineralization of human dental pulp cells. *J.Endod., 40*(1), 83-88.

Gough, J. E., Jones, J. R., & Hench, L. L. (2004). Nodule formation and mineralisation of human primary osteoblasts cultured on a porous bioactive glass scaffold. *Biomaterials, 25*(11), 2039-2046.

Greenblatt, M. B., Shim, J. H., & Glimcher, L. H. (2013). Mitogen-activated protein kinase pathways in osteoblasts. *Annu.Rev.Cell Dev.Biol., 29*, 63-79.

Greenblatt, M. B., Shim, J. H., Zou, W., Sitara, D., Schweitzer, M., Hu, D., Lotinun, S., Sano, Y., Baron, R., Park, J. M., Arthur, S., Xie, M., Schneider, M. D., Zhai, B., Gygi, S., Davis, R., & Glimcher, L. H. (2010). The p38 MAPK pathway is essential for skeletogenesis and bone homeostasis in mice. *J.Clin.Invest., 120*(7), 2457-2473.

Gronthos, S., Mankani, M., Brahim, J., Robey, P. G., & Shi, S. (2000). Postnatal human dental pulp stem cells (DPSCs) in vitro and in vivo. *Proc.Natl.Acad.Sci.U.S.A., 97*(25), 13625-13630.

Gu, H., Guo, F., Zhou, X., Gong, L., Zhang, Y., Zhai, W., Chen, L., Cen, L., Yin, S., Chang, J., & Cui, L. (2011). The stimulation of osteogenic differentiation of human adipose-derived stem cells by ionic products from akermanite dissolution via activation of the ERK pathway. *Biomaterials, 32*(29), 7023-7033.

Gu, H., Huang, Z., Yin, X., Zhang, J., Gong, L., Chen, J., Rong, K., Xu, J., Lu, L., & Cui, L. (2015). Role of c-jun N-terminal kinase in the osteogenic and adipogenic differentiation of human adipose-derived mesenchymal stem cells. *Exp.Cell Res., 339*(1), 112-121.

Guicheux, J., Lemonnier, J., Ghayor, C., Suzuki, A., Palmer, G., & Caverzasio, J. (2003). Activation of p38 mitogen-activated protein kinase and c-jun-NH2-terminal kinase by BMP-2 and their implication in the stimulation of osteoblastic cell differentiation. *J.Bone Miner.Res., 18*(11), 2060-2068.

Gupta, A., Leong, D. T., Bai, H. F., Singh, S. B., Lim, T. C., & Hutmacher, D. W. (2007). Osteo-maturation of adipose-derived stem cells required the combined action of vitamin D3, beta-glycerophosphate, and ascorbic acid. *Biochem.Biophys.Res.Commun., 362*(1), 17-24.

Haimi, S., Moimas, L., Pirhonen, E., Lindroos, B., Huhtala, H., Räty, S., Kuokkanen, H., Sandor, G. K., Miettinen, S., & Suuronen, R. (2009b). Calcium phosphate surface treatment of bioactive glass causes a delay in early osteogenic differentiation of adipose stem cells. *J.Biomed.Mater.Res.A., 91*(2), 540-547.

Haimi, S., Suuriniemi, N., Haaparanta, A. M., Ellä, V., Lindroos, B., Huhtala, H., Räty, S., Kuokkanen, H., Sandor, G. K., Kellomäki, M., Miettinen, S., & Suuronen, R.

(2009a). Growth and osteogenic differentiation of adipose stem cells on PLA/bioactive glass and PLA/beta-TCP scaffolds. *Tissue Eng.Part A., 15*(7), 1473-1480.

Hakki, S. S., Bozkurt, B. S., & Hakki, E. E. (2010). Boron regulates mineralized tissue-associated proteins in osteoblasts (MC3T3-E1). *J.Trace Elem.Med.Biol., 24*(4), 243-250.

Halvorsen, Y. D., Franklin, D., Bond, A. L., Hitt, D. C., Auchter, C., Boskey, A. L., Paschalis, E. P., Wilkison, W. O., & Gimble, J. M. (2001). Extracellular matrix mineralization and osteoblast gene expression by human adipose tissue-derived stromal cells. *Tissue Eng., 7*(6), 729-741.

Halvorsen, Y. D., Wilkison, W. O., & Gimble, J. M. (2000). Adipose-derived stromal cells--their utility and potential in bone formation. *Int.J.Obes.Relat.Metab.Disord., 24 Suppl 4*, S41-4.

Hamidouche, Z., Hay, E., Vaudin, P., Charbord, P., Schule, R., Marie, P. J., & Fromigue, O. (2008). FHL2 mediates dexamethasone-induced mesenchymal cell differentiation into osteoblasts by activating wnt/beta-catenin signaling-dependent Runx2 expression. *FASEB J., 22*(11), 3813-3822.

Hamilton, D. W., & Brunette, D. M. (2007). The effect of substratum topography on osteoblast adhesion mediated signal transduction and phosphorylation. *Biomaterials, 28*(10), 1806-1819.

Han, S. M., Coh, Y. R., Ahn, J. O., Jang, G., Yum, S. Y., Kang, S. K., Lee, H. W., & Youn, H. Y. (2015). Enhanced hepatogenic transdifferentiation of human adipose tissue mesenchymal stem cells by gene engineering with Oct4 and Sox2. *PLoS One, 10*(3), e0108874.

Harada, N., Watanabe, Y., Sato, K., Abe, S., Yamanaka, K., Sakai, Y., Kaneko, T., & Matsushita, T. (2014). Bone regeneration in a massive rat femur defect through endochondral ossification achieved with chondrogenically differentiated MSCs in a degradable scaffold. *Biomaterials, 35*(27), 7800-7810.

Hata, K., Nishimura, R., Ikeda, F., Yamashita, K., Matsubara, T., Nokubi, T., & Yoneda, T. (2003). Differential roles of Smad1 and p38 kinase in regulation of peroxisome proliferator-activating receptor gamma during bone morphogenetic protein 2-induced adipogenesis. *Mol.Biol.Cell, 14*(2), 545-555.

Hattori, H., Masuoka, K., Sato, M., Ishihara, M., Asazuma, T., Takase, B., Kikuchi, M., Nemoto, K., & Ishihara, M. (2006). Bone formation using human adipose tissue-derived stromal cells and a biodegradable scaffold. *J.Biomed.Mater.Res.B.Appl.Biomater., 76*(1), 230-239.

Hayrapetyan, A., Jansen, J. A., & van den Beucken, J. J. (2015). Signaling pathways involved in osteogenesis and their application for bone regenerative medicine. *Tissue Eng.Part B.Rev., 21*(1), 75-87.

Hench, L. L. (1988). Bioactive ceramics. *Ann.N.Y.Acad.Sci., 523*, 54-71.

Hench, L. L. (2006). The story of bioglass. *J.Mater.Sci.Mater.Med., 17*(11), 967-978.

Hench, L. L., Splinter, R. J., Allen, W. C., & Greenlee, T. K. (1971). Bonding mechanisms at the interface of ceramic prosthetic materials. *J.Biomed.Mater.Res., 5*(6), 117-141.

Hench, L. L. (1991). Bioceramics: From concept to clinic. *J Am Ceram Soc, 74*(7), 1487-1510.

Hench, L. L. (1998). Bioceramics. *J Am Ceram Soc, 81*(7), 1705-1728.

Higuchi, C., Myoui, A., Hashimoto, N., Kuriyama, K., Yoshioka, K., Yoshikawa, H., & Itoh, K. (2002). Continuous inhibition of MAPK signaling promotes the early osteoblastic differentiation and mineralization of the extracellular matrix. *J.Bone Miner.Res., 17*(10), 1785-1794.

Hilton, M. J., Tu, X., Wu, X., Bai, S., Zhao, H., Kobayashi, T., Kronenberg, H. M., Teitelbaum, S. L., Ross, F. P., Kopan, R., & Long, F. (2008). Notch signaling maintains bone marrow mesenchymal progenitors by suppressing osteoblast differentiation. *Nat.Med., 14*(3), 306-314.

Hong, D., Chen, H. X., Xue, Y., Li, D. M., Wan, X. C., Ge, R., & Li, J. C. (2009). Osteoblastogenic effects of dexamethasone through upregulation of TAZ expression in rat mesenchymal stem cells. *J.Steroid Biochem.Mol.Biol., 116*(1-2), 86-92.

Hoppe, A., Guldal, N. S., & Boccaccini, A. R. (2011). A review of the biological response to ionic dissolution products from bioactive glasses and glass-ceramics. *Biomaterials, 32*(11), 2757-2774.

Horwitz, E. M., Le Blanc, K., Dominici, M., Mueller, I., Slaper-Cortenbach, I., Marini, F. C., Deans, R. J., Krause, D. S., Keating, A., & International Society for Cellular Therapy. (2005). Clarification of the nomenclature for MSC: The international society for cellular therapy position statement. *Cytotherapy, 7*(5), 393-395.

Hsieh, W. T., Liu, Y. S., Lee, Y. H., Rimando, M. G., Lin, K. H., & Lee, O. K. (2016). Matrix dimensionality and stiffness cooperatively regulate osteogenesis of mesenchymal stromal cells. *Acta Biomater., 32*, 210-222.

Huang, H., Song, T. J., Li, X., Hu, L., He, Q., Liu, M., Lane, M. D., & Tang, Q. Q. (2009). BMP signaling pathway is required for commitment of C3H10T1/2 pluripotent stem cells to the adipocyte lineage. *Proc.Natl.Acad.Sci.U.S.A., 106*(31), 12670-12675.

Huang, S., Wang, S., Bian, C., Yang, Z., Zhou, H., Zeng, Y., Li, H., Han, Q., & Zhao, R. C. (2012). Upregulation of miR-22 promotes osteogenic differentiation and inhibits adipogenic differentiation of human adipose tissue-derived mesenchymal stem cells by repressing HDAC6 protein expression. *Stem Cells Dev., 21*(13), 2531-2540.

Huebsch, N., Arany, P. R., Mao, A. S., Shvartsman, D., Ali, O. A., Bencherif, S. A., Rivera-Feliciano, J., & Mooney, D. J. (2010). Harnessing traction-mediated manipulation of the cell/matrix interface to control stem-cell fate. *Nat.Mater., 9*(6), 518-526.

Hwang, J. H., Byun, M. R., Kim, A. R., Kim, K. M., Cho, H. J., Lee, Y. H., Kim, J., Jeong, M. G., Hwang, E. S., & Hong, J. H. (2015). Extracellular matrix stiffness regulates osteogenic differentiation through MAPK activation. *PLoS One, 10*(8), e0135519.

Hynes, K., Menicanin, D., Mrozik, K., Gronthos, S., & Bartold, P. M. (2014). Generation of functional mesenchymal stem cells from different induced pluripotent stem cell lines. *Stem Cells Dev., 23*(10), 1084-1096.

Hynes, R. O. (2002). Integrins: Bidirectional, allosteric signaling machines. *Cell, 110*(6), 673-687.

Igura, K., Zhang, X., Takahashi, K., Mitsuru, A., Yamaguchi, S., & Takashi, T. A. (2004). Isolation and characterization of mesenchymal progenitor cells from chorionic villi of human placenta. *Cytotherapy, 6*(6), 543-553.

Ivaska, J., Reunanen, H., Westermarck, J., Koivisto, L., Kähäri, V. M., & Heino, J. (1999). Integrin alpha2beta1 mediates isoform-specific activation of p38 and upregulation of collagen gene transcription by a mechanism involving the alpha2 cytoplasmic tail. *J.Cell Biol., 147*(2), 401-416.

Jaiswal, R. K., Jaiswal, N., Bruder, S. P., Mbalaviele, G., Marshak, D. R., & Pittenger, M. F. (2000). Adult human mesenchymal stem cell differentiation to the osteogenic or adipogenic lineage is regulated by mitogen-activated protein kinase. *J.Biol.Chem., 275*(13), 9645-9652.

Jakob, M., Saxer, F., Scotti, C., Schreiner, S., Studer, P., Scherberich, A., Heberer, M., & Martin, I. (2012). Perspective on the evolution of cell-based bone tissue engineering strategies. *Eur.Surg.Res., 49*(1), 1-7.

James, A. W. (2013). Review of signaling pathways governing MSC osteogenic and adipogenic differentiation. *Scientifica (Cairo), 2013*, 684736.

James, A. W., LaChaud, G., Shen, J., Asatrian, G., Nguyen, V., Zhang, X., Ting, K., & Soo, C. (2016). A review of the clinical side effects of bone morphogenetic protein-2. *Tissue Eng.Part B.Rev.,*

James, A. W., Pang, S., Askarinam, A., Corselli, M., Zara, J. N., Goyal, R., Chang, L., Pan, A., Shen, J., Yuan, W., Stoker, D., Zhang, X., Adams, J. S., Ting, K., & Soo, C. (2012). Additive effects of sonic hedgehog and nell-1 signaling in osteogenic versus adipogenic differentiation of human adipose-derived stromal cells. *Stem Cells Dev., 21*(12), 2170-2178.

Janderova, L., McNeil, M., Murrell, A. N., Mynatt, R. L., & Smith, S. R. (2003). Human mesenchymal stem cells as an in vitro model for human adipogenesis. *Obes.Res., 11*(1), 65-74.

Jang, S., Cho, H. H., Cho, Y. B., Park, J. S., & Jeong, H. S. (2010). Functional neural differentiation of human adipose tissue-derived stem cells using bFGF and forskolin. *BMC Cell Biol., 11*, 25-2121-11-25.

Javed, A., Afzal, F., Bae, J. S., Gutierrez, S., Zaidi, K., Pratap, J., van Wijnen, A. J., Stein, J. L., Stein, G. S., & Lian, J. B. (2009). Specific residues of RUNX2 are obligatory for formation of BMP2-induced RUNX2-SMAD complex to promote osteoblast differentiation. *Cells Tissues Organs, 189*(1-4), 133-137.

Jell, G., Notingher, I., Tsigkou, O., Notingher, P., Polak, J. M., Hench, L. L., & Stevens, M. M. (2008). Bioactive glass-induced osteoblast differentiation: A noninvasive spectroscopic study. *J.Biomed.Mater.Res.A., 86*(1), 31-40.

Jeon, O., Rhie, J. W., Kwon, I. K., Kim, J. H., Kim, B. S., & Lee, S. H. (2008). In vivo bone formation following transplantation of human adipose-derived stromal cells that are not differentiated osteogenically. *Tissue Eng.Part A., 14*(8), 1285-1294.

Jikko, A., Harris, S. E., Chen, D., Mendrick, D. L., & Damsky, C. H. (1999). Collagen integrin receptors regulate early osteoblast differentiation induced by BMP-2. *J.Bone Miner.Res., 14*(7), 1075-1083.

Jin, Y., Zhang, W., Liu, Y., Zhang, M., Xu, L., Wu, Q., Zhang, X., Zhu, Z., Huang, Q., & Jiang, X. (2014). rhPDGF-BB via ERK pathway osteogenesis and adipogenesis balancing in ADSCs for critical-sized calvarial defect repair. *Tissue Eng.Part A., 20*(23-24), 3303-3313.

Jones, J. R. (2015). Reprint of: Review of bioactive glass: From hench to hybrids. *Acta Biomater., 23 Suppl*, S53-82.

Jones, J. R., Tsigkou, O., Coates, E. E., Stevens, M. M., Polak, J. M., & Hench, L. L. (2007). Extracellular matrix formation and mineralization on a phosphate-free porous bioactive glass scaffold using primary human osteoblast (HOB) cells. *Biomaterials, 28*(9), 1653-1663.

Jung, K. W. (2009). Perspectives on human stem cell research. *J.Cell.Physiol., 220*(3), 535-537.

Kakudo, N., Shimotsuma, A., & Kusumoto, K. (2007). Fibroblast growth factor-2 stimulates adipogenic differentiation of human adipose-derived stem cells. *Biochem.Biophys.Res.Commun., 359*(2), 239-244.

Kang, Q., Song, W. X., Luo, Q., Tang, N., Luo, J., Luo, X., Chen, J., Bi, Y., He, B. C., Park, J. K., Jiang, W., Tang, Y., Huang, J., Su, Y., Zhu, G. H., He, Y., Yin, H., Hu, Z., Wang, Y., Chen, L., Zuo, G. W., Pan, X., Shen, J., Vokes, T., Reid, R. R., Haydon, R. C., Luu, H. H., & He, T. C. (2009). A comprehensive analysis of the dual roles of BMPs in regulating adipogenic and osteogenic differentiation of mesenchymal progenitor cells. *Stem Cells Dev., 18*(4), 545-559.

Kanno, T., Takahashi, T., Tsujisawa, T., Ariyoshi, W., & Nishihara, T. (2007). Mechanical stress-mediated Runx2 activation is dependent on ras/ERK1/2 MAPK signaling in osteoblasts. *J.Cell.Biochem., 101*(5), 1266-1277.

Khanna-Jain, R., Mannerström, B., Vuorinen, A., Sandor, G. K., Suuronen, R., & Miettinen, S. (2012). Osteogenic differentiation of human dental pulp stem cells on beta-tricalcium phosphate/poly (l-lactic acid/caprolactone) three-dimensional scaffolds. *J.Tissue Eng., 3*(1), 2041731412467998.

Khetan, S., Guvendiren, M., Legant, W. R., Cohen, D. M., Chen, C. S., & Burdick, J. A. (2013). Degradation-mediated cellular traction directs stem cell fate in covalently crosslinked three-dimensional hydrogels. *Nat.Mater., 12*(5), 458-465.

Khojasteh, A., Behnia, H., Hosseini, F. S., Dehghan, M. M., Abbasnia, P., & Abbas, F. M. (2013). The effect of PCL-TCP scaffold loaded with mesenchymal stem cells on vertical bone augmentation in dog mandible: A preliminary report. *J.Biomed.Mater.Res.B.Appl.Biomater.,*

Kilian, K. A., Bugarija, B., Lahn, B. T., & Mrksich, M. (2010). Geometric cues for directing the differentiation of mesenchymal stem cells. *Proc.Natl.Acad.Sci.U.S.A., 107*(11), 4872-4877.

Kim, G. H., Park, Y. D., Lee, S. Y., El-Fiqi, A., Kim, J. J., Lee, E. J., Kim, H. W., & Kim, E. C. (2015). Odontogenic stimulation of human dental pulp cells with bioactive nanocomposite fiber. *J.Biomater.Appl., 29*(6), 854-866.

Kim, H. P., Ji, Y. H., Rhee, S. C., Dhong, E. S., Park, S. H., & Yoon, E. S. (2012). Enhancement of bone regeneration using osteogenic-induced adipose-derived stem cells combined with demineralized bone matrix in a rat critically-sized calvarial defect model. *Curr.Stem Cell.Res.Ther., 7*(3), 165-172.

Kim, S. P., Ha, J. M., Yun, S. J., Kim, E. K., Chung, S. W., Hong, K. W., Kim, C. D., & Bae, S. S. (2010). Transcriptional activation of peroxisome proliferator-activated receptor-gamma requires activation of both protein kinase A and akt during adipocyte differentiation. *Biochem.Biophys.Res.Commun., 399*(1), 55-59.

Kimbrel, E. A., & Lanza, R. (2015). Current status of pluripotent stem cells: Moving the first therapies to the clinic. *Nat.Rev.Drug Discov., 14*(10), 681-692.

Klees, R. F., Salasznyk, R. M., Kingsley, K., Williams, W. A., Boskey, A., & Plopper, G. E. (2005). Laminin-5 induces osteogenic gene expression in human mesenchymal stem cells through an ERK-dependent pathway. *Mol.Biol.Cell, 16*(2), 881-890.

Knippenberg, M., Helder, M. N., Doulabi, B. Z., Semeins, C. M., Wuisman, P. I., & Klein-Nulend, J. (2005). Adipose tissue-derived mesenchymal stem cells acquire bone cell-like responsiveness to fluid shear stress on osteogenic stimulation. *Tissue Eng., 11*(11-12), 1780-1788.

Komori, T., Yagi, H., Nomura, S., Yamaguchi, A., Sasaki, K., Deguchi, K., Shimizu, Y., Bronson, R. T., Gao, Y. H., Inada, M., Sato, M., Okamoto, R., Kitamura, Y., Yoshiki, S., & Kishimoto, T. (1997). Targeted disruption of Cbfa1 results in a complete lack of bone formation owing to maturational arrest of osteoblasts. *Cell, 89*(5), 755-764.

Kono, S. J., Oshima, Y., Hoshi, K., Bonewald, L. F., Oda, H., Nakamura, K., Kawaguchi, H., & Tanaka, S. (2007). Erk pathways negatively regulate matrix mineralization. *Bone, 40*(1), 68-74.

Kornicka, K., Marycz, K., Tomaszewski, K. A., Maredziak, M., & Smieszek, A. (2015). The effect of age on osteogenic and adipogenic differentiation potential of human adipose derived stromal stem cells (hASCs) and the impact of stress factors in the course of the differentiation process. *Oxid Med.Cell.Longev, 2015*, 309169.

Kozawa, O., Hatakeyama, D., & Uematsu, T. (2002). Divergent regulation by p44/p42 MAP kinase and p38 MAP kinase of bone morphogenetic protein-4-stimulated osteocalcin synthesis in osteoblasts. *J.Cell.Biochem., 84*(3), 583-589.

Krampera, M., Marconi, S., Pasini, A., Galie, M., Rigotti, G., Mosna, F., Tinelli, M., Lovato, L., Anghileri, E., Andreini, A., Pizzolo, G., Sbarbati, A., & Bonetti, B. (2007). Induction of neural-like differentiation in human mesenchymal stem cells derived from bone marrow, fat, spleen and thymus. *Bone, 40*(2), 382-390.

Kyllönen, L., Haimi, S., Mannerström, B., Huhtala, H., Rajala, K. M., Skottman, H., Sandor, G. K., & Miettinen, S. (2013). Effects of different serum conditions on

osteogenic differentiation of human adipose stem cells in vitro. *Stem Cell.Res.Ther., 4*(1), 17.

Lai, C. F., Chaudhary, L., Fausto, A., Halstead, L. R., Ory, D. S., Avioli, L. V., & Cheng, S. L. (2001). Erk is essential for growth, differentiation, integrin expression, and cell function in human osteoblastic cells. *J.Biol.Chem., 276*(17), 14443-14450.

Lai, C. F., & Cheng, S. L. (2002). Signal transductions induced by bone morphogenetic protein-2 and transforming growth factor-beta in normal human osteoblastic cells. *J.Biol.Chem., 277*(18), 15514-15522.

Lakhkar, N. J., Lee, I. H., Kim, H. W., Salih, V., Wall, I. B., & Knowles, J. C. (2013). Bone formation controlled by biologically relevant inorganic ions: Role and controlled delivery from phosphate-based glasses. *Adv.Drug Deliv.Rev., 65*(4), 405-420.

Landis, W. J., & Silver, F. H. (2009). Mineral deposition in the extracellular matrices of vertebrate tissues: Identification of possible apatite nucleation sites on type I collagen. *Cells Tissues Organs, 189*(1-4), 20-24.

Langenbach, F., & Handschel, J. (2013). Effects of dexamethasone, ascorbic acid and beta-glycerophosphate on the osteogenic differentiation of stem cells in vitro. *Stem Cell.Res.Ther., 4*(5), 117.

Langer, R., & Vacanti, J. P. (1993). Tissue engineering. *Science, 260*(5110), 920-926.

Larranaga, A., Alonso-Varona, A., Palomares, T., Rubio-Azpeitia, E., Aldazabal, P., Martin, F. J., & Sarasua, J. R. (2015). Effect of bioactive glass particles on osteogenic differentiation of adipose-derived mesenchymal stem cells seeded on lactide and caprolactone based scaffolds. *J.Biomed.Mater.Res.A., 103*(12), 3815-3824.

Larsen, K. H., Frederiksen, C. M., Burns, J. S., Abdallah, B. M., & Kassem, M. (2010). Identifying a molecular phenotype for bone marrow stromal cells with in vivo bone-forming capacity. *J.Bone Miner.Res., 25*(4), 796-808.

Lee, J., Abdeen, A. A., & Kilian, K. A. (2014). Rewiring mesenchymal stem cell lineage specification by switching the biophysical microenvironment. *Sci.Rep., 4*, 5188.

Lee, M. H., Kim, Y. J., Yoon, W. J., Kim, J. I., Kim, B. G., Hwang, Y. S., Wozney, J. M., Chi, X. Z., Bae, S. C., Choi, K. Y., Cho, J. Y., Choi, J. Y., & Ryoo, H. M. (2005). Dlx5 specifically regulates Runx2 type II expression by binding to homeodomain-response elements in the Runx2 distal promoter. *J.Biol.Chem., 280*(42), 35579-35587.

Lefterova, M. I., & Lazar, M. A. (2009). New developments in adipogenesis. *Trends Endocrinol.Metab., 20*(3), 107-114.

Lehmann, J. M., Lenhard, J. M., Oliver, B. B., Ringold, G. M., & Kliewer, S. A. (1997). Peroxisome proliferator-activated receptors alpha and gamma are activated by indomethacin and other non-steroidal anti-inflammatory drugs. *J.Biol.Chem., 272*(6), 3406-3410.

Lei, B., Chen, X., Wang, Y., Zhao, N., Du, C., & Fang, L. (2010). Surface nanoscale patterning of bioactive glass to support cellular growth and differentiation. *J.Biomed.Mater.Res.A., 94*(4), 1091-1099.

Leidi, M., Dellera, F., Mariotti, M., & Maier, J. A. (2011). High magnesium inhibits human osteoblast differentiation in vitro. *Magnes.Res., 24*(1), 1-6.

Lendeckel, S., Jodicke, A., Christophis, P., Heidinger, K., Wolff, J., Fraser, J. K., Hedrick, M. H., Berthold, L., & Howaldt, H. P. (2004). Autologous stem cells (adipose) and fibrin glue used to treat widespread traumatic calvarial defects: Case report. *J.Craniomaxillofac.Surg., 32*(6), 370-373.

Leppäranta, O., Vaahtio, M., Peltola, T., Zhang, D., Hupa, L., Hupa, M., Ylänen, H., Salonen, J. I., Viljanen, M. K., & Eerola, E. (2008). Antibacterial effect of bioactive glasses on clinically important anaerobic bacteria in vitro. *J.Mater.Sci.Mater.Med., 19*(2), 547-551.

Leu, A., & Leach, J. K. (2008). Proangiogenic potential of a collagen/bioactive glass substrate. *Pharm.Res., 25*(5), 1222-1229.

Leucht, P., Jiang, J., Cheng, D., Liu, B., Dhamdhere, G., Fang, M. Y., Monica, S. D., Urena, J. J., Cole, W., Smith, L. R., Castillo, A. B., Longaker, M. T., & Helms, J. A. (2013). Wnt3a reestablishes osteogenic capacity to bone grafts from aged animals. *J.Bone Joint Surg.Am., 95*(14), 1278-1288.

Li, C., Vepari, C., Jin, H. J., Kim, H. J., & Kaplan, D. L. (2006). Electrospun silk-BMP-2 scaffolds for bone tissue engineering. *Biomaterials, 27*(16), 3115-3124.

Li, C. J., Madhu, V., Balian, G., Dighe, A. S., & Cui, Q. (2015). Cross-talk between VEGF and BMP-6 pathways accelerates osteogenic differentiation of human adipose-derived stem cells. *J.Cell.Physiol., 230*(11), 2671-2682.

Li, H., Li, T., Wang, S., Wei, J., Fan, J., Li, J., Han, Q., Liao, L., Shao, C., & Zhao, R. C. (2013). miR-17-5p and miR-106a are involved in the balance between osteogenic and adipogenic differentiation of adipose-derived mesenchymal stem cells. *Stem Cell.Res., 10*(3), 313-324.

Li, X., Yuan, J., Li, W., Liu, S., Hua, M., Lu, X., & Zhang, H. (2014). Direct differentiation of homogeneous human adipose stem cells into functional hepatocytes by mimicking liver embryogenesis. *J.Cell.Physiol., 229*(6), 801-812.

Lian, J. B., & Stein, G. S. (1995). Development of the osteoblast phenotype: Molecular mechanisms mediating osteoblast growth and differentiation. *Iowa Orthop.J., 15*, 118-140.

Lian, J. B., Stein, G. S., van Wijnen, A. J., Stein, J. L., Hassan, M. Q., Gaur, T., & Zhang, Y. (2012). MicroRNA control of bone formation and homeostasis. *Nat.Rev.Endocrinol., 8*(4), 212-227.

Liao, Y. H., Chang, Y. H., Sung, L. Y., Li, K. C., Yeh, C. L., Yen, T. C., Hwang, S. M., Lin, K. J., & Hu, Y. C. (2014). Osteogenic differentiation of adipose-derived stem cells and calvarial defect repair using baculovirus-mediated co-expression of BMP-2 and miR-148b. *Biomaterials, 35*(18), 4901-4910.

Lindroos, B., Aho, K. L., Kuokkanen, H., Räty, S., Huhtala, H., Lemponen, R., Yli-Harja, O., Suuronen, R., & Miettinen, S. (2010). Differential gene expression in adipose stem cells cultured in allogeneic human serum versus fetal bovine serum. *Tissue Eng.Part A., 16*(7), 2281-2294.

Lindroos, B., Boucher, S., Chase, L., Kuokkanen, H., Huhtala, H., Haataja, R., Vemuri, M., Suuronen, R., & Miettinen, S. (2009). Serum-free, xeno-free culture media maintain the proliferation rate and multipotentiality of adipose stem cells in vitro. *Cytotherapy, 11*(7), 958-972.

Lindroos, B., Suuronen, R., & Miettinen, S. (2011). The potential of adipose stem cells in regenerative medicine. *Stem Cell.Rev., 7*(2), 269-291.

Liu, Q., Cen, L., Zhou, H., Yin, S., Liu, G., Liu, W., Cao, Y., & Cui, L. (2009). The role of the extracellular signal-related kinase signaling pathway in osteogenic differentiation of human adipose-derived stem cells and in adipogenic transition initiated by dexamethasone. *Tissue Eng.Part A., 15*(11), 3487-3497.

Liu, Y., Chen, C., He, H., Wang, D., E, L., Liu, Z., & Liu, H. (2012). Lentiviral-mediated gene transfer into human adipose-derived stem cells: Role of NELL1 versus BMP2 in osteogenesis and adipogenesis in vitro. *Acta Biochim.Biophys.Sin.(Shanghai), 44*(10), 856-865.

Long, F. (2011). Building strong bones: Molecular regulation of the osteoblast lineage. *Nat.Rev.Mol.Cell Biol., 13*(1), 27-38.

Loty, C., Sautier, J. M., Tan, M. T., Oboeuf, M., Jallot, E., Boulekbache, H., Greenspan, D., & Forest, N. (2001). Bioactive glass stimulates in vitro osteoblast differentiation and creates a favorable template for bone tissue formation. *J.Bone Miner.Res., 16*(2), 231-239.

Lou, J., Tu, Y., Li, S., & Manske, P. R. (2000). Involvement of ERK in BMP-2 induced osteoblastic differentiation of mesenchymal progenitor cell line C3H10T1/2. *Biochem.Biophys.Res.Commun., 268*(3), 757-762.

Lu, Z., Roohani-Esfahani, S. I., Li, J., & Zreiqat, H. (2015). Synergistic effect of nanomaterials and BMP-2 signalling in inducing osteogenic differentiation of adipose tissue-derived mesenchymal stem cells. *Nanomedicine, 11*(1), 219-228.

Lu, Z., Roohani-Esfahani, S. I., Wang, G., & Zreiqat, H. (2012). Bone biomimetic microenvironment induces osteogenic differentiation of adipose tissue-derived mesenchymal stem cells. *Nanomedicine, 8*(4), 507-515.

Lu, Z., & Zreiqat, H. (2010). Beta-tricalcium phosphate exerts osteoconductivity through alpha2beta1 integrin and down-stream MAPK/ERK signaling pathway. *Biochem.Biophys.Res.Commun., 394*(2), 323-329.

Luyten, F. P., Cunningham, N. S., Ma, S., Muthukumaran, N., Hammonds, R. G., Nevins, W. B., Woods, W. I., & Reddi, A. H. (1989). Purification and partial amino acid sequence of osteogenin, a protein initiating bone differentiation. *J.Biol.Chem., 264*(23), 13377-13380.

Luzi, E., Marini, F., Sala, S. C., Tognarini, I., Galli, G., & Brandi, M. L. (2008). Osteogenic differentiation of human adipose tissue-derived stem cells is modulated by the miR-26a targeting of the SMAD1 transcription factor. *J.Bone Miner.Res., 23*(2), 287-295.

Madras, N., Gibbs, A. L., Zhou, Y., Zandstra, P. W., & Aubin, J. E. (2002). Modeling stem cell development by retrospective analysis of gene expression profiles in single progenitor-derived colonies. *Stem Cells, 20*(3), 230-240.

Maeno, S., Niki, Y., Matsumoto, H., Morioka, H., Yatabe, T., Funayama, A., Toyama, Y., Taguchi, T., & Tanaka, J. (2005). The effect of calcium ion concentration on osteoblast viability, proliferation and differentiation in monolayer and 3D culture. *Biomaterials, 26*(23), 4847-4855.

Mannello, F., & Tonti, G. A. (2007). Concise review: No breakthroughs for human mesenchymal and embryonic stem cell culture: Conditioned medium, feeder layer, or feeder-free; medium with fetal calf serum, human serum, or enriched plasma; serum-free, serum replacement nonconditioned medium, or ad hoc formula? all that glitters is not gold! *Stem Cells, 25*(7), 1603-1609.

Marelli, B., Ghezzi, C. E., Mohn, D., Stark, W. J., Barralet, J. E., Boccaccini, A. R., & Nazhat, S. N. (2011). Accelerated mineralization of dense collagen-nano bioactive glass hybrid gels increases scaffold stiffness and regulates osteoblastic function. *Biomaterials, 32*(34), 8915-8926.

Margoni, A., Fotis, L., & Papavassiliou, A. G. (2012). The transforming growth factor-beta/bone morphogenetic protein signalling pathway in adipogenesis. *Int.J.Biochem.Cell Biol., 44*(3), 475-479.

Marino, G., Rosso, F., Cafiero, G., Tortora, C., Moraci, M., Barbarisi, M., & Barbarisi, A. (2010). Beta-tricalcium phosphate 3D scaffold promote alone osteogenic differentiation of human adipose stem cells: In vitro study. *J.Mater.Sci.Mater.Med., 21*(1), 353-363.

Marklein, R. A., Lo Surdo, J. L., Bellayr, I. H., Godil, S. A., Puri, R. K., & Bauer, S. R. (2016). High content imaging of early morphological signatures predicts long term mineralization capacity of human mesenchymal stem cells upon osteogenic induction. *Stem Cells, 34*(4), 935-947.

Martin, G. R. (1981). Isolation of a pluripotent cell line from early mouse embryos cultured in medium conditioned by teratocarcinoma stem cells. *Proc.Natl.Acad.Sci.U.S.A., 78*(12), 7634-7638.

Matsuguchi, T., Chiba, N., Bandow, K., Kakimoto, K., Masuda, A., & Ohnishi, T. (2009). JNK activity is essential for Atf4 expression and late-stage osteoblast differentiation. *J.Bone Miner.Res., 24*(3), 398-410.

Matsuoka, F., Takeuchi, I., Agata, H., Kagami, H., Shiono, H., Kiyota, Y., Honda, H., & Kato, R. (2013). Morphology-based prediction of osteogenic differentiation potential of human mesenchymal stem cells. *PLoS One, 8*(2), e55082.

Matsushita, T., Chan, Y. Y., Kawanami, A., Balmes, G., Landreth, G. E., & Murakami, S. (2009). Extracellular signal-regulated kinase 1 (ERK1) and ERK2 play essential roles in osteoblast differentiation and in supporting osteoclastogenesis. *Mol.Cell.Biol., 29*(21), 5843-5857.

Maumus, M., Peyrafitte, J. A., D'Angelo, R., Fournier-Wirth, C., Bouloumie, A., Casteilla, L., Sengenes, C., & Bourin, P. (2011). Native human adipose stromal cells: Localization, morphology and phenotype. *Int.J.Obes.(Lond), 35*(9), 1141-1153.

McArdle, A., Chung, M. T., Paik, K. J., Duldulao, C., Chan, C., Rennert, R., Walmsley, G. G., Senarath-Yapa, K., Hu, M., Seo, E., Lee, M., Wan, D. C., & Longaker, M. T.

(2014). Positive selection for bone morphogenetic protein receptor type-IB promotes differentiation and specification of human adipose-derived stromal cells toward an osteogenic lineage. *Tissue Eng.Part A., 20*(21-22), 3031-3040.

McBeath, R., Pirone, D. M., Nelson, C. M., Bhadriraju, K., & Chen, C. S. (2004). Cell shape, cytoskeletal tension, and RhoA regulate stem cell lineage commitment. *Dev.Cell., 6*(4), 483-495.

McIntosh, K., Zvonic, S., Garrett, S., Mitchell, J. B., Floyd, Z. E., Hammill, L., Kloster, A., Di Halvorsen, Y., Ting, J. P., Storms, R. W., Goh, B., Kilroy, G., Wu, X., & Gimble, J. M. (2006). The immunogenicity of human adipose-derived cells: Temporal changes in vitro. *Stem Cells, 24*(5), 1246-1253.

Mehrkens, A., Saxer, F., Güven, S., Hoffmann, W., Müller, A. M., Jakob, M., Weber, F. E., Martin, I., & Scherberich, A. (2012). Intraoperative engineering of osteogenic grafts combining freshly harvested, human adipose-derived cells and physiological doses of bone morphogenetic protein-2. *Eur.Cell.Mater., 24*, 308-319.

Mendes, S. C., Tibbe, J. M., Veenhof, M., Both, S., Oner, F. C., van Blitterswijk, C. A., & de Bruijn, J. D. (2004). Relation between in vitro and in vivo osteogenic potential of cultured human bone marrow stromal cells. *J.Mater.Sci.Mater.Med., 15*(10), 1123-1128.

Mentink, A., Hulsman, M., Groen, N., Licht, R., Dechering, K. J., van der Stok, J., Alves, H. A., Dhert, W. J., van Someren, E. P., Reinders, M. J., van Blitterswijk, C. A., & de Boer, J. (2013). Predicting the therapeutic efficacy of MSC in bone tissue engineering using the molecular marker CADM1. *Biomaterials, 34*(19), 4592-4601.

Merceron, C., Vinatier, C., Portron, S., Masson, M., Amiaud, J., Guigand, L., Cherel, Y., Weiss, P., & Guicheux, J. (2010). Differential effects of hypoxia on osteochondrogenic potential of human adipose-derived stem cells. *Am.J.Physiol.Cell.Physiol., 298*(2), C355-64.

Mesimäki, K., Lindroos, B., Törnwall, J., Mauno, J., Lindqvist, C., Kontio, R., Miettinen, S., & Suuronen, R. (2009). Novel maxillary reconstruction with ectopic bone formation by GMP adipose stem cells. *Int.J.Oral Maxillofac.Surg., 38*(3), 201-209.

Miguez-Pacheco, V., Hench, L. L., & Boccaccini, A. R. (2015). Bioactive glasses beyond bone and teeth: Emerging applications in contact with soft tissues. *Acta Biomater., 13*, 1-15.

Millan, J. L. (2013). The role of phosphatases in the initiation of skeletal mineralization. *Calcif.Tissue Int., 93*(4), 299-306.

Millard, M., Odde, S., & Neamati, N. (2011). Integrin targeted therapeutics. *Theranostics, 1*, 154-188.

Miri, A. K., Muja, N., Kamranpour, N. O., Lepry, W. C., Boccaccini, A. R., Clarke, S. A., & Nazhat, S. N. (2016). Ectopic bone formation in rapidly fabricated acellular injectable dense collagen-bioglass hybrid scaffolds via gel aspiration-ejection. *Biomaterials, 85*, 128-141.

Mitchell, J. B., McIntosh, K., Zvonic, S., Garrett, S., Floyd, Z. E., Kloster, A., Di Halvorsen, Y., Storms, R. W., Goh, B., Kilroy, G., Wu, X., & Gimble, J. M. (2006).

Immunophenotype of human adipose-derived cells: Temporal changes in stromal-associated and stem cell-associated markers. *Stem Cells, 24*(2), 376-385.

Miyazono, K., Kamiya, Y., & Morikawa, M. (2010). Bone morphogenetic protein receptors and signal transduction. *J.Biochem., 147*(1), 35-51.

Modica, S., & Wolfrum, C. (2013). Bone morphogenic proteins signaling in adipogenesis and energy homeostasis. *Biochim.Biophys.Acta, 1831*(5), 915-923.

Monfoulet, L. E., Becquart, P., Marchat, D., Vandamme, K., Bourguignon, M., Pacard, E., Viateau, V., Petite, H., & Logeart-Avramoglou, D. (2014). The pH in the microenvironment of human mesenchymal stem cells is a critical factor for optimal osteogenesis in tissue-engineered constructs. *Tissue Eng.Part A., 20*(13-14), 1827-1840.

Moseti, D., Regassa, A., & Kim, W. K. (2016). Molecular regulation of adipogenesis and potential anti-adipogenic bioactive molecules. *Int.J.Mol.Sci., 17*(1), 10.3390/ijms17010124.

Munukka, E., Leppäranta, O., Korkeamäki, M., Vaahtio, M., Peltola, T., Zhang, D., Hupa, L., Ylänen, H., Salonen, J. I., Viljanen, M. K., & Eerola, E. (2008). Bactericidal effects of bioactive glasses on clinically important aerobic bacteria. *J.Mater.Sci.Mater.Med., 19*(1), 27-32.

Murray, I. R., West, C. C., Hardy, W. R., James, A. W., Park, T. S., Nguyen, A., Tawonsawatruk, T., Lazzari, L., Soo, C., & Peault, B. (2014). Natural history of mesenchymal stem cells, from vessel walls to culture vessels. *Cell Mol.Life Sci., 71*(8), 1353-1374.

Murshed, M., Harmey, D., Millan, J. L., McKee, M. D., & Karsenty, G. (2005). Unique coexpression in osteoblasts of broadly expressed genes accounts for the spatial restriction of ECM mineralization to bone. *Genes Dev., 19*(9), 1093-1104.

Murshed, M., & McKee, M. D. (2010). Molecular determinants of extracellular matrix mineralization in bone and blood vessels. *Curr.Opin.Nephrol.Hypertens., 19*(4), 359-365.

Muruganandan, S., Roman, A. A., & Sinal, C. J. (2009). Adipocyte differentiation of bone marrow-derived mesenchymal stem cells: Cross talk with the osteoblastogenic program. *Cell Mol.Life Sci., 66*(2), 236-253.

Myers, T. J., Granero-Molto, F., Longobardi, L., Li, T., Yan, Y., & Spagnoli, A. (2010). Mesenchymal stem cells at the intersection of cell and gene therapy. *Expert Opin.Biol.Ther., 10*(12), 1663-1679.

Nakashima, K., Zhou, X., Kunkel, G., Zhang, Z., Deng, J. M., Behringer, R. R., & de Crombrugghe, B. (2002). The novel zinc finger-containing transcription factor osterix is required for osteoblast differentiation and bone formation. *Cell, 108*(1), 17-29.

Niemeyer, P., Kasten, P., Simank, H. G., Fellenberg, J., Seckinger, A., Kreuz, P. C., Mehlhorn, A., Sudkamp, N. P., & Krause, U. (2006). Transplantation of mesenchymal stromal cells on mineralized collagen leads to ectopic matrix synthesis in vivo independently from prior in vitro differentiation. *Cytotherapy, 8*(4), 354-366.

Niemeyer, P., Kornacker, M., Mehlhorn, A., Seckinger, A., Vohrer, J., Schmal, H., Kasten, P., Eckstein, V., Sudkamp, N. P., & Krause, U. (2007). Comparison of immunological properties of bone marrow stromal cells and adipose tissue-derived stem cells before and after osteogenic differentiation in vitro. *Tissue Eng., 13*(1), 111-121.

Nohe, A., Hassel, S., Ehrlich, M., Neubauer, F., Sebald, W., Henis, Y. I., & Knaus, P. (2002). The mode of bone morphogenetic protein (BMP) receptor oligomerization determines different BMP-2 signaling pathways. *J.Biol.Chem., 277*(7), 5330-5338.

Nohe, A., Keating, E., Knaus, P., & Petersen, N. O. (2004). Signal transduction of bone morphogenetic protein receptors. *Cell.Signal., 16*(3), 291-299.

Nöth, U., Tuli, R., Seghatoleslami, R., Howard, M., Shah, A., Hall, D. J., Hickok, N. J., & Tuan, R. S. (2003). Activation of p38 and smads mediates BMP-2 effects on human trabecular bone-derived osteoblasts. *Exp.Cell Res., 291*(1), 201-211.

Oh, C. H., Hong, S. J., Jeong, I., Yu, H. S., Jegal, S. H., & Kim, H. W. (2010). Development of robotic dispensed bioactive scaffolds and human adipose-derived stem cell culturing for bone tissue engineering. *Tissue Eng.Part C.Methods, 16*(4), 561-571.

Olmos Buitrago, J., Perez, R. A., El-Fiqi, A., Singh, R. K., Kim, J. H., & Kim, H. W. (2015). Core-shell fibrous stem cell carriers incorporating osteogenic nanoparticulate cues for bone tissue engineering. *Acta Biomater., 28*, 183-192.

Ono, K., & Han, J. (2000). The p38 signal transduction pathway: Activation and function. *Cell.Signal., 12*(1), 1-13.

Oonishi, H., Hench, L. L., Wilson, J., Sugihara, F., Tsuji, E., Matsuura, M., Kin, S., Yamamoto, T., & Mizokawa, S. (2000). Quantitative comparison of bone growth behavior in granules of bioglass, A-W glass-ceramic, and hydroxyapatite. *J.Biomed.Mater.Res., 51*(1), 37-46.

Ortuno, M. J., Ruiz-Gaspa, S., Rodriguez-Carballo, E., Susperregui, A. R., Bartrons, R., Rosa, J. L., & Ventura, F. (2010). P38 regulates expression of osteoblast-specific genes by phosphorylation of osterix. *J.Biol.Chem., 285*(42), 31985-31994.

Oswald, J., Boxberger, S., Jorgensen, B., Feldmann, S., Ehninger, G., Bornhäuser, M., & Werner, C. (2004). Mesenchymal stem cells can be differentiated into endothelial cells in vitro. *Stem Cells, 22*(3), 377-384.

Otto, F., Thornell, A. P., Crompton, T., Denzel, A., Gilmour, K. C., Rosewell, I. R., Stamp, G. W., Beddington, R. S., Mundlos, S., Olsen, B. R., Selby, P. B., & Owen, M. J. (1997). Cbfa1, a candidate gene for cleidocranial dysplasia syndrome, is essential for osteoblast differentiation and bone development. *Cell, 89*(5), 765-771.

Otto, T. C., & Lane, M. D. (2005). Adipose development: From stem cell to adipocyte. *Crit.Rev.Biochem.Mol.Biol., 40*(4), 229-242.

Pachon-Pena, G., Yu, G., Tucker, A., Wu, X., Vendrell, J., Bunnell, B. A., & Gimble, J. M. (2011). Stromal stem cells from adipose tissue and bone marrow of age-matched female donors display distinct immunophenotypic profiles. *J.Cell.Physiol., 226*(3), 843-851.

Pak, J. (2011). Regeneration of human bones in hip osteonecrosis and human cartilage in knee osteoarthritis with autologous adipose-tissue-derived stem cells: A case series. *J.Med.Case Rep., 5*, 296-1947-5-296.

Pak, J. (2012). Autologous adipose tissue-derived stem cells induce persistent bone-like tissue in osteonecrotic femoral heads. *Pain Physician., 15*(1), 75-85.

Pamula, E., Kokoszka, J., Cholewa-Kowalska, K., Laczka, M., Kantor, L., Niedzwiedzki, L., Reilly, G. C., Filipowska, J., Madej, W., Kolodziejczyk, M., Tylko, G., & Osyczka, A. M. (2011). Degradation, bioactivity, and osteogenic potential of composites made of PLGA and two different sol-gel bioactive glasses. *Ann.Biomed.Eng., 39*(8), 2114-2129.

Panetta, N. J., Gupta, D. M., Lee, J. K., Wan, D. C., Commons, G. W., & Longaker, M. T. (2010). Human adipose-derived stromal cells respond to and elaborate bone morphogenetic protein-2 during in vitro osteogenic differentiation. *Plast.Reconstr.Surg., 125*(2), 483-493.

Park, J. C., Kim, J. C., Kim, B. K., Cho, K. S., Im, G. I., Kim, B. S., & Kim, C. S. (2012). Dose- and time-dependent effects of recombinant human bone morphogenetic protein-2 on the osteogenic and adipogenic potentials of alveolar bone-derived stromal cells. *J.Periodontal.Res., 47*(5), 645-654.

Patrikoski, M., Juntunen, M., Boucher, S., Campbell, A., Vemuri, M. C., Mannerström, B., & Miettinen, S. (2013). Development of fully defined xeno-free culture system for the preparation and propagation of cell therapy-compliant human adipose stem cells. *Stem Cell.Res.Ther., 4*(2), 27.

Payne, K. A., Meszaros, L. B., Phillippi, J. A., & Huard, J. (2010). Effect of phosphatidyl inositol 3-kinase, extracellular signal-regulated kinases 1/2, and p38 mitogen-activated protein kinase inhibition on osteogenic differentiation of muscle-derived stem cells. *Tissue Eng.Part A., 16*(12), 3647-3655.

Pearson, G., Robinson, F., Beers Gibson, T., Xu, B. E., Karandikar, M., Berman, K., & Cobb, M. H. (2001). Mitogen-activated protein (MAP) kinase pathways: Regulation and physiological functions. *Endocr.Rev., 22*(2), 153-183.

Peltola, M. J., Aitasalo, K. M., Suonpää, J. T., Yli-Urpo, A., & Laippala, P. J. (2001). In vivo model for frontal sinus and calvarial bone defect obliteration with bioactive glass S53P4 and hydroxyapatite. *J.Biomed.Mater.Res., 58*(3), 261-269.

Pennisi, C. P., Dolatshahi-Pirouz, A., Foss, M., Chevallier, J., Fink, T., Zachar, V., Besenbacher, F., & Yoshida, K. (2011). Nanoscale topography reduces fibroblast growth, focal adhesion size and migration-related gene expression on platinum surfaces. *Colloids Surf.B Biointerfaces, 85*(2), 189-197.

Petit, V., & Thiery, J. P. (2000). Focal adhesions: Structure and dynamics. *Biol.Cell., 92*(7), 477-494.

Pfaffl, M. W. (2001). A new mathematical model for relative quantification in real-time RT-PCR. *Nucleic Acids Res., 29*(9), e45.

Phillips, J. E., Gersbach, C. A., Wojtowicz, A. M., & Garcia, A. J. (2006). Glucocorticoid-induced osteogenesis is negatively regulated by Runx2/Cbfa1 serine phosphorylation. *J.Cell.Sci., 119*(Pt 3), 581-591.

Platt, M. O., Wilder, C. L., Wells, A., Griffith, L. G., & Lauffenburger, D. A. (2009). Multipathway kinase signatures of multipotent stromal cells are predictive for osteogenic differentiation: Tissue-specific stem cells. *Stem Cells, 27*(11), 2804-2814.

Pre, D., Ceccarelli, G., Gastaldi, G., Asti, A., Saino, E., Visai, L., Benazzo, F., Cusella De Angelis, M. G., & Magenes, G. (2011). The differentiation of human adipose-derived stem cells (hASCs) into osteoblasts is promoted by low amplitude, high frequency vibration treatment. *Bone, 49*(2), 295-303.

Prins, H. J., Braat, A. K., Gawlitta, D., Dhert, W. J., Egan, D. A., Tijssen-Slump, E., Yuan, H., Coffer, P. J., Rozemuller, H., & Martens, A. C. (2014). In vitro induction of alkaline phosphatase levels predicts in vivo bone forming capacity of human bone marrow stromal cells. *Stem Cell.Res., 12*(2), 428-440.

Qiu, W., Chen, L., & Kassem, M. (2011). Activation of non-canonical wnt/JNK pathway by Wnt3a is associated with differentiation fate determination of human bone marrow stromal (mesenchymal) stem cells. *Biochem.Biophys.Res.Commun., 413*(1), 98-104.

Rahaman, M. N., Day, D. E., Bal, B. S., Fu, Q., Jung, S. B., Bonewald, L. F., & Tomsia, A. P. (2011). Bioactive glass in tissue engineering. *Acta Biomater., 7*(6), 2355-2373.

Rajala, K., Lindroos, B., Hussein, S. M., Lappalainen, R. S., Pekkanen-Mattila, M., Inzunza, J., Rozell, B., Miettinen, S., Narkilahti, S., Kerkelä, E., Aalto-Setälä, K., Otonkoski, T., Suuronen, R., Hovatta, O., & Skottman, H. (2010). A defined and xeno-free culture method enabling the establishment of clinical-grade human embryonic, induced pluripotent and adipose stem cells. *PLoS One, 5*(4), e10246.

Ramasubramanian, A., Shiigi, S., Lee, G. K., & Yang, F. (2011). Non-viral delivery of inductive and suppressive genes to adipose-derived stem cells for osteogenic differentiation. *Pharm.Res., 28*(6), 1328-1337.

Rath, S. N., Nooeaid, P., Arkudas, A., Beier, J. P., Strobel, L. A., Brandl, A., Roether, J. A., Horch, R. E., Boccaccini, A. R., & Kneser, U. (2013). Adipose- and bone marrow-derived mesenchymal stem cells display different osteogenic differentiation patterns in 3D bioactive glass-based scaffolds. *J.Tissue Eng.Regen.Med.,*

Reffitt, D. M., Ogston, N., Jugdaohsingh, R., Cheung, H. F., Evans, B. A., Thompson, R. P., Powell, J. J., & Hampson, G. N. (2003). Orthosilicic acid stimulates collagen type 1 synthesis and osteoblastic differentiation in human osteoblast-like cells in vitro. *Bone, 32*(2), 127-135.

Reilly, G. C., Radin, S., Chen, A. T., & Ducheyne, P. (2007). Differential alkaline phosphatase responses of rat and human bone marrow derived mesenchymal stem cells to 45S5 bioactive glass. *Biomaterials, 28*(28), 4091-4097.

Ren, G., Chen, X., Dong, F., Li, W., Ren, X., Zhang, Y., & Shi, Y. (2012). Concise review: Mesenchymal stem cells and translational medicine: Emerging issues. *Stem Cells Transl.Med., 1*(1), 51-58.

Rezwan, K., Chen, Q. Z., Blaker, J. J., & Boccaccini, A. R. (2006). Biodegradable and bioactive porous polymer/inorganic composite scaffolds for bone tissue engineering. *Biomaterials, 27*(18), 3413-3431.

Rodbell, M. (1964). Metabolism of isolated fat cells. I. effects of hormones on glucose metabolism and lipolysis. *J.Biol.Chem., 239*, 375-380.

Rodriguez, J. P., Gonzalez, M., Rios, S., & Cambiazo, V. (2004). Cytoskeletal organization of human mesenchymal stem cells (MSC) changes during their osteogenic differentiation. *J.Cell.Biochem., 93*(4), 721-731.

Rosen, E. D., & MacDougald, O. A. (2006). Adipocyte differentiation from the inside out. *Nat.Rev.Mol.Cell Biol., 7*(12), 885-896.

Roux, P. P., & Blenis, J. (2004). ERK and p38 MAPK-activated protein kinases: A family of protein kinases with diverse biological functions. *Microbiol.Mol.Biol.Rev., 68*(2), 320-344.

Rubinfeld, H., & Seger, R. (2005). The ERK cascade: A prototype of MAPK signaling. *Mol.Biotechnol., 31*(2), 151-174.

Ruokola, P., Dadu, E., Kazmertsuk, A., Häkkänen, H., Marjomäki, V., & Ihalainen, J. A. (2014). Raman spectroscopic signatures of echovirus 1 uncoating. *J.Virol., 88*(15), 8504-8513.

Russell, K. C., Phinney, D. G., Lacey, M. R., Barrilleaux, B. L., Meyertholen, K. E., & O'Connor, K. C. (2010). In vitro high-capacity assay to quantify the clonal heterogeneity in trilineage potential of mesenchymal stem cells reveals a complex hierarchy of lineage commitment. *Stem Cells, 28*(4), 788-798.

Rust, K. R., Singleton, G. T., Wilson, J., & Antonelli, P. J. (1996). Bioglass middle ear prosthesis: Long-term results. *Am.J.Otol., 17*(3), 371-374.

Ryoo, H. M., Lee, M. H., & Kim, Y. J. (2006). Critical molecular switches involved in BMP-2-induced osteogenic differentiation of mesenchymal cells. *Gene, 366*(1), 51-57.

Sacak, B., Certel, F., Akdeniz, Z. D., Karademir, B., Ercan, F., Ozkan, N., Akpinar, I. N., & Celebiler, O. (2016). Repair of critical size defects using bioactive glass seeded with adipose-derived mesenchymal stem cells. *J.Biomed.Mater.Res.B.Appl.Biomater.,*

Saffarian Tousi, N., Velten, M. F., Bishop, T. J., Leong, K. K., Barkhordar, N. S., Marshall, G. W., Loomer, P. M., Aswath, P. B., & Varanasi, V. G. (2013). Combinatorial effect of Si4+, Ca2+, and Mg2+ released from bioactive glasses on osteoblast osteocalcin expression and biomineralization. *Mater.Sci.Eng.C.Mater.Biol.Appl., 33*(5), 2757-2765.

Salasznyk, R. M., Klees, R. F., Boskey, A., & Plopper, G. E. (2007b). Activation of FAK is necessary for the osteogenic differentiation of human mesenchymal stem cells on laminin-5. *J.Cell.Biochem., 100*(2), 499-514.

Salasznyk, R. M., Klees, R. F., Williams, W. A., Boskey, A., & Plopper, G. E. (2007a). Focal adhesion kinase signaling pathways regulate the osteogenic differentiation of human mesenchymal stem cells. *Exp.Cell Res., 313*(1), 22-37.

Salingcarnboriboon, R., Yoshitake, H., Tsuji, K., Obinata, M., Amagasa, T., Nifuji, A., & Noda, M. (2003). Establishment of tendon-derived cell lines exhibiting pluripotent mesenchymal stem cell-like property. *Exp.Cell Res., 287*(2), 289-300.

Samavedi, S., Whittington, A. R., & Goldstein, A. S. (2013). Calcium phosphate ceramics in bone tissue engineering: A review of properties and their influence on cell behavior. *Acta Biomater., 9*(9), 8037-8045.

Sanchez-Duffhues, G., Hiepen, C., Knaus, P., & Ten Dijke, P. (2015). Bone morphogenetic protein signaling in bone homeostasis. *Bone, 80*, 43-59.

Sandor, G. K., Numminen, J., Wolff, J., Thesleff, T., Miettinen, A., Tuovinen, V. J., Mannerström, B., Patrikoski, M., Seppänen, R., Miettinen, S., Rautiainen, M., & Ohman, J. (2014). Adipose stem cells used to reconstruct 13 cases with cranio-maxillofacial hard-tissue defects. *Stem Cells Transl.Med., 3*(4), 530-540.

Sandor, G. K., Tuovinen, V. J., Wolff, J., Patrikoski, M., Jokinen, J., Nieminen, E., Mannerström, B., Lappalainen, O. P., Seppänen, R., & Miettinen, S. (2013). Adipose stem cell tissue-engineered construct used to treat large anterior mandibular defect: A case report and review of the clinical application of good manufacturing practice-level adipose stem cells for bone regeneration. *J.Oral Maxillofac.Surg., 71*(5), 938-950.

Sapkota, G., Alarcon, C., Spagnoli, F. M., Brivanlou, A. H., & Massague, J. (2007). Balancing BMP signaling through integrated inputs into the Smad1 linker. *Mol.Cell, 25*(3), 441-454.

Schaller, M. D. (2001). Biochemical signals and biological responses elicited by the focal adhesion kinase. *Biochim.Biophys.Acta, 1540*(1), 1-21.

Schlaepfer, D. D., Hauck, C. R., & Sieg, D. J. (1999). Signaling through focal adhesion kinase. *Prog.Biophys.Mol.Biol., 71*(3-4), 435-478.

Scott, M. A., Nguyen, V. T., Levi, B., & James, A. W. (2011). Current methods of adipogenic differentiation of mesenchymal stem cells. *Stem Cells Dev., 20*(10), 1793-1804.

Shah, F. S., Li, J., Dietrich, M., Wu, X., Hausmann, M. G., LeBlanc, K. A., Wade, J. W., & Gimble, J. M. (2014). Comparison of stromal/stem cells isolated from human omental and subcutaneous adipose depots: Differentiation and immunophenotypic characterization. *Cells Tissues Organs, 200*(3-4), 204-211.

Shi, J., Zhang, X., Zhu, J., Pi, Y., Hu, X., Zhou, C., & Ao, Y. (2013). Nanoparticle delivery of the bone morphogenetic protein 4 gene to adipose-derived stem cells promotes articular cartilage repair in vitro and in vivo. *Arthroscopy, 29*(12), 2001-2011.e2.

Shie, M. Y., & Ding, S. J. (2013). Integrin binding and MAPK signal pathways in primary cell responses to surface chemistry of calcium silicate cements. *Biomaterials, 34*(28), 6589-6606.

Shie, M. Y., Ding, S. J., & Chang, H. C. (2011). The role of silicon in osteoblast-like cell proliferation and apoptosis. *Acta Biomater., 7*(6), 2604-2614.

Shih, Y. R., Tseng, K. F., Lai, H. Y., Lin, C. H., & Lee, O. K. (2011). Matrix stiffness regulation of integrin-mediated mechanotransduction during osteogenic differentiation of human mesenchymal stem cells. *J.Bone Miner.Res., 26*(4), 730-738.

Shim, W. S., Jiang, S., Wong, P., Tan, J., Chua, Y. L., Tan, Y. S., Sin, Y. K., Lim, C. H., Chua, T., Teh, M., Liu, T. C., & Sim, E. (2004). Ex vivo differentiation of human adult bone marrow stem cells into cardiomyocyte-like cells. *Biochem.Biophys.Res.Commun., 324*(2), 481-488.

Shin, M. K., Kim, M. K., Bae, Y. S., Jo, I., Lee, S. J., Chung, C. P., Park, Y. J., & Min do, S. (2008). A novel collagen-binding peptide promotes osteogenic differentiation via Ca2+/calmodulin-dependent protein kinase II/ERK/AP-1 signaling pathway in human bone marrow-derived mesenchymal stem cells. *Cell.Signal., 20*(4), 613-624.

Shiraishi, T., Sumita, Y., Wakamastu, Y., Nagai, K., & Asahina, I. (2012). Formation of engineered bone with adipose stromal cells from buccal fat pad. *J.Dent.Res., 91*(6), 592-597.

Song, I., Kim, B. S., Kim, C. S., & Im, G. I. (2011). Effects of BMP-2 and vitamin D3 on the osteogenic differentiation of adipose stem cells. *Biochem.Biophys.Res.Commun., 408*(1), 126-131.

Stevens, B., Yang, Y., Mohandas, A., Stucker, B., & Nguyen, K. T. (2008). A review of materials, fabrication methods, and strategies used to enhance bone regeneration in engineered bone tissues. *J.Biomed.Mater.Res.B.Appl.Biomater., 85*(2), 573-582.

Stoor, P., Söderling, E., & Salonen, J. I. (1998). Antibacterial effects of a bioactive glass paste on oral microorganisms. *Acta Odontol.Scand., 56*(3), 161-165.

Strioga, M., Viswanathan, S., Darinskas, A., Slaby, O., & Michalek, J. (2012). Same or not the same? comparison of adipose tissue-derived versus bone marrow-derived mesenchymal stem and stromal cells. *Stem Cells Dev., 21*(14), 2724-2752.

Stromps, J. P., Paul, N. E., Rath, B., Nourbakhsh, M., Bernhagen, J., & Pallua, N. (2014). Chondrogenic differentiation of human adipose-derived stem cells: A new path in articular cartilage defect management? *Biomed.Res.Int., 2014*, 740926.

Strong, A. L., Hunter, R. S., Jones, R. B., Bowles, A. C., Dutreil, M. F., Gaupp, D., Hayes, D. J., Gimble, J. M., Levi, B., McNulty, M. A., & Bunnell, B. A. (2016). Obesity inhibits the osteogenic differentiation of human adipose-derived stem cells. *J.Transl.Med., 14*, 27-016-0776-1.

Suzawa, M., Tamura, Y., Fukumoto, S., Miyazono, K., Fujita, T., Kato, S., & Takeuchi, Y. (2002). Stimulation of Smad1 transcriptional activity by ras-extracellular signal-regulated kinase pathway: A possible mechanism for collagen-dependent osteoblastic differentiation. *J.Bone Miner.Res., 17*(2), 240-248.

Suzuki, A., Guicheux, J., Palmer, G., Miura, Y., Oiso, Y., Bonjour, J. P., & Caverzasio, J. (2002). Evidence for a role of p38 MAP kinase in expression of alkaline phosphatase during osteoblastic cell differentiation. *Bone, 30*(1), 91-98.

Takagishi, Y., Kawakami, T., Hara, Y., Shinkai, M., Takezawa, T., & Nagamune, T. (2006). Bone-like tissue formation by three-dimensional culture of MG63 osteosarcoma cells in gelatin hydrogels using calcium-enriched medium. *Tissue Eng., 12*(4), 927-937.

Takahashi, K., Tanabe, K., Ohnuki, M., Narita, M., Ichisaka, T., Tomoda, K., & Yamanaka, S. (2007). Induction of pluripotent stem cells from adult human fibroblasts by defined factors. *Cell, 131*(5), 861-872.

Takahashi, K., & Yamanaka, S. (2006). Induction of pluripotent stem cells from mouse embryonic and adult fibroblast cultures by defined factors. *Cell, 126*(4), 663-676.

Takeuchi, Y., Nakayama, K., & Matsumoto, T. (1996). Differentiation and cell surface expression of transforming growth factor-beta receptors are regulated by interaction with matrix collagen in murine osteoblastic cells. *J.Biol.Chem., 271*(7), 3938-3944.

Takeuchi, Y., Suzawa, M., Kikuchi, T., Nishida, E., Fujita, T., & Matsumoto, T. (1997). Differentiation and transforming growth factor-beta receptor down-regulation by collagen-alpha2beta1 integrin interaction is mediated by focal adhesion kinase and its downstream signals in murine osteoblastic cells. *J.Biol.Chem., 272*(46), 29309-29316.

Talley, A. D., Kalpakci, K. N., Shimko, D. A., Zienkiewicz, K. J., Cochran, D. L., & Guelcher, S. A. (2016). Effects of recombinant human bone morphogenetic protein-2 dose and ceramic composition on new bone formation and space maintenance in a canine mandibular ridge saddle defect model. *Tissue Eng.Part A., 22*(5-6), 469-479.

Tamura, Y., Takeuchi, Y., Suzawa, M., Fukumoto, S., Kato, M., Miyazono, K., & Fujita, T. (2001). Focal adhesion kinase activity is required for bone morphogenetic protein-Smad1 signaling and osteoblastic differentiation in murine MC3T3-E1 cells. *J.Bone Miner.Res., 16*(10), 1772-1779.

Tang, Q. Q., & Lane, M. D. (2012). Adipogenesis: From stem cell to adipocyte. *Annu.Rev.Biochem., 81*, 715-736.

Taylor, J. A. (2010). Bilateral orbitozygomatic reconstruction with tissue-engineered bone. *J.Craniofac.Surg., 21*(5), 1612-1614.

Teng, N. Y., Liu, Y. S., Wu, H. H., Liu, Y. A., Ho, J. H., & Lee, O. K. (2015). Promotion of mesenchymal-to-epithelial transition by Rac1 inhibition with small molecules accelerates hepatic differentiation of mesenchymal stromal cells. *Tissue Eng.Part A., 21*(7-8), 1444-1454.

Thesleff, T., Lehtimäki, K., Niskakangas, T., Mannerström, B., Miettinen, S., Suuronen, R., & Ohman, J. (2011). Cranioplasty with adipose-derived stem cells and biomaterial: A novel method for cranial reconstruction. *Neurosurgery, 68*(6), 1535-1540.

Thompson, E. M., Matsiko, A., Kelly, D. J., Gleeson, J. P., & O'Brien, F. J. (2016). An endochondral ossification-based approach to bone repair: Chondrogenically primed mesenchymal stem cell-laden scaffolds support greater repair of critical-sized cranial defects than osteogenically stimulated constructs in vivo. *Tissue Eng.Part A., 22*(5-6), 556-567.

Thomson, J. A., Itskovitz-Eldor, J., Shapiro, S. S., Waknitz, M. A., Swiergiel, J. J., Marshall, V. S., & Jones, J. M. (1998). Embryonic stem cell lines derived from human blastocysts. *Science, 282*(5391), 1145-1147.

Thornton, T. M., Pedraza-Alva, G., Deng, B., Wood, C. D., Aronshtam, A., Clements, J. L., Sabio, G., Davis, R. J., Matthews, D. E., Doble, B., & Rincon, M. (2008). Phosphorylation by p38 MAPK as an alternative pathway for GSK3beta inactivation. *Science, 320*(5876), 667-670.

Tirkkonen, L., Haimi, S., Huttunen, S., Wolff, J., Pirhonen, E., Sandor, G. K., & Miettinen, S. (2013). Osteogenic medium is superior to growth factors in differentiation of human adipose stem cells towards bone-forming cells in 3D culture. *Eur.Cell.Mater., 25*, 144-158.

Tirkkonen, L., Halonen, H., Hyttinen, J., Kuokkanen, H., Sievänen, H., Koivisto, A. M., Mannerström, B., Sandor, G. K., Suuronen, R., Miettinen, S., & Haimi, S. (2011). The effects of vibration loading on adipose stem cell number, viability and differentiation towards bone-forming cells. *J.R.Soc.Interface, 8*(65), 1736-1747.

Tomakidi, P., Schulz, S., Proksch, S., Weber, W., & Steinberg, T. (2014). Focal adhesion kinase (FAK) perspectives in mechanobiology: Implications for cell behaviour. *Cell Tissue Res., 357*(3), 515-526.

Tominaga, S., Yamaguchi, T., Takahashi, S., Hirose, F., & Osumi, T. (2005). Negative regulation of adipogenesis from human mesenchymal stem cells by jun N-terminal kinase. *Biochem.Biophys.Res.Commun., 326*(2), 499-504.

Toyoda, M., Matsubara, Y., Lin, K., Sugimachi, K., & Furue, M. (2009). Characterization and comparison of adipose tissue-derived cells from human subcutaneous and omental adipose tissues. *Cell Biochem.Funct., 27*(7), 440-447.

Troyer, D. L., & Weiss, M. L. (2008). Wharton's jelly-derived cells are a primitive stromal cell population. *Stem Cells, 26*(3), 591-599.

Tsai, K. S., Kao, S. Y., Wang, C. Y., Wang, Y. J., Wang, J. P., & Hung, S. C. (2010). Type I collagen promotes proliferation and osteogenesis of human mesenchymal stem cells via activation of ERK and akt pathways. *J.Biomed.Mater.Res.A., 94*(3), 673-682.

Tsigkou, O., Jones, J. R., Polak, J. M., & Stevens, M. M. (2009). Differentiation of fetal osteoblasts and formation of mineralized bone nodules by 45S5 bioglass conditioned medium in the absence of osteogenic supplements. *Biomaterials, 30*(21), 3542-3550.

Ulsamer, A., Ortuno, M. J., Ruiz, S., Susperregui, A. R., Osses, N., Rosa, J. L., & Ventura, F. (2008). BMP-2 induces osterix expression through up-regulation of Dlx5 and its phosphorylation by p38. *J.Biol.Chem., 283*(7), 3816-3826.

Urist, M. R. (1965). Bone: Formation by autoinduction. *Science, 150*(3698), 893-899.

Vacanti, J. P., & Langer, R. (1999). Tissue engineering: The design and fabrication of living replacement devices for surgical reconstruction and transplantation. *Lancet, 354 Suppl 1*, SI32-4.

Valerio, P., Pereira, M. M., Goes, A. M., & Leite, M. F. (2004). The effect of ionic products from bioactive glass dissolution on osteoblast proliferation and collagen production. *Biomaterials, 25*(15), 2941-2948.

Välimäki, V. V., & Aro, H. T. (2006). Molecular basis for action of bioactive glasses as bone graft substitute. *Scand.J.Surg., 95*(2), 95-102.

van de Watering, F. C., van den Beucken, J. J., van der Woning, S. P., Briest, A., Eek, A., Qureshi, H., Winnubst, L., Boerman, O. C., & Jansen, J. A. (2012). Non-glycosylated BMP-2 can induce ectopic bone formation at lower concentrations compared to glycosylated BMP-2. *J.Control.Release, 159*(1), 69-77.

Vangsness, C. T.,Jr, Sternberg, H., & Harris, L. (2015). Umbilical cord tissue offers the greatest number of harvestable mesenchymal stem cells for research and clinical application: A literature review of different harvest sites. *Arthroscopy, 31*(9), 1836-1843.

Varanasi, V. G., Owyoung, J. B., Saiz, E., Marshall, S. J., Marshall, G. W., & Loomer, P. M. (2011). The ionic products of bioactive glass particle dissolution enhance periodontal ligament fibroblast osteocalcin expression and enhance early mineralized tissue development. *J.Biomed.Mater.Res.A., 98*(2), 177-184.

Varanasi, V. G., Saiz, E., Loomer, P. M., Ancheta, B., Uritani, N., Ho, S. P., Tomsia, A. P., Marshall, S. J., & Marshall, G. W. (2009). Enhanced osteocalcin expression by osteoblast-like cells (MC3T3-E1) exposed to bioactive coating glass (SiO2-CaO-P2O5-MgO-K2O-Na2O system) ions. *Acta Biomater., 5*(9), 3536-3547.

Varma, M. J., Breuls, R. G., Schouten, T. E., Jurgens, W. J., Bontkes, H. J., Schuurhuis, G. J., van Ham, S. M., & van Milligen, F. J. (2007). Phenotypical and functional characterization of freshly isolated adipose tissue-derived stem cells. *Stem Cells Dev., 16*(1), 91-104.

Vater, C., Kasten, P., & Stiehler, M. (2011). Culture media for the differentiation of mesenchymal stromal cells. *Acta Biomater., 7*(2), 463-477.

Viale-Bouroncle, S., Gosau, M., & Morsczeck, C. (2014a). Collagen I induces the expression of alkaline phosphatase and osteopontin via independent activations of FAK and ERK signalling pathways. *Arch.Oral Biol., 59*(12), 1249-1255.

Viale-Bouroncle, S., Gosau, M., & Morsczeck, C. (2014b). Laminin regulates the osteogenic differentiation of dental follicle cells via integrin-alpha2/-beta1 and the activation of the FAK/ERK signaling pathway. *Cell Tissue Res., 357*(1), 345-354.

Vimalraj, S., Arumugam, B., Miranda, P. J., & Selvamurugan, N. (2015). Runx2: Structure, function, and phosphorylation in osteoblast differentiation. *Int.J.Biol.Macromol., 78*, 202-208.

Vinals, F., Lopez-Rovira, T., Rosa, J. L., & Ventura, F. (2002). Inhibition of PI3K/p70 S6K and p38 MAPK cascades increases osteoblastic differentiation induced by BMP-2. *FEBS Lett., 510*(1-2), 99-104.

Visvader, J. E., & Clevers, H. (2016). Tissue-specific designs of stem cell hierarchies. *Nat.Cell Biol.,*

Viti, F., Landini, M., Mezzelani, A., Petecchia, L., Milanesi, L., & Scaglione, S. (2016). Osteogenic differentiation of MSC through calcium signaling activation: Transcriptomics and functional analysis. *PLoS One, 11*(2), e0148173.

Vuornos, K., Björninen, M., Talvitie, E., Paakinaho, K., Kellomäki, M., Huhtala, H., Miettinen, S., Seppänen-Kaijansinkko, R., & Haimi, S. (2016). Human adipose stem cells differentiated on braided polylactide scaffolds is a potential approach for tendon tissue engineering. *Tissue Eng.Part A., 22*(5-6), 513-523.

Wan, D. C., Shi, Y. Y., Nacamuli, R. P., Quarto, N., Lyons, K. M., & Longaker, M. T. (2006). Osteogenic differentiation of mouse adipose-derived adult stromal cells

requires retinoic acid and bone morphogenetic protein receptor type IB signaling. *Proc.Natl.Acad.Sci.U.S.A., 103*(33), 12335-12340.

Wang, S., Qu, X., & Zhao, R. C. (2011). Mesenchymal stem cells hold promise for regenerative medicine. *Front.Med., 5*(4), 372-378.

Wang, W., Liu, Q., Zhang, Y., & Zhao, L. (2014). Involvement of ILK/ERK1/2 and ILK/p38 pathways in mediating the enhanced osteoblast differentiation by micro/nanotopography. *Acta Biomater., 10*(8), 3705-3715.

Wang, Y., Azais, T., Robin, M., Vallee, A., Catania, C., Legriel, P., Pehau-Arnaudet, G., Babonneau, F., Giraud-Guille, M. M., & Nassif, N. (2012). The predominant role of collagen in the nucleation, growth, structure and orientation of bone apatite. *Nat.Mater., 11*(8), 724-733.

Wang, Y. K., Yu, X., Cohen, D. M., Wozniak, M. A., Yang, M. T., Gao, L., Eyckmans, J., & Chen, C. S. (2012). Bone morphogenetic protein-2-induced signaling and osteogenesis is regulated by cell shape, RhoA/ROCK, and cytoskeletal tension. *Stem Cells Dev., 21*(7), 1176-1186.

Wang, Z., Lu, B., Chen, L., & Chang, J. (2011). Evaluation of an osteostimulative putty in the sheep spine. *J.Mater.Sci.Mater.Med., 22*(1), 185-191.

Waselau, M., Patrikoski, M., Juntunen, M., Kujala, K., Kääriäinen, M., Kuokkanen, H., Sandor, G. K., Vapaavuori, O., Suuronen, R., Mannerström, B., von Rechenberg, B., & Miettinen, S. (2012). Effects of bioactive glass S53P4 or beta-tricalcium phosphate and bone morphogenetic protein-2 and bone morphogenetic protein-7 on osteogenic differentiation of human adipose stem cells. *J.Tissue Eng., 3*(1), 2041731412467789.

Wei, Y., Sun, X., Wang, W., & Hu, Y. (2007). Adipose-derived stem cells and chondrogenesis. *Cytotherapy, 9*(8), 712-716.

Weijers, E. M., Van Den Broek, L. J., Waaijman, T., Van Hinsbergh, V. W., Gibbs, S., & Koolwijk, P. (2011). The influence of hypoxia and fibrinogen variants on the expansion and differentiation of adipose tissue-derived mesenchymal stem cells. *Tissue Eng.Part A., 17*(21-22), 2675-2685.

Wolff, J., Sandor, G. K., Miettinen, A., Tuovinen, V. J., Mannerström, B., Patrikoski, M., & Miettinen, S. (2013). GMP-level adipose stem cells combined with computer-aided manufacturing to reconstruct mandibular ameloblastoma resection defects: Experience with three cases. *Ann.Maxillofac.Surg., 3*(2), 114-125.

Woo, K. M., Seo, J., Zhang, R., & Ma, P. X. (2007). Suppression of apoptosis by enhanced protein adsorption on polymer/hydroxyapatite composite scaffolds. *Biomaterials, 28*(16), 2622-2630.

Wozney, J. M., Rosen, V., Celeste, A. J., Mitsock, L. M., Whitters, M. J., Kriz, R. W., Hewick, R. M., & Wang, E. A. (1988). Novel regulators of bone formation: Molecular clones and activities. *Science, 242*(4885), 1528-1534.

Wu, C., Zhang, Y., Zhou, Y., Fan, W., & Xiao, Y. (2011). A comparative study of mesoporous glass/silk and non-mesoporous glass/silk scaffolds: Physiochemistry and in vivo osteogenesis. *Acta Biomater., 7*(5), 2229-2236.

Wu, C., Zhou, Y., Xu, M., Han, P., Chen, L., Chang, J., & Xiao, Y. (2013). Copper-containing mesoporous bioactive glass scaffolds with multifunctional properties of angiogenesis capacity, osteostimulation and antibacterial activity. *Biomaterials, 34*(2), 422-433.

Wu, X., Tu, X., Joeng, K. S., Hilton, M. J., Williams, D. A., & Long, F. (2008). Rac1 activation controls nuclear localization of beta-catenin during canonical wnt signaling. *Cell, 133*(2), 340-353.

Xian, L., Wu, X., Pang, L., Lou, M., Rosen, C. J., Qiu, T., Crane, J., Frassica, F., Zhang, L., Rodriguez, J. P., Xiaofeng, J., Shoshana, Y., Shouhong, X., Argiris, E., Mei, W., & Xu, C. (2012). Matrix IGF-1 maintains bone mass by activation of mTOR in mesenchymal stem cells. *Nat.Med., 18*(7), 1095-1101.

Xiao, G., Jiang, D., Thomas, P., Benson, M. D., Guan, K., Karsenty, G., & Franceschi, R. T. (2000). MAPK pathways activate and phosphorylate the osteoblast-specific transcription factor, Cbfa1. *J.Biol.Chem., 275*(6), 4453-4459.

Xie, Q., Wang, Z., Zhou, H., Yu, Z., Huang, Y., Sun, H., Bi, X., Wang, Y., Shi, W., Gu, P., & Fan, X. (2016). The role of miR-135-modified adipose-derived mesenchymal stem cells in bone regeneration. *Biomaterials, 75*, 279-294.

Xu, C., Su, P., Chen, X., Meng, Y., Yu, W., Xiang, A. P., & Wang, Y. (2011). Biocompatibility and osteogenesis of biomimetic bioglass-collagen-phosphatidylserine composite scaffolds for bone tissue engineering. *Biomaterials, 32*(4), 1051-1058.

Xynos, I. D., Edgar, A. J., Buttery, L. D., Hench, L. L., & Polak, J. M. (2000). Ionic products of bioactive glass dissolution increase proliferation of human osteoblasts and induce insulin-like growth factor II mRNA expression and protein synthesis. *Biochem.Biophys.Res.Commun., 276*(2), 461-465.

Xynos, I. D., Edgar, A. J., Buttery, L. D., Hench, L. L., & Polak, J. M. (2001). Gene-expression profiling of human osteoblasts following treatment with the ionic products of bioglass 45S5 dissolution. *J.Biomed.Mater.Res., 55*(2), 151-157.

Yang, H. J., Kim, K. J., Kim, M. K., Lee, S. J., Ryu, Y. H., Seo, B. F., Oh, D. Y., Ahn, S. T., Lee, H. Y., & Rhie, J. W. (2014). The stem cell potential and multipotency of human adipose tissue-derived stem cells vary by cell donor and are different from those of other types of stem cells. *Cells Tissues Organs, 199*(5-6), 373-383.

Yang, S., Wang, J., Tang, L., Ao, H., Tan, H., Tang, T., & Liu, C. (2014). Mesoporous bioactive glass doped-poly (3-hydroxybutyrate-co-3-hydroxyhexanoate) composite scaffolds with 3-dimensionally hierarchical pore networks for bone regeneration. *Colloids Surf.B Biointerfaces, 116*, 72-80.

Yang, X., Gong, P., Lin, Y., Zhang, L., Li, X., Yuan, Q., Tan, Z., Wang, Y., Man, Y., & Tang, H. (2010). Cyclic tensile stretch modulates osteogenic differentiation of adipose-derived stem cells via the BMP-2 pathway. *Arch.Med.Sci., 6*(2), 152-159.

Ye, X., Yin, X., Yang, D., Tan, J., & Liu, G. (2012). Ectopic bone regeneration by human bone marrow mononucleated cells, undifferentiated and osteogenically differentiated

bone marrow mesenchymal stem cells in beta-tricalcium phosphate scaffolds. *Tissue Eng.Part C.Methods, 18*(7), 545-556.

Yi, T., Jun, C. M., Kim, S. J., & Yun, J. H. (2016). Evaluation of in vivo osteogenic potential of bone morphogenetic protein 2-overexpressing human periodontal ligament stem cells combined with biphasic calcium phosphate block scaffolds in a critical-size bone defect model. *Tissue Eng.Part A., 22*(5-6), 501-512.

Ying, X., Cheng, S., Wang, W., Lin, Z., Chen, Q., Zhang, W., Kou, D., Shen, Y., Cheng, X., Rompis, F. A., Peng, L., & Zhu Lu, C. (2011). Effect of boron on osteogenic differentiation of human bone marrow stromal cells. *Biol.Trace Elem.Res., 144*(1-3), 306-315.

Yoon, E., Dhar, S., Chun, D. E., Gharibjanian, N. A., & Evans, G. R. (2007). In vivo osteogenic potential of human adipose-derived stem cells/poly lactide-co-glycolic acid constructs for bone regeneration in a rat critical-sized calvarial defect model. *Tissue Eng., 13*(3), 619-627.

Yourek, G., Hussain, M. A., & Mao, J. J. (2007). Cytoskeletal changes of mesenchymal stem cells during differentiation. *ASAIO J., 53*(2), 219-228.

Zanetti, A. S., Sabliov, C., Gimble, J. M., & Hayes, D. J. (2013). Human adipose-derived stem cells and three-dimensional scaffold constructs: A review of the biomaterials and models currently used for bone regeneration. *J.Biomed.Mater.Res.B.Appl.Biomater., 101*(1), 187-199.

Zeng, Q., Han, Y., Li, H., & Chang, J. (2014). Bioglass/alginate composite hydrogel beads as cell carriers for bone regeneration. *J.Biomed.Mater.Res.B.Appl.Biomater., 102*(1), 42-51.

Zhang, D., Leppäranta, O., Munukka, E., Ylänen, H., Viljanen, M. K., Eerola, E., Hupa, M., & Hupa, L. (2010). Antibacterial effects and dissolution behavior of six bioactive glasses. *J.Biomed.Mater.Res.A., 93*(2), 475-483.

Zhang, H. H., Huang, J., Duvel, K., Boback, B., Wu, S., Squillace, R. M., Wu, C. L., & Manning, B. D. (2009). Insulin stimulates adipogenesis through the akt-TSC2-mTORC1 pathway. *PLoS One, 4*(7), e6189.

Zhang, J., Park, Y. D., Bae, W. J., El-Fiqi, A., Shin, S. H., Lee, E. J., Kim, H. W., & Kim, E. C. (2015). Effects of bioactive cements incorporating zinc-bioglass nanoparticles on odontogenic and angiogenic potential of human dental pulp cells. *J.Biomater.Appl., 29*(7), 954-964.

Zhang, P., Wu, Y., Jiang, Z., Jiang, L., & Fang, B. (2012). Osteogenic response of mesenchymal stem cells to continuous mechanical strain is dependent on ERK1/2-Runx2 signaling. *Int.J.Mol.Med., 29*(6), 1083-1089.

Zhang, W. B., Zhong, W. J., & Wang, L. (2014). A signal-amplification circuit between miR-218 and wnt/beta-catenin signal promotes human adipose tissue-derived stem cells osteogenic differentiation. *Bone, 58*, 59-66.

Zhang, X., Guo, J., Zhou, Y., & Wu, G. (2014). The roles of bone morphogenetic proteins and their signaling in the osteogenesis of adipose-derived stem cells. *Tissue Eng.Part B.Rev., 20*(1), 84-92.

Zhao, Y., Song, T., Wang, W., Wang, J., He, J., Wu, N., Tang, M., He, B., & Luo, J. (2012). P38 and ERK1/2 MAPKs act in opposition to regulate BMP9-induced osteogenic differentiation of mesenchymal progenitor cells. *PLoS One, 7*(8), e43383.

Zhou, Q., Li, B., Zhao, J., Pan, W., Xu, J., & Chen, S. (2016). IGF-I induces adipose derived mesenchymal cell chondrogenic differentiation in vitro and enhances chondrogenesis in vivo. *In Vitro Cell.Dev.Biol.Anim., 52*(3), 356-364.

Zhou, Y., Guan, X., Wang, H., Zhu, Z., Li, C., Wu, S., & Yu, H. (2013). Hypoxia induces osteogenic/angiogenic responses of bone marrow-derived mesenchymal stromal cells seeded on bone-derived scaffolds via ERK1/2 and p38 pathways. *Biotechnol.Bioeng., 110*(6), 1794-1804.

Zielins, E. R., Paik, K., Ransom, R. C., Brett, E. A., Blackshear, C. P., Luan, A., Walmsley, G. G., Atashroo, D. A., Senarath-Yapa, K., Momeni, A., Rennert, R., Sorkin, M., Seo, E. Y., Chan, C. K., Gurtner, G. C., Longaker, M. T., & Wan, D. C. (2016). Enrichment of adipose-derived stromal cells for BMPR1A facilitates enhanced adipogenesis. *Tissue Eng.Part A., 22*(3-4), 214-221.

Zoch, M. L., Clemens, T. L., & Riddle, R. C. (2016). New insights into the biology of osteocalcin. *Bone, 82*, 42-49.

Zuk, P. A., Chou, Y. F., Mussano, F., Benhaim, P., & Wu, B. M. (2011). Adipose-derived stem cells and BMP2: Part 2. BMP2 may not influence the osteogenic fate of human adipose-derived stem cells. *Connect.Tissue Res., 52*(2), 119-132.

Zuk, P. A., Zhu, M., Ashjian, P., De Ugarte, D. A., Huang, J. I., Mizuno, H., Alfonso, Z. C., Fraser, J. K., Benhaim, P., & Hedrick, M. H. (2002). Human adipose tissue is a source of multipotent stem cells. *Mol.Biol.Cell, 13*(12), 4279-4295.

Zuk, P. A., Zhu, M., Mizuno, H., Huang, J., Futrell, J. W., Katz, A. J., Benhaim, P., Lorenz, H. P., & Hedrick, M. H. (2001). Multilineage cells from human adipose tissue: Implications for cell-based therapies. *Tissue Eng., 7*(2), 211-228.

9   Original publications

Bone Morphogenetic Protein-2 Induces Donor-Dependent Osteogenic and Adipogenic Differentiation in Human Adipose Stem Cells

SARI VANHATUPA,[a,b,c] MIINA OJANSIVU,[a,b,c] REIJA AUTIO,[d] MIIA JUNTUNEN,[a,b,c]
SUSANNA MIETTINEN[a,b,c]

[a]Adult Stem Cell Research
Group, [b]BioMediTech, and
[d]School of Health Sciences,
University of Tampere,
Tampere, Finland; [c]Science
Center, Tampere, University
Hospital, Tampere, Finland

Correspondence: Sari Vanhatupa,
Ph.D., Adult Stem Cell Group,
BioMediTech, Institute of
Biosciences, and Medical
Technology, University of
Tampere, Biokatu 12, FM 5, 6th
floor, 33520 Tampere, Finland.
Telephone: 358 40 1909825;
E-Mail: sari.vanhatupa@uta.fi

ABSTRACT

Bone morphogenetic protein-2 (BMP-2) is a growth factor used to stimulate bone regeneration in clinical applications. However, there are contradicting reports on the functionality of BMP-2 in human adipose stem cells (hASCs), which are frequently used in tissue engineering. In this study, we analyzed the effects of BMP-2 on SMAD1/5 signaling, proliferation, and differentiation in hASCs. Our results indicated that BMP-2 induced dose-dependent (25–100 ng/ml) activation of SMAD signaling. Furthermore, the cell proliferation analysis revealed that BMP-2 (100 ng/ml) consistently decreased the proliferation in all the cell lines studied. However, the analysis of the differentiation potential revealed that BMP-2 (100 ng/ml) exhibited a donor-dependent dual role, inducing both osteogenic and adipogenic differentiation in hASCs. The quantitative alkaline phosphatase (qALP) activity and mineralization levels were clearly enhanced in particular donor cell lines by BMP-2 stimulus. On the contrary, in other cell lines, qALP and mineralization levels were diminished and the lipid formation was enhanced. The current study also suggests that hASCs have accelerated biochemical responsiveness to BMP-2 stimulus in human serum-supplemented culture medium compared with fetal bovine serum. The production origin of the BMP-2 growth factor is also important for its response: BMP-2 produced in mammalian cells enhanced signaling and differentiation responses compared with BMP-2 produced in *Escherichia coli*. These results explain the existing contradiction in the reported BMP-2 studies and indicate the variability in the functional end mechanism of BMP-2-stimulated hASCs. STEM CELLS TRANSLATIONAL MEDICINE *2015;4:1–12*

SIGNIFICANCE

This study examined how bone morphogenetic protein-2 (BMP-2) modulates the SMAD signaling mechanism and the proliferation and differentiation outcome of human adipose stem cells (hASCs) derived from several donors. The results indicate that BMP-2 triggers molecular SMAD signaling mechanisms in hASCs and regulates differentiation processes in human serum-culture conditions. Importantly, BMP-2 has dual activity, inducing osteogenic and adipogenic differentiation, subject to hASC donor line studied. These findings explain contradictory previous results and highlight the importance of further studies to understand how signaling pathways guide mesenchymal stem cell functions at the molecular level.

INTRODUCTION

The bone morphogenetic proteins (BMPs) are the best characterized cytokines proposed to drive osteogenic differentiation and are used in clinical applications to stimulate bone regeneration [1]. The BMPs, which belong to the transforming growth factor-β family, mediate their biological function through forming a complex with type I and II serine/threonine kinase receptors. These receptors, in turn, phosphorylate receptor-mediated SMAD-proteins, including SMAD1, 5, and 8. Activated SMAD proteins form complexes with SMAD4 protein and subsequently translocate to the nucleus,

where they cooperate with other DNA-binding proteins to target specific genes such as distal-less homeobox (Dlx)-2/5 and osterix (Osx) for transcriptional regulation [2–4].

Among the BMPs, BMP-2 is best studied in the context of osteogenesis and has been indicated to have potential in bone formation. However, multiple studies have reported contradictory results of BMP-2 treatment in vitro and in vivo. The BMP-2 growth factor has been shown to induce osteogenesis [2, 5] and adipogenesis [6] in bone marrow-derived mesenchymal stem cell (BMSC) cultures in vitro as well as in live animal models

[7, 8]. Also, viral BMP-2 transduction of human adipose stem cells (hASCs) has been shown to produce more bone precursor cells and calcified matrix than osteoblasts, indicating excellent response of hASCs to endogenous production of BMP-2 [9]. However, there are also opposing studies proposing that externally supplemented BMP-2 has only a very weak response, lack of response, or even a negative response in MSC osteogenesis [10–12]. There are indications that BMP-2 stimulus had no impact on its downstream SMAD-signaling mechanisms, or on expression of osteogenic genes or osteogenic responses such as mineralization in hASCs [11]. These contradicting results imply that functionality and osteogenic impact of BMP-2 on BMSCs and hASCs require further study to verify the benefit of BMP-2 use in clinical applications.

The function of BMP-2 in osteogenic differentiation of BMSCs and osteoblasts has been proposed to be highly dependent on cellular shape and molecular feedback loops [2, 13], such as cooperative mechanisms with Wnt/β-catenin, fibroblast growth factor (FGF) [14], and Notch signaling [15–17]. This indicates that the function of BMPs is intricately regulated by internal and external factors both positively and negatively, addressing complex molecular mechanisms functioning cooperatively in BMSC and ASC differentiation processes, as well. The complexity of the regulatory mechanisms also raises the question of whether there is variation in cellular growth factor responses of cell lines derived from different individuals. In this study, we investigated the effect of BMP-2 growth factor on signaling mechanisms and on the differentiation potential of the several hASC donor lines. Our results indicated that in all the cell lines studied, BMP-2 induced phosphorylation of SMAD1/5 signaling proteins, activation and translocation into cell nuclei. Furthermore, hASCs showed variable differentiation responses to BMP-2 treatment in osteogenic culture conditions, displaying osteogenic or adipogenic outcome depending on the donor cell line studied. BMP-2 responses in hASCs also showed clear dependence on culture conditions. BMP-2 induced higher SMAD activation in human serum (HS) conditions versus fetal bovine serum conditions (FBS). Finally, our results indicated that BMP-2 production origin plays an important role in its functionality since BMP-2 produced in mammalian cells induced stronger responses on hASCs when compared with growth factor produced in *E. coli.*

MATERIALS AND METHODS

Ethics Statement

This study was conducted in accordance with the Ethics Committee of the Pirkanmaa Hospital District, Tampere, Finland (R03058). The hASCs used in this study were isolated from adipose tissue samples acquired from 10 female donors (mean age: 46 ± 25 years) undergoing surgery in the Department of Plastic Surgery, Tampere University Hospital. A written informed consent from all the donors was obtained for the use of the adipose tissue samples for research purposes.

Adipose Stem Cell Isolation and Culture

Human ASCs were isolated by mechanical and enzymatic procedure as described previously by Lindroos and coworkers [18]. Isolated hASCs were cultured in Dulbecco's Modified Eagle Medium/ Ham's Nutrient Mixture F-12 1:1 mixture (Thermo Fisher Scientific Inc., Carlsbad, CA, https://www.thermofisher.com) supplemented with 5% HS (GE Healthcare, Buckinghamshire, U.K., http://www.gelifesciences.com), 1% L-glutamine (GlutaMAX;

Thermo Fisher Scientific Inc.) and 1% antibiotics (100 U/ml penicillin and 0.1 mg/ml streptomycin; Thermo Fisher Scientific Inc.). This medium composition is referred to as basic medium (BM) in this article. After primary cell culture (passages 1–2), the surface marker expression of hASCs was analyzed by flow cytometry (fluorescence-activated cell sorting) (FACSAria; Becton, Dickinson and Company, Erembodegem, Belgium, http://www.bdbiosciences.com) (supplemental online data) [18]. The experiments with hASCs were carried out in passages 1–5.

For the quantitative alkaline phosphatase (qALP) activity, Alizarin red mineralization analyses, and Oil Red O analyses, 500 cells per well were plated on 24-well plates. In qALP and Oil Red O analyses, Nunc 24-well plates (Thermo Fisher Scientific Inc.) and in mineralization studies CellBIND (Corning Inc., Corning, NY, https://www.corning.com), 24-well plates were used. hASCs were cultured in 4 different culturing conditions: BM, BM supplemented with BMP-2, osteogenic medium (OM; supplemented with 10 mM β-glycerophosphate, 200 μM L-ascorbic acid 2-phosphate, and 5 nM dexamethasone), and OM supplemented with BMP-2. BMP-2 originated from either mammalian cultures (Chinese hamster ovary cells [CHO]; R&D Systems, Minneapolis, MN, https://www.rndsystems.com) or from *Escherichia coli* (Sigma-Aldrich, St. Louis, MO, https://www.sigmaaldrich.com). BMP-2 was used in concentration of 100 ng/ml unless otherwise mentioned. For the Western blot analysis, cells were cultured in 1% HS (GE Healthcare) and 1% FBS (Thermo Fisher Scientific Inc.).

Real-Time Polymerase Chain Reaction

Quantitative real-time polymerase chain reaction (qRT-PCR) analysis of osteogenic and adipogenic marker genes was performed as described by Mesimäki and coworkers [1]. Briefly, 2,000 cells per well were plated on a 6-well plate (Thermo Fisher Scientific Inc.). CHO BMP-2 was used in RT-PCR experiments (R&D Systems). The total mRNA was isolated at the time points of days 7 and 14 using the NucleoSpin RNA II kit (Macherey-Nagel GmbH & Co., Düren, Germany, http://www.mn-net.com). The isolated mRNA was reverse transcribed to cDNA with the High-Capacity cDNA Reverse Transcriptase Kit (Thermo Fisher Scientific Inc.). The data were normalized to the expression of housekeeping gene *RPLP0* (human acidic ribosomal phosphoprotein P0) and the relative expression of each gene was calculated using a mathematical model described previously [19]. The primer sequences (Oligomer Oy, Helsinki, Finland, http://www.oligomer.fi) and the accession numbers are presented in Table 1.

Cell Number

The cell number of hASCs cultured in different conditions was analyzed at 14 and 19 days by CyQUANT Cell Proliferation Assay Kit (Thermo Fisher Scientific Inc.), according to the manufacturer's protocol as described by Lindroos et al. and Tirkkonen et al. [18, 20].

Alkaline Phosphatase Activity, Mineralization, and Oil Red O-Lipid Formation

Analyses of the qALP activity, mineralization, and lipid formation were conducted as previously described [18, 20]. The activity of ALP was studied quantitatively at day 14, as described in the Sigma ALP procedure (Sigma-Aldrich). The qALP activity results were normalized with the cell number from the CyQUANT analysis.

The Alizarin red S staining of minerals was analyzed at days 14 and 19. Briefly, the cells were fixed with 70% ethanol for 1 hour

Table 1. The sequences and accession numbers of the primers used in quantitative real-time polymerase chain reaction

Gene abbreviation	5'-Sequence-3'		Product size (bp)	Accession number
AP2	Forward	GGTGGTGGAATGCGTCATG	71	NM_001442
	Reverse	CAACGTCCCTTGGCTTATGC		
Dlx5	Forward	ACCATCCGTCTCAGGAATCG	75	NM_005221.5
	Reverse	CCCCCGTAGGGCTGTAGTAGT		
Osterix	Forward	TGAGCTGGAGCGTCATGTG	79	AF_477981
	Reverse	TCGGGTAAAGCGCTTGGA		
RPLP0	Forward	AATCTCCAGGGGCACCATT	70	NM_001002
	Reverse	CGCTGGCTCCCACTTTGT		

Abbreviation: bp, base pair.

(−20°C) followed by staining with 2% Alizarin red S solution (pH 4.1–4.3; Sigma-Aldrich) for 10 minutes at room temperature. Finally, for the quantitative analysis, the dye staining the calcium minerals was extracted from the samples with 100 mM cetylpyridinium chloride (Sigma-Aldrich). The intensity of the dye was analyzed with Victor 1420 multiplate reader (PerkinElmer Inc., Turku, Finland, http://www.perkinelmer.com) at 540 nm and the results were normalized with the cell number from the CyQUANT analysis [18, 20].

To assess the adipogenic differentiation of hASCs at 19 days, Oil Red O staining was conducted as previously described [18, 20], with slight modifications [18, 20]. Cell nuclei were stained with 4′,6-diamidino-2-phenylindole (DAPI) for 5 minutes before the last washing steps. DAPI-stained nuclei and the formation of the large lipid droplets stained with the fluorescent Oil Red O were analyzed from the microscopy images by using the ImageJ program (U.S. National Institutes of Health, Bethesda, MD, http://imagej.nih.gov/ij/). The number of the lipid droplets was normalized with the number of the counted nuclei.

Immunocytochemical Staining

For the analysis of the subcellular localization of activated SMAD1/5, mesenchymal vimentin and phosphorylated SMAD1/5 were analyzed by immunocytochemical staining after 0 minutes, 30 minutes, and 2 hours of BMP-2 stimulation (*E. coli*). For the staining, 10,000 cells per well were plated on a 48-well plate (Thermo Fisher Scientific Inc.). Prior to BMP-2 induction, hASCs were starved for 24 hours in 1% HS medium. At each time point, cells were fixed with 4% paraformaldehyde (Sigma-Aldrich) supplemented with 0.2% Triton X-100 for 15 minutes at room temperature. Blocking was done with 1% bovine serum albumin (Sigma-Aldrich) for 1 hour at 4°C. Subsequently, a double staining was conducted with the following primary antibodies: rabbit monoclonal anti-human-phosphorylated SMAD1/5 (pSMAD1/5; Cell Signaling Technology, Danvers, MA, http://www.cellsignal.com) and goat polyclonal anti-human vimentin (Merck Millipore, Billerica, MA, http://www.merckmillipore.com) overnight followed by secondary antibody staining with anti-goat Alexa 568 (Thermo Fisher Scientific Inc.) and anti-rabbit Alexa 488 (Thermo Fisher Scientific Inc.). Finally, samples were imaged using an Olympus microscope (IX51; Olympus Corp., Tokyo, Japan, http://www.olympus-global.com) equipped with a fluorescence unit and camera (DP30BW; Olympus Corp.).

Western Blotting and Immunodetection

For the analysis, 40,000 cells per well were plated on a 6-well plate (Thermo Fisher Scientific Inc.) and starved as described above for immunocytochemical staining, before treatment with BMP-2 from either CHO cells or *E. coli*. The medium was changed every third day. After a culture period of 24 hours, 3 and 7 days hASCs were lysed directly into 2× Laemmli sample buffer (20% glycerol, 6% SDS, 50 mM Tris pH 6.8, 10% β-mercaptoethanol) and samples were separated with SDS electrophoresis. After the electrophoretic separation, the proteins were transferred to polyvinylidene fluoride membrane (GE Healthcare, Waukesha, WI, http://www3.gehealthcare.com). After blocking, the target proteins were probed with the following primary antibodies: rabbit monoclonal anti-pSMAD1/5 (Cell Signaling Technology) and mouse monoclonal anti-β-actin (Santa Cruz Biotechnology, Dallas, TX, http://www.scbt.com) followed by horseradish peroxidase-conjugated secondary antibodies goat anti-mouse IgG (Santa Cruz Biotechnology) and anti-rabbit IgG (Cell Signaling Technology). Proteins were detected using enhanced chemiluminescence detection reagent (GE Healthcare). To analyze the basal levels of non-phosphorylated SMAD1, the pSMAD1/5 blots were stripped and blotted by rabbit monoclonal anti-SMAD1 antibody, followed by anti-rabbit IgG detection (supplemental online data). Semiquantitative normalization of pSMAD1/5 levels by SMAD1 basal levels was performed using ImageJ analysis software.

Statistical Analysis

Statistical analyses were performed with SPSS version 22 (IBM Corp., Armonk, NY, http://www.ibm.com). Alizarin red, qALP analysis, and CyQUANT measurements were performed with three to four hASC lines with three replicate samples of each. Oil Red O quantification was analyzed from three to four hASC lines with five replicative spots from each condition or treatment. Data are presented as mean ± SD. The pairwise comparisons between the effects of BMP-2 stimulus on ALP activity, mineralization, lipid formation, and cell proliferation were analyzed by using a nonparametric Mann-Whitney U test. The resulting p values were corrected with the Bonferroni multiple adjustment method based on the number of planned comparisons (supplemental online data; calculated p values are listed in supplemental online Tables 2–5). All the differences between and within the groups with adjusted $p \leq .05$ were considered to be significant.

RESULTS

BMP-2 Induces Donor Cell Line-Independent Activation of SMAD 1/5 Protein in hASCs

To analyze the biological functionality of BMP-2 in MSCs, we examined whether BMP-2 activates the internal SMAD pathway. For this, five different hASC lines (HFSC 41/12, 11/12, 15/12, 6/12,

and 8/12) were analyzed after BMP-2 induction at time points 24 hours and 7 days by Western blotting of levels of phosphorylated SMAD 1/5, total SMAD1, and β-actin as an internal control. Quantitative results of the pSMAD1/5 levels revealed that SMAD1/5 was activated robustly by BMP-2 at both time points in all the hASC lines studied (Fig. 1A). Also, small hASC line-dependent variations of the pSMAD1/5 levels at BMP-2 stimulus were observed at both time points. However, minor levels of constitutively phosphorylated SMAD were apparent also in unstimulated control samples. Comparison of the effectiveness of BMP-2 produced in *E. coli* and in CHO revealed modest SMAD1/5 induction by BMP-2 produced in *E. coli*, but clearly enhanced induction by BMP-2 produced in CHO cells (Fig. 1A).

We also studied the effect of culture conditions on SMAD activation. For this purpose, hASCs were cultured in HS or in FBS medium. In both media, pSMAD was activated dose dependently with BMP-2 stimulus. Surprisingly, BMP-2 produced in *E. coli* induced higher levels of pSMAD activation in the HS medium (Fig. 2A, 2B). Quantification of the intensity of the pSMAD bands and normalization to SMAD1 levels revealed that the difference between HS and FBS media was most apparent at 24 hours and at 7 days. Only higher doses of BMP-2 induced minor induction of pSMAD in the FBS medium (Fig. 2A, 2B). Similar findings were apparent also when SMAD activation of the osteoblast cell line and hBMSC line was analyzed in HS and FBS media in the presence of BMP-2: The SMAD was activated dose dependently by BMP-2 in the HS medium, whereas in the FBS medium, the overall levels of pSMAD were decreased at all time points (supplemental online Fig. 1; supplemental online data).

BMP-2 Activated SMAD Translocates to Nucleus in hASCs

In a first step, the functionality of recombinant human BMP-2 signaling was analyzed from the total cell lysates by Western blot. However, we wanted to study whether the phosphorylated SMAD retains its functionality and the signal is actually transferred to the nucleus of hASCs for the transcriptional processes. To further analyze the functionality of BMP-2, we performed analysis of the translocation of activated SMAD1/5 by immunocytochemical staining (human fat stem cell [HFSC] 7/12). Our results indicated that after 30 minutes of BMP-2 growth factor stimulus, pSMAD 1/5, stained with green, translocated into cell nuclei and remained there after 2 hours from the start of the stimulation. The red staining in Figure 1B indicates mesenchymal vimentin protein. Some of the pSMAD1/5 were also observed in unstimulated cells, indicating a minor level of basal SMAD activation (Fig. 1B). To gain a broader picture, we also performed the analysis of the SMAD translocation in BMSCs, 3 other hASC lines (HFSC 41/12, 15/12, and 25/12), and osteoblasts. These results indicate that SMAD1/5 is activated and translocated to nuclei in all the cell types studied by both BMP-2 growth factors (ie, those produced in *E. coli* and in the CHO cell line) (supplemental online Figs. 2, 3) and confirms that BMP-2 is a functional trigger for the SMAD-related molecular mechanisms in MSCs.

The Activity of the Early Osteogenic Marker ALP Is Differentially Enhanced by BMP-2 in hASCs Lines

To analyze the functional outcome of BMP-2-SMAD signaling, we performed quantitative analysis of the early osteogenic marker,

normalized alkaline phosphatase (ALP) enzymatic activity in BM and OM culture conditions in different hASC lines. Our results indicated that the BMP-2-induced response of ALP activity was highly variable between hASC lines. Based on our results, BMP-2 does not modulate qALP levels in BM; however, clear differences were apparent when cells were treated with BMP-2 in OM. From the studied hASC lines, we could clearly distinguish 2 types of responses to BMP-2 stimuli. Some cell lines showed enhancement of the qALP levels due to BMP-2 stimulus (Fig. 3A), whereas in others, qALP levels were diminished or retained at the same level by BMP-2 treatment (Fig. 3B). However, cell proliferation analysis by the CyQUANT method revealed that BMP-2 treatment decreases the proliferation efficiency in all the cell lines studied in both BM and OM (Fig. 3A, 3B). To further analyze this differential behavior, we used hASC lines expressing opposing responses to BMP-2 stimulus. hASCs were separated into 2 groups, group I (HFSC 41/12, 11/12, 9/12) and group II (HFSC 15/12, 6/12, and 7/12), based on whether the BMP-2 enhanced or decreased ALP activity, respectively. As indicated in Figure 3C and 3D, qALP results from cell lines in each group were combined, showing that BMP-2 enhanced ALP activity in group I and decreased activity in group II. Also, BMP-2 addition significantly decreased proliferation levels of hASCs in BM and OM in both groups (Fig. 3C).

### Mineralization of hASCs Is Differentially Promoted by BMP-2

To further analyze the osteogenic differentiation potential of BMP-2 (CHO), we performed Alizarin red mineralization analysis at time points of 14 and 19 days in BM and OM conditions. Alizarin red color formation due to mineralization of the samples was analyzed qualitatively (Fig. 4C) but also quantitatively (Fig. 4A, 4B, and 4D) by extraction of the color and measurement of the intensity of the extracted stain. Altogether, eight different hASC lines were analyzed and divided into groups I and II based on their response to BMP-2 in ALP analysis (HFSC41/12, 9/13, 11/12, and 19/11 in group I; HFSC 15/12, 44/12, 6/12, and 7/12 in group II). There was a significant difference between hASCs in their BMP-2-induced mineralization in OM. hASC lines in group I showed prominent enhancement of the mineralization at day 19. Also 3 of 4 cell lines showed a significant increase at day 14 (Fig. 4A, 4D).

On the contrary, hASC lines in group II did not show any significant enhancement of mineralization in response to BMP-2 stimulus at any of the analyzed time points or in either medium. Actually, some hASC lines in group II had decreased mineralization levels in BMP-2-supplemented OM (Fig. 4B). Qualitative analysis of mineralization of hASC lines HFSC 41/12 from group I versus HFSC 15/12 from group II confirmed this finding, showing clearly enhanced mineralization in the hASC line from group I and decreased levels of mineralization in hASC of group II in BMP-2-supplemented OM (Fig. 4C). Finally, the mineralization results from the hASC lines in each group were combined, and showed that BMP-2 significantly increased mineralization in group I and decreased it in group II (Fig. 4D).

BMP-2 Growth Factor From Mammalian Origin Efficiently Modulates ALP Activity and Mineralization of hASCs

In order to study whether the production origin of the BMP-2 growth factor influences the response of hASCs, we analyzed the effect of BMP-2 from *E. coli* and mammalian CHO cells. We
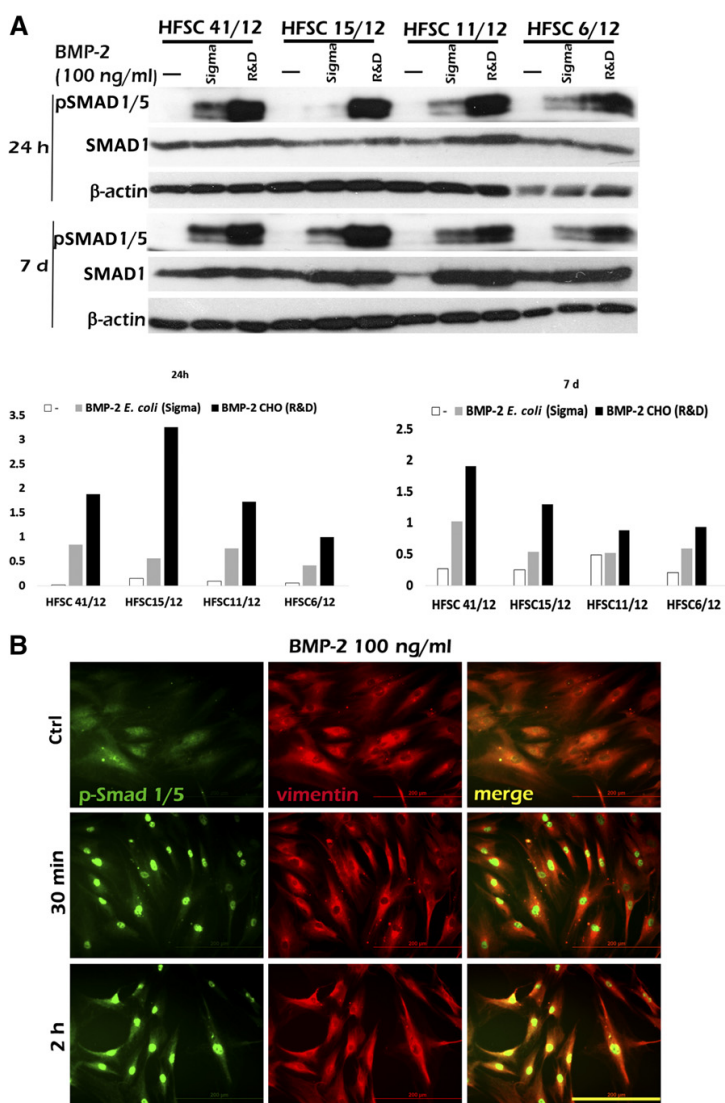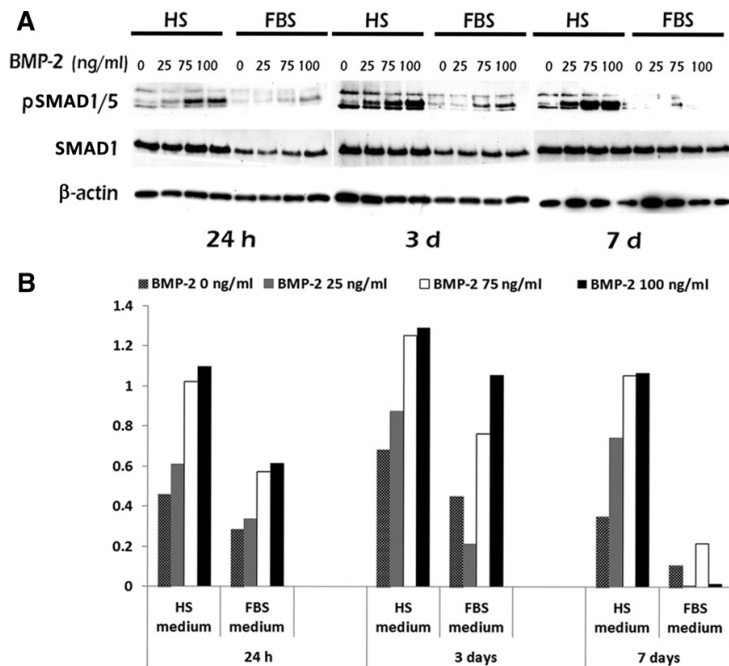
Figure 1. BMP-2 induced phosphorylation of SMAD1/5 and translocation into nuclei. **(A):** Representative image of Western Blot analysis of SMAD1/5 phosphorylation, basal SMAD1, and β-actin levels in BMP-2 induction. BMP-2 was used in amount of 100 ng/ml, and BMP-2 from Sigma was produced in *Escherichia coli*, whereas BMP-2 from R&D was produced in CHO cells. Analysis time points were 24 hours and 7 days, and human adipose stem cell (hASC) lines used were HFSC 41/12, 15/12, 11/12, and 6/12. Phosphorylated SMAD levels were quantified by normalizing them with SMAD1 basal protein levels by using the ImageJ analysis tool. **(B):** Immunocytochemical analysis of translocation of *p*-SMAD1/5 was performed at 3 time points: 0 minutes (Ctrl), 30 minutes, and 2 hours. In the representative images, the hASC line used was HFSC 7/12; BMP-2 (*E. coli*) was used in a concentration of 100 ng/ml. Primary antibodies (*p*-SMAD1/5 [green] and vimentin [red]) and secondary antibodies (Alexa fluor 568 and 488) were used to detect the subcellular localization of *p*-SMAD1/5 and cytoplasmic vimentin proteins. Scale bar = 200 μm. Abbreviations: BMP-2, bone morphogenetic protein-2; CHO, Chinese hamster ovary; HFSC, human fat stem cell; R&D, R&D Systems; Sigma, Sigma-Aldrich.

analyzed cell proliferation, qALP activity, and mineralization capacity of two donor cell lines, 15/12 (group II) and 41/12 (group I), stimulated with BMP-2 produced in *E.coli* and CHO. CyQUANT proliferation analysis revealed that with both BMPs, the proliferation of hASCs was decreased under all conditions. However,

BMP-2 produced in CHO cells decreased proliferation more efficiently compared with BMP-2 from *E. coli* (Fig. 5A, 5B). Analysis of qALP and mineralization revealed that BMP-2 produced in CHO cells had a greater capacity to modulate the changes in OM in both cell lines. Also, the results between the cell lines

Figure 2. BMP-2 induced SMAD activation in HS and FBS media. **(A):** Representative image of Western Blot analysis of BMP-2-induced SMAD1/5 phosphorylation, basal SMAD1, and β-actin levels in HS and FBS media. BMP-2 (*Escherichia coli*) was used in amount of 0, 25, 75, and 100 ng/ml. Analysis time points were 24 h, 3 days, and 7 days, and the hASC line used was human fat stem cell (HFSC) 8/12. **(B):** Semiquantitative analysis of phosphorylated SMAD1/5 levels normalized with SMAD1 levels. Quantification was performed with the ImageJ analysis program. Abbreviations: BMP-2, bone morphogenetic protein-2; FBS, fetal bovine serum; HS, human serum.

were opposing, so the 15/12 cell line showed decreased qALP activity and mineralization, whereas cell line 41/12 clearly showed increased qALP activity and mineralization in OM supplemented with BMP-2 (Fig. 5A, 5B). Our results indicated that as in ALP activation and mineral formation, BMP-2 produced in CHO cells was the most efficient inducer of hASCs.

BMP-2 Induces High Expression of Osteogenic and Adipogenic Markers and Formation of Lipid Vacuoles in hASCs

During the mineralization assays, we observed that some of the hASC lines produced large amounts of lipid vacuoles in the presence of BMP-2. Thus, we investigated further whether BMP-2 actually induces adipogenic differentiation in some of the hASC lines studied. We analyzed expression levels of the adipogenic marker adipocyte protein 2 (*AP2*), and the osteogenic markers osterix (*Osx*) and *Dlx5* in hASC lines from group I and II. At day 7, BMP-2 (CHO) induced elevated expression of osteogenic markers *osterix* and *Dlx5* and, at day 14, remarkably high levels of *AP2*. Expression levels of both osteogenic and adipogenic markers varied among hASC lines (Fig. 6A), but levels were not dependent on the group in which they were previously classified (data not shown). These results suggested that BMP-2 growth factor could induce osteogenic as well as adipogenic differentiation in hASCs and prompted us to further analyze the effect of BMP-2 stimulus on adipogenic differentiation in BM and OM. For this purpose, we performed Oil Red O staining of lipid vacuoles

and semiquantitative analysis of lipid formation with ImageJ analysis at day 19.

BM and OM induced modest lipid formation in all the hASC lines studied. However, BMP-2 treatment induced statistically significant lipid formation in hASC lines from group II, whereas in hASCs from group I, we did not observe any significant enhancement of the lipid formation (Fig. 6B, 6C).

We also wanted to analyze further the relevance of the BMP-2 production origin (ie, *E. coli* or CHO). Qualitative and semiquantitative Oil Red O analysis of the lipid formation of hASC lines 41/12 (group I) and 6/12 (group II) revealed that lipid formation was significantly enhanced with both types of BMP-2 in hASC line 6/12, although, CHO-produced BMP-2 induced higher levels of lipid formation compared with BMP-2 of *E. coli* origin. None of the BMP-2 types induced any significant lipid formation in hASC line 41/12 (Fig. 6B, 6D).

DISCUSSION

Osteoinductive BMP-2 is the most prominent growth factor used in clinics in recent years [1, 21–23]. Unfortunately, recent publications describing BMP-2 efficacy on BMSCs and ASCs have been contradictory, and its role as an osteoinducer has been questioned [6, 11, 12, 20]. The current study aimed to further analyze the effect of BMP-2 growth factor in vitro on several hASC lines derived from different donors and to untangle the existing contradictions in previous results in our laboratory and among other laboratories.
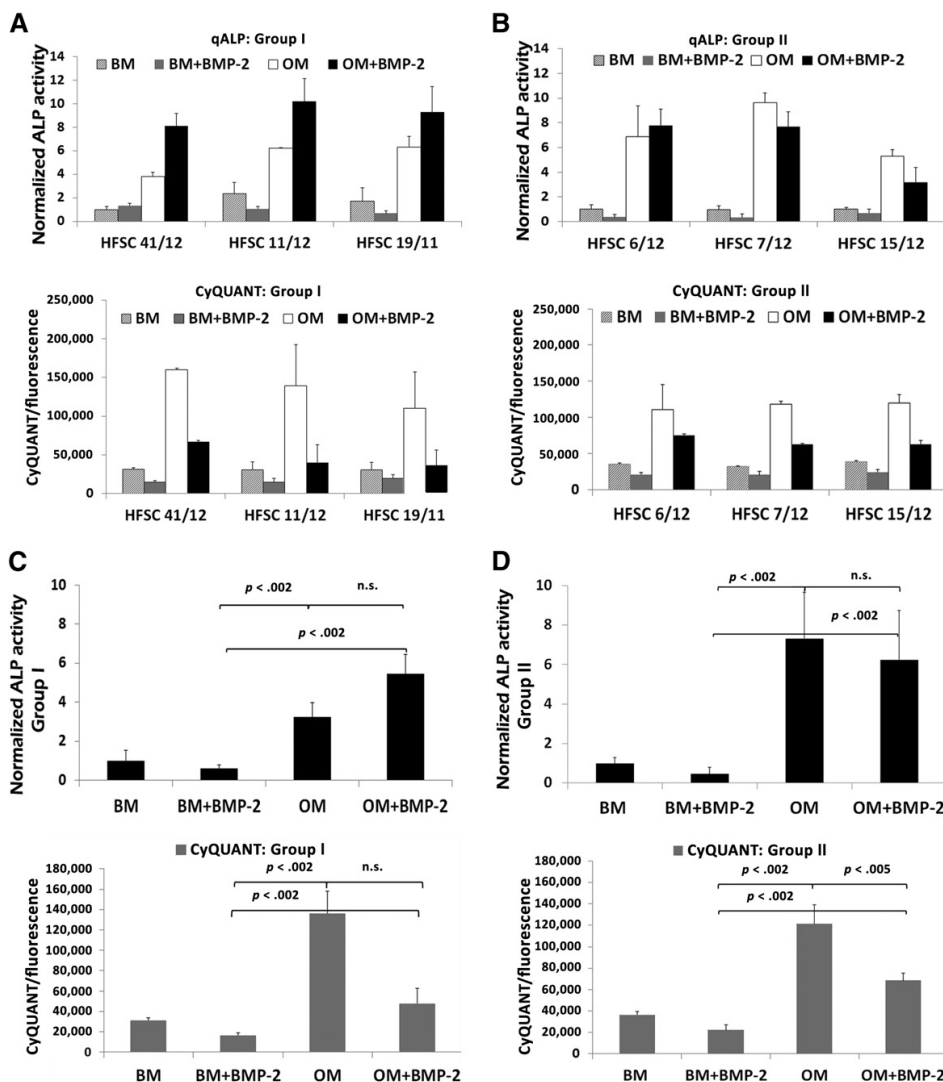
Figure 3. BMP-2 induction of ALP activity in human adipose stem cells. **(A, B):** qALP activity (three replicate samples per condition) normalized with fluorescent values from CyQUANT cell number analysis. Lower panels present fluorescence values from CyQUANT cell number analysis. hASC lines HFSC 41/12, 11/12, 19/11 represent group I **(A)** and hASC lines HFSC 6/12, 7/12, and 15/12 represent group II **(B)**. **(C):** Results from group I were grouped together and given as normalized qALP values and fluorescence values from CyQUANT cell number analysis (three cell lines and three replicate samples per condition). **(D):** The same was done to group II. Results are expressed as mean $\pm$ SD. ALP results were standardized to the control condition. The BMP-2 (CHO) concentration was 100 ng/ml. Statistical analysis was performed with the Mann-Whitney U test and with Bonferroni correction. The level of significance was set at $p < .05$. Abbreviations: ALP, alkaline phosphatase; BM, basic culture medium; BMP-2, bone morphogenetic protein-2; HFSC, human fat stem cell; n.s., not significant; OM, osteogenic medium; qALP, quantitative alkaline phosphatase.

Our results indicated that the functional mechanism of BMP-2-induced SMAD activation was present in all studied hASCs, hBMSCs, and osteoblasts, testifying to the molecular functionality of the BMP-2 growth factor and its receptor. Previous in vitro studies investigating the action of the BMP-2 in hASCs have suggested a lack of the BMP-2 effect or even a decreasing effect on the osteogenic differentiation of hASCs [11, 12, 20]. In these studies, ALP activity, mineralization, or gene expression of osteogenic markers such as *Dlx5* and *Osx* were not affected by BMP-2 supplementation. Also BMP-2-related SMAD phosphorylation levels analyzed by Western blot and immunocytochemical staining were unaffected [11]. Our results with BMP-2 indicated that all of the studied hASC lines do respond to mammalian BMP-2, but the biological outcome in the differentiation process varies
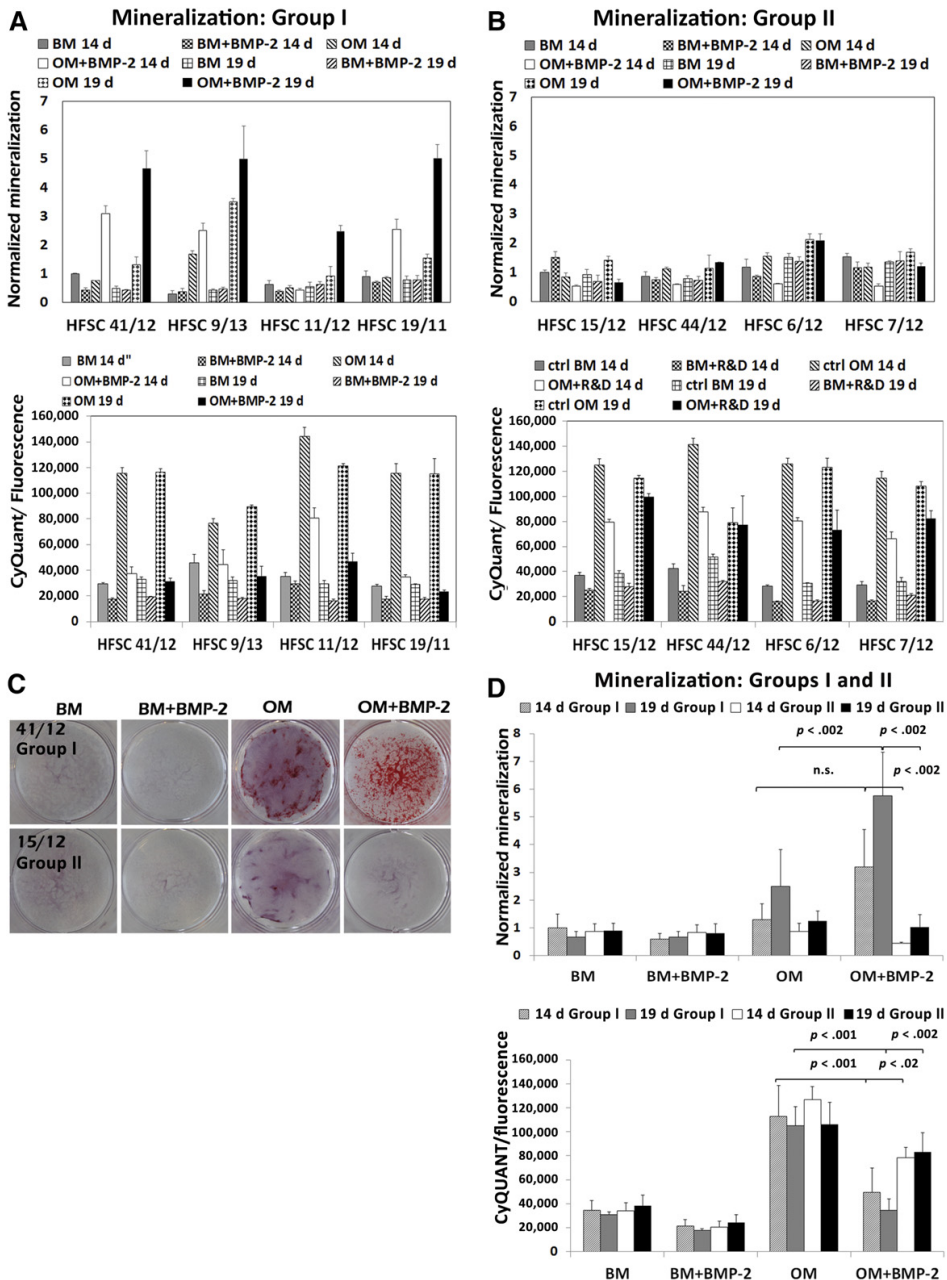
Figure 4. Impact of BMP-2 on mineralization of human adipose stem cells (hASCs). **(A, B):** Quantitative analysis of Alizarin red S mineralization assay normalized with fluorescence values from CyQUANT cell number analysis (three replicate samples per condition). Fluorescence values in the lower panels are from CyQUANT cell number analysis of hASC lines HFSC 41/12, 11/12, 19/11, and 9/13 representing group I **(A)**, and hASC lines HFSC 6/12, 7/12, 44/12, and 15/12 representing group II **(B)**. Results from group I were grouped together and represented as normalized Alizarin red S values; the lower panel presents fluorescence values from CyQUANT cell number analysis. **(D):** The same was done to group II (four cell lines and three replicates per condition). **(C):** Qualitative analysis of mineralization by Alizarin red S staining of HFSC lines 41/12 (group I) and 15/12 (group II). Images are from the whole 24-well area. Results are expressed as mean ± SD. Alizarin red S results were standardized to the control condition. The amount of BMP-2 (CHO) used was 100 ng/ml. Statistical analysis was performed with the Mann-Whitney *U* test and with Bonferroni correction. The level of significance was set at *p* < .05. Abbreviations: BM, basic culture medium; BMP-2, bone morphogenetic protein-2; ctrl, control; HFSC, human fat stem cell; OM, osteogenic medium; R&D, R&D Systems.
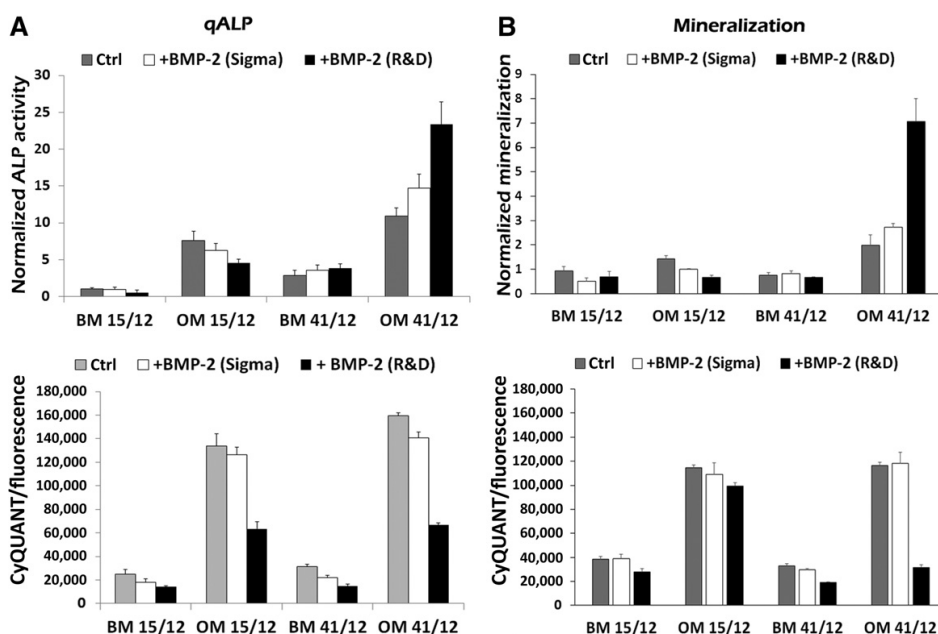
Figure 5. Comparison of the effectiveness of BMP-2 produced in mammalian cells (Chinese hamster ovary [CHO]) and in *Escherichia coli*. **(A, B):** qALP activity **(A)** and Alizarin red S values **(B)** normalized with fluorescence values from CyQUANT cell number analysis. Lower panels present fluorescence values from CyQUANT cell number analysis. Presented human adipose stem cell lines are HFSC 41/12 (group I) and 15/12 (group II). Results are expressed as mean ± SD. ALP results were standardized to the control condition. The amount of BMP-2 (E. coli [Sigma] or CHO [R&D]) used was 100 ng/ml. Abbreviations: ALP, alkaline phosphatase; BM, basic culture medium; BMP-2, bone morphogenetic protein-2; ctrl, control; OM, osteogenic medium; qALP, quantitative alkaline phosphatase; R&D, R&D Systems; Sigma, Sigma-Aldrich.

from one donor line to another. However, one common function for BMP-2 was observed in all hASCs studied: BMP-2 considerably decreased hASC proliferation rates. The same effect can be seen also in our previous work, where BMP-2 was studied in combination with biomaterials, bioactive glass, and β-tricalcium phosphate [12].

Our current results revealed that BMP-2 exerts dual action in differentiation processes of hASCs, and two types of donor cell lines could be distinguished based on their responses. High levels of BMP-2-induced mineralization were expected because of our results of SMAD activation at the molecular level. However, analysis of the expression of adipogenic marker gene *AP2* revealed that in the presence of OM and BMP-2 stimulus, all hASC lines studied expressed remarkably high levels of this marker regardless of indicated group. Furthermore, some hASC lines clearly had a greater tendency toward adipogenic differentiation, as indicated by qualitative and quantitative Oil Red O lipid staining (Fig. 6). We also observed heterogeneity in the differentiation capacity within some donor cell lines, with simultaneous mineralization and lipid formation seen in some phase of the differentiation process. However, broader analysis of hASC lines would be required to confirm this heterogeneous behavior.

Our findings indicate that the functional outcome differs substantially among hASC lines; most likely, this is dependent on the other cooperative signaling mechanisms in addition to BMP-2. There are several reports and reviews describing molecular mechanisms of osteogenic and adipogenic differentiation of BMSCs and ASCs, indicating that critical molecular switches are usually

part of Wnt, BMP, Notch, and FGF signaling cascades functioning cooperatively in regulation of these events [7, 24–26]. It is plausible that some hASC donor lines used in our studies have more adipocyte commitment and more functional adipogenic signaling pathways compared with others. Thus, hypothetically, these cells might be sensitized for BMP-2 functions toward adipogenic signaling mechanisms and, as a result, we observed enhanced lipid formation instead of mineralization upon BMP-2 stimulus. Park and coworkers reported that BMP-2 induces osteogenic and adipogenic differentiation of human alveolar bone-derived stromal cells [6]. In their study, dose-dependent adipogenic and osteogenic effects of BMP-2 were studied separately in adipogenic and osteogenic media. However, as a further distinction from their work, our study was performed in its entirety in basic and osteogenic culture conditions.

Cell surface marker analysis of the hASCs (supplemental online Table 1; supplemental online Fig. 4) revealed that average expression of the CD marker 34 was relatively high, whereas CD marker 73 expression was lower than stated in the International Society for Cellular Therapy minimal criteria for multipotent MSCs [27]. Based on previous publications by Patrikoski and coworkers [28] and Mitchell and coworkers [29], hASCs have changes in surface marker expression levels due to multiplied passages of the cells. However, in this study, hASCs in groups I and II had a similar CD marker expression pattern (supplemental online Fig. 4), suggesting that variation in expression of CD markers analyzed in this study was not related to differentiation outcome of BMP-2 stimulus. hASC lines in
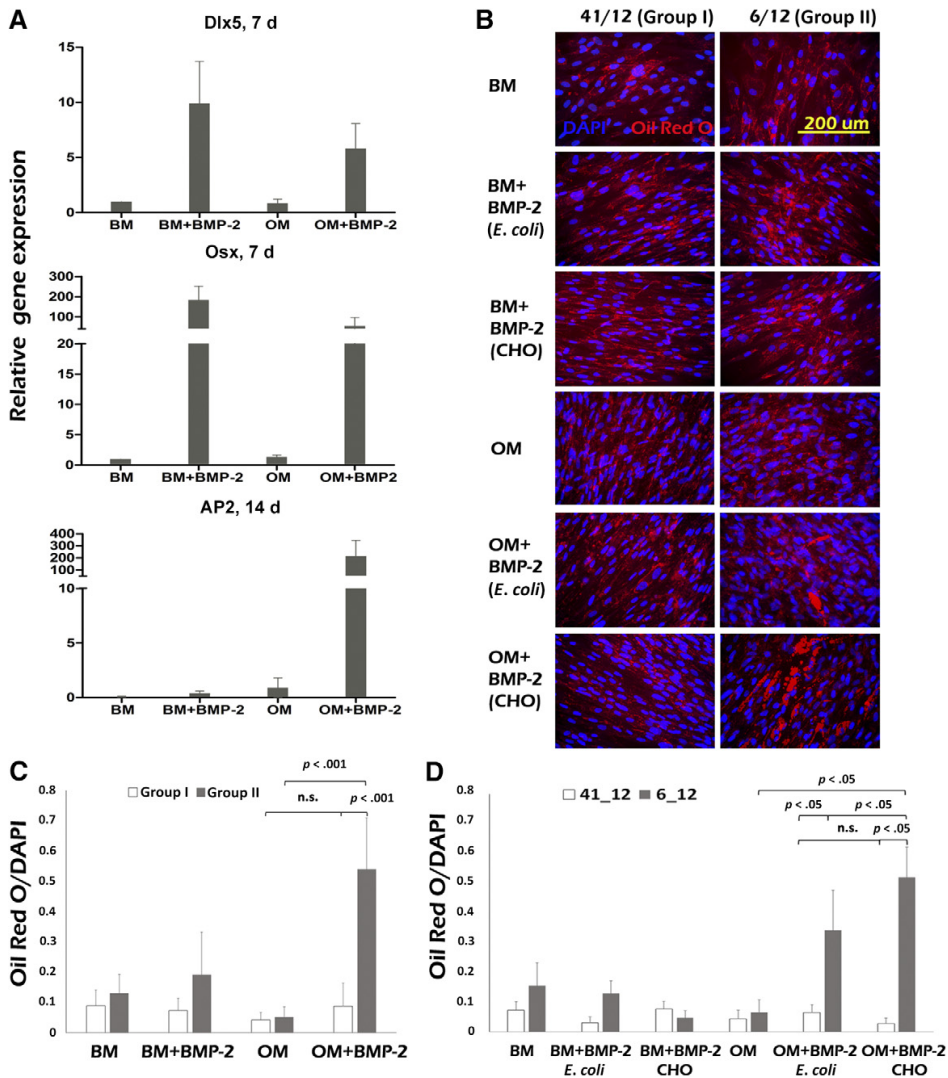
Figure 6. Expression of osteogenic/adipogenic marker genes and lipid formation in human adipose stem cells (hASCs). **(A):** Quantitative polymerase chain reaction analysis of relative mRNA expression of osteogenic markers *Dlx5* and *osterix (Osx)* at the 7-day time point and adipogenic marker *AP2* at the 14-day time point (3 hASC lines from group I and group II each were used). The amount of BMP-2 (CHO; R&D) used was 100 ng/ml. **(B):** Qualitative analysis of Oil Red O staining of lipid vacuoles (bright red) and nuclei of the cells (blue) at the 19-day time point. The amount of BMP-2 (CHO and *Escherichia coli*) used was 100 ng/ml. **(C):** Quantitative analysis of the Oil Red O lipid formation normalized with amount of nuclei in hASC lines in group I ($n = 15$) and group II ($n = 20$). The amount of BMP-2 (CHO) used was 100 ng/ml. **(D):** Quantitative analysis of the Oil Red O lipid formation normalized with the amount of nuclei in hASC lines 41/12 and 6/12 ($n = 5$). The amount of BMP-2 (*E. coli* and CHO) used was 100 ng/ml. Statistical analysis was performed with the Mann-Whitney *U* test and with Bonferroni correction. The level of significance was set at $p < .05$. Quantitative analysis was performed by the ImageJ analysis program. Abbreviations: AP2, adipocyte protein 2; BM, basic culture medium; BMP-2, bone morphogenetic protein-2; CHO, Chinese hamster ovary; Dlx, distal-less homeobox; OM= osteogenic medium; DAPI, 4′,6-diamidino-2-phenylindole.

groups I and II had variation in donor age such that the average age in group I was 36 ± 15 years and, in group II, 56 ± 14 years (data not shown). Based on this finding, it is tempting to speculate that hASCs derived from younger donors would have higher potential to demonstrate BMP-2-induced osteogenesis than cells from older individuals.

Our results indicate that the functionality of BMP-2 is distinctly dependent on culture conditions. Western blot analysis of the phosphorylated SMAD1/5 indicated that the intracellular impact of BMP-2 in hASCs, hBMSCs, and osteoblasts was stronger in the HS medium than the FBS medium. The explanation for the different response to BMP-2 in HS and FBS media might be found

in the differential expression of BMP receptors on the cell surface of hASCs. Most critical for the functionality of the BMP-2 growth factor is the responsive BMP receptor complex. BMPs exert their diverse biological effects through two types of transmembrane receptors, BMPR-I and BMPR-II, possessing the intrinsic serine/threonine kinase activity [30–32]. The binding of dimeric BMP ligands to heterotetrameric receptors activates their cytoplasmic kinase domain and further receptor-specific SMADs [33, 34]. However, the existence of the BMP-2 receptor on the hASC surface in the FBS medium has been indicated in the extensive studies by Zuk and coworkers [11, 35], suggesting that this might not be the definitive cause for the dysfunction of SMAD signaling mechanisms in hASCs. Furthermore, in this study, we tested only 1 brand of FBS; presumably, FBS from different manufacturers might have displayed a variable impact on BMP-2 functionality. Also, the bioactivity of the actual growth factor can vary in different culture conditions, since components of the FBS could actually inhibit the action of otherwise functional BMP-2 growth factor. Zuk and coworkers also disclosed an interesting possibility in their discussion referring to the differential miRNA expression of the hASCs as at the root of their BMP-2 responsiveness [11].

The conformation of the BMP-2 growth factor is also a very important issue for its biological functionality [36]. We compared the effect of human recombinant BMP-2 produced in *E. coli* and mammalian CHO cells on proliferation and osteogenic and adipogenic differentiation of hASCs. Our results clearly indicated that hASCs responded to mammalian-produced BMP-2 more efficiently. BMP-2 produced in CHO cells had a marked but donor-dependent impact on mineralization and lipid formation of hASCs. BMP-2 produced in *E. coli* also induced these processes, but the effect was clearly diminished compared with CHO-produced BMP-2. In all the hASC lines studied, both BMP-2 types also decreased proliferation of the donor cell line independently, although CHO-produced BMP-2 was more effective. This is probably due to more physiological conformation of the CHO-produced growth factor and that proteins produced in the mammalian system have been processed by cells with posttranslational glycosylation, unlike proteins produced in bacterial systems [36]. Therefore, the use of different types of growth factors might also partially explain variable results reported from several BMP-MSC studies. Variability in culture conditions, arrangements of responsive receptors, expression of growth factors by cells in certain conditions, status of the different populations, and internal cellular mechanisms might explain the fluctuating outcome of hASCs in

BMP-2 stimulus and further studies are required to clarify molecular signaling and functional outcome in this context.

CONCLUSION

We examined how BMP-2 modulates signaling mechanisms, proliferation, and differentiation outcome of hASCs derived from several donors. Our results show that BMP-2 triggers molecular SMAD signaling mechanisms in hASCs and regulates differentiation processes in HS medium. The production origin of BMP-2 has an important role in its functionality on hASCs, since BMP-2 produced in mammalian cells induced higher responses than counterparts produced in *E. coli*. Based on our results, BMP-2 has two mechanisms of action, inducing osteogenic and adipogenic differentiation, depending on the hASC donor line. These findings partially explain contradictory previous results and highlight the importance of further studies to understand how signaling pathways guide MSC functions at the molecular level.

AUTHOR CONTRIBUTIONS

S.V.: conception and design, collection and assembly of the data, data analysis and interpretation, manuscript writing, final approval of the manuscript; M.O.: collection and assembly of the data, data analysis and interpretation, manuscript writing, final approval of the manuscript; R.A.: data analysis and interpretation, manuscript writing, final approval of the manuscript; M.J.: collection and assembly of the data, data analysis and interpretation, final approval of the manuscript; S.M.: data analysis and interpretation, manuscript writing, final approval of the manuscript, financial support.

DISCLOSURE OF POTENTIAL CONFLICTS OF INTEREST

The authors indicated no potential conflicts of interest.

REFERENCES

1 Mesimäki K, Lindroos B, Törnwall J et al. Novel maxillary reconstruction with ectopic bone formation by GMP adipose stem cells. Int J Oral Maxillofac Surg 2009;38:201–209.

2 Wang YK, Yu X, Cohen DM et al. Bone morphogenetic protein-2-induced signaling and osteogenesis is regulated by cell shape, RhoA/ROCK, and cytoskeletal tension. Stem Cells Dev 2012;21: 1176–1186.

3 Zhang X, Guo J, Zhou Y et al. The roles of bone morphogenetic proteins and their signaling in the osteogenesis of adipose-derived stem cells. Tissue Eng Part B Rev 2014;20:84–92.

4 Ryoo HM, Lee MH, Kim YJ. Critical molecular switches involved in BMP-2-induced

osteogenic differentiation of mesenchymal cells. Gene 2006;366:51–57.

5 Castro-Govea Y, Cervantes-Kardasch VH, Borrego-Soto G et al. Human bone morphogenetic protein 2-transduced mesenchymal stem cells improve bone regeneration in a model of mandible distraction surgery. J Craniofac Surg 2012;23:392–396.

6 Park JC, Kim JC, Kim BK et al. Dose- and time-dependent effects of recombinant human bone morphogenetic protein-2 on the osteogenic and adipogenic potentials of alveolar bone-derived stromal cells. J Periodontal Res 2012;47:645–654.

7 James AW, Zara JN, Zhang X et al. Perivascular stem cells: A prospectively purified mesenchymal stem cell population for bone tissue

engineering. STEM CELLS TRANSLATIONAL MEDICINE 2012;1:510–519.

8 Montgomery SR, Nargizyan T, Meliton V et al. A novel osteogenic oxysterol compound for therapeutic development to promote bone growth: Activation of hedgehog signaling and osteogenesis through smoothened binding. J Bone Miner Res 2014;29:1872–1885.

9 Dragoo JL, Choi JY, Lieberman JR et al. Bone induction by BMP-2 transduced stem cells derived from human fat. J Orthop Res 2003;21: 622–629.

10 Chou YF, Zuk PA, Chang TL et al. Adipose-derived stem cells and BMP2: Part 1. BMP2-treated adipose-derived stem cells do not improve repair of segmental femoral defects. Connect Tissue Res 2011;52:109–118.

11 Zuk P, Chou YF, Mussano F et al. Adipose-derived stem cells and BMP2: Part 2. BMP2 may not influence the osteogenic fate of human adipose-derived stem cells. Connect Tissue Res 2011;52:119–132.

12 Waselau M, Patrikoski M, Juntunen M et al. Effects of bioactive glass S53P4 or beta-tricalcium phosphate and bone morphogenetic protein-2 and bone morphogenetic protein-7 on osteogenic differentiation of human adipose stem cells. J Tissue Eng 2012;3:2041731412467789.

13 Fan J, Park H, Lee MK et al. Adipose-derived stem cells and BMP-2 delivery in chitosan-based 3D constructs to enhance bone regeneration in a rat mandibular defect model. Tissue Eng Part A 2014;20:2169–2179.

14 Maegawa N, Kawamura K, Hirose M et al. Enhancement of osteoblastic differentiation of mesenchymal stromal cells cultured by selective combination of bone morphogenetic protein-2 (BMP-2) and fibroblast growth factor-2 (FGF-2). J Tissue Eng Regen Med 2007;1:306–313.

15 Lin GL, Hankenson KD. Integration of BMP, Wnt, and notch signaling pathways in osteoblast differentiation. J Cell Biochem 2011;112:3491–3501.

16 Viale-Bouroncle S, Gosau M, Morsczeck C. NOTCH1 signaling regulates the BMP2/DLX-3 directed osteogenic differentiation of dental follicle cells. Biochem Biophys Res Commun 2014;443:500–504.

17 Viale-Bouroncle S, Klingelhoffer C, Ettl T et al. A protein kinase A (PKA)/beta-catenin pathway sustains the BMP2/DLX3-induced osteogenic differentiation in dental follicle cells (DFCs). Cell Signal 2015;27:598–605.

18 Lindroos B, Boucher S, Chase L et al. Serum-free, xeno-free culture media maintain the proliferation rate and multipotentiality of adipose stem cells in vitro. Cytotherapy 2009;11:958–972.

19 Pfaffl W. A new mathematical model for relative quantification in real-time RT-PCR. Nuclei Acids Res 2001;29:e45.

20 Tirkkonen L, Haimi S, Huttunen S et al. Osteogenic medium is superior to growth factors in differentiation of human adipose stem cells towards bone-forming cells in 3D culture. Eur Cell Mater 2013;25:144–158.

21 Sándor GK, Tuovinen VJ, Wolff J et al. Adipose stem cell tissue-engineered construct used to treat large anterior mandibular defect: a case report and review of the clinical application of good manufacturing practice-level adipose stem cells for bone regeneration. J Oral Maxillofac Surg 2013;71:938–950.

22 Sándor GK, Numminen J, Wolff J et al. Adipose stem cells used to reconstruct 13 cases with cranio-maxillofacial hard-tissue defects. STEM CELLS TRANSLATIONAL MEDICINE 2014;3:530–540.

23 Schuckert KH, Jopp S, Osadnik M. The use of platelet rich plasma, bone morphogenetic protein-2 and different scaffolds in oral and maxillofacial surgery—literature review in comparison with own clinical experience. J Oral Maxillofac Res 2011;2:e2.

24 Chatakun P, Núñez-Toldrà R, Díaz López EJ et al. The effect of five proteins on stem cells used for osteoblast differentiation and proliferation: a current review of the literature. Cell Mol Life Sci 2014;71:113–142.

25 Titorencu I, Pruna V, Jinga VV et al. Osteoblast ontogeny and implications for bone pathology: An overview. Cell Tissue Res 2014;355:23–33.

26 Takada I, Kouzmenko AP, Kato S. Wnt and PPARgamma signaling in osteoblastogenesis and adipogenesis. Nat Rev Rheumatol 2009;5:442–447.

27 Bourin P, Bunnell BA, Casteilla L et al. Stromal cells from the adipose tissue-derived stromal vascular fraction and culture expanded adipose tissue-derived stromal/stem cells: A joint statement of the International Federation for Adipose Therapeutics and Science (IFATS) and the International Society for Cellular Therapy (ISCT). Cytotherapy 2013;15:641–648.

28 Patrikoski M, Juntunen M, Boucher S et al. Development of fully defined xeno-free culture system for the preparation and propagation of cell therapy-compliant human adipose stem cells. Stem Cell Res Ther 2013;4:27.

29 Mitchell JB, McIntosh K, Zvonic S et al. Immunophenotype of human adipose-derived cells: temporal changes in stromal-associated and stem cell-associated markers. STEM CELLS 2006;24:376–385.

30 Ehrlich M, Horbelt D, Marom B et al. Homomeric and heteromeric complexes among TGF-β and BMP receptors and their roles in signaling. Cell Signal 2011;23:1424–1432.

31 Ehrlich M, Gutman O, Knaus P et al. Oligomeric interactions of TGF-β and BMP receptors. FEBS Lett 2012;586:1885–1896.

32 Miyazono K, Kamiya Y, Morikawa M. Bone morphogenetic protein receptors and signal transduction. J Biochem 2010;147:35–51.

33 Heldin CH, Moustakas A. Role of Smads in TGFβ signaling. Cell Tissue Res 2012;347:21–36.

34 Zieba A, Pardali K, Soderberg O et al. Intercellular variation in signaling through the TGF-beta pathway and its relation to cell density and cell cycle phase. Mol Cell Proteomics 2012;11:M111.013482.

35 Zuk PA, Zhu M, Ashjian P et al. Human adipose tissue is a source of multipotent stem cells. Mol Biol Cell 2002;13:4279–4295.

36 Carreira AC, Lojudice FH, Halcsik E et al. Bone morphogenetic proteins: Facts, challenges, and future perspectives. J Dent Res 2014;93:335–345.

See www.StemCellsTM.com for supporting information available online.

Bioactive glass ions as strong enhancers of osteogenic differentiation in human adipose stem cells

Miina Ojansivu [a,b,c,*,1,2,3], Sari Vanhatupa [a,b,c,1,2,3], Leena Björkvik [d,4], Heikki Häkkänen [e,5], Minna Kellomäki [b,f,2,6], Reija Autio [g,7], Janne A. Ihalainen [e,5], Leena Hupa [d,4], Susanna Miettinen [a,b,c,1,2,c]

[a] Adult Stem Cell Research Group, University of Tampere, Tampere, Finland
[b] BioMediTech, University of Tampere and Tampere University of Technology, Tampere, Finland
[c] Science Centre, Tampere University Hospital, Tampere, Finland
[d] Johan Gadolin Process Chemistry Centre, Åbo Akademi University, Turku, Finland
[e] Nanoscience Center, University of Jyväskylä, Jyväskylä, Finland
[f] Biomaterials and Tissue Engineering Group, Department of Electronics and Communications Engineering, Tampere University of Technology, Tampere, Finland
[g] School of Health Sciences, University of Tampere, Tampere, Finland

ARTICLE INFO

ABSTRACT

Bioactive glasses are known for their ability to induce osteogenic differentiation of stem cells. To elucidate the mechanism of the osteoinductivity in more detail, we studied whether ionic extracts prepared from a commercial glass S53P4 and from three experimental glasses (2-06, 1-06 and 3-06) are alone sufficient to induce osteogenic differentiation of human adipose stem cells. Cells were cultured using basic medium or osteogenic medium as extract basis. Our results indicate that cells stay viable in all the glass extracts for the whole culturing period, 14 days. At 14 days the mineralization in osteogenic medium extracts was excessive compared to the control. Parallel to the increased mineralization we observed a decrease in the cell amount. Raman and Laser Induced Breakdown Spectroscopy analyses confirmed that the mineral consisted of calcium phosphates. Consistently, the osteogenic medium extracts also increased osteocalcin production and collagen Type-I accumulation in the extracellular matrix at 13 days. Of the four osteogenic medium extracts, 2-06 and 3-06 induced the best responses of osteogenesis. However, regardless of the enhanced mineral formation, alkaline phosphatase activity was not promoted by the extracts. The osteogenic medium extracts could potentially provide a fast and effective way to differentiate human adipose stem cells in vitro.

© 2015 Acta Materialia Inc. Published by Elsevier Ltd. All rights reserved.

1. Introduction

With the aging population in the Western countries the amount of bone injuries is constantly growing highlighting the need for novel tissue engineering-based treatment solutions which could circumvent the drawbacks of the traditionally used autologous bone grafts (e.g., donor site morbidity, lack of adequate amount and quality of bone). Of the various biomaterials tested for bone tissue engineering applications, bioactive glasses (BaGs), originally described by Hench and coworkers [1], have proven to be especially advantageous due to their strong bonding to bone, biocompatibility and biodegradation (for thorough reviews of BaGs, see Jones et al. [2] and Rahaman et al. [3]). Importantly, BaGs are osteoinductive materials able to stimulate the osteogenic differentiation of stem and progenitor cells without any added chemical supplements [4–7].

Recently, the mechanism of BaG osteoinductivity has evoked interest. It has been observed that also when cells are cultured in media containing ions released from BaGs and having no contact to the BaG surface, osteogenic differentiation is enhanced, implying that the ions from BaG are alone capable of inducing osteogenic

differentiation [8–14]. However, the majority of the studies investigating the effect of BaG ions on osteogenic differentiation have used either osteosarcoma cell lines [15–17] or osteoblasts [10–14,18–21] and currently no knowledge exists about the response of mesenchymal stem cells to the ions dissolved from BaGs. Furthermore, of the various BaG compositions designed for biological applications, only those named as 45S5 [9–13,22], 58S [8,9,18,19], 6P53-b [11,13,22], MBG85 [15] and BG60S [20] have been studied in the context of ionic dissolution products in cell culture. Since the glass composition and dissolution kinetics between the different BaG types vary, the results obtained with a few glasses can by no means be applied to the other BaG compositions. To promote the utilization of the BaG materials in bone tissue engineering, a better understanding of the mechanisms of BaG induced osteogenic differentiation as well as the role of BaG ions in cell responses are required.

S53P4 glass, commercially available as BonAlive®, is known to induce osteogenic differentiation of human ASCs (hASCs) cultured in direct contact with the surface [7] and it has also proven to perform well in clinical settings [23–25]. We therefore wanted to test the performance of this otherwise well-characterized glass type in the context of ionic dissolution. The other three BaG types used in this study (2-06, 1-06 and 3-06) are experimental silica-based glass compositions which have not been characterized in cell culture experiments. However, 1-06 and 3-06 glasses have shown good bone and soft tissue bonding properties in *in vivo* studies [26,27] raising interest in their mechanism of action in cellular level.

In the present study, we hypothesized that ionic extracts dissolved from four different BaG compositions, S53P4, 2-06, 1-06 and 3-06, could stimulate the osteogenic differentiation of hASCs. To examine the validity of our hypothesis, we analyzed the viability, proliferation and osteogenic differentiation of hASCs after culturing the cells in BaG extract media prepared from each glass type using either basic medium (BM) or osteogenic medium (OM) as a base composition. This is the first study in which the BaG ion supplemented BM and OM are systematically compared in their ability to induce osteogenic differentiation. Unlike the other studies conducted thus far with ionic species, we carried out all the experiments in HS supplemented media which represents the natural growth environment of human-originated cells. The use of animal-origin free culture conditions enables the extrapolation of our results to the development of clinical-oriented bone tissue engineering applications.

2. Materials and methods

2.1. Ethics statement

This study was conducted in accordance with the Ethics Committee of the Pirkanmaa Hospital District, Tampere, Finland (R03058). The hASCs were isolated from adipose tissue samples obtained from surgical procedures conducted in the Department of Plastic Surgery, Tampere University Hospital. There were five women donors of age 52 ± 12 years. All the donors gave a written informed consent for the utilization of the adipose tissue samples in research settings.

2.2. Manufacturing bioactive glass granules

Bioactive glasses 2-06, 1-06, 3-06 and S53P4 were prepared from batches of analytical grade reagents Na_2CO_3, K_2CO_3, $CaCO_3$, MgO, $CaHPO_4 \cdot 2H_2O$, and Belgian quartz sand (Sigma–Aldrich, MO, USA). The batches giving 300 g glass were melted in a platinum crucible for 3 h at 1360 °C, cast, annealed, crushed and remelted to ensure homogeneity. The oxide compositions of the glasses S53P4, 2-06, 1-06 and 3-06 are depicted in Table 1. Annealed glass blocks were crushed and sieved to give a 500–1000 µm size range fraction. The crushing was done according to the ISO 719 procedure without milling. After crushing, the granules were washed with acetone in an ultrasound batch at least five times to minimize the fine grained particles attached on their surface. Finally, the acetone was evaporated and the particles were dried at 120 °C.

2.3. Preparation of bioactive glass extracts

The BaG granules (500–1000 µm) to be used in the extract preparation were first disinfected with ethanol (10 min in absolute ethanol +10 min in 70% ethanol) after which they were let to dry at room temperature for 2 h. In order to dissolute ions from the BaG granules 87.5 mg/ml granules were incubated for 24 h at +37 °C in cell culture dishes (diameter 10 cm). The extraction medium contained Dulbecco's Modified Eagle Medium/Ham's Nutrient Mixture F-12 (DMEM/F-12 1:1; Life Technologies, Gibco, Carlsbad, CA, USA) supplemented with 1% antibiotics (100 U/ml penicillin and 0.1 mg/ml streptomycin; Lonza, BioWhittaker, Verviers, Belgium) and 1% L-glutamine (GlutaMAX I; Life Technologies, Gibco). After incubation the extracts were sterile filtered (0.2 µm) and human serum (HS; PAA Laboratories, Pasching, Austria) was added to the concentration of 5%. This medium composition is referred to as basic medium extract (BM extract). In order to obtain osteomedium extracts (OM extracts), BM extracts were supplemented with osteogenic factors (10 mM β-glycerophosphate, 250 µM L-ascorbic acid 2-phosphate and 5 nM dexamethasone). The BaG extracts were freshly made for each 2 week experiment so the maximum storage time of the extracts was 14 days at +4 °C. No visible precipitate was formed during this time. A schematic representation of the BaG extract preparation is shown in Fig. 1.

2.4. Determination of the ion concentrations of the bioactive glass extracts

The ion concentrations of the BaG extracts after 24 h of extraction were determined using inductively coupled plasma optical emission spectrometer (ICP-OES; Optima 5300 DV, Perkin Elmer, Waltham, MA, USA). The extract samples containing 1% antibiotics (100 U/ml penicillin and 0.1 mg/ml streptomycin, Lonza) and 1% L-glutamine (GlutaMAX, Life Technologies) were sterile filtered (0.2 µm) prior to the analysis but neither serum nor the osteogenic supplements were added. The elements analyzed by ICP-OES were sodium ($\lambda = 589.592$ nm), potassium ($\lambda = 766.490$ nm), magnesium ($\lambda = 285.213$ nm), calcium ($\lambda = 317.933$ nm), phosphorus ($\lambda = 213.617$ nm), boron ($\lambda = 249.667$ nm) and silicon ($\lambda = 251.611$ nm). The results of the analysis are depicted in Table 2.

2.5. Adipose stem cell isolation, expansion and culture

The isolation of hASCs was conducted using a mechanical and enzymatic procedure described previously [28,29]. The isolated hASCs were maintained in T-75 polystyrene flasks (Nunc, Roskilde, Denmark) in DMEM/F-12 (Life Technologies) supplemented with 5% HS (PAA Laboratories), 1% L-glutamine (GlutaMAX I, Life Technologies) and 1% antibiotics (100 U/ml penicillin and 0.1 mg/ml streptomycin; Lonza, BioWhittaker). This medium composition will be denoted by control basic medium (BM). When 80–100% confluence was reached hASCs were cryo-preserved in gas-phase nitrogen in freezing solution (HS supplemented with 10% dimethyl sulfoxide; DMSO HybriMax®, Sigma–Aldrich) and thawed when needed for the experiments. The hASCs used in the experiments

Table 1
Compositions of bioactive glasses.

	wt.%						
	Na$_2$O	K$_2$O	MgO	CaO	P$_2$O$_5$	B$_2$O$_3$	SiO$_2$
S53P4	23.0	0.0	0.0	20.0	4.0	0.0	53.0
2-06	12.1	14.0	0.0	19.8	2.5	1.6	50.0
1-06	5.9	12.0	5.3	22.6	4.0	0.2	50.0
3-06	24.6	0.0	0.0	21.6	2.5	1.6	50.0

had strong expression for surface proteins of CD73, CD90 and CD105, whereas the expression of CD3, CD11a, CD14, CD19, CD45, CD80, CD86, HLA-DR, CD34 and CD54 was negative or very low (<15%), verifying the mesenchymal origin of the cells. Cell lines used were in passages 2–4.

For all the experiments the plating density was 400 cells/cm². The cell viability, proliferation, qALP and mineralization analyses were conducted in 24-well plates (Nunc). For immunocytochemical stainings cells were plated into 48-well plates (Nunc). In qRT-PCR and Raman analyses the 6-well format (Nunc) was used. In all, there were 10 different culturing conditions: control BM and control osteogenic medium (OM; BM supplemented with 10 mM β-glycerophosphate, 250 μM L-ascorbic acid 2-phosphate and 5 nM dexamethasone), and BM and OM extracts made from all the four BaG types (S53P4, 2-06, 1-06 and 3-06). During the experiments fresh media was given to the cells twice a week.

2.6. Cell viability

Cell viability in the various culturing conditions at 7 and 14 days was analyzed by live/dead staining (Invitrogen, Life Technologies) as described previously [29]. Briefly, cells were incubated in working solution containing 0.25 μM EthD-1 (stains dead cells red) and 0.5 μM Calcein-AM (stains living cells green) for 30 min. After the incubation, samples were imaged immediately with fluorescence microscope (Olympus, Tokyo, Japan).

2.7. Cell proliferation

Cell proliferation was studied by determining the DNA amount using CyQUANT Cell Proliferation Assay kit (Invitrogen, Life Technologies), according to the manufacturer's protocol. Briefly, at 11 and 14 days time points cells were lysed with 0.1% Triton-X 100 (Sigma–Aldrich) buffer. After one freeze–thaw-cycle (−70 °C), three parallel 20 μl samples of each lysate were pipetted to a 96-well plate (Nunc) and mixed with 180 μl working solution containing CyQUANT GR dye and cell lysis buffer. The fluorescence at 480/520 nm was measured with Victor 1420 Multilabel counter (Wallac, Turku, Finland).

2.8. Alkaline phosphatase activity

Alkaline phosphatase activity (ALP) was determined quantitatively after 11 and 14 days of culture, as previously described [29]. The activity was analyzed from the same Triton-X 100 lysates as the DNA amount. In short, 20 μl of each lysate was pipetted in three parallel samples into the wells of a MicroAmp™ Optical 96-well plate (Applied Biosystems, Life Technologies). In order to initiate the ALP enzyme reaction, 90 μl of working solution containing 1:1 stock substrate solution (p-nitrophenol phosphate) (Sigma–Aldrich) and 1.5 M alkaline buffer solution (2-amino-2-methyl propanol) (Sigma–Aldrich) were added to each well with a multichannel pipette. After 15 min incubation at +37 °C 50 μl of 1 M NaOH (Sigma–Aldrich) was added to the wells to stop the reaction. Finally, the absorbances were measured with Victor 1420 Multilabel counter at 405 nm.

2.9. Mineralization

Mineralization at 11 and 14 days was assessed by Alizarin red S staining, which stains the calcium minerals red. The staining followed a previously described protocol [30]. Briefly, cells were fixed with 70% ethanol for 1 h (−20 °C) and stained with 2% Alizarin red S (pH 4.1–4.3; Sigma–Aldrich) solution for 10 min at room temperature. The excess color was washed away with three consecutive water washes and one wash with 70% ethanol after which the samples were photographed. Finally, the dye was extracted with 100 mM cetylpyridinium chloride (Sigma–Aldrich) in order to quantify the result. After 3.5 h of extraction, the absorbances were measured at 544 nm.
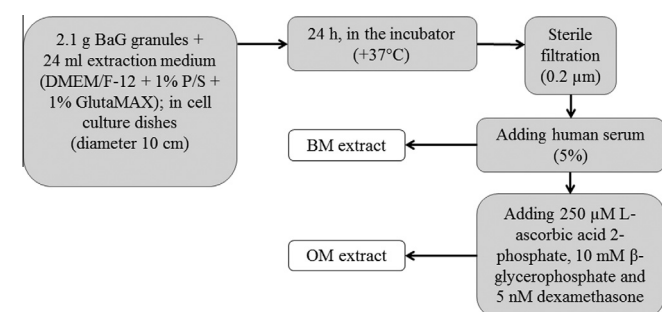
2.10. Quantitative real-time PCR

The relative expression of osteogenic marker genes under the different culturing conditions was studied at 7 and 14 days by quantitative real-time reverse transcription polymerase chain reaction (qRT-PCR) as described previously [30]. In short, the total messenger RNA (mRNA) was isolated from the samples using NucleoSpin RNA II kit (Macherey–Nagel, Düren, Germany) after which the isolated mRNA was reverse transcribed to cDNA with the High-Capacity cDNA Reverse Transcriptase Kit (Applied Biosystems, Life Technologies). The expressions of genes *DLX5*, *OSTERIX* and *RUNX2a* were analyzed and the data were normalized to the expression of housekeeping gene *RPLP0* (human acidic ribosomal phosphoprotein P0). *RPLP0* was chosen because it has been shown to have stable expression in adipose tissue [31,32]. In the calculation of relative expressions a previously described mathematical model was used [33]. The sequences of the primers (Oligomer Oy, Helsinki, Finland) and the accession numbers of the genes studied are presented in Table 3. The qRT-PCR mixture contained 50 ng cDNA, 300 nM forward and reverse primers and Power SYBR® Green PCR Master Mix (Applied Biosystems, Life Technologies). The reactions were conducted and monitored with

Fig. 1. Schematic representation of the BaG extract preparation. BaG = bioactive glass, BM = basic culture medium, OM = osteogenic medium.

Table 2
Ion concentrations of the BaG extracts analyzed by ICP-OES. All concentrations are mg/kg and they were analyzed after 24 h of extraction. The samples contained P/S and GlutaMAX but no serum or osteogenic supplements. (<LOQ = below limit of quantification.)

	Ca	K	Mg	P	Si	Na	B
DMEM/F-12	41	173	18	30	<LOQ	3480	<LOQ
S53P4	115	180	16	<LOQ	61	3760	<LOQ
2-06	153	360	16	<LOQ	53	3730	3.4
1-06	116	243	40	21	52	3620	<LOQ
3-06	131	172	16	<LOQ	56	3750	2.6

Table 3
The Sequences of the primers used in qRT-PCR.

Name	5′-Sequence-3′		Product size (bp)	Accession number
hDLX5	Forward	ACCATCCGTCTCAGGAATCG	75	NM_005221.5
	Reverse	CCCCCGTAGGGCTGTAGTAGT		
hOSTERIX	Forward	TGAGCTGGAGCGTCATGTG	79	AF477981
	Reverse	TCGGGTAAAGCGCTTGGA		
hRPLP0	Forward	AATCTCCAGGGGCACCATT	70	NM_001002
	Reverse	CGCTGGCTCCCACTTTGT		
hRUNX2a	Forward	CTTCATTCGCCTCACAAACAAC	62	NM_001024630.3
	Reverse	TCCTCCTGGAGAAAGTTTGCA		

AbiPrism 7000 Sequence Detection System (Applied Biosystems, Life Technologies) with initial enzyme activation at 95 °C for 10 min, followed by 45 cycles at 95 °C/15 s and 60 °C/60 s.

2.11. Immunocytochemical stainings

The amount and localization of collagen Type-I and osteocalcin was studied after 13 days of culture using immunocytochemical stainings (ICCs). Cells were fixed with 4% paraformaldehyde (PFA) supplemented with 0.2% Triton-X 100 (15 min at RT) and blocked with 1% bovine serum albumin (BSA) for 1 h at +4 °C. The primary antibodies (mouse monoclonal anti-collagen Type-I (dilution 1:2000) and mouse monoclonal anti-osteocalcin (dilution 1:100) (both antibodies produced by Abcam, Cambridge, UK) were diluted in 1% BSA and incubated overnight at +4 °C in slight shaking. After washes, both stainings were treated with the same secondary antibody (donkey anti-mouse alexa fluor 488 IgG, dilution 1:1000; Invitrogen, Life Technologies) for 45 min at RT. In case of the collagen Type-I ICC the actin cytoskeleton was stained with phalloidin-TRITC (dilution 1:500; Sigma–Aldrich) which was incubated simultaneously with the secondary antibody. In both collagen Type-I and osteocalcin ICCs the nuclei were stained with DAPI (dilution 1:2000) during the 3rd wash after the secondary antibody treatment. Imaging with fluorescent microscope (Olympus, Tokyo, Japan) was conducted immediately after staining.

2.12. Raman and Laser Induced Breakdown Spectroscopy

For Raman spectroscopy and Laser Induced Breakdown Spectroscopy (LIBS) cells were cultured in phenol red free medium (DMEM/F-12, +glutamine, −phenol red; Life Technologies, Gibco) since phenol red strongly interferes with Raman. Antibiotics (100 U/ml penicillin and 0.1 mg/ml streptomycin; Lonza, BioWhittaker) were added to 1% and HS (PAA Laboratories) to 5% as before. The BaG extract preparation followed the same procedure as described above. For these analyses cells were cultured only in osteogenic media (control OM and extract OMs) since no mineral formation was observed in extract BMs. The culturing time was extended to 17 days because the slightly different culturing conditions apparently delayed the onset of mineralization. At the time point the samples were washed twice with sterile H_2O and collected from the wells by scraping with 200 µl of sterile H_2O.

The Raman spectra were obtained as described in [34]. A laser excitation wavelength at 532 nm and 100 mW power was focused onto a dried sample with a microscope objective (Zeiss, 10×, 0.30 N.A.) and the backscattered light was collected with the same objective. The scattering was recorded using a CCD camera (Andor) and imaging spectrograph (Princeton Instruments) with entrance slit of 50 µm and grating of 600 grooves/mm. The data accumulation time was 30 s for each sample. From the detected data, the dark noise was subtracted.

The LIBS spectra were obtained using KrF excimer laser (Lambda Physik) for production of plasma and the detection was performed with spectrograph (Acton Research Corp) and ICCD camera (Oriel). A more detailed description of the setup can be found from [35].

2.13. Statistical analyses

Statistical analyses were performed with SPSS Statistics version 22 (IBM, Armonk, NY, USA). All the quantitative data are presented as mean and standard deviation (SD). CyQUANT and qALP analyses were repeated with 5 cell lines with 4 parallel samples in each culturing condition ($n = 20$). Alizarin red S staining was repeated with 4 cell lines with 4 parallel samples in each condition ($n = 16$). Gene expression analyses were conducted with 4 cell lines ($n = 4$). The significance of the effect of BaG extracts on hASC proliferation, ALP activity, mineralization and osteogenic gene expression was evaluated with non-parametric statistics using Mann–Whitney test, which analyses the differences between non-normally distributed data samples. In order to control the familywise error-rate, all the resulted p-values were corrected using Bonferroni adjustment based on the number of the planned comparisons. In the Alizarin red S and CyQUANT analyses we performed 20 planned comparisons within the time point. Further, in qALP analysis, we were additionally interested about differences between the BM and OM conditions of each sample and thus the number of planned comparisons was 25. The result was considered to be statistically significant when the adjusted p-value <0.05.

3. Results

3.1. BaG extracts do not compromise hASC viability but affect proliferation

In order to evaluate the survival of hASCs in the various culturing conditions live/dead staining was conducted after 7 and 14 days of culture. Based on this staining, all the culture conditions supported the viability of the cells as indicated in Fig. 2A. No dead cells were detected in any of the conditions at neither of the time points studied. At 7 days also the cell amount and morphology appeared similar to the control cells in both BM and OM extracts. However, at 14 days very distinct morphological changes were detectable. In S53P4 and 1-06 BM extracts the appearance of the cells did not differ from the control cells, but in 2-06 and 3-06 BM extracts the cells had adopted a small and rounded morphology compared to the spindle-shaped appearance of the control cells. In OM extracts no similar pattern could be seen. However, in OM at 14 days all of the extracts, but most notably 2-06 and 3-06 extracts, decreased the cell amount compared to the OM control. This same phenomenon was also observed in the quantitative CyQUANT cell proliferation assay which indicated that the decrease in cell amount in all the OM extracts at 14 days was also statistically significant (Fig. 2B). At 11 days only 2-06 OM extract decreased the cell amount; otherwise there were no differences in the proliferation between the OM extracts and the OM control at 11 days, which suggests that the OM extracts do not compromise the proliferation of hASCs per se. In case of the BM extracts the situation was opposite: at 14 days, 2-06, 1-06 and 3-06 BM
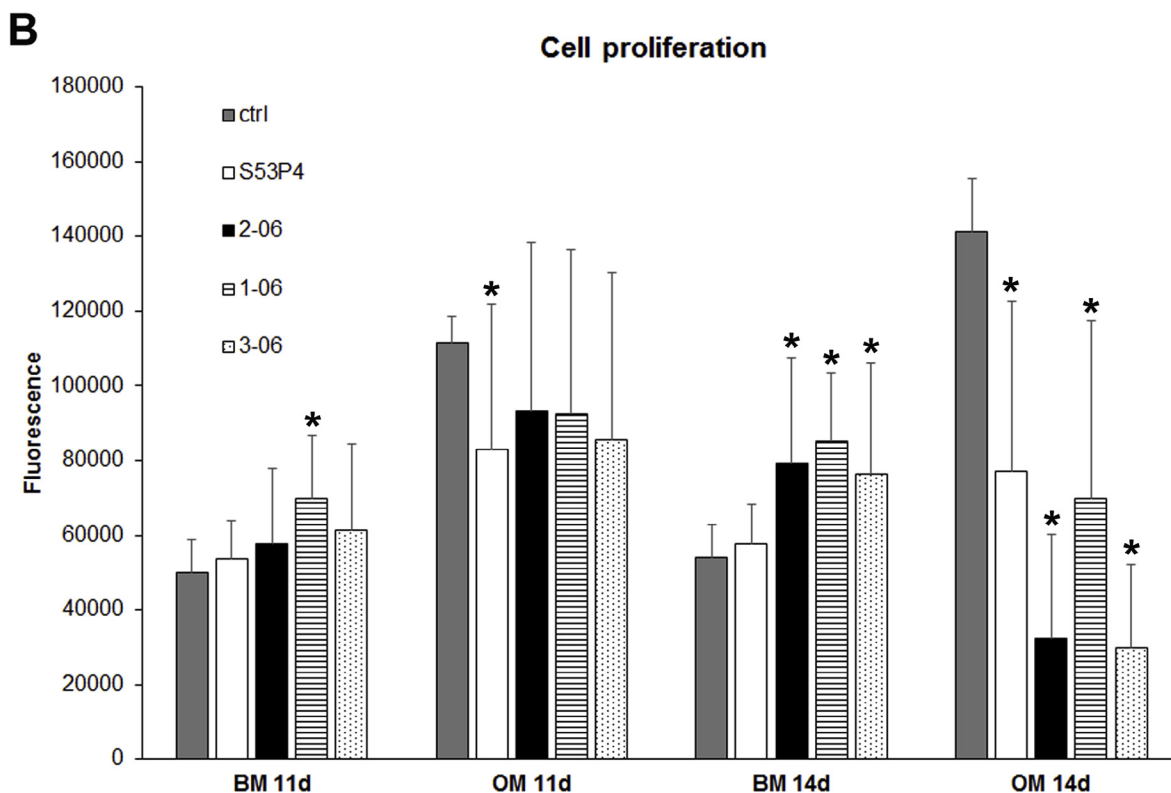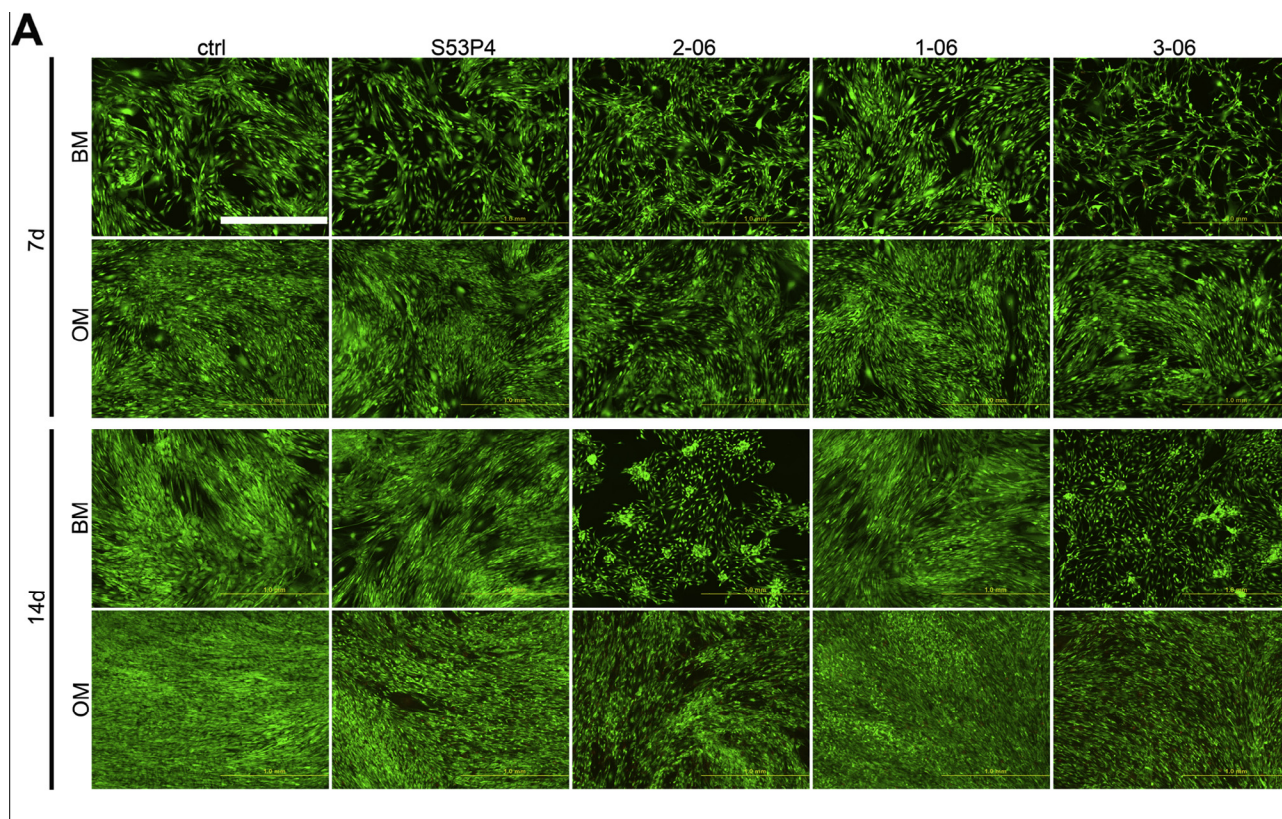
Fig. 2. Viability and proliferation of hASCs cultured on BaG extract media. (A) The viability of hASCs in the BaG extracts and control media was analyzed by live/dead staining (Invitrogen) after 7 and 14 days of culture. Scale bar 1.0 mm. (B) The proliferation of hASCs in BaG extracts was analyzed with CyQUANT Cell Proliferation Assay kit (Invitrogen). At 11 days in 1-06 BM the proliferation exceeded the control BM ($p = 0.00282$) and in 2-06 OM there were less cells compared to the OM control ($p = 0.0123$). At 14 days the cell amount in all the OM extracts had significantly decreased (S53P4: $p = 0.00222$, 2-06: $p < 0.001$, 1-06: $p < 0.001$, 3-06: $p < 0.001$) whereas in 2-06, 1-06 and 3-06 BM extracts there were more cells than in control BM (2-06: $p < 0.001$, 1-06: $p < 0.001$, 3-06: $p = 0.01106$). $n = 20$.

extracts significantly increased the proliferation of hASCs. Thus, even though the morphology of the cells was affected by the 2-06 and 3-06 BM extracts, this change was not accompanied by deterioration in the proliferative capacity.

3.2. Alkaline phosphatase activity is downregulated by the BaG extracts

To study the effect of the BaG extracts on the early osteogenic differentiation of hASCs, we determined the total ALP activity after 11 and 14 days of culture. As depicted in Fig. 3, the total ALP activity of the BaG extract treated samples did not exceed the control values at neither of the time points nor the culturing conditions (BM and OM). On the contrary, the ALP activity at 14 days was significantly decreased by the S53P4, 2-06 and 3-06 OM extract treatment compared to the control OM. At 11 days, however, no significant differences existed between any of the OM extracts and the OM control. In the BM extracts hASCs followed a similar behavioral pattern as in OM extracts. None of the BM extracts raised the total ALP activity above the control level and in case of 2-06 BM extract at 11 days, the ALP activity was significantly decreased.

3.3. BaG extracts change the gene expression profile of osteogenic markers

The gene expression of osteogenic marker genes *RUNX2a*, *OSTERIX* and *DLX5* was studied at time points 7 and 14 days in order to further analyze the osteogenic differentiation of hASCs in response to the BaG extract treatment. First of all, it was observed that there were some differences in the gene expression patterns between the four cell lines studied (data not shown). However, some general trends in the combined gene expression data were possible to identify. In case of *RUNX2a*, all the OM extracts decreased *RUNX2a* expression at both time points (7 and 14 days) (Fig. 4A). In BM condition 2-06, 1-06 and 3-06 extracts increased the *RUNX2a* mRNA levels at 14 days. *OSTERIX* and *DLX5* expressions followed a similar pattern: at 7 days the difference of the BaG extracts to the controls was small in both BM and OM, but at 14 days all the OM extracts (most prominently 3-06)

induced elevation in the gene expression (Fig. 4B and C). In case of *OSTERIX* there was a slight increase also in all the BM extracts at 14 days while *DLX5* was mildly elevated only in 2-06 and 3-06 BM extracts at this later time point.

3.4. Collagen Type-I production and secretion is enhanced in hASCs cultured in OM extracts

As seen in Fig. 5, in all the BM conditions collagen Type-I, the major organic component of the extracellular matrix (ECM) of bone, was still predominantly located intracellularly around the nucleus. The same applied to the hASCs cultured in control OM, even though the amount of collagen Type-I inside the cells was greater than in the BM conditions. In OM extracts the situation was completely different to the aforementioned conditions. Instead of being mainly intracellularly localized, in OM extracts collagen Type-I was secreted to the ECM. Moreover, in S53P4, 2-06 and 3-06 OM extracts the secreted collagen Type-I had initiated fibril-like structure formation implying well-progressed ECM maturation.

Collagen Type-I ICC was combined to the phalloidin-based staining of the actin cytoskeleton. Therefore, in addition to the collagen Type-I production, observations could be made about the effect of the BaG extracts on the cytoskeletal organization. In control samples, as well as in S53P4 and 1-06 BM extracts, the actin cytoskeleton was well-organized and aligned straight actin fibers could be seen inside the cells (Fig. 5). In OM extracts, and most notably in 2-06 and 3-06 BM extracts, the actin cytoskeleton looked disrupted and uneven, lacking the aligned appearance seen in the other samples.

3.5. Osteomedium extracts strongly increase mineral formation

In order to study the later stages of osteogenic differentiation, we conducted Alizarin red S staining at time points 11 and 14 days to see whether the BaG extracts can induce mineralization of hASCs. As seen in Fig. 6A, after 14 days of culture all the OM extracts induced extensive mineral formation compared to the control OM. The difference was significant with all the OM extracts as seen after quantification of the result (Fig. 6B) and in some cases
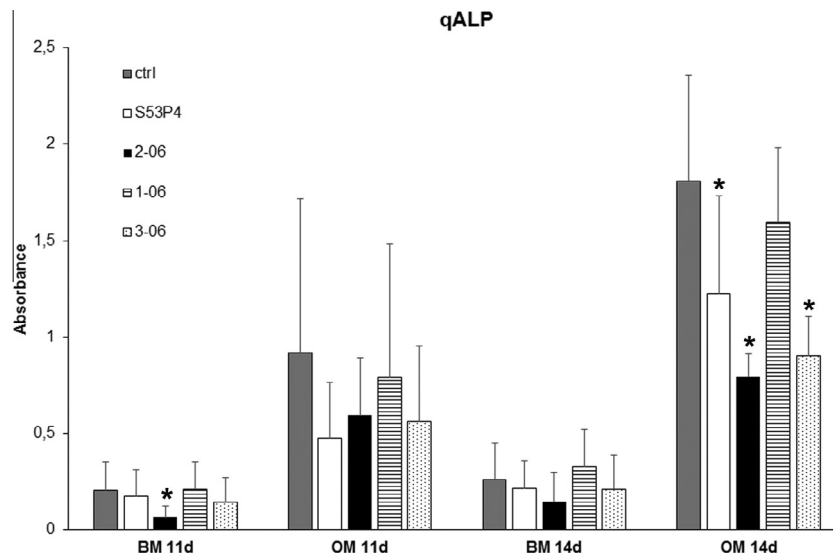
Fig. 3. Effect of BaG extracts on alkaline phosphatase activity. Quantitative ALP activity (qALP) was determined after 11 and 14 days of culture using a colorimetric assay. At 14 days S53P4, 2-06 and 3-06 OM extracts significantly decreased the total ALP activity compared to the control OM (S53P4: $p = 0.03702$, 2-06: $p < 0.001$, 3-06: $p < 0.001$). At 11 days also in 2-06 BM there were significantly less ALP activity than in control BM ($p = 0.00318$). However, each OM extract increased the total ALP activity when compared to the corresponding BM extract at both time points studied (11 days: $p = 0.001975$ (S53P4), $p < 0.001$ (2-06), $p = 0.0073$ (1-06), $p = 0.0026$ (3-06); 14 days: $p < 0.001$ with all the four extracts). $n = 20$.
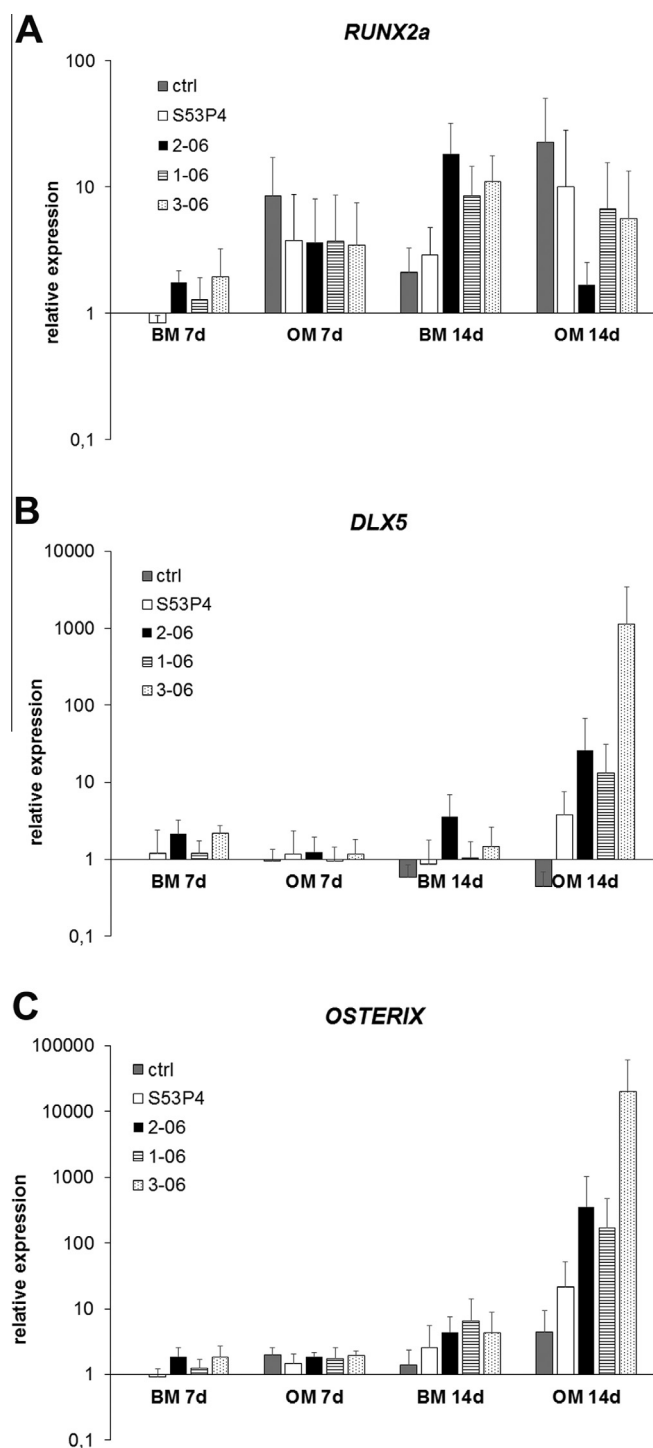
Fig. 4. BaG extract-induced changes in the expression of osteogenic marker genes. The expression of osteogenic marker genes *RUNX2a*, *DLX5* and *OSTERIX* was analyzed by qRT-PCR at 7 and 14 days. *n* = 4.

even one order of magnitude higher than in the control OM. Of the four OM extracts 2-06 and 3-06 turned out to be the best inducers of mineral formation. The onset of mineralization in OM extracts occurred between the 11 and 14 days time points since at 11 days no mineralization could be detected. However, none of the BM conditions could induce mineralization at neither of the time points. The mild staining of 2-06 and 3-06 BM samples seen in Fig. 6A and the elevation in the quantified result in Fig. 6B reflect the presence of a precipitate, which was also present in the blank samples

and was thus not a sign of cell-originated mineral deposition. The precipitate in these two extract types was detectable from the beginning of the culture (see Supplementary Fig. 1S) but was not present in any of the OM extracts or in S53P4 or 1-06 BM extracts. The precipitate formation in 2-06 and 3-06 BM extracts was very likely independent of pH change since there were no apparent differences in the pH between BM and OM extracts neither before or after the application of the media to the cells (see Supplementary Tables 1 and 2).

3.6. Analysis of the minerals in the osteomedium extracts with Raman and LIBS spectroscopies

To study the composition and amount of the mineral formed in the OM extracts, two laser spectroscopic methods, Raman and LIBS spectroscopy, were utilized. Raman spectroscopy reveals information about the molecular vibrations of the system, indicating the type of molecular groups in the sample. Full Raman spectra of the samples are shown in Fig. 7A. Fig. 7B shows the PO_4^{3-} and CO_3^{2-} vibration modes in more detail. The maximum of phosphate band locates at 964 cm^{-1}, which is a characteristic position for hydroxyapatite (HA) [36], shown also in Fig. 7B on top of the Raman spectra of the samples. However, a somewhat broader band does not exclude the presence of other phosphate species, like octacalcium phosphate (OCP) at 957 cm^{-1}, and β-tricalcium phosphate (β-TCP) at 970 cm^{-1} with two maxima at 951 and 971 cm^{-1} (the top most spectrum in Fig. 7B) [37]. On the other hand, the Raman signals of HA precursors, amorphous calcium phosphate (ACP) and dicalcium phosphate dehydrate (DCPD), locating at wavenumber positions of 952 and 985 cm^{-1}, respectively, are less extent in our spectra. At 1008 cm^{-1} a typical signal from phenylalanine (Phe) can be observed. In the region of 1030–1085 cm^{-1} vibrations from PO_4^{3-} and CO_3^{2-} are observed. The control sample shows a peak maximum at 1084 cm^{-1}. In the case of S53P4, 1-06, 2-06 and 3-06 samples the 1084 cm^{-1} band is still present in 1-06 and slightly in the 2-06 sample, but is invisible in the 3-06 and S53P4 samples. In the case of 1-06 also a band at 1064 cm^{-1} can be observed, whereas a maximum of the peak for 2-06, 3-06 and S53P4 samples are at 1078 cm^{-1}. This hints for differences in the CaP mineral species between the samples, but precise assignment of this region to particular chemical compositions is challenging. Fig. 7C shows, however, that a general PO_4^{3-} vibration intensity at around 960 cm^{-1} increases with respect to C–H vibrations representing the amount of organic material (cells) in the samples. This indicates that all the studied samples had a higher PO_4^{3-} content compared to the control sample, implying higher phosphate-containing mineral amounts in these samples.

LIBS measures atomic emission from the laser induced plasma, and therefore measures signals from each element in the sample. Thus, the Raman spectroscopy and LIBS spectroscopy are complementary techniques. In Fig. 8, the overall atomic emission spectrum after laser-induced breakdown is shown. The peaks inform the relative amount of each element present in the samples. In all the OM extract samples there are distinct peaks of Ca and P implying the presence of large amounts of CaP mineral, whereas in the control sample hardly any inorganic material is observed. However, since LIBS can only produce semi-quantitative results at best, the actual amount of the elements in each sample was not tried to quantify based on the LIBS experiments.

3.7. Osteocalcin protein production is induced by the osteomedium extracts

To further assess the later stages of osteogenic differentiation, we studied the amount and localization of osteocalcin, a component of the bone matrix, by ICC technique at time point 13 days.
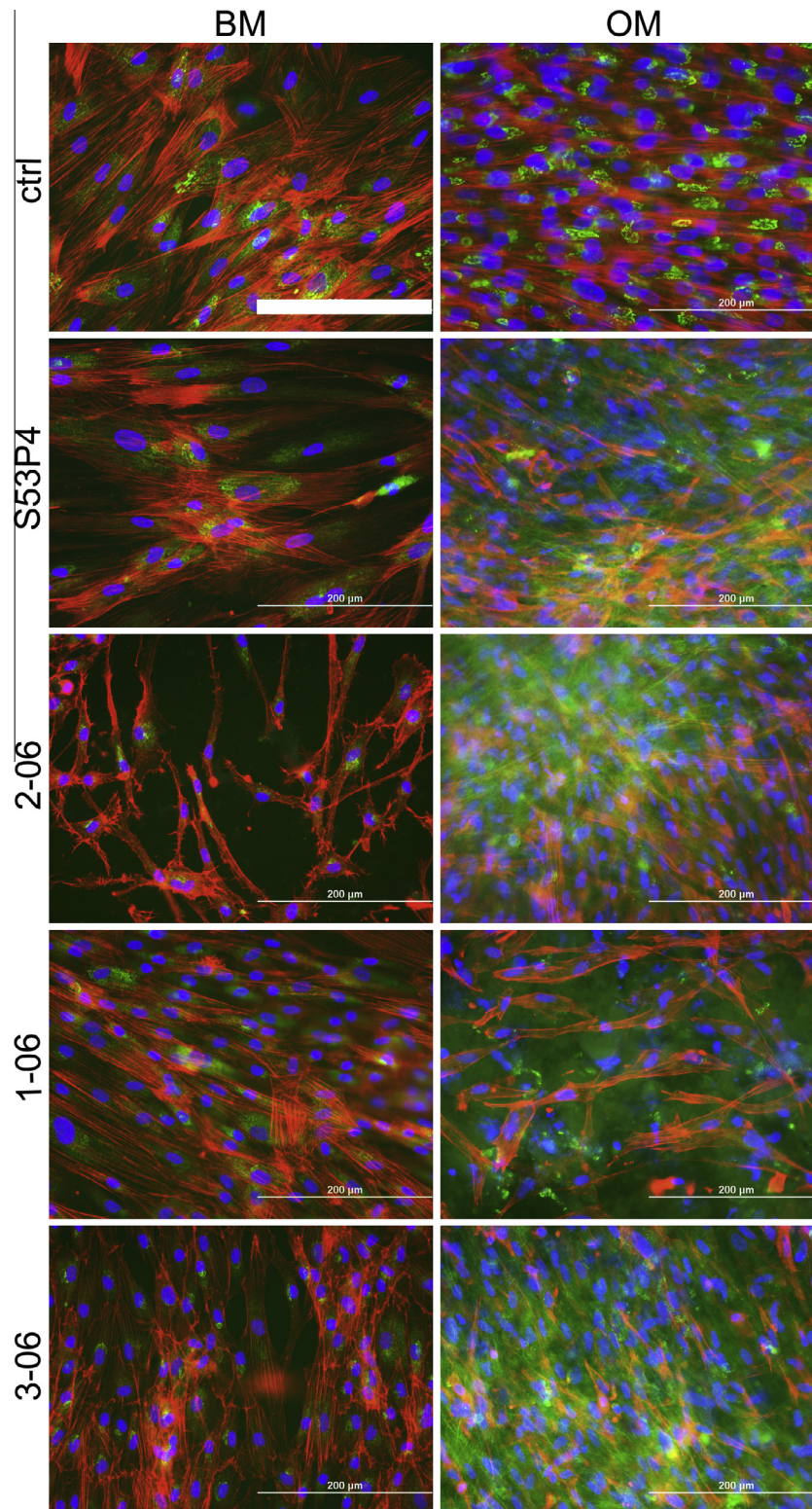
Fig. 5. Effect of BaG extracts on collagen Type-I production and cytoskeletal organization. The amount and localization of collagen Type-I as well as the structure of the actin cytoskeleton were assessed by ICC staining after 13 days of culture. Collagen Type-I is stained green, actin cytoskeleton is stained red with phalloidin and nuclei are stained blue with DAPI. Scale bar 200 μm.

As seen in Fig. 9, none of the BM conditions nor the control OM could induce the production of osteocalcin at this relatively early time point. However, in all the OM extract samples there were large amounts of osteocalcin present indicating the ability of OM extracts to stimulate osteocalcin production from the hASCs.

Majority of the osteocalcin detected seemed to be located in the ECM implying that the hASCs had secreted the protein to be part of the mineralized matrix. In 2-06 and 3-06 OM samples there was also clearly intracellular osteocalcin present. Thus, in these samples the osteocalcin production was still ongoing.
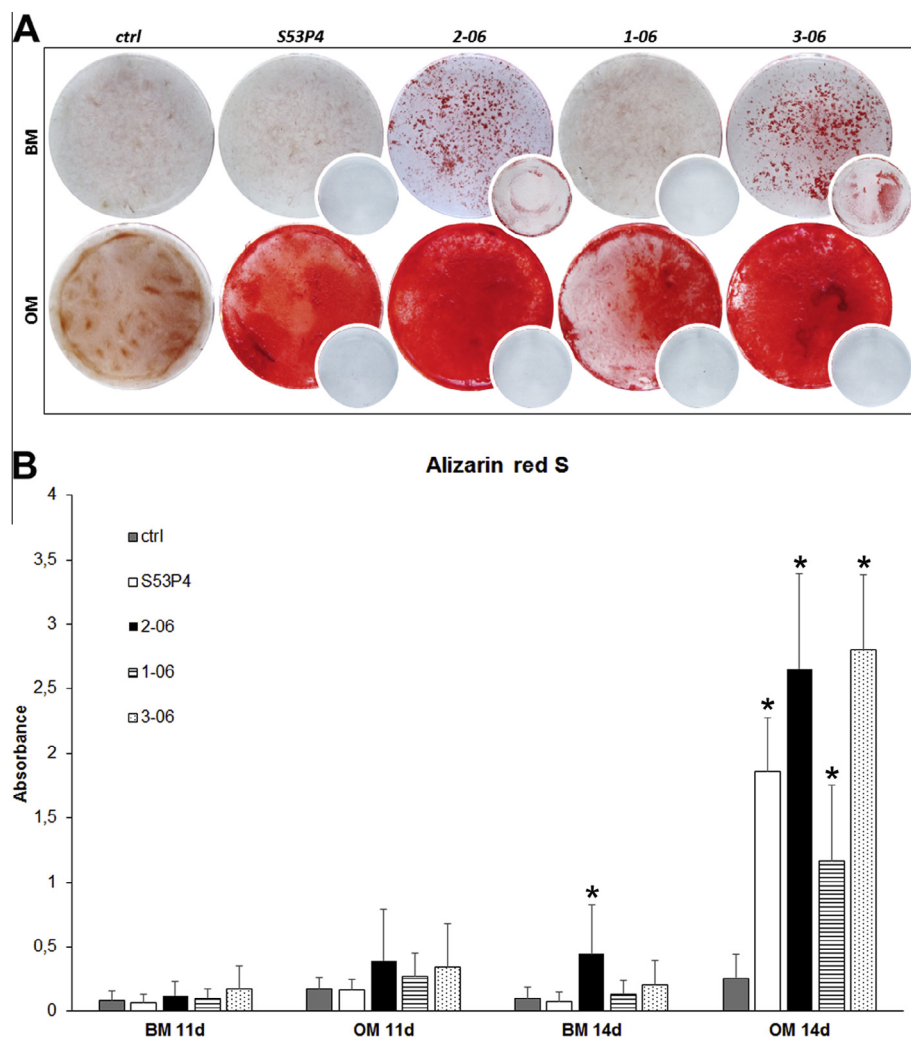
Fig. 6. Mineral formation as a consequence of BaG extract treatment. (A) The mineralization of hASCs in the BaG extract media was studied with Alizarin red S staining after 11 and 14 days of culture. Images of only 14 days samples are shown since at 11 days no mineralization was detected. The small images represent blank samples (media were incubated in the wells for 14 days without any cells). Each image represents a whole well in a 24-well plate (diameter 1.5 cm). (B) Alizarin red S staining was quantified by extracting the color with cetylpyridinium chloride and measuring the absorbances at 544 nm. The difference between control OM and extract OM samples at 14 days was statistically significant (with all the four OM extracts $p < 0.001$). $n = 16$.

4. Discussion

Bioactive glasses have been shown to be advantageous biomaterials for bone tissue engineering due to their inherent ability to induce osteogenic differentiation of stem cells without any additional chemical supplements [4–7]. When considering the mechanisms behind this highly interesting phenomenon it is likely that, the ionic dissolution products from the glasses play a role in the osteogenic cell responses. Unfortunately, the knowledge of the effects of BaG ions on cell behavior, especially on mesenchymal stem cells, is currently still insufficient. This prompted us to elucidate the response of hASCs to ionic extracts prepared from four different BaG types, commercial S53P4 and experimental glass compositions 2-06, 1-06 and 3-06. None of these glass types has been previously studied in the context of cell responses to the ionic dissolution products.

Based on the previous studies suggesting that osteoblasts adopt a more differentiated phenotype when treated with 45S5 dissolution products with no added osteogenic supplements [10,12], we hypothesized that the BM extracts prepared from S53P4, 2-06, 1-06 and 3-06 would induce osteogenic differentiation of hASCs with no OM supplements needed. Against our hypothesis, none of the
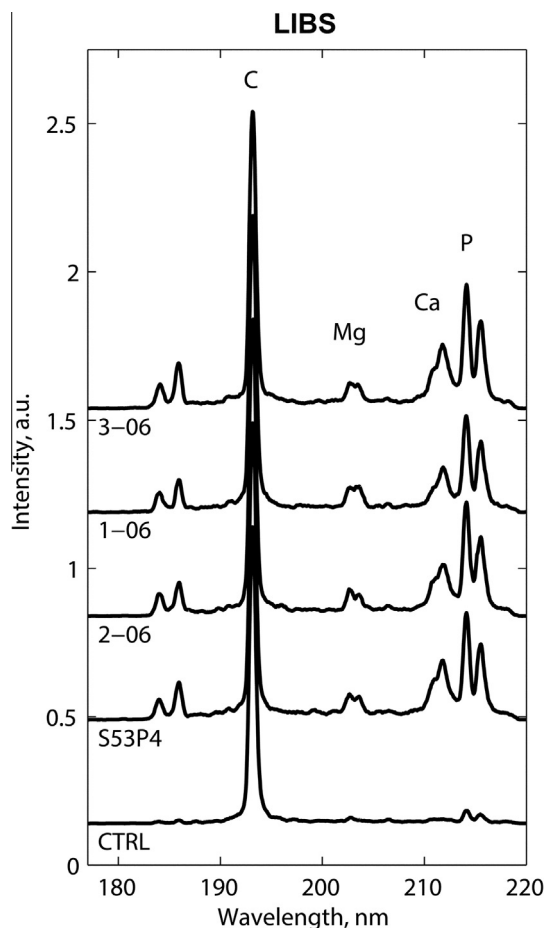
BM extracts used in this study could induce osteogenic differentiation of hASCs. Yet, as determined by mineral formation and osteocalcin and collagen Type-I production, the supplementation of the extracts with ascorbic acid, β-glycerophsophate and dexamethasone made a drastic improvement in the ability of hASCs to shift toward a mature osteoblastic phenotype when compared to the control OM and BM, and BM extracts. The lack of osteogenic differentiation in BM extracts might be at least partly explained by the ionic composition of the extracts. As seen from Table 2, the amount of phosphorous, as a result of specific surface reactions during the ion dissolution phase, was close to zero in all of the four extracts. Therefore in BM extracts there was no source of phosphate, an essential substrate for mineralization, whereas in OM extracts the added β-glycerophosphate and L-ascorbic acid 2-phosphate served as a phosphate sources required for the mineralization to occur. In fact, some previous studies have indicated that the initiation of mineral formation is highly dependent on the presence of β-glycerophosphate [38]. Furthermore, OM extracts increased the production, secretion and organization of collagen Type-I which were not observed in the BM extract treated samples nor the control samples. Formation of mature collagen Type-I containing ECM is a necessary prerequisite for the onset of mineralization since it
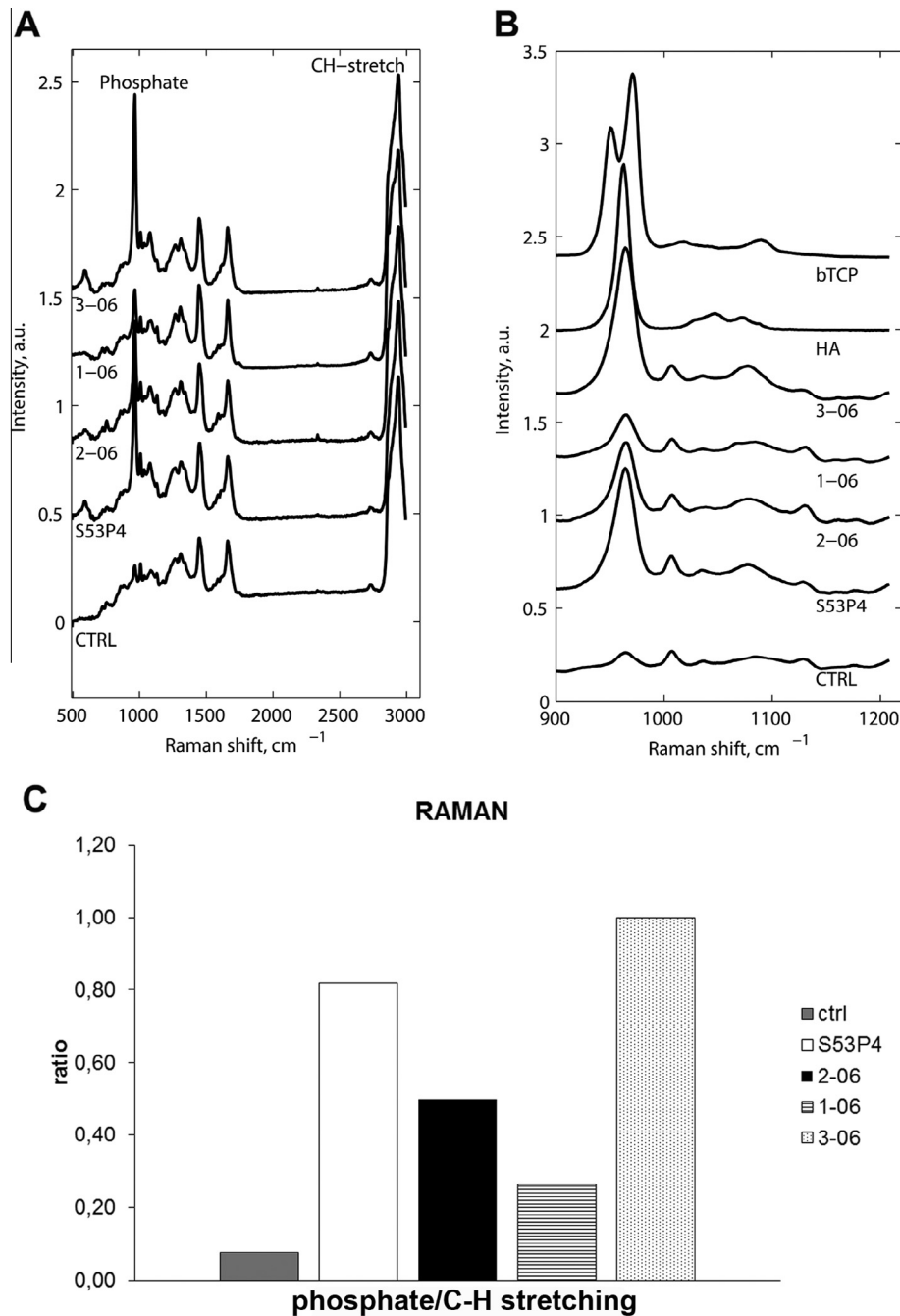
Fig. 7. Analysis of the minerals in OM extract samples by Raman spectroscopy. (A) A complete Raman spectra of the studied samples (control OM, S53P4 OM, 2-06 OM, 1-06 OM and 3-06 OM) at 17 days time point. (B) A Raman spectra of the studied samples, and standard samples of hydroxyapatite (HA) and β-tricalcium phosphate (β-TCP) in the range of PO_4^{3-} and CO_3^{2-} vibration modes. The 960, 1008, 1030, and the broad band between 1060 and 1100 cm^{-1} originate from, PO_4^{3-}, phenylalanine, PO_4^{3-}, and PO_4^{3-} and CO_3^{2-} bands, respectively. (C) The intensity ratio between PO_4^{3-}-vibration and C–H-vibration which reports the amount of phosphate in the samples relative to the amount of organic material (cells).

functions as a platform for mineral crystal growth and can even support spontaneous mineral formation without the need for cellular functions [38–41]. However, in our case the mineralization was not just a spontaneous phenomenon due to the presence of mature collagen since high amounts of osteocalcin were also detected in the OM extracts, implying that the hASCs had adopted a mature osteoblastic phenotype. Parallel to the increased mineralization and osteocalcin production, we observed a decrease in the cell amount which has been also considered a natural part of the bone-like tissue development *in vitro* [42], further supporting the well-progressed and rapid osteogenic differentiation of hASCs in the OM extracts.

The concept of combining BaG ions and OM supplements has been shown to enhance mineralization also with 45S5 and 58S glasses but these media have been only studied with MC3T3-E1 cells, fibroblasts and murine embryonic stem cells, and in neither of these cases the onset of mineralization occurred as early as with our extracts [8,11,22]. On the other hand, there are also opposing results indicating that BaG extract prepared from 58S glass does not significantly affect the osteogenic differentiation of human fetal osteoblasts even when the OM supplements are present [18]. Similar to our results, 45S5 and 6P53-b extracts have been shown to increase osteocalcin and collagen Type-I expression or protein production in MC3T3-E1 and periodontal fibroblast cells

LIBS

Fig. 8. Analysis of the mineralized OM extract samples by LIBS. Atomic emission spectra of control OM and OM extract (S53P4, 2-06, 1-06 and 3-06) samples measured by LIBS at 17 days time point. The elements responsible for each peak are marked. LIBS = Laser Induced Breakdown Spectroscopy.

the OM extract samples while the control OM sample contained only minimal amounts of inorganic material. Unexpectedly, the order of samples in Raman, presented as an inorganic phosphate (PO_4^{3-}) to organic (C–H) ratio slightly differed from the quantified Alizarin red S result. However, in order to diminish the fluorescence background in Raman experiments, the cells, unlike in Alizarin red S analysis, were cultured in phenol red-free media. Since phenol red is known to act as a hormone and affect osteogenic differentiation [43,44], this might explain the differing results between the different analyses. Indeed, the onset of mineralization in phenol red-free medium occurred later and forced us to lengthen the culturing time from 14 to 17 days. Interestingly, based on the spectral differences in Raman, this analysis suggested that in different extracts different CaP species were formed. Thus, the extract treated samples did not only differ in mineral amount but also in mineral composition. However, the determination of the exact mineral species present in the samples necessitates further analyses.

Alkaline phosphatase activity is one of the most widely used markers of osteogenic differentiation in the literature and it is considered a necessary prerequisite for the onset on mineralization e.g., [12,30,45,46]. ALP has been proposed to have a dual role as an initiator of mineral formation: firstly, it generates P_i, a raw material for calcium phosphates, by hydrolyzing various substrates but most importantly, it decreases the level of pyrophosphate, a known inhibitor of mineralization, by catalyzing its degradation [47]. To our surprise, both BM and OM extracts either decreased the total ALP activity or did not affect it at all compared to the controls at both time points (11 and 14 days). This unexpected finding might be explained by the high Ca^{2+} ion concentrations in the extract media, since it has been previously observed that elevated Ca^{2+} inhibits ALP activity in human periodontal ligament cells [48], mouse primary osteoblasts [49], MG63 cells [50] and in human osteoblasts [21], implying that this might be also the case with hASCs. It is also possible that ALP activity reached its peak outside the time points studied (11 and 14 days) and thus remained undetected. For this reason we followed the ALP activity of two hASC lines cultured in 2-06 OM and control OM at time intervals of 2 from 4 days time point until 14 days (Supplementary Fig. 2S). However, this closer inspection did not reveal any peaks in the total ALP activity in extract OM, leading us to the conclusion that the extract treatment does not promote the total ALP activity. Still, in each extract OM the ALP activity was significantly elevated compared to the corresponding BM extract in both time points studied (11 and 14 days). It is therefore likely that this mild elevation in the total ALP activity was enough to support the initiation of the extensive mineralization observed in the extract OMs. One of the goals of the present study was to compare the osteogenesis inducing ability of different extract compositions. Based on Alizarin red S staining and the expression of *DLX5* and *OSTERIX*, as well as visual evaluation of the amount of osteocalcin and collagen Type-I produced, 2-06 and 3-06 OM extracts turned out to be the strongest stimulators of hASC osteogenic differentiation. Consistently, these two extracts contained the largest amount Ca^{2+} which, apart from being a component of biological apatite and thus serving as a raw material for mineralization, has a role in various cell signaling events related to osteogenic differentiation [51–53]. In addition, 2-06 and 3-06 were the only extracts containing traces of boron, which has been previously shown to induce osteogenic differentiation of hBMSCs *in vitro* [54].

Of the four OM extracts 1-06, the only extract containing magnesium, induced the mildest responses of osteogenesis. It has been previously observed that magnesium inhibits the osteogenic differentiation of human osteoblasts [55] which might also partially explain the slightly poorer performance of 1-06 when compared to the other OM extracts. When it comes to silicon, there were no clear differences in the concentrations of the four

in the presence of OM supplements [13,22] whereas other studies with dental pulp cells, human osteoblasts and rat osteoblasts have reported a similar effect with 45S5, 58S and BG60S extracts even without the OM supplements [9,12,20]. Controversial results also exist in regard to proliferation: the proliferation of MC3T3-E1 cells and human osteoblasts was increased when cultured in 45S5 extracts [13,21] whereas in case of Saos-2 cells treated with MBG85 extract the proliferation was decreased [15]. The reason for this large variation and controversial results in the studies conducted with BaG extracts can most probably be explained by the significant differences in the experimental setup between the various studies (different glass compositions, cell types, medium substituents etc.). This makes a proper comparison difficult and highlights the need for standardized protocols.

The BM extracts, especially 2-06 and 3-06, even though lacking an osteogenic response in hASCs, still clearly affected the cells as seen from the morphology and cytoskeletal organization. In these extracts the cells adopted a small and rounded appearance and the cytoskeleton was less oriented than in the control. Furthermore, 2-06, 1-06 and 3-06 extracts increased proliferation as well as expression of *RUNX2a*. A more detailed assessment of the fate of hASCs in BM extracts, however, still requires further elucidation.
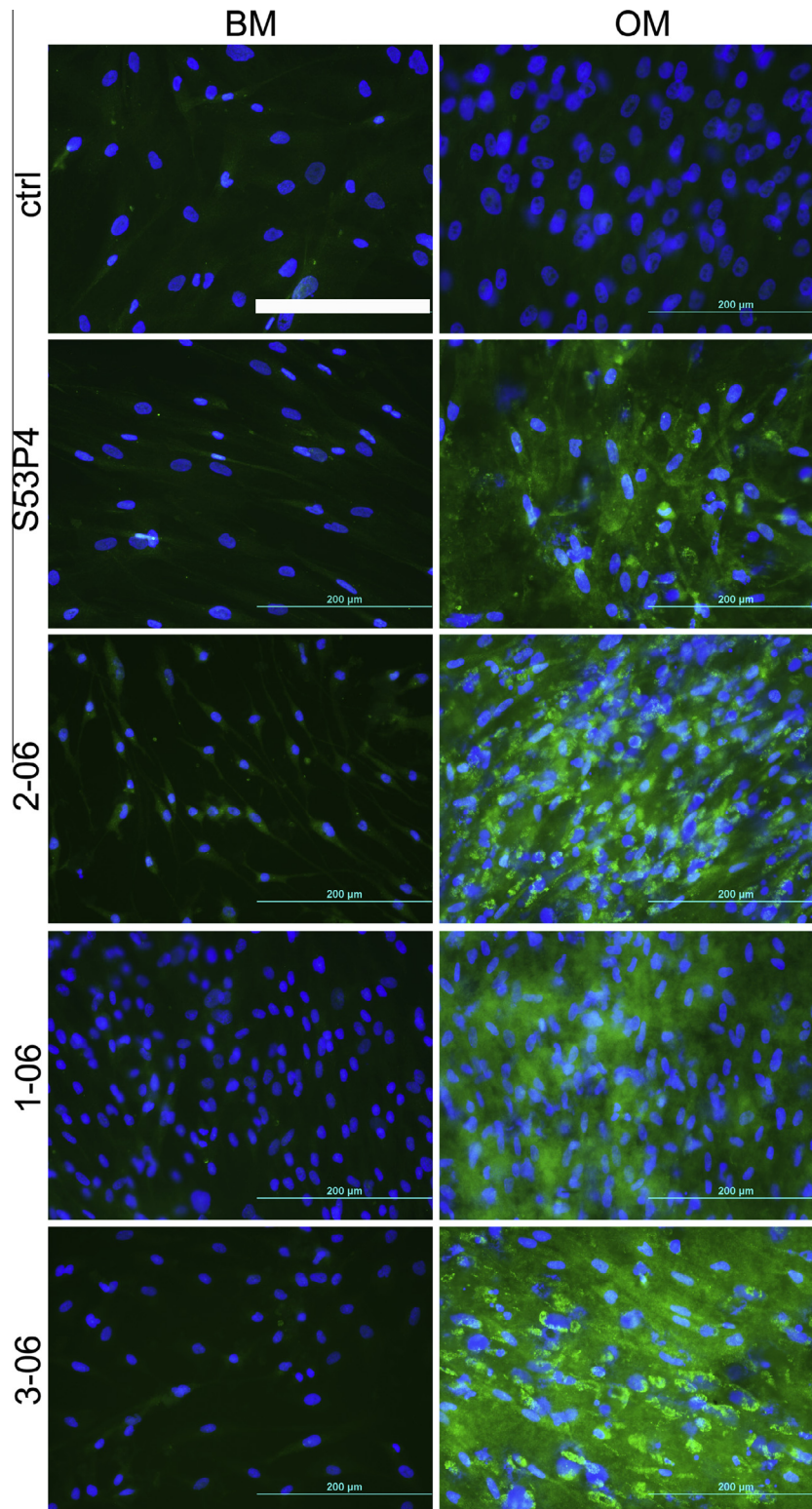
Due to the surprisingly extensive and early mineral formation in the OM extract samples we studied the mineral composition and amount by two representative spectroscopic techniques, namely Raman and LIBS. As expected, these methods confirmed the presence of large amounts of calcium and phosphate/phosphorous in

Fig. 9. Effect of BaG extracts on osteocalcin production. Osteocalcin amount and localization in the cells were studied with ICC staining at 13 days. Osteocalcin is stained green and the nuclei are stained blue with DAPI. Scale bar 200 µm.

extracts which could potentially explain the differences observed at the cellular level. However, silicon supplementation in the cell culture medium has been shown to stimulate osteogenic differentiation of human bone marrow mesenchymal stem cells and MG63 osteosarcoma cells [56,57] implying that silicon might be an essential osteogenesis-inducing component of our extracts as

well. Despite this speculation about the effects of the different ions, we need to keep in mind that the outcome observed is most likely a result of a complex combinatorial effect of different ions rather than an impact of single ionic species. Therefore, even though the specific roles of each individual ion would be interesting to further investigate, a similar outcome might not be

possible to reach by simply supplementing the media by single ionic species.

The excellent performance of all the OM extracts used in this study inevitably encourages to utilize them in various bone tissue engineering applications as effective inducers of osteogenic differentiation of mesenchymal stem cells. For example, augmentation of polymeric scaffolds, mechanically better suitable for bone tissue engineering than pure BaG, with these glass types might lead to an osteogenesis favoring environment as a consequence of BaG ion dissolution. Alternatively, culturing cells on polymeric scaffolds in the extract OM media would potentially be a favorable approach.

5. Conclusions

In the present study, we evaluated the osteogenic response of hASCs to BaG ionic extracts prepared from four different glass types, S53P4, 2-06, 1-06 and 3-06, using either BM or OM as a base medium. Even though none of the BM extracts could stimulate osteogenic differentiation of hASCs, all the OM extracts induced excessive CaP mineral formation with an exceptionally early onset (14 days). Mineralization was accompanied with increased collagen Type-I and osteocalcin production, elevated expression of *OSTERIX* and *DLX5* and a decrease in the cell amount, further confirming the well-progressed differentiation toward a mature osteoblastic phenotype. Of the four studied osteogenic medium extracts, 2-06 and 3-06 were the best inducers of osteogenesis. The OM extracts could potentially provide a fast and effective way to differentiate hASCs *in vitro*, possibly also in 3D environment such as polymeric scaffolds, prior to their implantation into the defect site. However, further studies are still required for the understanding of the molecular level mechanism responsible for this exceptionally good outcome.

Disclosures

The authors report no conflict of interest.

Acknowledgments

Appendix A. Figures with essential color discrimination

Certain figures in this article, particularly Figs. 2, 5,6 and 9 are difficult to interpret in black and white. The full color images can be found in the on-line version, at http://dx.doi.org/10.1016/j.act-bio.2015.04.017.

Appendix B. Supplementary data

Supplementary data associated with this article can be found, in the online version, at http://dx.doi.org/10.1016/j.actbio.2015.04.017.

References

[1] Hench LL, Splinter RJ, Allen WC, Greenlee TK. Bonding mechanisms at the interface of ceramic prosthetic materials. J Biomed Mater Res 1971;5:117–41.

[2] Jones JR. Review of bioactive glass: from Hench to hybrids. Acta Biomater 2013;9:4457–86.

[3] Rahaman MN, Day DE, Bal BS, Fu Q, Jung SB, Bonewald LF, et al. Bioactive glass in tissue engineering. Acta Biomater 2011;7:2355–73.

[4] Bosetti M, Cannas M. The effect of bioactive glasses on bone marrow stromal cells differentiation. Biomaterials 2005;26:3873–9.

[5] Gough JE, Jones JR, Hench LL. Nodule formation and mineralisation of human primary osteoblasts cultured on a porous bioactive glass scaffold. Biomaterials 2004;25:2039–46.

[6] Haimi S, Moimas L, Pirhonen E, Lindroos B, Huhtala H, Räty S, et al. Calcium phosphate surface treatment of bioactive glass causes a delay in early osteogenic differentiation of adipose stem cells. J Biomed Mater Res A 2009;91:540–7.

[7] Waselau M, Patrikoski M, Juntunen M, Kujala K, Kääriäinen M, Kuokkanen H, et al. Effects of bioactive glass S53P4 or beta-tricalcium phosphate and bone morphogenetic protein-2 and bone morphogenetic protein-7 on osteogenic differentiation of human adipose stem cells. J Tissue Eng 2012;3. 2041731412467789.

[8] Bielby RC, Pryce RS, Hench LL, Polak JM. Enhanced derivation of osteogenic cells from murine embryonic stem cells after treatment with ionic dissolution products of 58S bioactive sol–gel glass. Tissue Eng 2005;11:479–88.

[9] Gong W, Huang Z, Dong Y, Gan Y, Li S, Gao X, et al. Ionic extraction of a novel nano-sized bioactive glass enhances differentiation and mineralization of human dental pulp cells. J Endod 2014;40:83–8.

[10] Jell G, Notingher I, Tsigkou O, Notingher P, Polak JM, Hench LL, et al. Bioactive glass-induced osteoblast differentiation: a noninvasive spectroscopic study. J Biomed Mater Res A 2008;86:31–40.

[11] Saffarian Tousi N, Velten MF, Bishop TJ, Leong KK, Barkhordar NS, Marshall GW, et al. Combinatorial effect of Si^{4+}, Ca^{2+}, and Mg^{2+} released from bioactive glasses on osteoblast osteocalcin expression and biomineralization. Mater Sci Eng C Mater Biol Appl 2013;33:2757–65.

[12] Tsigkou O, Jones JR, Polak JM, Stevens MM. Differentiation of fetal osteoblasts and formation of mineralized bone nodules by 45S5 Bioglass conditioned medium in the absence of osteogenic supplements. Biomaterials 2009;30:3542–50.

[13] Varanasi VG, Saiz E, Loomer PM, Ancheta B, Uritani N, Ho SP, et al. Enhanced osteocalcin expression by osteoblast-like cells (MC3T3-E1) exposed to bioactive coating glass (SiO_2–CaO–P_2O_5–MgO–K_2O–Na_2O system) ions. Acta Biomater 2009;5:3536–47.

[14] Xynos ID, Edgar AJ, Buttery LD, Hench LL, Polak JM. Gene-expression profiling of human osteoblasts following treatment with the ionic products of Bioglass 45S5 dissolution. J Biomed Mater Res 2001;55:151–7.

[15] Alcaide M, Portoles P, Lopez-Noriega A, Arcos D, Vallet-Regi M, Portoles MT. Interaction of an ordered mesoporous bioactive glass with osteoblasts, fibroblasts and lymphocytes, demonstrating its biocompatibility as a potential bone graft material. Acta Biomater 2010;6:892–9.

[16] Gentleman E, Stevens MM, Hill RG, Brauer DS. Surface properties and ion release from fluoride-containing bioactive glasses promote osteoblast differentiation and mineralization in vitro. Acta Biomater 2013;9: 5771–9.

[17] Sun J, Wei L, Liu X, Li J, Li B, Wang G, et al. Influences of ionic dissolution products of dicalcium silicate coating on osteoblastic proliferation, differentiation and gene expression. Acta Biomater 2009;5:1284–93.

[18] Christodoulou I, Buttery LD, Saravanapavan P, Tai G, Hench LL, Polak JM. Dose- and time-dependent effect of bioactive gel-glass ionic-dissolution products on human fetal osteoblast-specific gene expression. J Biomed Mater Res B Appl Biomater 2005;74:529–37.

[19] Christodoulou I, Buttery LD, Tai G, Hench LL, Polak JM. Characterization of human fetal osteoblasts by microarray analysis following stimulation with 58S bioactive gel-glass ionic dissolution products. J Biomed Mater Res B Appl Biomater 2006;77:431–46.

[20] Valerio P, Pereira MM, Goes AM, Leite MF. The effect of ionic products from bioactive glass dissolution on osteoblast proliferation and collagen production. Biomaterials 2004;25:2941–8.

[21] Xynos ID, Edgar AJ, Buttery LD, Hench LL, Polak JM. Ionic products of bioactive glass dissolution increase proliferation of human osteoblasts and induce insulin-like growth factor II mRNA expression and protein synthesis. Biochem Biophys Res Commun 2000;276:461–5.

[22] Varanasi VG, Owyoung JB, Saiz E, Marshall SJ, Marshall GW, Loomer PM. The ionic products of bioactive glass particle dissolution enhance periodontal ligament fibroblast osteocalcin expression and enhance early mineralized tissue development. J Biomed Mater Res A 2011;98:177–84.

[23] Lindfors NC, Hyvönen P, Nyyssönen M, Kirjavainen M, Kankare J, Gullichsen E, et al. Bioactive glass S53P4 as bone graft substitute in treatment of osteomyelitis. Bone 2010;47:212–8.

[24] Turunen T, Peltola J, Yli-Urpo A, Happonen RP. Bioactive glass granules as a bone adjunctive material in maxillary sinus floor augmentation. Clin Oral Implants Res 2004;15:135–41.

[25] Sandor GK, Numminen J, Wolff J, Thesleff T, Miettinen A, Tuovinen VJ, et al. Adipose stem cells used to reconstruct 13 cases with cranio-maxillofacial hard-tissue defects. Stem Cells Transl Med 2014;3:530–40.

[26] Madanat R, Moritz N, Vedel E, Svedström E, Hupa HT. Radio-opaque bioactive glass markers for radiostereometric analysis. Acta Biomater 2009;5:3497–505.

[27] Zhao D, Moritz N, Vedel E, Hupa L, Aro HT. Mechanical verification of soft-tissue attachment on bioactive glasses and titanium implants. Acta Biomater 2008;4:1118–22.

[28] Zuk PA, Zhu M, Mizuno H, Huang J, Futrell JW, Katz AJ, et al. Multilineage cells from human adipose tissue: implications for cell-based therapies. Tissue Eng 2001;7:211–28.

[29] Tirkkonen L, Haimi S, Huttunen S, Wolff J, Pirhonen E, Sandor GK, et al. Osteogenic medium is superior to growth factors in differentiation of human adipose stem cells towards bone-forming cells in 3D culture. Eur Cell Mater 2013;25:144–58.

[30] Kyllönen L, Haimi S, Mannerström B, Huhtala H, Rajala KM, Skottman H, et al. Effects of different serum conditions on osteogenic differentiation of human adipose stem cells in vitro. Stem Cell Res Ther 2013;4:17.

[31] Fink T, Lund P, Pilgaard L, Rasmussen JG, Duroux M, Zachar V. Instability of standard PCR reference genes in adipose-derived stem cells during propagation, differentiation and hypoxic exposure. BMC Mol Biol 2008;9:98-2199-9-98.

[32] Gabrielsson BG, Olofsson LE, Sjögren A, Jernås M, Elander A, Lönn M, et al. Evaluation of reference genes for studies of gene expression in human adipose tissue. Obes Res 2005;13:649–52.

[33] Pfaffl MW. A new mathematical model for relative quantification in real-time RT-PCR. Nucleic Acids Res 2001;29:e45.

[34] Ruokola P, Dadu E, Kazmertsuk A, Häkkänen H, Marjomäki V, Ihalainen JA. Raman spectroscopic signatures of echovirus 1 uncoating. J Virol 2014;88:8504–13.

[35] Häkkänen HJ, Korppi-Tommola J. Laser-induced plasma emission spectrometric study of pigments and binders in paper coatings: matrix effects. Anal Chem 1998;70:4724–9.

[36] Penel G, Leroy G, Rey C, Bres E. MicroRaman spectral study of the PO_4 and CO_3 vibrational modes in synthetic and biological apatites. Calcif Tissue Int 1998;63:475–81.

[37] Hung PS, Kuo YC, Chen HG, Chiang HH, Lee OK. Detection of osteogenic differentiation by differential mineralized matrix production in mesenchymal stromal cells by Raman spectroscopy. PLoS ONE 2013;8:e65438.

[38] Fratzl-Zelman N, Fratzl P, Horandner H, Grabner B, Varga F, Ellinger A, et al. Matrix mineralization in MC3T3-E1 cell cultures initiated by beta-glycerophosphate pulse. Bone 1998;23:511–20.

[39] Landis WJ, Silver FH. Mineral deposition in the extracellular matrices of vertebrate tissues: identification of possible apatite nucleation sites on type I collagen. Cells Tissues Organs 2009;189:20–4.

[40] Nudelman F, Pieterse K, George A, Bomans PH, Friedrich H, Brylka LJ, et al. The role of collagen in bone apatite formation in the presence of hydroxyapatite nucleation inhibitors. Nat Mater 2010;9:1004–9.

[41] Wang Y, Azais T, Robin M, Vallee A, Catania C, Legriel P, et al. The predominant role of collagen in the nucleation, growth, structure and orientation of bone apatite. Nat Mater 2012;11:724–33.

[42] Lynch MP, Capparelli C, Stein JL, Stein GS, Lian JB. Apoptosis during bone-like tissue development in vitro. J Cell Biochem 1998;68:31–49.

[43] Ernst M, Schmid C, Froesch ER. Phenol red mimics biological actions of estradiol: enhancement of osteoblast proliferation in vitro and of type I collagen gene expression in bone and uterus of rats in vivo. J Steroid Biochem 1989;33:907–14.

[44] Still K, Reading L, Scutt A. Effects of phenol red on CFU-f differentiation and formation. Calcif Tissue Int 2003;73:173–9.

[45] Haimi S, Suuriniemi N, Haaparanta AM, Ellä V, Lindroos B, Huhtala H, et al. Growth and osteogenic differentiation of adipose stem cells on PLA/bioactive glass and PLA/beta-TCP scaffolds. Tissue Eng Part A 2009;15:1473–80.

[46] Murshed M, Harmey D, Millan JL, McKee MD, Karsenty G. Unique coexpression in osteoblasts of broadly expressed genes accounts for the spatial restriction of ECM mineralization to bone. Genes Dev 2005;19:1093–104.

[47] Millan JL. The role of phosphatases in the initiation of skeletal mineralization. Calcif Tissue Int 2013;93:299–306.

[48] An S, Gao Y, Ling J, Wei X, Xiao Y. Calcium ions promote osteogenic differentiation and mineralization of human dental pulp cells: implications for pulp capping materials. J Mater Sci Mater Med 2012;23:789–95.

[49] Maeno S, Niki Y, Matsumoto H, Morioka H, Yatabe T, Funayama A, et al. The effect of calcium ion concentration on osteoblast viability, proliferation and differentiation in monolayer and 3D culture. Biomaterials 2005;26:4847–55.

[50] Takagishi Y, Kawakami T, Hara Y, Shinkai M, Takezawa T, Nagamune T. Bone-like tissue formation by three-dimensional culture of MG63 osteosarcoma cells in gelatin hydrogels using calcium-enriched medium. Tissue Eng 2006;12:927–37.

[51] Danciu TE, Adam RM, Naruse K, Freeman MR, Hauschka PV. Calcium regulates the PI3K-Akt pathway in stretched osteoblasts. FEBS Lett 2003;536:193–7.

[52] Riddle RC, Taylor AF, Genetos DC, Donahue HJ. MAP kinase and calcium signaling mediate fluid flow-induced human mesenchymal stem cell proliferation. Am J Physiol Cell Physiol 2006;290:C776–84.

[53] Shin MK, Kim MK, Bae YS, Jo I, Lee SJ, Chung CP, et al. A novel collagen-binding peptide promotes osteogenic differentiation via Ca^{2+}/calmodulin-dependent protein kinase II/ERK/AP-1 signaling pathway in human bone marrow-derived mesenchymal stem cells. Cell Signal 2008;20:613–24.

[54] Ying X, Cheng S, Wang W, Lin Z, Chen Q, Zhang W, et al. Effect of boron on osteogenic differentiation of human bone marrow stromal cells. Biol Trace Elem Res 2011;144:306–15.

[55] Leidi M, Dellera F, Mariotti M, Maier JA. High magnesium inhibits human osteoblast differentiation in vitro. Magnes Res 2011;24:1–6.

[56] Reffitt DM, Ogston N, Jugdaohsingh R, Cheung HF, Evans BA, Thompson RP, et al. Orthosilicic acid stimulates collagen type 1 synthesis and osteoblastic differentiation in human osteoblast-like cells in vitro. Bone 2003;32:127–35.

[57] Shie MY, Ding SJ, Chang HC. The role of silicon in osteoblast-like cell proliferation and apoptosis. Acta Biomater 2011;7:2604–14.

The role of mitogen-activated protein kinases and cell attachment mechanism on bioactive glasses S53P4 and 1-06 in glass-induced osteogenic differentiation of human adipose stem cells

Miina Ojansivu[1,2,3*], Sari Vanhatupa[1,2,3], Xiaoju Wang [4], Minna Kellomäki[2,5], Leena Hupa[4] and Susanna Miettinen[1,2,3]

1 *Adult Stem Cell Research Group, University of Tampere, Tampere, Finland*

2 *BioMediTech, University of Tampere and Tampere University of Technology, Tampere, Finland*

3 *Science Centre, Tampere University Hospital, Tampere, Finland*

4 *Johan Gadolin Process Chemistry Centre, Åbo Akademi University, Turku, Finland*

5 *Biomaterials and Tissue Engineering Group, Department of Electronics and Communications Engineering, Tampere University of Technology, Tampere, Finland*

[*]*Corresponding author*

e-mail: miina.ojansivu@uta.fi

tel. +358 50 494 7925

fax: +358 3 3551 8498

Postal address: University of Tampere

> *BMT / Regenerative Medicine / Adult Stem Cell Group*
>
> *33014 University of Tampere*
>
> *FINLAND*

ABSTRACT

Bioactive glasses (BaGs) have been widely utilized in bone tissue engineering but the molecular response of cells to BaGs is poorly understood. To elucidate the mechanism of BaG-induced cell attachment and osteogenic differentiation we cultured human adipose stem cells (hASCs) on silica-based BaG discs S53P4 (BonAlive®) and 1-06 which includes also boron, magnesium and potassium. Both BaGs induced osteogenic differentiation by increasing alkaline phosphatase activity (ALP) and the expression of osteogenic markers *RUNX2a* and *OSTERIX*. Based on ALP, the less reactive 1-06 was a stronger osteoinducer. Regarding the cell attachment, cells cultured on BaGs had enhanced integrinβ1 and vinculin production, and mature focal adhesions were smaller but more dispersed than on polystyrene. Focal adhesion kinase (FAK), extracellular signal-regulated kinase (ERK1/2) and c-Jun N-terminal kinase (JNK)-induced c-Jun phosphorylations were upregulated by glass contact, and BaG-stimulated osteoinduction was significantly reduced by FAK and MAPK inhibitors. Interestingly, the presence of cells increased the concentration of ions released from both glasses, suggesting an active role for the cells as BaG modifiers. Such active and reciprocal interaction between the cells and the BaG surface likely affects the cell attachment mechanisms and thus explains the changes in the attachment and signaling observed on the BaGs.

1. INTRODUCTION

Of the various biomaterials tested for bone tissue engineering applications bioactive glasses (BaGs) have proven to be especially advantageous due to their strong bonding to bone, biocompatibility and biodegradation, but most importantly due to their inherent ability to stimulate the osteogenic differentiation of stem and progenitor cells [1,2]. Of the different BaG compositions S53P4, commercially available as BonAlive®, is known to induce osteogenic differentiation *in vitro* [3], and to support bone formation in *in vivo* models [4,5] as well as in clinical settings [6-8]. In addition to the well-known glass formulations, novel glass compositions are being constantly developed to further improve the glass properties. One interesting experimental glass type is 1-06, which contains potassium, magnesium and boron in addition to the traditional sodium, calcium, phosphorous and silica. 1-06 can be hot-worked, e.g. using the foam replica method, to highly porous amorphous scaffolds for bone tissue engineering [9]. Unlike 1-06, S53P4 partly crystallizes in thermal treatments during the scaffold manufacture which may affect its bioactivity [10]. In our previous study we observed that ionic extract prepared from 1-06 glass induced a strong osteogenic response in human adipose stem cells (hASCs) [11]. 1-06 has also shown good bone tissue bonding *in vivo* [12] but otherwise the behavior of this experimental glass in biological settings remains largely unknown.

When considering bone tissue engineering in which the cells are typically combined with a biomaterial structure, it would be important to understand how the cell functions in response to biomaterial contacts are guided by different signaling pathways. Despite the vast amount of studies conducted with BaGs very little is currently known about the cell signaling events related to the BaG-induced cellular responses. Au and coworkers [13] observed fluctuation in the gene expression levels of mitogen-activated protein kinases (MAPKs) in MG-63 osteosarcoma cell line cultured on Consil® Bioglass® particles and two other studies reported activation of focal adhesion kinase (FAK) and MAPKs in human dental pulp cells in contact with either BaG nanoparticles containing polycaprolactone-gelatin matrices or α-tricalcium phosphate cement combined with zinc-containing BaG [14,15]. However, in these studies the activation of the signaling proteins was not linked to the osteogenic response and, since the BaGs were part of composites, the effect induced solely by BaGs is impossible to distinguish.

Anchorage-dependent cells attach on the growth surface via transmembrane integrins which are composed of two glycoprotein subunits, the α chain and the β chain, noncovalently bound to each other [16]. Integrins form the core of the cell adhesion sites called focal adhesions (FAs) which connect the extracellular matrix (ECM) to the cytoskeleton and initiate several intracellular signaling cascades [17]. Since the integrins lack enzymatic activity, the cell attachment initiated integrin-mediated signal transmission relies primarily on non-receptor protein tyrosine kinases which associate with the cytoplasmic tails of the integrins. The most notable of these protein kinases is FAK which regulates various cellular processes ranging from migration, survival and cell cycle control to differentiation [18]. With respect to the osteogenic differentiation it has been observed that natural ECM simulating collagen-I and laminin surfaces support osteogenic differentiation of mesenchymal stem cells and osteoblastic cells via FAK-extracellular signal-regulated kinase (ERK1/2) signaling route [19-24]. Furthermore, elevated FAK activation has been observed in cells cultured on osteogenesis-supporting bioceramic materials [14,15,25,26].

Apart from being an important player in the cell attachment-induced signaling cascades downstream of FAK, ERK1/2, which forms one of the three major groups of MAPKs, is regulated by a variety of other stimuli including growth factors and cytokines [27]. Several studies have indicated the important role of ERK1/2 in the osteogenic differentiation induced solely by chemical supplements [28-30], although there is also evidence of ERK1/2 being a negative regulator of osteogenesis [31,32]. In addition to ERK1/2, p38 and c-Jun N-terminal kinases (JNKs), which form the two remaining groups of MAPKs, have been also tightly connected to the regulation of osteogenic differentiation. Both of them have been shown to be involved in the cell attachment-related signaling cascades [33,34] but as with ERK1/2, are important players in the osteogenic differentiation induced also by chemical stimuli [35-37].

In the present study we hypothesized that cell attachment on the BaG surface plays a role in the BaG-induced osteogenic differentiation of hASCs, and FAK and MAPKs have a distinct function in the glass-induced bone formation. We were also interested to compare the effect of two different glass compositions, S53P4 and 1-06, on the cellular responses. To examine the validity of our hypothesis we analyzed the attachment of hASCs on S53P4 and 1-06 glasses using vinculin immunocytochemistry and immunoblotting of vinculin and integrinβ1. Furthermore, we studied the fibronectin and collagen-I ECM formation on the glass surfaces by immunocytochemistry. To determine the roles of FAK and MAPKs in the glass-induced osteogenic differentiation we cultured hASCs in the presence of inhibitor molecules for FAK, ERK, p38 or JNK, after which we analyzed the activity of alkaline phosphatase (ALP) and the expression of osteogenic marker genes *RUNX2a* and *OSTERIX*. In addition, the activation of FAK and MAPKs in response to the glass contact was studied. Finally, the dissolution and surface structures of the BaGs were analyzed with inductively coupled plasma optical emission spectrometry (ICP-OES) and scanning electron microscopy (SEM), respectively, to shed light on the underlying material properties affecting the cell attachment and signaling. To our knowledge this is the first study analyzing the effect of S53P4 and 1-06 glasses on the cell attachment and osteogenic differentiation related cell signaling mechanisms.

2. MATERIALS AND METHODS

2.1. Ethics statement

This study was conducted in accordance with the Ethics Committee of the Pirkanmaa Hospital District, Tampere, Finland (R15161). The hASCs were isolated from adipose tissue samples obtained from surgical procedures conducted in the Department of Plastic Surgery, Tampere University

Hospital. There were five female donors of age 56±8 years. All the donors gave a written informed consent for the utilization of the adipose tissue samples in the research settings.

2.2. Manufacturing of the BaG discs and their pretreatment

Bioactive glasses S53P4 and 1-06 were prepared from batches of analytical grade reagents Na_2CO_3, K_2CO_3, $CaCO_3$, MgO, $CaHPO_4 \cdot 2H_2O$, and Belgian quartz sand (Sigma-Aldrich, St. Louis, MO, USA). The batches were melted in a platinum crucible for 3 h at 1360°C, cast, annealed, crushed and remelted to ensure homogeneity. The melt was cast to give rods which after annealing were cut into circular discs, the thickness of which was 1.5 mm and the diameter either 14 mm or 10 mm. Both sides of the discs were polished with water on polishing paper (of which the finest was 2500 grit) until a mirror-like finish was achieved. The oxide compositions of the glasses S53P4 and 1-06 are depicted in Table 1.

Prior to the cell culture the discs were disinfected with ethanol treatment (10 min in absolute ethanol + 10 min in 70 % ethanol) after which they were let dry at room temperature for approximately 2 h. The discs were pre-incubated in cell culture medium in the cell culture incubator over night before plating the cells.

Table 1. *The nominal compositions of S53P4 and 1-06 BaGs.*

	wt-%						
	Na_2O	K_2O	MgO	CaO	P_2O_5	B_2O_3	SiO_2
S53P4	23.0	0.0	0.0	20.0	4.0	0.0	53.0
1-06	5.9	12.0	5.3	22.6	4.0	0.2	50.0

2.3. Adipose stem cell isolation and culture

The isolation of hASCs was conducted using a mechanical and enzymatic procedure described previously [38,39]. The isolated hASCs were maintained in T-75 polystyrene flasks (Nunc, Thermo Fisher Scientific, Waltham, MA, USA) in DMEM/F-12 (Life Technologies, Thermo Fisher Scientific) supplemented with 5 % human serum (HS; PAA Laboratories, GE Healthcare, Little Chalfont, Buckinghamshire, United Kingdom), 1 % L-glutamine (GlutaMAX I, Life Technologies, Thermo Fisher Scientific) and 1 % antibiotics (100 U/ml penicillin and 0.1 mg/ml streptomycin; BioWittaker, Lonza, Basel, Switzerland). When 80-100 % confluence was reached hASCs were cryo-preserved in gas-phase nitrogen in freezing solution (HS supplemented with 10 % dimethyl sulfoxide; DMSO HybriMax®, Sigma-Aldrich) and thawed when needed for the experiments. To verify the mesenchymal origin of the hASCs the surface marker expression was determined at passage 1 with flow cytometric analysis (fluorescence-activated cell sorting) (FACSAria, Becton, Dickinson and Company, Erembodegem, Belgium) as previously described [40]. The hASCs used in the experiments had strong expression for surface markers of CD73, CD90 and CD105, whereas the expression of CD3, CD11a, CD14, CD19, CD45, CD80, CD86, HLA-DR, CD34 and CD54 was very low (Supplementary Table S2). The surface marker expression thus confirmed the mesenchymal origin of the hASCs. Cells used in the experiments were in passages 2-5.

In the quantitative experiments (cell proliferation, alkaline phosphatase (ALP) activity and gene expression), SEM analysis and in the immunocytochemical stainings the plating density was 1100 cells/cm^2. In Western blot studies the plating density was 11 100 cells/cm^2. Immunocytochemical stainings were conducted in 48-well format (Nunc, Thermo Fisher Scientific) with 10 mm discs whereas all the other analyses were performed in 24-well format (Nunc, Thermo Fisher, Scientific)

with 14 mm discs. Control cells were grown in cell culture plastic (polystyrene). The medium composition in the experiments was otherwise the same as the maintenance medium described above except that the human serum was treated with dextran coated charcoal (Sigma-Aldrich; according to the manufacturer's protocol) to strip hormones from the serum to better observe the BaG-induced signaling events. No osteogenic medium supplements were used in order to detect the differentiation caused solely by the BaGs. FAK and MAPKs were inhibited during the culture using specific inhibitors listed in Table 2. The functionality of the inhibitors was tested with immunoblotting (Supplementary Figure S1). Furthermore, we also proved that none of the culture conditions severely compromised the cell viability or proliferation (Supplementary Figure S2) which enabled further studies with the BaGs and the indicated inhibitor concentrations. The media was changed twice a week.

Table 2. *The inhibitors used in the experiments.*

Target	Inhibitor	Final concentration	Manufacturer
FAK	PF562271	2 µM	Selleckchem, Munich, Germany
MEK-ERK	PD98059	60 µM	Calbiochem, Merck Millipore, Billerica, MA, USA
p38	SB202190	2 µM	Calbiochem, Merck Millipore
JNK	SP600125	10 µM	Selleckchem

2.4. Alkaline phosphatase activity

To analyze the osteogenic differentiation, ALP activity was determined quantitatively at 21d, as previously described [11,39]. This relatively late time point for ALP analysis was chosen based on our optimization which indicates that the osteogenic differentiation induced by the BaGs without any osteogenic supplements occurs later than in the osteogenic medium (data not shown). Briefly, the cells were lysed with 0.1 % Triton-X 100 (Sigma-Aldrich) buffer. 20 µl of each lysate was pipetted into the wells of a MicroAmp^{TM} Optical 96-well plate (Applied Biosystems, Thermo Fisher Scientific). 90 µl of working solution containing 1:1 stock substrate solution (p-nitrophenol phosphate; Sigma-Aldrich) and 1.5 M alkaline buffer solution (2-amino-2-methyl propanol; Sigma-Aldrich) was added to each well. After 15 min incubation at +37°C, 50 µl of 1 M NaOH (Sigma-Aldrich) was added to the wells to stop the reaction. Finally, the absorbances were measured with Victor 1420 Multilabel counter (Wallac, Turku, Finland) at 405 nm. The ALP results were normalized by dividing with the CyQUANT (Invitrogen, Thermo Fisher Scientific) cell proliferation values (Supplementary Figure S2B).

2.5. Quantitative real-time PCR

The relative expression of osteogenic marker genes was studied at 14d and 21d by quantitative real-time reverse transcription polymerase chain reaction (qRT-PCR) as described previously [41]. Briefly, the total messenger RNA (mRNA) was isolated from the samples using NucleoSpin RNA II kit (Macherey-Nagel, Düren, Germany) after which the isolated mRNA was reverse transcribed to cDNA with the High-Capacity cDNA Reverse Transcriptase Kit (Applied Biosystems, Thermo Fisher Scientific). The expressions of genes *OSTERIX* and *RUNX2a* were analyzed and the data was normalized to the expression of housekeeping gene *RPLP0* (human acidic ribosomal phosphoprotein

P0). *RPLP0* was used because it is known to have stable expression in adipose tissue [42,43]. In the calculation of relative expressions a previously described mathematical model was used [44]. The sequences of the primers (Oligomer Oy, Helsinki, Finland) and the accession numbers of the genes studied are depicted in Table 3. The qRT-PCR mixture contained 50 ng cDNA, 300 nM forward and reverse primers, and Power SYBR® Green PCR Master Mix (Applied Biosystems, Thermo Fisher Scientific). The reactions were conducted and monitored with AbiPrism 7000 Sequence Detection System (Applied Biosystems, Thermo Fisher Scientific) with initial enzyme activation at 95°C for 10 min, followed by 45 cycles at 95°C/15 s and 60°C/60 s.

Table 3. *The sequences of the primers used in qRT-PCR.*

Name	5'-Sequence-3'	Product size (bp)	Accession Number
OSTERIX	forward TGAGCTGGAGCGTCATGTG	79	AF477981
	reverse TCGGGTAAAGCGCTTGGA		
RPLP0	forward AATCTCCAGGGGCACCATT	70	NM_001002
	reverse CGCTGGCTCCCACTTTGT		
RUNX2a	forward CTTCATTCGCCTCACAAACAAC	62	NM_001024630.3
	reverse TCCTCCTGGAGAAAGTTTGCA		

2.6. Immunocytochemical stainings
The amount and localization of cell attachment related vinculin as well as extracellular matrix (ECM) proteins collagen-I and fibronectin were studied using immunocytochemical stainings (ICCs). Vinculin was stained at time points 24h and 7d, and collagen-I and fibronectin at 21d. The staining of actin cytoskeleton and nuclei were combined to all the stainings. Briefly, cells were fixed with 4 % paraformaldehyde (PFA, Sigma-Aldrich) supplemented with 0.2 % Triton-X 100 (Sigma-Aldrich) for 15 min at RT, and blocked with 1 % bovine serum albumin (BSA, Sigma-Aldrich) for 1-3 h at +4C°. The following primary antibodies were used: vinculin ABfinity™ recombinant rabbit antibody (Life Technologies, Thermo Fisher Scientific; dilution 1:100), mouse monoclonal anti-collagen-I (Abcam, Cambridge, United Kingdom; dilution 1:2000) and mouse anti-human fibronectin (Merck Millipore; dilution 1:200). The primary antibodies were diluted in 1 % BSA and incubated overnight at +4C°. After washes, the secondary antibodies (donkey anti-rabbit Alexa fluor 488 IgG for vinculin and donkey anti-mouse IgG for collagen-I and fibronectin; both from Invitrogen, Thermo Fisher Scientific; dilution 1:800) were applied together with actin-staining phalloidin-TRITC (Sigma-Aldrich, dilution 1:500) and incubated for 45 min at RT. The nuclei were stained with 4', 6-diamidino-2-phenylindole (DAPI; Molecular Probes, Thermo Fisher Scientific; dilution 1:2000) during the 3rd wash after the secondary antibody treatment. After the staining the discs were mounted between an objective glass and a cover slip with Shandon Immu-Mount (Thermo Fisher Scientific). The bottoms of the control wells were detached with a hollow punch and a hammer and mounted the same way as the discs. Samples were imaged with Zeiss Axio Scope.A1 fluorescence microscope (Oberkochen, Germany).

2.7. SDS-PAGE and immunoblotting

The effect of the BaGs on the activation of FAK and MAPKs and the production of vinculin and integrinβ1 was analyzed by SDS-PAGE and immunoblotting at 6h, 3d and 7d. At each time point hASCs were lysed directly into 2xLaemmli sample buffer (20% glycerol, 6% SDS, 50 mM Tris pH 6.8, 10% β-mercaptoethanol). After the electrophoretic separation the proteins were transferred to polyvinylidene fluoride membrane (PVDF; GE Healthcare). Followed by blocking with non-fat milk the target proteins were probed with the following primary antibodies: rabbit monoclonal anti-pFAK (Cell Signaling Technology, Danvers, MA, USA; dilution 1:1000), rabbit monoclonal anti-pERK (p-p44/42; Cell Signaling Technology; dilution 1:2000), rabbit monoclonal anti-p-p38 (Cell Signaling Technology; dilution 1:1000), rabbit polyclonal anti-p-c-Jun (Ser 63) (Cell Signaling Technology; dilution 1:1000), mouse monoclonal anti-integrinβ1 (Santa Cruz Biotechnology, Dallas, Texas, USA; dilution 1:500), vinculin ABfinity^{TM} recombinant rabbit antibody (Life Technologies, Thermo Fisher Scientific; dilution 1:500) and mouse monoclonal anti-β-actin (Santa Cruz Biotechnology; dilution 1:2000), followed by HRP-conjugated secondary antibodies goat anti-mouse IgG (Santa Cruz Biotechnology; dilution 1:2000) and anti-rabbit IgG (Cell Signaling Technology; dilution 1:2000). Proteins were detected with enhanced chemiluminescence detection reagent (ECL; GE Healthcare) using ChemiDoc MP imaging system (Bio-Rad, Hercules, CA, USA). To analyze the basal levels of non-phosphorylated proteins, the blots were stripped and blotted again by the following antibodies: rabbit anti-FAK (Cell Signaling Technology; dilution 1:1000), rabbit polyclonal anti-ERK2 (Santa Cruz Biotechnology; dilution 1:500), rabbit polyclonal anti-p38α (Santa Cruz Biotechnology; dilution 1:100) and rabbit monoclonal anti-c-Jun (Cell Signaling Technology; dilution 1:1000), followed by HRP-conjugated secondary antibody treatment and ECL detection as before.

2.8. Analysis of the glass surfaces by SEM

To study the changes in the BaG material surfaces and in the cell morphology on BaGs during the experimental period, the discs were characterized with SEM (Leo 1530, combined with energy dispersive X-ray analysis (EDXA, UltraDry, Thermo Fisher Scientific)) after 24h, 3d, 7d and 21d of culture. The surfaces were analyzed from both blank and cell containing samples. At each time point samples were washed once with PBS and fixed with 5% glutaraldehyde (Sigma-Aldrich) for 1h at RT. After fixation samples were stored in deionized water at +4°C and prior to imaging they were dehydrated by ascending series of ethanol (10%, 20%, 40%, 60%, 80% and 99.5%), followed by air drying.

2.9. Ionic release from the BaG discs

In order to determine the ionic release profile of the BaGs, the medium sample was collected at the time of each medium change and the ion concentrations in the culture medium were determined by ICP-OES (Optima 5300 DV, Perkin Elmer, Waltham, MA, USA). The concentrations were determined from both blank and cell containing samples. The elements analyzed by ICP-OES were sodium (k = 589.592 nm), potassium (k = 766.490 nm), magnesium (k = 285.213 nm), calcium (k = 317.933 nm), phosphorus (k = 213.617 nm), boron (k = 249.667 nm) and silicon (k = 251.611 nm).

2.10. Statistical analysis

Statistical analyses were performed with SPSS Statistics version 22 (IBM, Armonk, NY, USA). All the quantitative data is presented as mean and standard deviation (SD). Alkaline phosphatase activity analyses were repeated with 4 hASC donor lines with 3 parallel samples in each culturing condition (n=12). Gene expression analyses were conducted with 4 hASC donor lines (n=4). The significance of the effect of BaG discs and the various inhibitors on hASC ALP activity and osteogenic gene

expression was evaluated with non-parametric statistics using Kruskal-Wallis one-way analysis of variance by ranks to determine whether there are significant differences within a data set, and with Mann-Whitney post hoc test to analyze the specific sample pairs for significant differences. These non-parametric tests were chosen because, due to the relatively small n, it would have been unjustified to assume the data to be normally distributed. In order to control the familywise error-rate, all the resulted p-values were corrected using Bonferroni adjustment based on the number of planned comparisons. The result was considered to be statistically significant when the adjusted p-value < 0.05.

3. RESULTS

3.1. Osteogenic differentiation and ECM production of hASCs on BaGs

Bioactive glasses are known for their ability to induce osteogenic differentiation of stem and progenitor cells in the absence of chemical osteogenesis stimulating substances [3,45-47]. To find out whether this was the case also with our glasses and culture conditions we determined ALP activity at 21d and the expression of osteogenic marker genes *RUNX2a* and *OSTERIX* at 14d and 21d. As indicated in Figure 1A both glass types significantly increased ALP activity when compared to the control polystyrene (p<0.001). Furthermore, 1-06 induced a significantly higher ALP activity than S53P4 (p<0.001). Both glass types also increased the expression of *RUNX2a* (Figure 1B) and *OSTERIX* (Figure 1C) at both time points studied, confirming their ability to induce osteogenic differentiation of hASCs. In gene expression level, however, there were no clear differences between the two glass types.

In order to study the effect of the BaGs on the ECM production we conducted immunocytochemical staining of fibronectin and collagen-I at 21d time point. As seen in Figure 1D, cells produced high amounts of fibronectin independent of the culturing material. The production of collagen-I, on the other hand, was clearly upregulated on both of the glasses when compared to the polystyrene control (Figure 1E). However, the location of collagen-I was still clearly inside the cells implying that no mature collagen-I containing ECM had not yet been formed.

3.2. Cell attachment and actin cytoskeleton on BaGs

To analyze the attachment of the hASCs on the BaGs immunoblotting of integrinβ1 and vinculin as well as immunocytochemical staining of vinculin, combined with phalloidin staining of actin cytoskeleton and DAPI staining of the nuclei, were conducted. At 3d and 7d time points both glasses clearly increased the integrinβ1 production as seen in Figure 2A. In a similar manner the production of vinculin was also increased at all the studied time points when compared to the polystyrene control. Interestingly, the inhibition of FAK did not seem to affect the production of these proteins. Immunocytochemistry of vinculin, a marker of mature focal adhesions, revealed that at 24h time point no strong and clear focal adhesion sites were formed in either of the materials; instead, small adhesion sites were spread throughout the cells (Figure 2B). At 7d, on the other hand, typical looking pronounced focal adhesions were formed at the end of the actin fibers in control polystyrene material. On both of the glasses, on the contrary, focal adhesions were still small and covered most of the cell area (Figure 2C). On the glasses the inhibition of FAK did not seem to have notable effect on vinculin amount or arrangement but on control polystyrene at 7d it hindered the formation of large focal adhesion sites.

In addition to focal adhesions the glasses also had an effect on the organization of the actin cytoskeleton. Specifically, the actin fibers of the cells grown on BaGs were not as stretched or aligned as the fibers of the control cells grown on polystyrene. Moreover, at some spots the actin fibers on

BaGs were even partially disorganized. The inhibition of FAK did not affect the appearance of the fibers on the glasses but on control polystyrene it made the fibers even thicker than without the inhibitor.

3.3. The role of FAK in the BaG-induced osteogenic differentiation of hASCs

In order to further analyze the mechanisms of cell attachment on BaGs the activation of FAK was studied with Western blot analysis at 6h, 3d and 7d time points (Figure 3A). At 6h and 3d no activation of FAK could be detected in either of the conditions but at 7d FAK activation was upregulated by both glass types. Interestingly, also the basal levels of FAK were increased implying that the glasses had an effect on the protein production as well. The FAK inhibitor successfully diminished the activation of FAK. In order to evaluate the role of FAK in the BaG-induced osteogenic differentiation we analyzed ALP activity and the expression of osteogenic marker genes in the presence of FAK inhibitor. As seen in Figure 3B, the inhibition of FAK significantly decreased the normalized ALP activity on both glasses (p<0.001) and the effect was considerably large. A similar trend was seen in the expression of *RUNX2a* and *OSTERIX* (Figure 3C and 3D, respectively).

3.4. The role of ERK1/2 in the BaG-induced osteogenic differentiation of hASCs

Similar to the analyses of FAK we also determined the activation of MAPKs on the glasses and their role in the BaG-induced osteogenic differentiation using specific inhibitors. When it comes to ERK1/2, after the initial decreasing effect of the glasses on the ERK1/2 activation at 6h both glasses actually increased the activation of ERK1/2 at later time points (3d and 7d; Figure 4A). Unlike with FAK, the basal levels of ERK2 were not affected by the glasses. In the presence of FAK inhibition the activity of ERK1/2 was diminished on both glasses. As with the inhibition of FAK, the inhibition of ERK1/2 significantly decreased the normalized ALP activity on both glasses (p<0.001) (Figure 4B). The same effect was seen also in the expression of osteogenic marker genes *RUNX2a* and *OSTERIX* (Figure 4C and 4D, respectively).

3.5. The role of p38 in the BaG-induced osteogenic differentiation of hASCs

With respect to the activation of p38, we observed a similar initial decrease in the activity of p38 on the glasses at 6h time point as with ERK1/2 (Figure 5A). However, unlike with ERK1/2 and FAK, no upregulation of p38 activity was observed in either of the time points studied. On the contrary, 1-06 glass actually decreased the activation of p38 at 3d and the activation was even more downregulated in the presence of FAK inhibitor. S53P4 glass, on the other hand, seemed to have no clear effect on the p38 activation when compared to the control. With respect to the osteogenic differentiation, the inhibition of p38 significantly decreased the normalized ALP activity (S53P4: p=0.024, 1-06: p=0.035) (Figure 5B) but the extent of the decrease was much smaller than with FAK and ERK1/2 inhibitors. Furthermore, on *RUNX2a* and *OSTERIX* expression the inhibition of p38 seemed to have no effect at all (Figure 5C and 5D, respectively).

3.6. The role of JNK in the BaG-induced osteogenic differentiation of hASCs

Since the phosphorylation levels of JNK were extremely low in all the studied conditions and time points (Supplementary Figure S3) we decided to analyze the activation of c-Jun, a downstream target of JNK [48], in order to assess the effect of the BaGs on the JNK function. As seen in Figure 6A, the activation of c-Jun was upregulated by both of the glasses at 3d and 7d time points. Unlike with ERK1/2 and p38, however, the inhibition of FAK had no clear effect on the c-Jun activation. Both glasses also increased the basal levels of c-Jun at all the time points studied. In case of the osteogenic differentiation, the inhibition of JNK significantly decreased the normalized ALP activity on both

glass types (S53P4: p=0.007, 1-06: p<0.001) (Figure 6B) and a similar decreasing effect was also seen in the expression of *RUNX2a* and *OSTERIX* (Figure 6C and 6D, respectively).

3.7. Morphological changes of the BaG surfaces and the attached cells during the cell culture
Due to their reactivity, both S53P4 and 1-06 are subjected to dissolution during the cell culture period which results in changes in the BaG surface structures. Such changes in the surfaces can also explain changes in the cell attachment mode and signaling events related to it. The submicron scale morphological features of both glasses at 24h, 3d and 7d time points are displayed in the SEM images of Figure 7, which depicts both blank and cell-containing samples. S53P4 and 1-06 showed distinctive topographic features after immersion in the cell culture medium. When compared to 1-06, the submicron scale structure of the S53P4 surface was more porous and coral-like, and became denser as the immersion time increased. In contrast to S53P4, 1-06 showed a more compact and granule-like appearance, suggesting a lower rate of reactivity. The blank samples and the cell-containing samples, however, did not differ greatly on the surface morphology.

In order to visualize the attachment of the cells with respect to the surface, the cell-containing samples were imaged and displayed in smaller magnifications with SEM at time points 24h, 3d, 7d and 21d (Figure 8). The cells adopted a less flat appearance on the glasses when compared to the polystyrene control, but they were still equally distributed on all the surfaces. Notably, after 7d of culture the cells attached on S53P4 glass were covered with a precipitate of CaP which is formed in the glass dissolution. Such a precipitate was not observed on the cells on 1-06 glass. At 21d the entire glass surface was totally covered by a heavy cell layer and therefore no single cells could be distinguished.

3.8. Ionic release of the BaGs in the cell culture medium
Ionic release serves as an indicator of glass dissolution behavior and is also a key factor regulating cell responses. In order to determine the ionic concentrations and their variations in the culture media during the whole culture period, ICP-OES analysis was conducted to medium samples collected at each medium change. Figure 9 shows the ion concentrations of Ca, P, K, Mg, B, Si and Na in the culture medium at different time points for both S53P4 and 1-06 glasses, as well as for the control medium, for both cell-containing and blank samples. 1-06 glass contains K, Mg and B in its formulation and therefore elevated concentrations of these ions were only detected in 1-06 samples. The release of Si reached saturation during the pre-incubation of the glasses and the concentration of Si kept constant throughout the cell culture period for both S53P4 and 1-06. No Si was present in the control medium. With respect to the dissolution of Ca and P, a more profound depletion of Ca and P concentrations was seen in the S53P4 samples than in the 1-06 samples. This suggests that more CaP was most likely precipitated onto S53P4 than onto 1-06. The P concentrations in the S53P4 samples dropped even below the detection limit in 10d and 14d samples suggesting that all the P was consumed in the CaP layer formation. This is in agreement with the heavy CaP precipitate on the hASCs on S53P4 glass after a culture period of 7d (Figure 8) and the formation of visible CaP layers after 7d or more prolonged culture periods as seen in the cross-section images of S53P4 discs (Supplementary Figures S4 and S5). This data further supports the higher reactivity of S53P4 when compared to 1-06.

As part of the ionic dissolution studies we were also interested in to compare the corresponding blank and cell-containing samples with respect to the glass dissolution behavior. In 1-06 blank samples, the concentrations of K and Mg reached an approximately constant level of 300 and 50 mg/L after the 24h pre-incubation (0d), respectively, which correlated well with the ratio of the corresponding oxides in the glass formulation (Figure 9). In contrast to the blank samples, in 1-06

cell-containing samples K and Mg concentrations kept increasing during the culture period. Similarly, the release of B, though low in reality, was slightly higher from the cell-containing 1-06 samples than from the blanks samples. Notably, higher Ca concentrations were also seen in the cell-containing samples than in the blank samples with both S53P4 and 1-06. In polystyrene control samples, however, the presence of cells had no increasing effect on the ionic concentrations. It therefore seems evident that the presence of cells on the glass surface has a profound effect on the BaG dissolution behavior.

4. DISCUSSION

Bioactive glasses are widely studied biomaterials with long history in biomedical research and clinical applications. However, despite the vast amount of research conducted with BaGs, the molecular level effects of these materials on cells have not been studied. This prompted us to examine the signaling response of hASCs cultured on S53P4 and 1-06 BaG discs.

As expected based on a previous study conducted by us [3], S53P4 glass induced the osteogenic differentiation of hASCs as determined by ALP activity, *RUNX2a* and *OSTERIX* expression as well as collagen-I production. Interestingly, 1-06 induced significantly higher ALP activity than S53P4, implying that this experimental glass is a more effective inducer of osteogenic differentiation. This might be explained by the compositional differences between the glasses. 1-06, unlike S53P4, contains minuscule amount of boron (around 1 mg/L boron was found in the culture medium of the 1-06 cell-containing samples throughout the whole culturing period), which has been shown to be advantageous for the osteogenic differentiation of human bone marrow mesenchymal stem cells (hBMSCs) *in vitro* in similar concentrations as detected in our culture [49]. Differentiation responses are also affected by the structure of the material surface which differs between the glasses due to differences in reactivity. We observed that S53P4 reacts more rapidly than 1-06 in the cell culture medium, which resulted in thick CaP precipitate on S53P4 glass observed with SEM after 7d of culture. The precipitate, which covers the cells, might have a negative effect on the differentiation and thus possibly partly explains the poorer performance of S53P4 when compared to 1-06.

Cells adhere to the growth substrate via dynamic multiprotein structures called focal adhesions which link the ECM proteins to the actin cytoskeleton via transmembrane integrins [17]. Mature focal adhesions, characterized by the presence of vinculin, are strong attachment sites located primarily at the end of the actin fibers, and surfaces which induce the formation of such prominent focal adhesions have been shown to support osteogenic differentiation of stem and progenitor cells, whereas small and evenly spread focal adhesions have been linked to a decrease osteogenic and an increase in adipogenic commitment [50-52]. In contrast to these previous studies conducted with various surface topographies and micropatterns created in polystyrene and polyimide, our results indicated that the mature focal adhesions of hASCs on S53P4 and 1-06 were small and evenly dispersed despite the evidently osteogenic potential of both BaG types. It is therefore likely that the size and distribution of the focal adhesions as such do not dictate the cell fate exclusively. Furthermore, the amount of both integrinβ1 and vinculin increased on the glasses, suggesting that even though the focal adhesions were small the vast amount of them might make the attachment considerably strong. Pennisi and co-workers showed that on roughened platinum surface fibroblasts adopt a similar elongated shape with small focal adhesions as hASCs on BaGs [53] implying that the surface roughness of the glasses might be an underlying factor for the atypical attachment of the cells on BaGs. Moreover, due to the glass reactivity, the surfaces of the BaGs are very dynamic which might hinder the stable cell attachment with prominent focal adhesions but still stimulate the attachment mechanisms by inducing

the formation of the vast amount of smaller and possibly less stable attachment sites observed on the glasses.

The focal adhesions are tightly connected to the underlying actin cytoskeleton which changes dynamically in response to focal adhesion mediated forces and thus regulates cell behavior [54]. During osteogenic differentiation actin cytoskeleton typically turns from organized parallel actin fibers to a robust network of reorganized stress fibers with a more random patterning [55,56]. A reorganized actin network was observed on both of the glasses whereas on control polystyrene the actin cytoskeleton was still more organized. This was in line with the observed osteogenic differentiation on the glasses. At some spots the actin fibers on BaGs seemed even slightly disorganized but this might be due to the rapid cytoskeletal changes associated with osteogenic differentiation. Rodriguez and co-workers found that actin integrity is important at the initial steps of differentiation, but later on rapid changes occur in actin monomer/polymer equilibrium enabling the cytoskeletal reorganization [55]. Furthermore, it is also possible that the reactivity of the glass surfaces is reflected to the cytoskeletal organization via the atypical focal adhesion sites and therefore partly explains the actin arrangement.

Focal adhesion kinase is associated with the cytoplasmic parts of the integrin β chains and due to its catalytic activity it relies messages from the cell attachment site to the interior of the cell, thus affecting cell behavior in response to cell attachment [18,57,58]. We observed that FAK was activated on both of the glasses when compared to the polystyrene control at 7d and the inhibition of FAK significantly decreased the BaG-induced osteogenic differentiation. These observations were well in line with the previous studies highlighting the crucial role of FAK in cell attachment related osteogenic differentiation [19-24], although in these studies the attachment was analyzed on ECM protein surfaces like collagen-I, which in our cells was not secreted from the cells on the BaGs. We also looked into the fibronectin ECM but it was equally abundant on all the materials and therefore could not explain the signaling differences between the BaGs and polystyrene. However, there might have been differences in the amount of other ECM proteins not analyzed in this study. It is also possible that the abundance of the focal adhesion sites on the glasses is reflected to enhanced attachment-mediated signaling events which we observe as an increased FAK activation.

Similar to FAK, both BaGs stimulated the activation of ERK1/2 at 3d and 7d, and upon ERK1/2 inhibition the BaG-induced osteogenic differentiation was greatly diminished. As expected based on the previous studies [19-24], the inhibition of FAK affected negatively the ERK1/2 activation on BaGs suggesting that ERK1/2 acts downstream of FAK also in the BaG-induced osteogenic differentiation. However, the inhibition of FAK could not totally abolish the activation of ERK1/2 implying that there are also attachment-independent stimuli acting via ERK1/2. ERK1/2 is known to be activated in osteogenic medium (OM) induced osteogenic differentiation [28-30] but since we did not have OM in our cultures this cannot explain the residual ERK1/2 activation under FAK inhibition. Related to osteogenesis ERK1/2 activation has been also shown to be upregulated by silicon ions [62] and akermanite extract [63] suggesting that the ionic dissolution products from the BaGs might cause signaling responses leading to ERK1/2 activation.

p38 and JNK are typically thought to be activated mainly by cytokines and various environmental stresses but there are also evidence that they play a role as regulators of osteogenic differentiation [33-37]. We observed the activation of JNK downstream target c-Jun at 3d and 7d in response to both BaGs. Furthermore, the osteogenic differentiation of hASCs on BaGs was significantly decreased after treatment with JNK inhibitor, implying to a significant role for JNK in the BaG-induced osteogenesis. However, the levels of p-c-Jun were not clearly affected by the FAK inhibition suggesting that JNK activation is stimulated by mechanisms not related to the FAK

activation. JNK is known to be involved in the signaling mechanisms of bone morphogenetic protein 2 (BMP-2), Wnt3a and NEL-like protein 1 (NELL-1) [65-67] which might be differentially produced in cells cultured on BaGs and thus affect JNK signaling.

With respect to p38, no BaG-induced activation was observed and even though the ALP was significantly decreased upon p38 inhibition the magnitude of the decrease was lower than with the other inhibitors. Furthermore, in *RUNX2a* and *OSTERIX* gene expression levels no changes were detected in response to p38 inhibition. Although several studies suggest an important role for 38 in both cell attachment and chemical stimuli induced osteogenesis [34,36,37], there are also studies which could not demonstrate any role for 38 in the osteogenic differentiation of mesenchymal stem cells [52,68]. Thus the role of p38 in the BaG-induced osteogenic differentiation might not simply be as significant as that of FAK, ERK1/2 and JNK or, alternatively, the cells have a mechanism to compensate for the loss of p38 activity. Interestingly, while S53P4 did not affect the p38 activation after 3d or 7d of culture, 1-06 decreased the activation at 3d and when combined with the FAK inhibition the p-p38 was totally abolished. This was the only clear difference in the signaling response between the two glasses and therefore one might speculate whether it could explain the better ALP inducing ability of 1-06. However, since the inhibition of p38 in general was not advantageous for the ALP activity this might not be an underlying factor explaining the different behavior of the glasses.

The decreasing effect of FAK and MAPK inhibitions on osteogenic differentiation of hASCs lead us to speculate whether these molecules function as switches of cell fate in BaG-induced cellular responses. Based on the literature it is known that the inhibition of FAK, ERK and JNK, while decreasing osteogenesis, induces adipogenic differentiation of stem cells [28,30,37,52,66,69]. There is also evidence that strontium doped 45S5 glass upregulates the lipid metabolism and synthesis in hBMSCs [70] raising more questions related to the effect of BaGs on adipogenic differentiation. To test whether S53P4 and 1-06 BaGs and the inhibition of FAK and MAPKs affect adipogenic differentiation we analyzed the expression of adipogenic marker gene *aP2* (Supplementary Figure S6A). Glasses as such induced a minor increase in *aP2* expression but only after inhibition of FAK the *aP2* expression was increased to a larger extent, suggesting that FAK may serve as a crucial switch between osteogenesis and adipogenesis on BaGs. However, when the later stages of adipogenesis were analyzed with Oil red O staining and protein level analysis of FABP4/aP2 (Supplementary Figure S6B-C), no indications of adipogenesis could be observed. FAK inhibition on BaGs may therefore prime the cells towards adipogenesis but fails to induce maturation, at least in the absence of other chemical induction stimuli.

When considering the cell-BaG interface, it is clear that the cells respond to the glass surface properties via attachment related mechanisms ultimately leading to changes in cell fate (e.g. osteogenic differentiation), as we have observed. However, the interaction between the cells and the BaG surface is likely reciprocal, i.e. as the glass surface affects the cell behavior, the cells might also have a modifying effect on the glass surface. Indeed, with respect to the glass reactivity, we observed that the attachment of the hASCs on the glass surfaces had an impact on the reaction layer formation and dissolution of BaGs. Our results indicate that the attachment of cells onto the BaGs caused a slower accumulation of CaP at the glass surface and consequently a thinner CaP reaction layer was formed on the glass surfaces with cells attached when compared to the blank samples (Supplementary Figure S5). In line with this, comparatively higher Ca, K, Mg and B concentrations were always detected in the medium of cell-containing samples than in the blank samples, suggesting that in the presence of cells more network-modifying ions released from the glass network are free in the medium than entrapped into the formed CaP layer.

Our results suggest that the osteogenesis inducing effect of BaGs S53P4 and 1-06 is at least partly mediated via cell attachment mechanisms and FAK-ERK1/2 pathway related to them. However, besides the cell attachment related signaling the osteogenic differentiation of stem cells is known to be regulated by a variety of other molecular mechanisms including BMP, Wnt, Hedgehog and NELL-1 signaling, just to mention few. Furthermore, these signaling cascades are known to collaborate closely with the attachment related signaling cascades [71,72] and together they comprise a very complex intracellular signaling network. It is therefore likely that these other signaling routes are also involved in the BaG-induced osteogenic differentiation.

5. CONCLUSIONS

As a conclusion, we observed that the osteogenic differentiation of hASCs was stimulated by both S53P4 and 1-06 BaGs, of which less reactive 1-06 was a stronger inducer. Fibronectin ECM was equally well-formed on all the culturing substrates but in case of collagen-I, BaGs had an increasing effect on its production but not on secretion. With respect to the cell attachment, the production of integrinβ1 and vinculin was upregulated on both glasses implying to stronger attachment mechanisms in the cells on BaGs when compared to polystyrene control. The focal adhesions on BaGs, however, were exceptionally small and spread throughout the cells suggesting an unorthodox mode of attachment, possibly related to the glass surface reactivity. FAK, ERK1/2 and JNK turned out to be essential molecules in the BaG-induced osteogenic differentiation since the inhibition of these molecules significantly decreased ALP activity on both glasses and a reduction was also observed in the expression of *RUNX2a* and *OSTERIX*. Glasses also upregulated the activation of FAK and ERK1/2, as well as JNK downstream target c-Jun. The role of p38, however, was less significant. Interestingly, the cell-BaG interaction was observed to be reciprocal, i.e. in addition to the glass-induced attachment and signaling responses in cells, the cells had an active role as glass modifiers. This is the first study analyzing the molecular level responses of cells on BaGs S53P4 and 1-06 and thus gives a valuable insight into the mechanism of BaG-induced osteogenic differentiation. In the future the research should be extended to comprise also other signaling cascades to obtain a broader picture of the BaG-induced signaling events. Such a knowledge would aid in the design of new functional biomaterials for bone tissue engineering applications.

REFERENCES

1. Jones JR. Review of bioactive glass: From Hench to hybrids. Acta Biomater 2013;9:4457-4486.

2. Rahaman MN, Day DE, Bal BS, Fu Q, Jung SB, Bonewald LF, et al. Bioactive glass in tissue engineering. Acta Biomater 2011;7:2355-2373.

3. Waselau M, Patrikoski M, Juntunen M, Kujala K, Kääriäinen M, Kuokkanen H, et al. Effects of bioactive glass S53P4 or beta-tricalcium phosphate and bone morphogenetic protein-2 and bone morphogenetic protein-7 on osteogenic differentiation of human adipose stem cells. J Tissue Eng 2012;3:2041731412467789.

4. Peltola MJ, Aitasalo KM, Suonpaa JT, Yli-Urpo A, Laippala PJ. In vivo model for frontal sinus and calvarial bone defect obliteration with bioactive glass S53P4 and hydroxyapatite. J Biomed Mater Res 2001;58:261-269.

5. Virolainen P, Heikkila J, Yli-Urpo A, Vuorio E, Aro HT. Histomorphometric and molecular biologic comparison of bioactive glass granules and autogenous bone grafts in augmentation of bone defect healing. J Biomed Mater Res 1997;35:9-17.

6. Lindfors NC, Hyvönen P, Nyyssönen M, Kirjavainen M, Kankare J, Gullichsen E, et al. Bioactive glass S53P4 as bone graft substitute in treatment of osteomyelitis. Bone 2010;47:212-218.

7. Turunen T, Peltola J, Yli-Urpo A, Happonen RP. Bioactive glass granules as a bone adjunctive material in maxillary sinus floor augmentation. Clin Oral Implants Res 2004;15:135-141.

8. Sandor GK, Numminen J, Wolff J, Thesleff T, Miettinen A, Tuovinen VJ, et al. Adipose stem cells used to reconstruct 13 cases with cranio-maxillofacial hard-tissue defects. Stem Cells Transl Med 2014;3:530-540.

9. Mantsos T, Chatzistavrou X, Roether JA, Hupa L, Arstila H, Boccaccini AR. Non-crystalline composite tissue engineering scaffolds using boron-containing bioactive glass and poly(D,L-lactic acid) coatings. Biomed Mater 2009;4:055002-6041/4/5/055002. Epub 2009 Sep 23.

10. Fagerlund S, Massera J, Moritz N, Hupa L, Hupa M. Phase composition and in vitro bioactivity of porous implants made of bioactive glass S53P4. Acta Biomater 2012;8:2331-2339.

11. Ojansivu M, Vanhatupa S, Björkvik L, Häkkänen H, Kellomäki M, Autio R, et al. Bioactive glass ions as strong enhancers of osteogenic differentiation in human adipose stem cells. Acta Biomater 2015;21:190-203.

12. Madanat R, Moritz N, Vedel E, Svedström E, Aro HT. Radio-opaque bioactive glass markers for radiostereometric analysis. Acta Biomater 2009;5:3497-3505.

13. Au AY, Au RY, Demko JL, McLaughlin RM, Eves BE, Frondoza CG. Consil bioactive glass particles enhance osteoblast proliferation and selectively modulate cell signaling pathways in vitro. J Biomed Mater Res A 2010;94:380-388.

14. Kim GH, Park YD, Lee SY, El-Fiqi A, Kim JJ, Lee EJ, et al. Odontogenic stimulation of human dental pulp cells with bioactive nanocomposite fiber. J Biomater Appl 2015;29:854-866.

15. Zhang J, Park YD, Bae WJ, El-Fiqi A, Shin SH, Lee EJ, et al. Effects of bioactive cements incorporating zinc-bioglass nanoparticles on odontogenic and angiogenic potential of human dental pulp cells. J Biomater Appl 2015;29:954-964.

16. Hynes RO. Integrins: bidirectional, allosteric signaling machines. Cell 2002;110:673-687.

17. Burridge K, Chrzanowska-Wodnicka M. Focal adhesions, contractility, and signaling. Annu Rev Cell Dev Biol 1996;12:463-518.

18. Schaller MD. Biochemical signals and biological responses elicited by the focal adhesion kinase. Biochim Biophys Acta 2001;1540:1-21.

19. Salasznyk RM, Klees RF, Boskey A, Plopper GE. Activation of FAK is necessary for the osteogenic differentiation of human mesenchymal stem cells on laminin-5. J Cell Biochem 2007;100:499-514.

20. Salasznyk RM, Klees RF, Williams WA, Boskey A, Plopper GE. Focal adhesion kinase signaling pathways regulate the osteogenic differentiation of human mesenchymal stem cells. Exp Cell Res 2007;313:22-37.

21. Shih YR, Tseng KF, Lai HY, Lin CH, Lee OK. Matrix stiffness regulation of integrin-mediated mechanotransduction during osteogenic differentiation of human mesenchymal stem cells. J Bone Miner Res 2011;26:730-738.

22. Takeuchi Y, Suzawa M, Kikuchi T, Nishida E, Fujita T, Matsumoto T. Differentiation and transforming growth factor-beta receptor down-regulation by collagen-alpha2beta1 integrin interaction is mediated by focal adhesion kinase and its downstream signals in murine osteoblastic cells. J Biol Chem 1997;272:29309-29316.

23. Viale-Bouroncle S, Gosau M, Morsczeck C. Collagen I induces the expression of alkaline phosphatase and osteopontin via independent activations of FAK and ERK signalling pathways. Arch Oral Biol 2014;59:1249-1255.

24. Viale-Bouroncle S, Gosau M, Morsczeck C. Laminin regulates the osteogenic differentiation of dental follicle cells via integrin-alpha2/-beta1 and the activation of the FAK/ERK signaling pathway. Cell Tissue Res 2014;357:345-354.

25. Marino G, Rosso F, Cafiero G, Tortora C, Moraci M, Barbarisi M, et al. Beta-tricalcium phosphate 3D scaffold promote alone osteogenic differentiation of human adipose stem cells: in vitro study. J Mater Sci Mater Med 2010;21:353-363.

26. Shie MY, Ding SJ. Integrin binding and MAPK signal pathways in primary cell responses to surface chemistry of calcium silicate cements. Biomaterials 2013;34:6589-6606.

27. Rubinfeld H, Seger R. The ERK cascade: a prototype of MAPK signaling. Mol Biotechnol 2005;31:151-174.

28. Jaiswal RK, Jaiswal N, Bruder SP, Mbalaviele G, Marshak DR, Pittenger MF. Adult human mesenchymal stem cell differentiation to the osteogenic or adipogenic lineage is regulated by mitogen-activated protein kinase. J Biol Chem 2000;275:9645-9652.

29. Lai CF, Chaudhary L, Fausto A, Halstead LR, Ory DS, Avioli LV, et al. Erk is essential for growth, differentiation, integrin expression, and cell function in human osteoblastic cells. J Biol Chem 2001;276:14443-14450.

30. Liu Q, Cen L, Zhou H, Yin S, Liu G, Liu W, et al. The role of the extracellular signal-related kinase signaling pathway in osteogenic differentiation of human adipose-derived stem cells and in adipogenic transition initiated by dexamethasone. Tissue Eng Part A 2009;15:3487-3497.

31. Kono SJ, Oshima Y, Hoshi K, Bonewald LF, Oda H, Nakamura K, et al. Erk pathways negatively regulate matrix mineralization. Bone 2007;40:68-74.

32. Higuchi C, Myoui A, Hashimoto N, Kuriyama K, Yoshioka K, Yoshikawa H, et al. Continuous inhibition of MAPK signaling promotes the early osteoblastic differentiation and mineralization of the extracellular matrix. J Bone Miner Res 2002;17:1785-1794.

33. Chiu LH, Lai WF, Chang SF, Wong CC, Fan CY, Fang CL, et al. The effect of type II collagen on MSC osteogenic differentiation and bone defect repair. Biomaterials 2014;35:2680-2691.

34. Ivaska J, Reunanen H, Westermarck J, Koivisto L, Kahari VM, Heino J. Integrin alpha2beta1 mediates isoform-specific activation of p38 and upregulation of collagen gene transcription by a mechanism involving the alpha2 cytoplasmic tail. J Cell Biol 1999;147:401-416.

35. Gu H, Huang Z, Yin X, Zhang J, Gong L, Chen J, et al. Role of c-Jun N-terminal kinase in the osteogenic and adipogenic differentiation of human adipose-derived mesenchymal stem cells. Exp Cell Res 2015;339:112-121.

36. Suzuki A, Guicheux J, Palmer G, Miura Y, Oiso Y, Bonjour JP, et al. Evidence for a role of p38 MAP kinase in expression of alkaline phosphatase during osteoblastic cell differentiation. Bone 2002;30:91-98.

37. Tominaga S, Yamaguchi T, Takahashi S, Hirose F, Osumi T. Negative regulation of adipogenesis from human mesenchymal stem cells by Jun N-terminal kinase. Biochem Biophys Res Commun 2005;326:499-504.

38. Zuk PA, Zhu M, Mizuno H, Huang J, Futrell JW, Katz AJ, et al. Multilineage cells from human adipose tissue: implications for cell-based therapies. Tissue Eng 2001;7:211-228.

39. Tirkkonen L, Haimi S, Huttunen S, Wolff J, Pirhonen E, Sandor GK, et al. Osteogenic medium is superior to growth factors in differentiation of human adipose stem cells towards bone-forming cells in 3D culture. Eur Cell Mater 2013;25:144-158.

40. Lindroos B, Boucher S, Chase L, Kuokkanen H, Huhtala H, Haataja R, et al. Serum-free, xeno-free culture media maintain the proliferation rate and multipotentiality of adipose stem cells in vitro. Cytotherapy 2009;11:958-972.

41. Kyllönen L, Haimi S, Mannerström B, Huhtala H, Rajala KM, Skottman H, et al. Effects of different serum conditions on osteogenic differentiation of human adipose stem cells in vitro. Stem Cell Res Ther 2013;4:17.

42. Fink T, Lund P, Pilgaard L, Rasmussen JG, Duroux M, Zachar V. Instability of standard PCR reference genes in adipose-derived stem cells during propagation, differentiation and hypoxic exposure. BMC Mol Biol 2008;9:98-2199-9-98.

43. Gabrielsson BG, Olofsson LE, Sjögren A, Jernås M, Elander A, Lönn M, et al. Evaluation of reference genes for studies of gene expression in human adipose tissue. Obes Res 2005;13:649-652.

44. Pfaffl MW. A new mathematical model for relative quantification in real-time RT-PCR. Nucleic Acids Res 2001;29:e45.

45. Bosetti M, Cannas M. The effect of bioactive glasses on bone marrow stromal cells differentiation. Biomaterials 2005;26:3873-3879.

46. Gough JE, Jones JR, Hench LL. Nodule formation and mineralisation of human primary osteoblasts cultured on a porous bioactive glass scaffold. Biomaterials 2004;25:2039-2046.

47. Haimi S, Moimas L, Pirhonen E, Lindroos B, Huhtala H, Räty S, et al. Calcium phosphate surface treatment of bioactive glass causes a delay in early osteogenic differentiation of adipose stem cells. J Biomed Mater Res A 2009;91:540-547.

48. Pulverer BJ, Kyriakis JM, Avruch J, Nikolakaki E, Woodgett JR. Phosphorylation of c-jun mediated by MAP kinases. Nature 1991;353:670-674.

49. Ying X, Cheng S, Wang W, Lin Z, Chen Q, Zhang W, et al. Effect of boron on osteogenic differentiation of human bone marrow stromal cells. Biol Trace Elem Res 2011;144:306-315.

50. Abagnale G, Steger M, Nguyen VH, Hersch N, Sechi A, Joussen S, et al. Surface topography enhances differentiation of mesenchymal stem cells towards osteogenic and adipogenic lineages. Biomaterials 2015;61:316-326.

51. Biggs MJ, Richards RG, Gadegaard N, McMurray RJ, Affrossman S, Wilkinson CD, et al. Interactions with nanoscale topography: adhesion quantification and signal transduction in cells of osteogenic and multipotent lineage. J Biomed Mater Res A 2009;91:195-208.

52. Kilian KA, Bugarija B, Lahn BT, Mrksich M. Geometric cues for directing the differentiation of mesenchymal stem cells. Proc Natl Acad Sci U S A 2010;107:4872-4877.

53. Pennisi CP, Dolatshahi-Pirouz A, Foss M, Chevallier J, Fink T, Zachar V, et al. Nanoscale topography reduces fibroblast growth, focal adhesion size and migration-related gene expression on platinum surfaces. Colloids Surf B Biointerfaces 2011;85:189-197.

54. Di Cio S, Gautrot JE. Cell sensing of physical properties at the nanoscale: Mechanisms and control of cell adhesion and phenotype. Acta Biomater 2015.

55. Rodriguez JP, Gonzalez M, Rios S, Cambiazo V. Cytoskeletal organization of human mesenchymal stem cells (MSC) changes during their osteogenic differentiation. J Cell Biochem 2004;93:721-731.

56. Yourek G, Hussain MA, Mao JJ. Cytoskeletal changes of mesenchymal stem cells during differentiation. ASAIO J 2007;53:219-228.

57. Chatzizacharias NA, Kouraklis GP, Theocharis SE. Disruption of FAK signaling: a side mechanism in cytotoxicity. Toxicology 2008;245:1-10.

58. Schlaepfer DD, Hauck CR, Sieg DJ. Signaling through focal adhesion kinase. Prog Biophys Mol Biol 1999;71:435-478.

59. Engler AJ, Sen S, Sweeney HL, Discher DE. Matrix elasticity directs stem cell lineage specification. Cell 2006;126:677-689.

60. Hwang JH, Byun MR, Kim AR, Kim KM, Cho HJ, Lee YH, et al. Extracellular Matrix Stiffness Regulates Osteogenic Differentiation through MAPK Activation. PLoS One 2015;10:e0135519.

61. Docheva D, Padula D, Popov C, Mutschler W, Clausen-Schaumann H, Schieker M. Researching into the cellular shape, volume and elasticity of mesenchymal stem cells, osteoblasts and osteosarcoma cells by atomic force microscopy. J Cell Mol Med 2008;12:537-552.

62. Shie MY, Ding SJ, Chang HC. The role of silicon in osteoblast-like cell proliferation and apoptosis. Acta Biomater 2011;7:2604-2614.

63. Gu H, Guo F, Zhou X, Gong L, Zhang Y, Zhai W, et al. The stimulation of osteogenic differentiation of human adipose-derived stem cells by ionic products from akermanite dissolution via activation of the ERK pathway. Biomaterials 2011;32:7023-7033.

64. Hamilton DW, Brunette DM. The effect of substratum topography on osteoblast adhesion mediated signal transduction and phosphorylation. Biomaterials 2007;28:1806-1819.

65. Guicheux J, Lemonnier J, Ghayor C, Suzuki A, Palmer G, Caverzasio J. Activation of p38 mitogen-activated protein kinase and c-Jun-NH2-terminal kinase by BMP-2 and their implication in the stimulation of osteoblastic cell differentiation. J Bone Miner Res 2003;18:2060-2068.

66. Qiu W, Chen L, Kassem M. Activation of non-canonical Wnt/JNK pathway by Wnt3a is associated with differentiation fate determination of human bone marrow stromal (mesenchymal) stem cells. Biochem Biophys Res Commun 2011;413:98-104.

67. Chen F, Walder B, James AW, Soofer DE, Soo C, Ting K, et al. NELL-1-dependent mineralisation of Saos-2 human osteosarcoma cells is mediated via c-Jun N-terminal kinase pathway activation. Int Orthop 2012;36:2181-2187.

68. Fu L, Tang T, Miao Y, Zhang S, Qu Z, Dai K. Stimulation of osteogenic differentiation and inhibition of adipogenic differentiation in bone marrow stromal cells by alendronate via ERK and JNK activation. Bone 2008;43:40-47.

69. Xu B, Ju Y, Song G. Role of p38, ERK1/2, focal adhesion kinase, RhoA/ROCK and cytoskeleton in the adipogenesis of human mesenchymal stem cells. J Biosci Bioeng 2014;117:624-631.

70. Autefage H, Gentleman E, Littmann E, Hedegaard MA, Von Erlach T, O'Donnell M, et al. Sparse feature selection methods identify unexpected global cellular response to strontium-containing materials. Proc Natl Acad Sci U S A 2015;112:4280-4285.

71. Noth U, Tuli R, Seghatoleslami R, Howard M, Shah A, Hall DJ, et al. Activation of p38 and Smads mediates BMP-2 effects on human trabecular bone-derived osteoblasts. Exp Cell Res 2003;291:201-211.

72. Tamura Y, Takeuchi Y, Suzawa M, Fukumoto S, Kato M, Miyazono K, et al. Focal adhesion kinase activity is required for bone morphogenetic protein--Smad1 signaling and osteoblastic differentiation in murine MC3T3-E1 cells. J Bone Miner Res 2001;16:1772-1779.
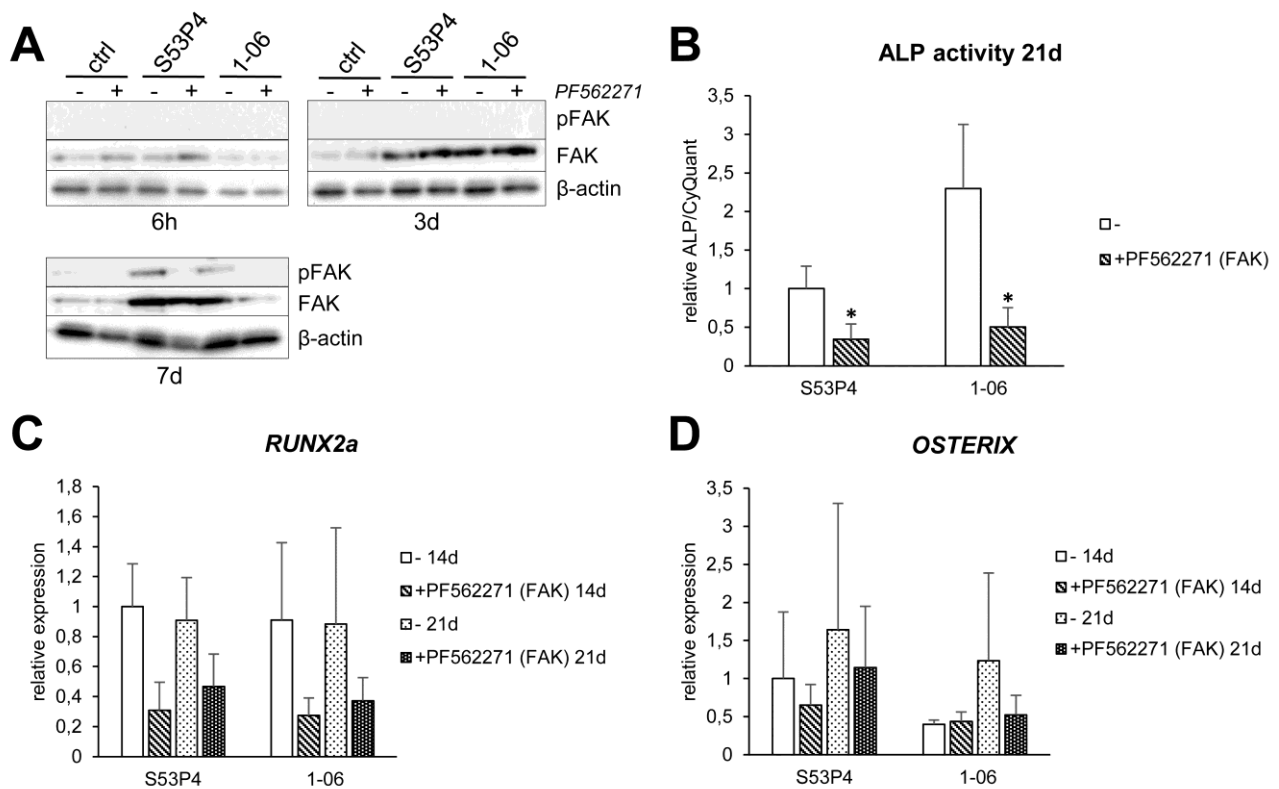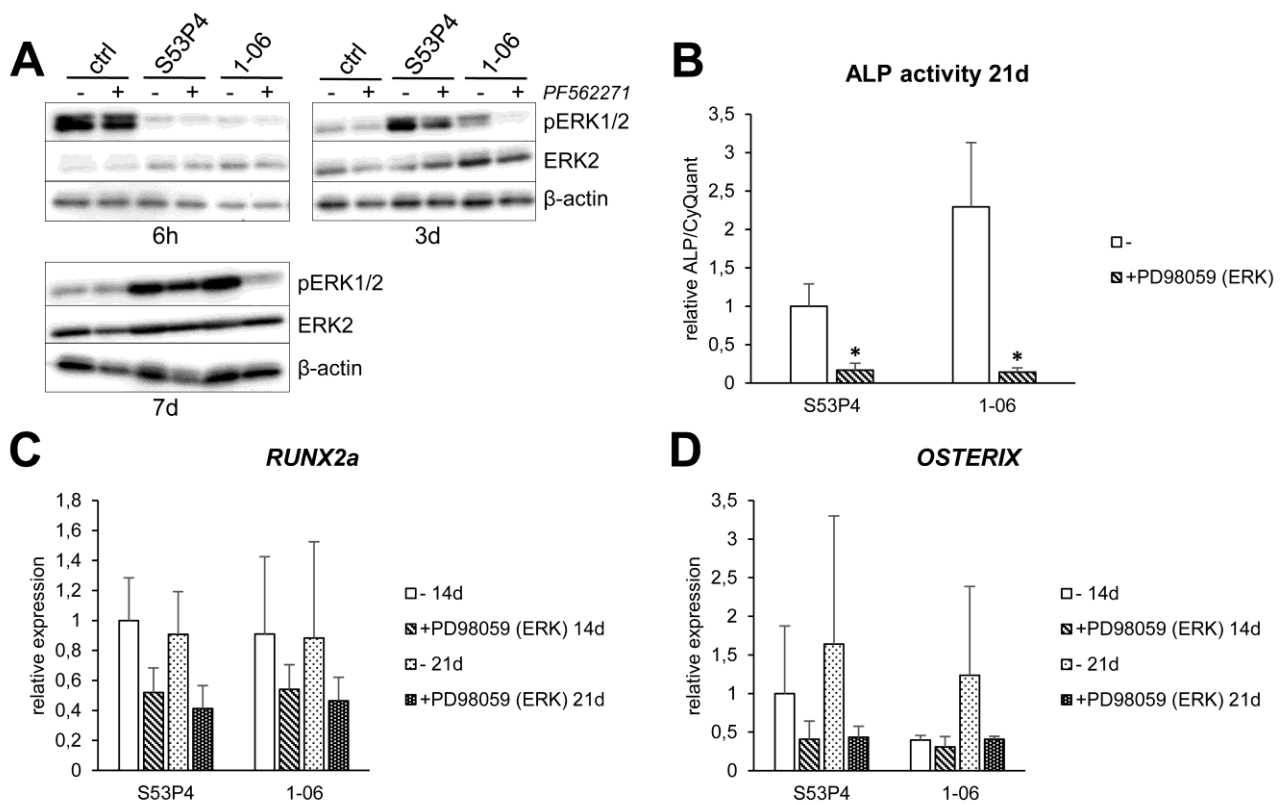
FIGURES
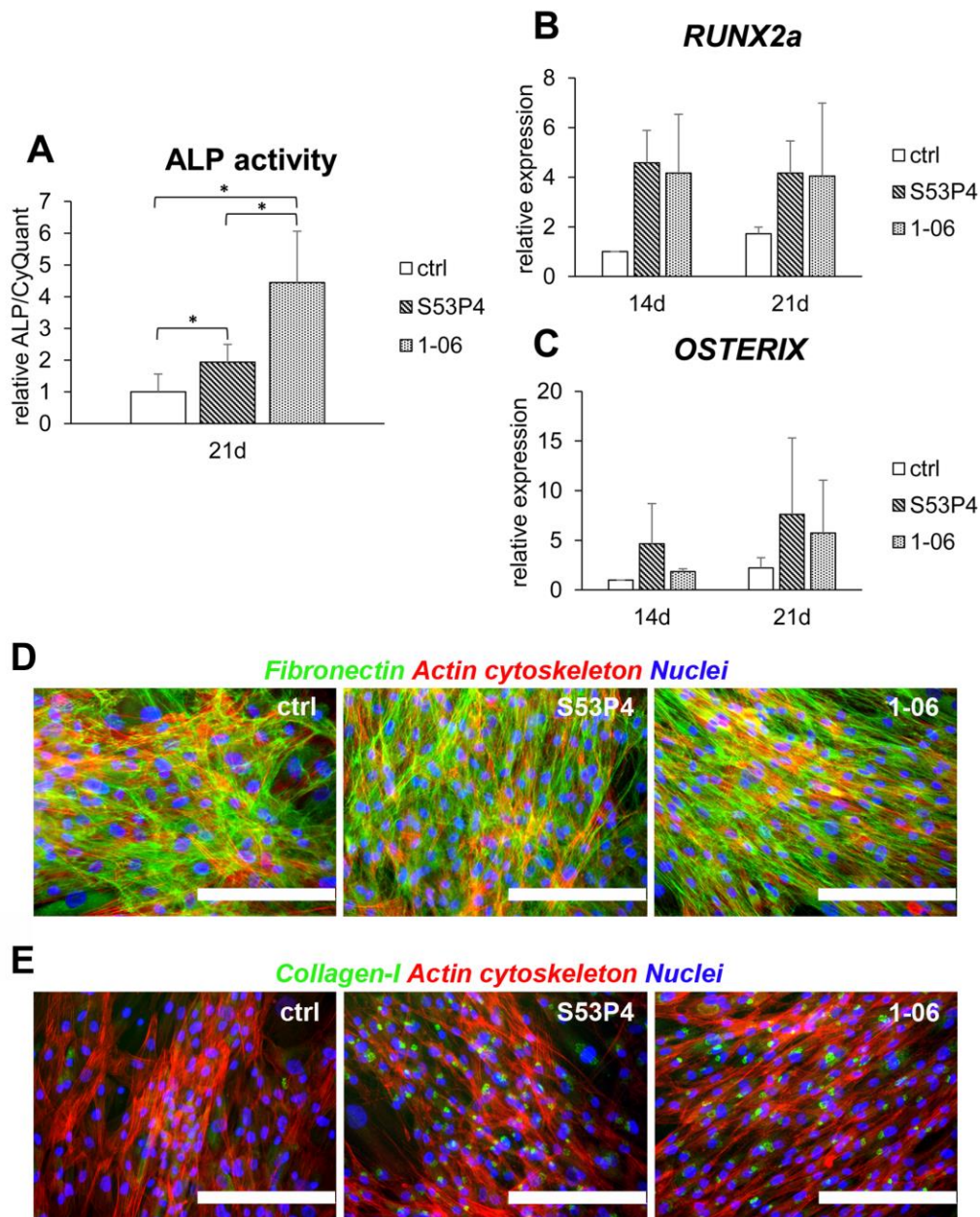
Figure 1. *Osteogenic differentiation and ECM production of hASCs on BaGs.* **A.** Alkaline phosphatase (ALP) activity at 21d normalized with cell amount determined by CyQUANT assay. *n*=12. **B.** *RUNX2a* expression at 14d and 21d. *n*=4. **C.** *OSTERIX* expression at 14d and 21d. *n*=4. The results are relative to the control (ctrl; polystyrene). *p<0.05. **D.** Immunocytochemical staining of fibronectin (green) at 21d. **E.** Immunocytochemical staining of collagen-I (green) at 21d. Scale bars 200 µM. Actin cytoskeleton was stained red with phalloidin and nuclei blue with DAPI. Ctrl=control (polystyrene).
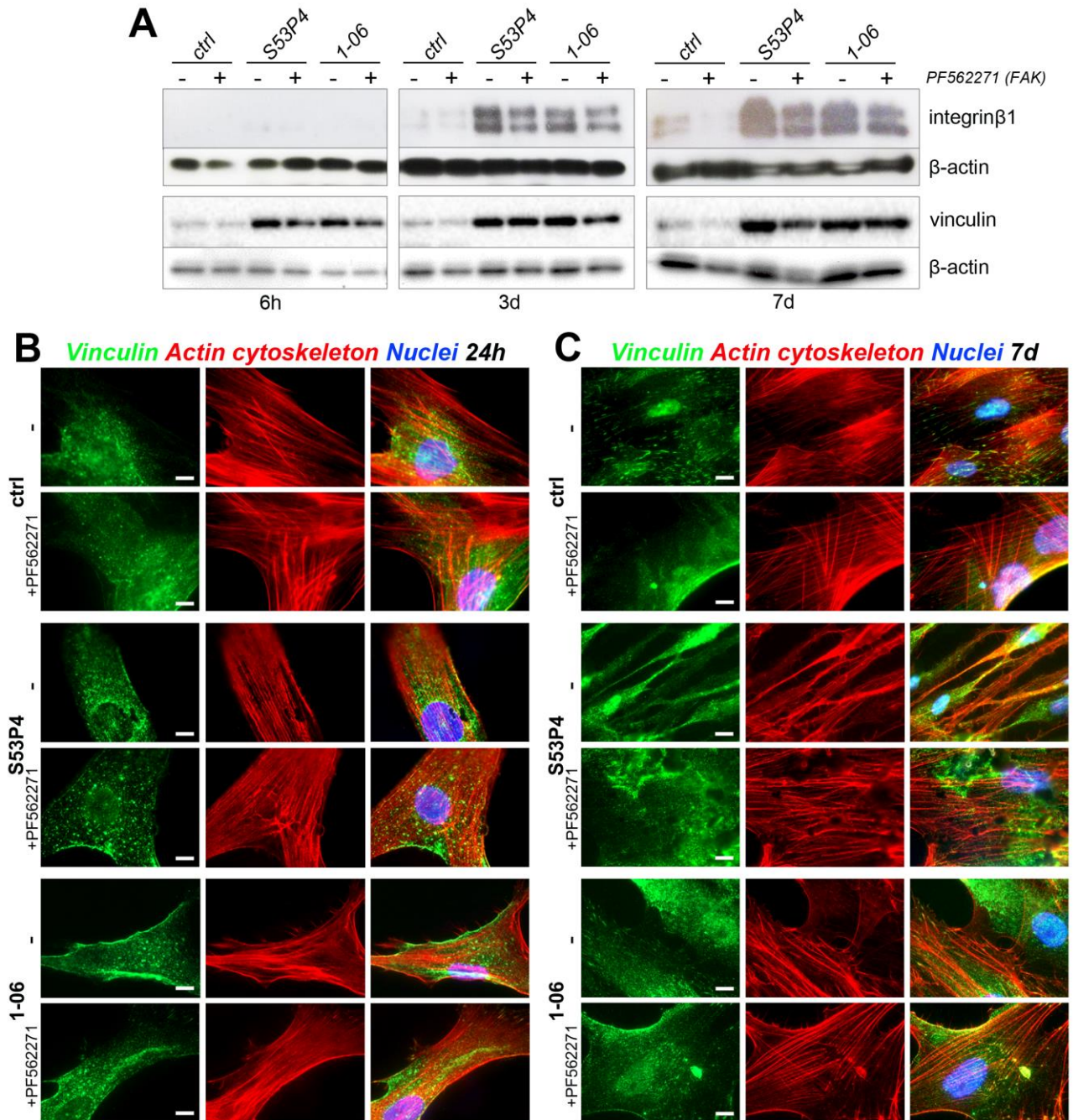
Figure 2. *Cell attachment and actin cytoskeleton on BaGs.* **A.** Western blot analysis of integrinβ1 and vinculin at 6h, 3d and 7d in the presence or absence of FAK inhibitor PF562271 (2 µM). β-actin served as a loading control. **B, C.** Immunocytochemical staining of vinculin at 24h and 7d, respectively, in the presence or absence of FAK inhibitor PF562271 (2 µM). Actin cytoskeleton was stained red with phalloidin and nuclei blue with DAPI. Scale bars 10 µM. ctrl=control (polystyrene).

Figure 3. *The role of FAK in the BaG-induced osteogenic differentiation of hASCs.* **A.** Western blot analysis of FAK activation (phosphorylation; pFAK) on the different materials at 6h, 3d and 7d. β-actin served as a loading control. ctrl=control (polystyrene). **B.** ALP activity at 21d normalized with cell amount determined by CyQUANT assay. The results are represented relative to the S53P4 without the inhibitor (-). $n=12$. **C.** *RUNX2a* expression at 14d and 21d. The results are relative to S53P4 without the inhibitor (-) at 14d. $n=4$. **D.** *OSTERIX* expression at 14d and 21d. The results are relative to the S53P4 without the inhibitor (-) at 14d. $n=4$. FAK inhibitor PF562271 (2 µM).
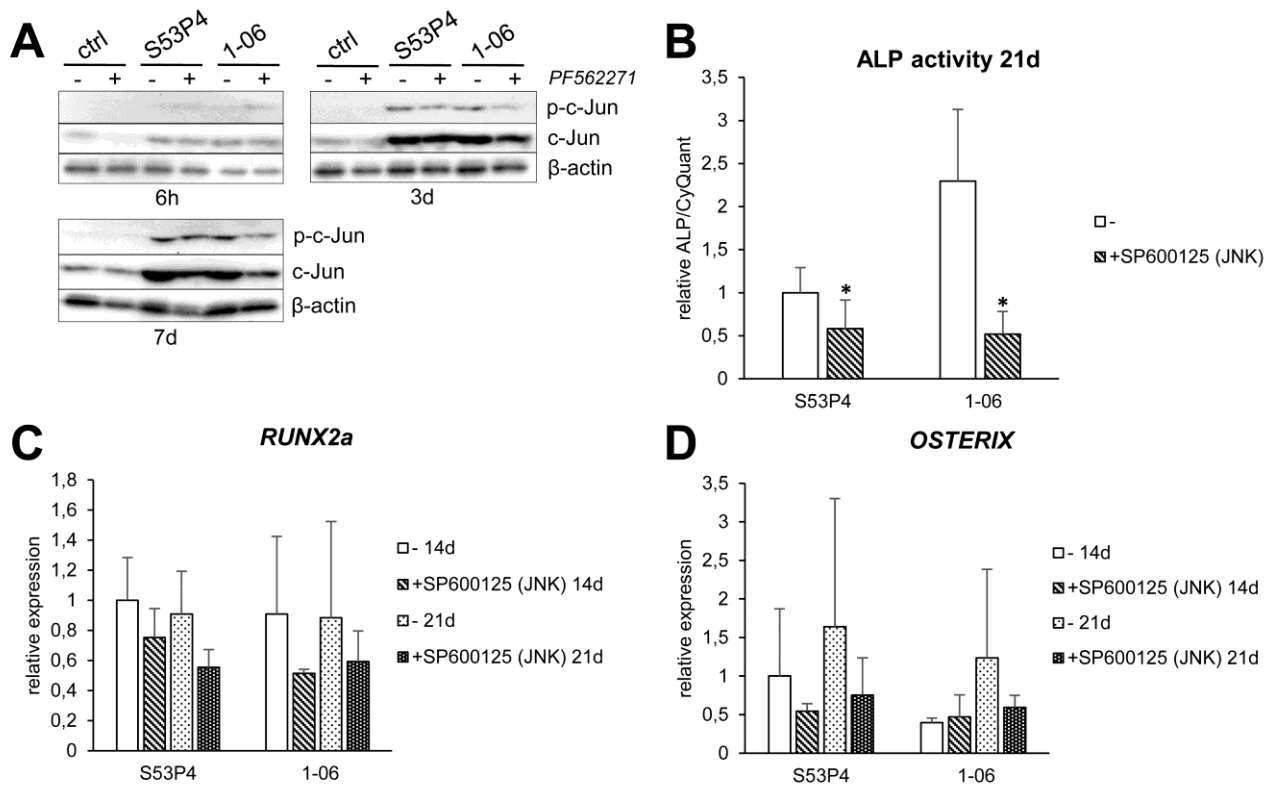
Figure 4. *The role of ERK1/2 in the BaG-induced osteogenic differentiation of hASCs*. **A.** Western blot analysis of ERK activation (phosphorylation; pERK1/2) on the different materials at 6h, 3d and 7d, in the presence or absence of the FAK inhibitor PF562271 (2 µM). β-actin served as a loading control. ctrl=control (polystyrene). **B.** ALP activity at 21d normalized with cell amount determined by CyQUANT assay. The results are represented relative to the S53P4 without the inhibitor (-). *n*=12. **C.** *RUNX2a* expression at 14d and 21d. The results are relative to S53P4 without the inhibitor (-) at 14d. *n*=4. **D.** *OSTERIX* expression at 14d and 21d. The results are relative to the S53P4 without the inhibitor (-) at 14d. *n*=4. ERK inhibitor PD98059 (60 µM).
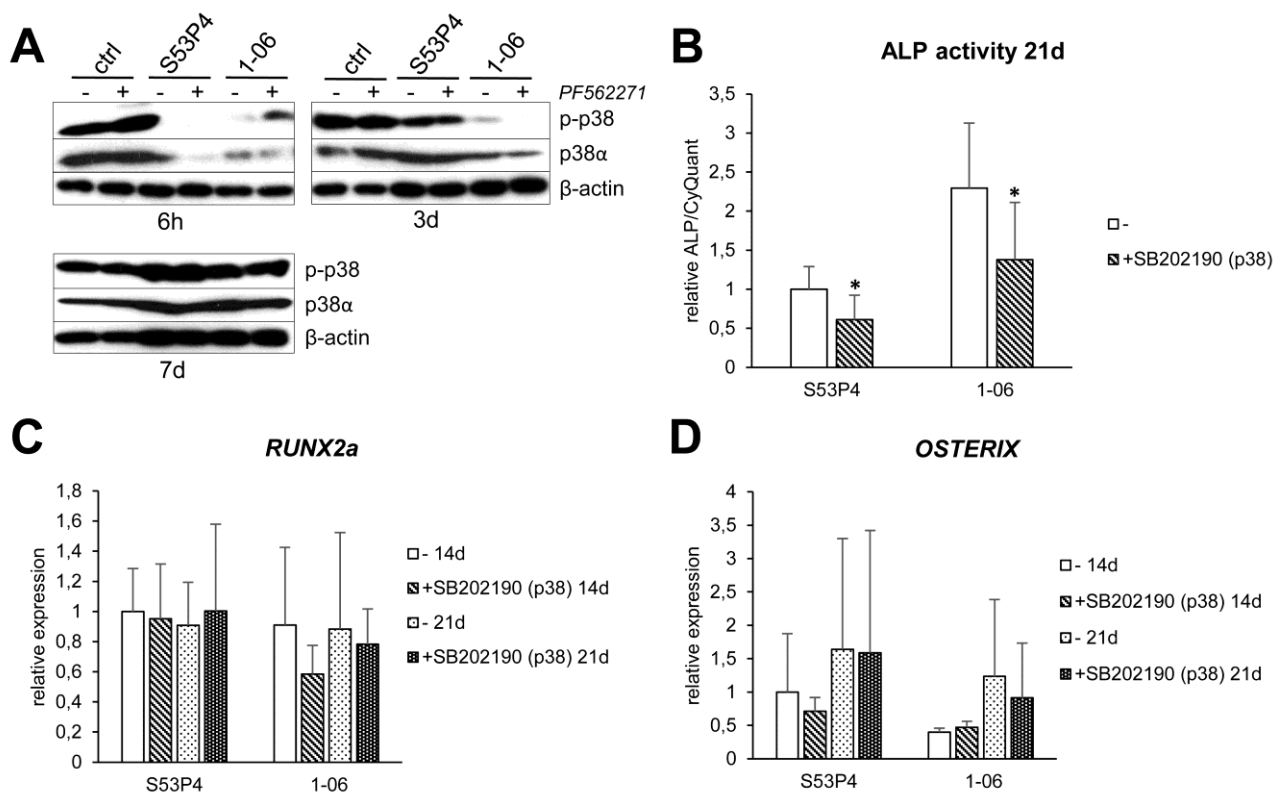
Figure 5. *The role of p38 in the BaG-induced osteogenic differentiation of hASCs.* **A.** Western blot analysis of p38 activation (phosphorylation; p-p38) on the different materials at 6h, 3d and 7d, in the presence or absence of FAK inhibitor PF562271 (2 µM). β-actin served as a loading control. ctrl=control (polystyrene). **B.** ALP activity at 21d normalized with cell amount determined by CyQUANT assay. The results are represented relative to the S53P4 without the inhibitor (-). *n*=12. **C.** *RUNX2a* expression at 14d and 21d. The results are relative to S53P4 without the inhibitor (-) at 14d. *n*=4. **D.** *OSTERIX* expression at 14d and 21d. The results are relative to the S53P4 without the inhibitor (-) at 14d. *n*=4. p38 inhibitor SB202190 (2 µM).

Figure 6. *The role of JNK in the BaG-induced osteogenic differentiation of hASCs.* **A.** Western blot analysis of c-Jun activation (phosphorylation; p-c-Jun) on the different materials at 6h, 3d and 7d, in the presence or absence of FAK inhibitor PF562271 (2 µM). β-actin served as a loading control. ctrl=control (polystyrene). **B.** ALP activity at 21d normalized with cell amount determined by CyQUANT assay. The results are represented relative to the S53P4 without the inhibitor (-). *n*=12. **C.** *RUNX2a* expression at 14d and 21d. The results are relative to S53P4 without the inhibitor (-) at 14d. *n*=4. **D.** *OSTERIX* expression at 14d and 21d. The results are relative to the S53P4 without the inhibitor (-) at 14d. *n*=4. JNK inhibitor SP600125 (10 µM).
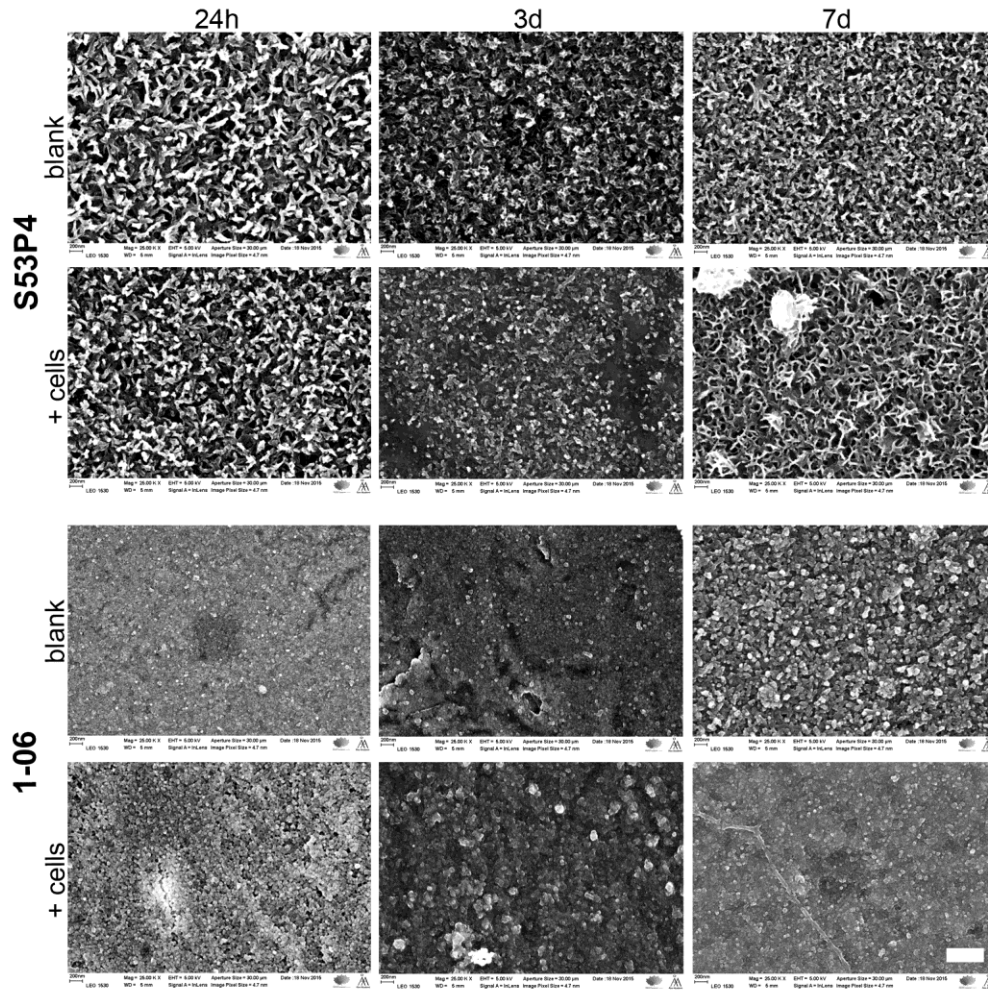
Figure 7. *Submicron scale structures of the BaG disc surfaces.* The submicron scale structures of the glass surfaces were evaluated at 24h, 3d and 7d time points with SEM imaging. Both blank samples (no cells) and cell-containing samples were imaged. From cell-containing samples a location with no covering cells was chosen. Scale bars 500 nm.
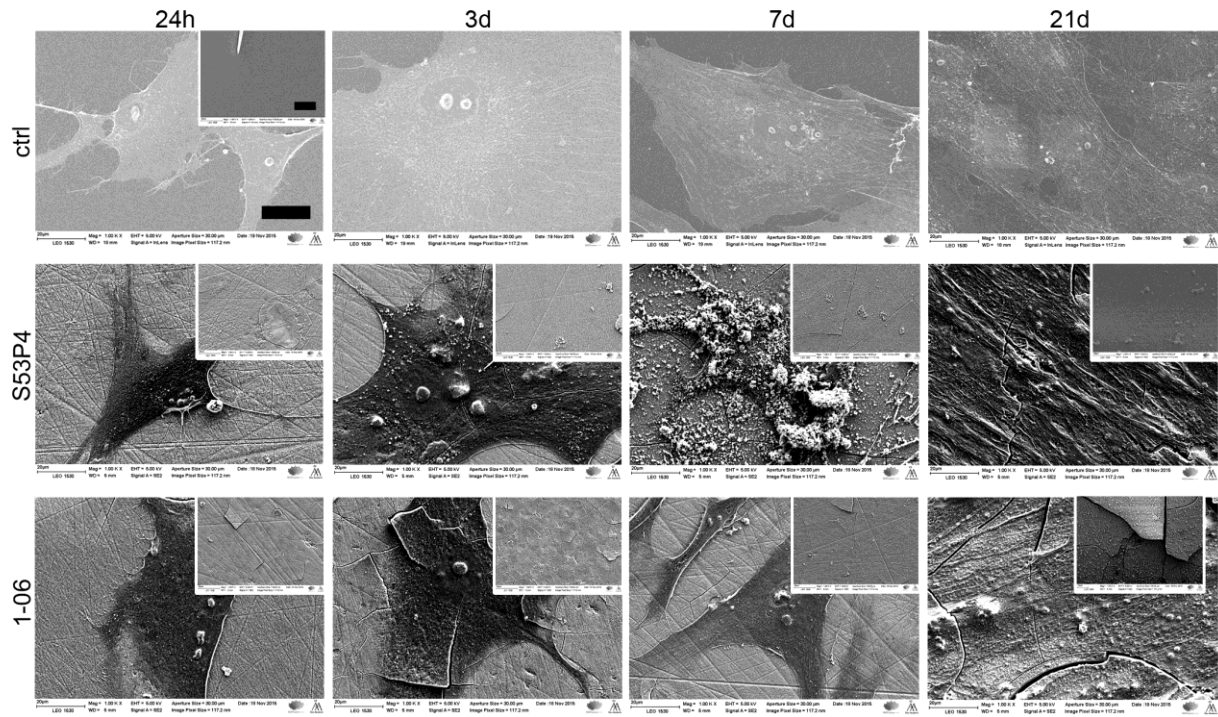
Figure 8. *Cell shape on the different surfaces.* hASCs grown on different surfaces were visualized at 24h, 3d, 7d and 21d time points with SEM imaging. Smaller images represent the surfaces of the blank samples (not containing cells). After 7d of culture a thick CaP precipitate covers the cells on S53P4 but not on 1-06 or on control polystyrene. Scale bars 20 μm. Ctrl=control (polystyrene).
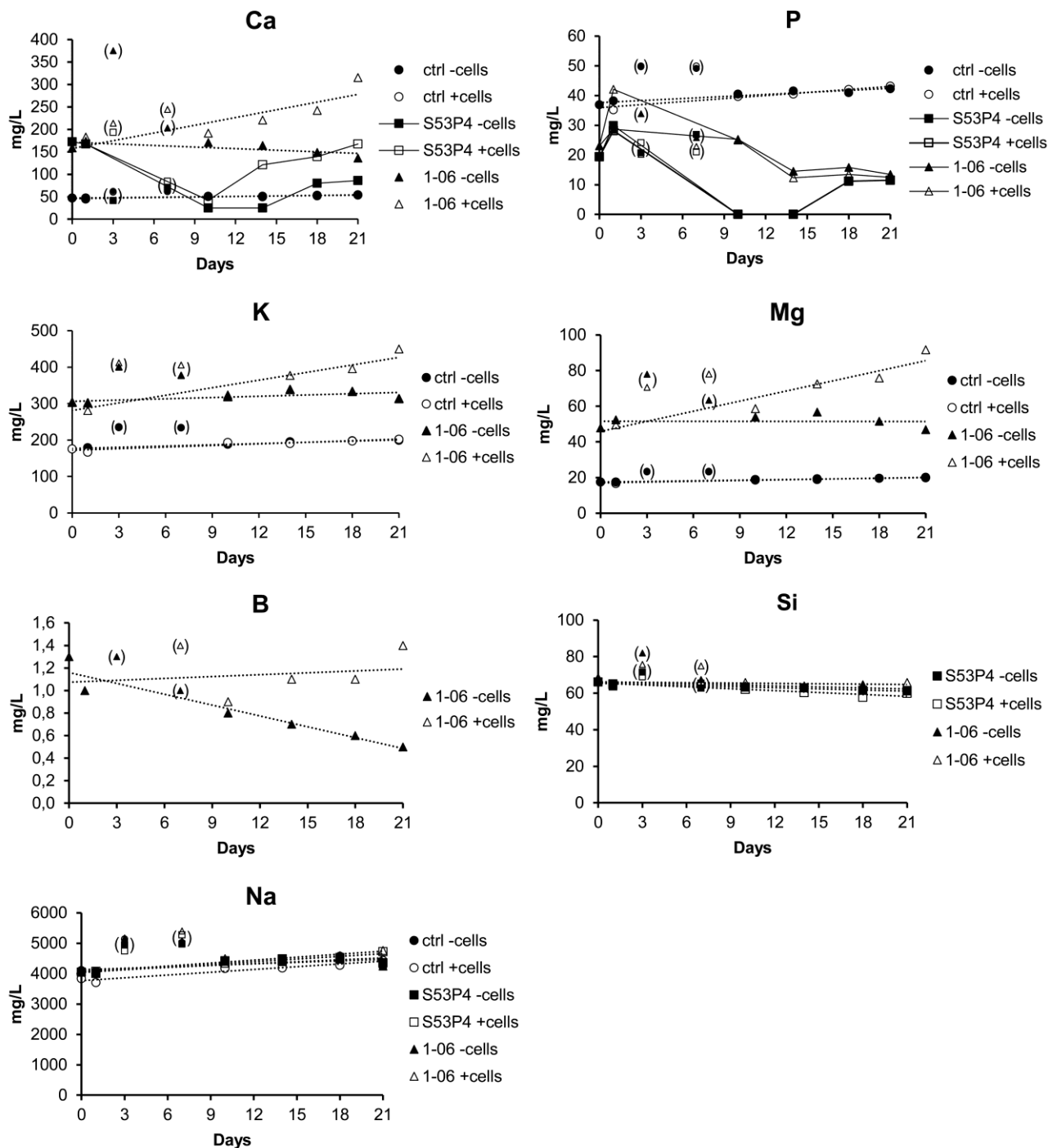
Figure 9. *Ionic release profiles of the BaG discs.* Ion concentrations of Ca, P, K, Mg, B, Si and Na were analyzed with ICP-OES from medium samples collected at each medium change. Both blank samples (-cells) and cell-containing samples (+cells) were analyzed at each time point. A linear trendline (dash line) was fitted when the release was approximately linear. In Ca and P graphs a continuous line was added to the BaG samples to make the temporal fluctuation in the ionic levels clearer. Measurement values of the 3d and 7d samples are shown in parentheses due to their systematically too high values, possibly caused by concentration of these particular samples due to transient humidity change in the cell culture incubator. Ctrl=control (polystyrene).